MODIFIED COILED-COIL PROTEINS FOR THE TREATMENT OF CHRONIC MYELOID LEUKEMIA

by

Benjamin James Bruno

A dissertation submitted to the faculty of
The University of Utah
in partial fulfillment of the requirements for the degree of

Doctor of Philosophy

Department of Pharmaceutics and Pharmaceutical Chemistry

The University of Utah

December 2017

The University of Utah Graduate School

STATEMENT OF DISSERTATION APPROVAL

The dissertation of **Benjamin James Bruno**

has been approved by the following supervisory committee members:

Carol S. Lim	, Chair	**07-27-2017** Date Approved
David W. Grainger	, Member	**07-27-2017** Date Approved
James N. Herron	, Member	**07-27-2017** Date Approved
Margit Janat-Amsbury	, Member	**07-31-2017** Date Approved
Shawn C. Owen	, Member	**07-27-2017** Date Approved

and by **Carol S. Lim** , Chair/Dean of

the Department/College/School of **Pharmaceutics and Pharmaceutical Chemistry**

and by David B. Kieda, Dean of The Graduate School.

ABSTRACT

Chronic myeloid leukemia (CML) is caused by the constitutive tyrosine kinase activity of the oncoprotein Bcr-Abl. This aberrant kinase activity activates a multitude of oncogenic signaling pathways resulting in myeloid cell proliferation. In the early 2000s, the development of tyrosine kinase inhibitors (TKIs) (such as the breakthrough drug imatinib) greatly improved the prognosis and overall survival of those diagnosed with CML. However, point mutations in the TK domain often limit the clinical effectiveness of TKIs. Second- and third-generation TKIs have been developed to treat those with mutant Bcr-Abl; however, off-target effects and subsequent toxicity of these newer drugs limits their use.

The N-terminal coil-coiled (CC) domain of Bcr-Abl allows for homooligomerization, a prerequisite to aberrant TK activity. Previous work in the lab has focused on designing a mutant CC which is capable of binding to the CC in Bcr-Abl, thereby inhibiting oligomerization and subsequent oncogenic signaling. The lead construct, the 72-amina acid CC^{mut3}, was effective against cells harboring both wild-type and clinically-relevant Bcr-Abl mutants when delivered as a gene. As gene therapy is still preclinical, the aim of this work was to create a translatable version of CC^{mut3}. In one study, a leukemia-specific cell-penetrating peptide was added to the N-terminus of the CC, which facilitated protein delivery to leukemic cells and subsequent induction of apoptosis in Bcr-Abl+ cells. Next, peptide stapling was implemented in an attempt to create a

proteolytically-resistant version of CC^{mut3}. Locking the peptide backbone of an α-helical peptide with an all-hydrocarbon staple can lead to increased helicity, target affinity, serum stability, and half-life. However, stapling of CC^{mut3} paradoxically led to increased sensitivity to proteolysis, which is explored in Chapter 4. The last chapter in this dissertation focuses on the use of alternative staples and other modifications that could be used to design CC constructs that are resistant to proteolysis.

TABLE OF CONTENTS

LIST OF TABLES

Tables

LIST OF FIGURES

Figures

LIST OF SCHEMES

Schemes

LIST OF ABBREVIATIONS

7-AAD	7-aminoactinomycin D
AA	Amino acid
ABC	ATP binding cassette
ABD	Actin binding domain
Arg	arginine
ALL	Acute lymphoblastic leukemia
ATP	Adenosine triphosphate
ATRP	Atom transfer radical polymerization
AUC	Area under the curve
BCR	Breakpoint cluster region
BLM	β-lactamase
BMT	Bone marrow transplant
c-Abl	Cellular Abelson protein tyrosine kinase
CC	Coiled-coil
CCmut	Mutant coiled-coil
CMC	Critical micelle concentration
CML	Chronic myeloid leukemia
CPP	Cell penetrating peptide
CSA	Cyclosporine
cyt-c	Cytochrome C
D-AA	D-amino acid
DAU	Diallylurea
DBD	DNA binding domain
ddH20	double distilled water
DH	Dbl homology domain
DM	Diabetes mellitus
DMAP	2,2-dimethoxy-2-phenyl-acetophenone
DMPA	2,2 dimethoxy-2-phenylacetophenone
DNA	Deoxyribonucleic acid
DOPE	dioleylphosphoethanolamine
DTT	Dithiothreitol
EDTA	Ethylenediaminetetraacetic acid
EPR	Enhanced permeability and retention

FDA	Food and Drug Administration
FITC	Fluorescin isothiocyanate
FRP	Free radical polymerization
GAP	GTPase-activating protein
GHRH	Growth hormone releasing hormone
GI	Gastrointestinal
GI-MAPS	Gastrointestional mucoadhesive patch system
GLP-1	Glucagon-like peptide 1
GRAS	generally recognized as safe
GTP	Guanosine triphosphate
HA	Hemagglutinin
HDAC	Histone deacetylase s
hEGF	Human epidermal growth factor
HER2	Human epidermal growth factor receptor 2
hGH	Human growth hormone
HPLC	High performance liquid chromatography
IFN	Interferon
IgG	Immunoglobulin G
Jak	Janus kinase
LCMS	Liquid chromatography/mass spectroscopy
IM	intramuscular, intramuscularly
IV	intravenous, intravenously
kDa	kilodalton
LRP	Living radical polymerization
LS-CPP	Leukemia-specific cell penetrating peptide
lys	lysine
MAb	Monoclonal antibody
MD	Molecular dynamics
MDCK	Madin-Darby Canine Kidney Cells
MDR	Multidrug resistance
MPS	Mononuclear phagocytic system
MUC2	Mucin 2
NES	Nuclear export signal
NLS	Nuclear localization signal
NMP	N-methyl-2-pyrrolidone
NP	Nanoparticle
o/w	oil in water emulsion
PAC	Poly(alkyl-cyano-acrylates)
PCL	Poly(ε-caprolactone)
PDGFR	platelet-derived growth factor receptor
PEG	Polyethylene glycol

PGP	P-glycoprotein
PH	Plekstrin homology domain
Ph+	Philadelphia chromosome
PLA	Poly(lactic acid)
PLGA	Poly(lactic-co-glyclic acid)
PPI	Protein-protein interaction
PTH	Parathyroid hormone
RA	Rheumatoid arthritis
RAFT	Reversible addition fragment transfer
RCM	Ruthenium-catalyzed ring closing metathesis
REAL	Reversible aqueous lipidization
RES	Reticuloendothelial system
RhoGEF	Rho GTPase-specific guanine nucleotide exchange factor
RMSD	Root-mean-square deviation
Rx	Prescription
S/T	Serine/theronine
sCT	Salmon calcitonin
SDS	Sodium dodecyl sulfate
SFK	Src family kinases
SH2	Src homology 2 domain
SH3	Src homology 3 domain
siRNA	small interfering RNA
SL	Sublingual
SLN	Solid lipid nanoparticle
SNAC	n-(8-[2-hydroxylbenzoyl]amino)caprylic acid
SNEDDS	Self-nanoemulsifying drug delivery system
SoS	Son of Sevenless
SubQ	subcutaneous, subcutaneously
TAT	Trans-activating transcriptional activator
TCEP	Tris(2-carboxyethyl)phosphine hydrochloride
TKI	Tyrosine kinase inhibitor
TJ	Tight junction
TMC	Trimethyl chitosan chloride
UAA	Unnatural amino acid
VA044	2,2'-Azobis[2-(2-imidazolin-2-yl)propane]dihydrochloride
w/o	water in oil emulsion
XPB	Xeroderma pigmentosum protein
Y-kinase	Tyrosine kinase
ZOT	Zonula occludens toxin

ACKNOWLEDGMENTS

First, I must thank those who preceded me in the Lim Lab, specifically, those who worked on the CML project. Dr. Andrew Dixon trained me from when I first joined the lab until he left Utah for a postdoctoral position, and again ever since he took his position in Dr. Owen's lab. Importantly, he was the originator of the coiled-coil project, which is the foundation for the work in this dissertation. Dr. Jonathan Constance is always available for my questions, even today when he is a research assistant professor in the Department of Pediatrics. Beyond having the original idea for the stapled peptide project, Dr. David Woessner has continued to help me develop professionally through emails and interactions at scientific meetings. Dr. Geoffrey Miller worked with the Walensky group at Harvard to design the original stapled peptides, and was instrumental in the initiation of this project. Beyond scientific support, he is always available to grab a beer or watch an RSL game when we need a break from the lab.

Of course, none of this would have been possible without the leadership and guidance of Dr. Carol Lim. You cultivate a lab environment in which students truly want to help each other succeed. I don't know of any other lab where the members are so willing to help out not only their fellow lab mates, but graduate students in other labs as well. Of course, this longstanding environment and the generosity of her students made others more willing to help me, both in and outside of the department.

More personally, Dr. Lim treats her graduate students as individuals and uses a variety of

mentoring methods to fit each student's needs. She treated me with a soft hand, often allowing me to make mistakes or learn the error in my thoughts, rather than tell me what to do or why I am wrong. With this, she gave me great freedom to carry out my research as I saw necessary (despite occasional overzealous controls), while simultaneously always being available if I had questions. Despite knowing the complications it would surely entail, Dr. Lim was willing to take me into her lab as a dual PharmD/PhD student. This greatly limited my time in the lab, even keeping me out for a full year during PharmD clinical rotations. I think all of the aforementioned can be boiled down to one sentence: her number one concern is the wellbeing and success of her students.

I would not have been able to enter or complete the dual degree pathway without the financial support of the College of Pharmacy; you removed the major hurdle that could have prevented me from pursuing both clinical and research degrees. In that same vein, I would like to thank both the College of Pharmacy and Department of Pharmaceutics and Pharmaceutical Chemistry for allowing me the flexibility to dual enroll. I would like to thank the American Association of Pharmaceutical Sciences, for awarding me their predoctoral fellowship. Further, support from the University of Utah's Graduate Research Fellowship and HCI Experimental Therapeutics pilot funding 170303 allowed me to continue work on this stapled peptide project after NIH funding (R01 CA129528) had ended. I must also acknowledge the University of Michigan, whose undergraduate Biology program truly prepared me for graduate school.

During my time in the College of Pharmacy, I have been lucky to have many opportunities to work with my fellow student scientists. Lim Lab, p53-group members Mohanad Mossalam, Abood Okal, and Karina Matissek give great scientific feedback,

whether it be on a paper, presentation, or experimental design. Current Lim lab members Phong Lu, Katherine Redd, and Erica Vander Mause continued to help with lab work during the conclusion of my PhD studies, and continue much of the work on various projects started during my tenure in the Lim lab. Owen lab members Sun Jin Kim and Jessica McCombs, Chen lab members Peng Zhao and Peng Wang, you are always willing to discuss a problem I am having, or lend me a reagent I forgot to reorder. Jonathan Falconer helped in running the DLS experiment, and his comedy makes for a great break from the lab, even if we never actually leave. Amanda Smith and Sarah Safran helped me whenever I sporadically needed their scientific advice, or to use a piece of their equipment, and possibly more importantly, also liked to escape to the Utah desert with friends. The size-exclusion chromatography experiment would not have been possible without the help of Zach Cruz and Mark Petersen. It is great to work with a group of students who truly want to help each other.

I would also like to thank the Core facility directors, who were instrumental in this work, from training to experimental troubleshooting. Dr. James Marvin, director of flow cytometry, Dr. Chris Roedesch, Cell Imaging core director, and in particular Dr. Krishna Parsawar, co-director of the mass spectroscopy core. Krishna spent many hours aiding in the design, running, and analysis of all the mass spectroscopy data herein.

The stapled protein study in Chapter 4 would not have been possible without our collaboration with the Chou lab, Biochemistry, and in particular Drs. Chou and Wang. I truly enjoyed this collaboration – our meetings were productive, and by our scientific discussions were able to create, test, and hypothesize efficiently. Further, proteases used for the included studies (HRV3C and TEV) were a kind gift from Katherine Ferrell, of the

Hill lab.

Next, I would like to thank my committee members, Drs. David Grainger, James Herron, Margit Janat-Amsbury, and Shawn Owen, for their scientific input and guidance. In particular, Shawn Owen and I have worked together closely over the past 2 years. Even though I probably ask him on average a question a day, he always makes time to help me. Of course, this would not have been possible without the support of my family. To my parents, Amy and Mike Bruno – not only did you support my love for science from an early age, you've done so in a way that isn't overbearing. You let us kids make our own mistakes, and there were plenty, and I can't thank you enough for that. And to my siblings, Anthony (liquid nitrogen specialist), Katie (on-call editing director), Nick (chief layman consultant), and Maria (AP Biology expert) – thanks for your encouragement, discussions, and your ever willingness to proof read whatever I send you. Also, thanks for all making multiple trips out to Utah, and to all who came to Salt Lake for my graduation, from Chicago, Denver, Iowa, Wyoming, and California. I am lucky to have such a caring, involved family. To my girlfriend Vanja, thank you for your constant support, and for pushing me when I became jaded about science.

While I always appreciated the help others are willing to give me, I didn't realize how many people helped me complete this degree until I began to write these acknowledgements. After reading this section, it is clear to me that I could never have finished the PhD without the help and support of dozens of people, from all walks of life. Thank you all!

CHAPTER 1

BACKGROUND AND SIGNIFICANCE

Summary

Chronic myeloid leukemia (CML) is caused by the oncoprotein Bcr-Abl, created by a reciprocal chromosomal translocation resulting in a truncated chromosome 22, known as the Philadelphia chromosome (Ph). The fusion protein Bcr-Abl activates numerous oncogenic signaling pathways through a constitutively active tyrosine kinase (TK) domain, resulting in cell growth and survival. Conventional therapies target this TK domain, inhibiting the kinase activity and subsequent downstream signaling. While these 'tyrosine kinase inhibitors' (TKIs) have converted CML from a deadly cancer to a chronic condition, mutations in the TK domain often leave these TKIs ineffective. Second and third generation TKIs have been developed to treat those with mutated Bcr-Abl, but off-target effects limit their use. Another class of resistance, known as Bcr-Abl-independent resistance, appears in the absence of TK domain mutations, and is especially difficult to treat.

Bcr-Abl oligomerization through an N-terminal coiled-coil (CC) domain is a prerequisite to the aberrant kinase activity of Bcr-Abl. Indeed, previous work has shown that removing this oligomerization domain abolishes the oncogenic activity of Bcr-Abl. Previous work in the lab focused on creating a mutated version of this CC (known as

CC^{mut}), which would preferentially bind the CC in Bcr-Abl while avoiding homo-oligomerization. This CC^{mut} was effective against both wild-type and clinically-relevant Bcr-Abl mutants. However, this work was all performed using gene delivery (transfection, lentiviral infection). Chapters 2-5 focus on translating CC^{mut3} into a deliverable, biologically stable protein, utilizing cell-penetrating peptides (Chapters 2 and 3) and peptide/protein stapling (Chapters 2, 4, and 5).

Background

The Breakpoint Cluster Region

The breakpoint cluster region gene (BCR) is located on the long arm of chromosome 22, specifically 22q11. While the Bcr protein is involved in development, its functions in adult organisms are unclear. For instance, BCR-knockout mice develop with only mild cognitive impairment and neutrophil development [1, 2]. In adults, Bcr protein levels are highest in the brain and hematopoietic cells, specifically during the early stages of myeloid differentiation [3]. Bcr and homologous protein Abr are now believed to play a role in cell polarity, inflammation, memory, and may even be involved in bipolar disorder [4-7].

The ubiquitously expressed Bcr protein is almost entirely cytoplasmic, and is involved in G protein signal transduction pathways, trafficking of growth factors, and mediating transcription through peroxisome-proliferator-activated receptor gamma [1, 3, 4]. Specifically, the C-terminal region of the Bcr protein activates guanosine triphosphate hydrolyzing enzymes (GTPases), also known as GTPase-activating proteins (GAPs) (Figure 1.1) [3, 8]. Bcr accelerates the GTPase activity of RAC1, a family of proteins that

link extracellular signals to cellular responses, including cytoskeletal reorganization and subsequent membrane ruffling [3]. RAC1 binding to Bcr and subsequent activation requires the GAP domain of Bcr first bind GTP [9]. While this region is important in the endogenous activity of Bcr, the RAC-GAP domain is lost upon recombination with the ABL1 gene [10]. Bcr also associates with the xeroderma pigmentosum protein (XPB) via its DH/PH domain (Figure 1.1), which is involved in DNA repair, cell cycle regulation, and the initiation of transcription [3].

The BCR gene contains 23 exons, and its transcripts are either 4.5 or 7.0 kilobases (kb) in length [3]. The 5' untranslated region (5' UTR) containing the transcription regulatory regions are important, as this same region will control the transcription of the fusion gene BCR-ABL1 [3]. The two resulting proteins are 130 and 160 kilodaltons (kDa), respectively, with the 130kDa protein being primarily nuclear, and the 160 kDa protein cytoplasmic [3].

Structurally, the Bcr protein contains a number of domains, including N-terminal oligomerization domain, serine/threonine kinase domain, Src homology (SH2) binding domain, Dbl homology domain (DH), Pleckstrin homology domain (PH), also known as the Rho GTPase-specific guanine nucleotide exchange factor (RhoGEF) (Figure 1.1) [3]. At the N-terminus of the protein is a coiled-coil (CC) oligomerization domain, which interacts with F-actin and is thought to be required for the cytoplasmic location of Bcr and the fusion protein Bcr-Abl [3, 11]. This will be discussed in detail later in this chapter, as will the activity of the DH/PH domain. The serine/threonine kinase domain can both auto- and trans-autophosphorylate Bcr proteins [3, 12]. Trans- or autophosphorylation of Y-177

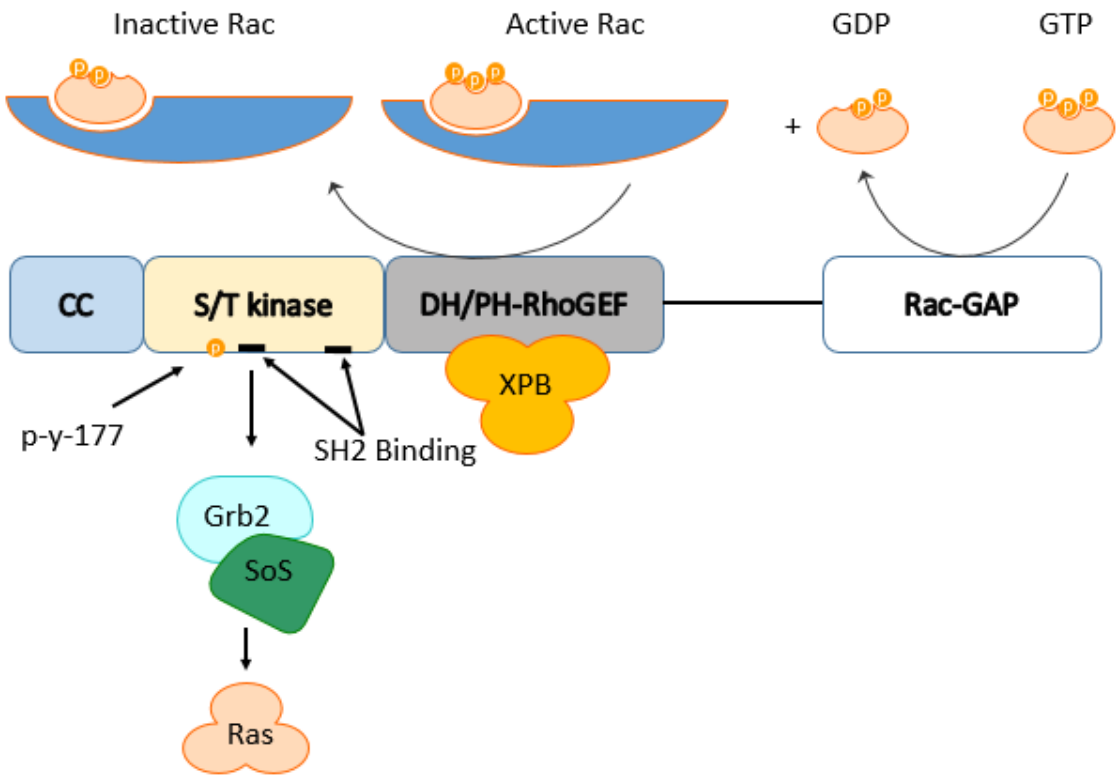

Figure 1.1 Bcr protein domains and select functions. Starting with the N-terminus, domains include the coiled-coil (CC) oligomerization domain, serine/threonine kinase domain, DH/PH and RhoGEF domains, and finally the Rac-GAP domain. Phosphorylation of the serine/threonine kinase domain at tyrosine-177 allows binding of the adaptor protein Grb2 (via SH2 domains) and subsequent Ras signaling. The DH/PH domain binds the xeroderma pigmentosum protein (XPB), which is involved in transcription initiation and DNA repair. Finally, the RhoGEF and Rac-GAP domains work together to inactivate Rac. Abbreviations: CC, coiled-coil; S/T, serine/threonine; DH/PH, Dbl homolgiy/Pl; GEF, GTPase-specific guanine nucleotide exchange factor; GAP, GTPase-activating protein; SH2, Src homology domain 2; SoS, Sons of Sevenless; XPB, xeroderma pigmentosum protein.

in the SH2 binding domain permits Bcr to interact with the adapter protein Grb2 which subsequently binds Son of Sevenless (SoS), resulting in increased Ras signaling [3, 13]. SH2 binding domains are highly conserved sequences of approximately 100 amino acids that bear no catalytic activity [3]. The SH2 binding domains of Bcr are different from other SH2 domains in that those in Bcr can bind SH2 binding sites with phospho-serine and phospho-threonine, as well as the standard phospho-tyrosines [3]. The Rac-GAP domain is important in the negative regulation of Rac and Cdc42, and along with the RhoGEF domain converts Rac from the active (Rac-GTP) to inactive (Rac-GDP) form [9]. Loss of Bcr Rac-GAP function in vivo results in severe inflammatory response to lipopolysaccharides as well as increased ROS production by neutrophils innate immune responses in mice, [14] while in vitro experiments noted increased actin reorganization and membrane ruffling [15].

Abelson Tyrosine-Protein Kinase 1 (ABL1)

Cellular Abelson protein tyrosine kinase (c-Abl) is encoded by the ABL1 gene, closely related to the Src family of kinases [16]. Located on the long arm of chromosome 9 (9q34) [3], this 140 kDa ubiquitously-expressed nonreceptor tyrosine kinase is found both in the cytoplasm and nucleus, as it often shuttles between the two compartments via myristoylation and regulation of its nuclear localization (NLS) and nuclear export signals (NES) [2, 17-19]. Unlike BCR1 knockouts, ABL1 knockouts clearly suffer developmental anomalies; these mice have increased perinatal mortality, lower birth weight, deficient bone and leukocyte development, and suffer from abnormal head and eye development [2, 17, 20].

Cytoplasmic c-Abl is commonly activated by numerous surface receptors, including platelet-derived growth factors receptors (PDGFR), cadherins, neurotrophin receptors, and other ligand-gated ion channels [17]. Nuclear c-Abl is involved in a myriad of proapoptotic functions. When in the nucleus, c-Abl is involved in responses to genotoxic stress and cell cycle progression [17]. Specifically, DNA damage activates c-Abl, which in turn regulates the PI3K-related proteins ATM and ATR and their substrates Chk1 and Chk2 [21], resulting in cell cycle arrest, DNA repair, or apoptosis [22]. Additionally, c-Abl is known to be involved in the regulation of caspase cleavage, a key stage of apoptosis induction [23]. The stark differences between pro-apoptotic c-Abl and antiapoptotic Bcr-Abl will be discussed in the next section.

The kinase activity of c-Abl is negatively regulated by myristoylation of its N-terminal 'cap' region [16] (Figure 1.2B). Upon myristoylation, this cap is buried in the kinase domain, thus inhibiting kinase activity [19]. Further, this causes the SH2 and SH3 domains of c-Abl to form an inhibitory scaffold that holds the protein in this inactive state [17]. This regulatory cap is lost upon fusing with BCR1 (Figure 1.2 A and C), and is generally responsible for the increased kinase activity of Bcr-Abl compared to that of c-Abl (discussed in detail in the next section) [19]. It is likely that ligand binding to the SH2/SH3 domains releases them from their inhibitory binding state, but further tyrosine phosphorylation of c-Abl (including, but not limited to Y412) is necessary for its kinase activity [17]. When unbound, the SH2 and SH3 domains are free to bind cell surface receptors, which regulate c-Abl activity [17].

C-terminal to the SH2 domain is the tyrosine kinase domain and active site (Figure 1.2B). The center of the protein contains a DNA-binding domain interacts preferentially

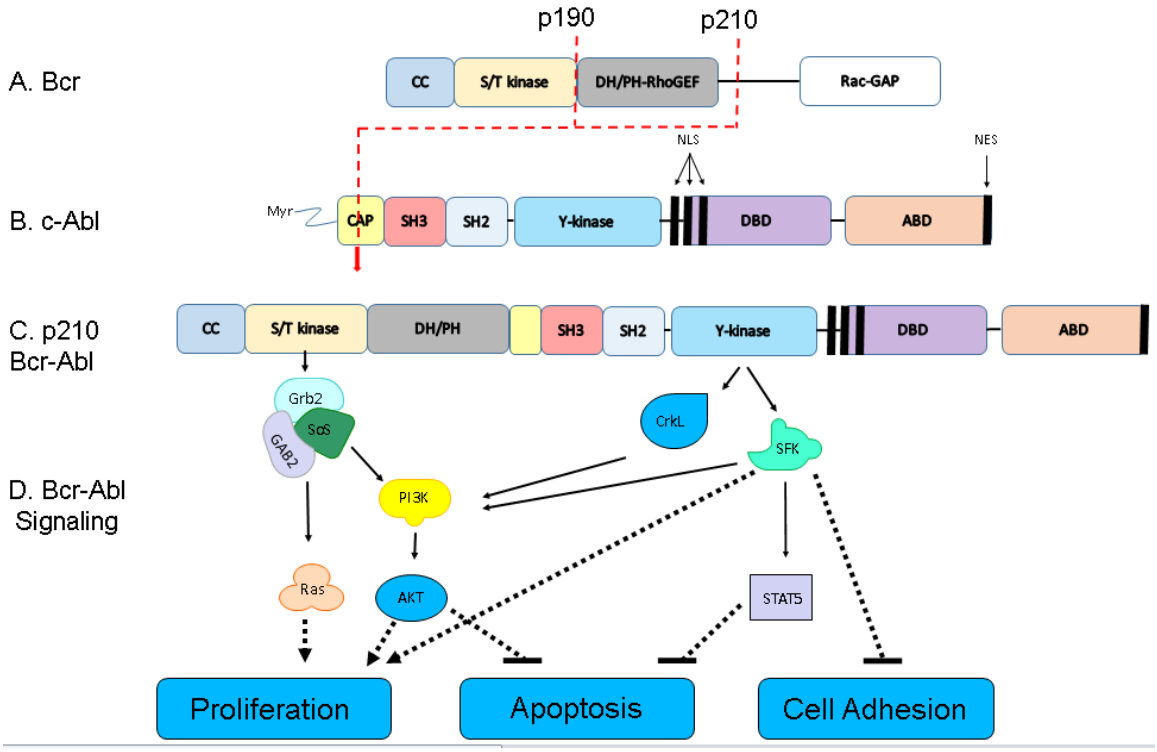

Figure 1.2: Bcr-Abl domains and signaling. A) Bcr protein domains. B) c-Abl protein domains. The dotted red line represents the location of the reciprocal translocation between chromosomes 9 and 22, which results in the creation of C) Bcr-Abl. D) downstream signaling of Bcr-Abl. Dashed lines represent indirect interactions.
Abbreviations: CC, coiled-coil; S/T, serine/threonine; DH/PH, Dbl homolgiy/Pl; GEF, GTPase-specific guanine nucleotide exchange factor; GAP, GTPase-activating protein; SH, Src Homology domain; Y-kinase, tyrosine kinase; NLS, nuclear localization signal; DBD, DNA binding domain; ABD, actin binding domain; NES, nuclear export signal; SoS, Son of Sevenless; SFK, Src family kinases

with deformed DNA in a sequence-dependent manner [24]. Finally, the C-terminus contains an F-actin binding domain for direct binding the cytoskeleton, which is uncommon in tyrosine kinases [17]. Binding interactions between c-Abl and F-actin/microtubules may also partially regulate c-Abl activity [17]. See Figure 1.2 B for domain positions in c-Abl.

Bcr-Abl

A head-to-tail reciprocal translocation between BCR and ABL1 on chromosomes 22 and 9, t(9;22)[q34.1;q11.21] creates the fusion gene BCR-ABL1, which encodes for the Bcr-Abl protein, responsible for chronic myeloid leukemia (CML) (Figure 1.2C) [3]. The result, a truncated chromosome 22 known as the 'Philadelphia chromosome' (Ph), was first discovered and associated with CML in 1960[25], and a more precise understanding of the reciprocal translocation was published by Janet Rowley in 1973 [26]. However, it was not until 1990 that studies confirmed Ph is the causative agent of CML [27, 28]. Bcr-Abl is now known to be necessary and sufficient to cause CML. That is, the expression of Bcr-Abl in normal hematopoietic stem cells is sufficient to induce a CML phenotype [27, 28]. While this work is primarily concerned with Bcr-Abl as it relates to CML it is important to note that 20% of adult and 5% of pediatric acute lymphoblastic leukemias (ALL) are Ph+ [3].

The translocation sites of both BCR and ABL1 contain the Alu transposable repeat sequence, the sites of translocation. Chromosomes 9 and 22 are in close proximity during the S to G2 transition, which is likely partially responsible for the increased frequency of this specific translocation event [3]. While the break occurs in only one region in ABL1

(C-terminal of the cap), BCR has two known break points. Therefore, the Bcr-Abl protein is typically 190 or 210 kDa, depending on the site of recombination in Bcr [3]. While p210 is typically seen in CML, p190 Bcr-Abl is more common in acute leukemias and is generally more active than p210 Bcr-Abl [3]. In both cases, the resulting proteins contain the N-terminal oligomerization domain of Bcr and have constitutive tyrosine kinase activity (Figure 1.2D) [3].

The Bcr-Abl fusion protein contains most of the same domains present in both Bcr and c-Abl, but the C-terminus of Bcr and the N-terminus of Abl is lost (Figure 1.2). The N-terminus of c-Abl plays a key role in tyrosine kinase autoregulation, and its loss is partially responsible for the constitutive tyrosine kinase activity of Bcr-Abl [25]. While c-Abl is primarily a nuclear protein, the fusion protein Bcr-Abl is wholly cytoplasmic [29]. The N-terminus of Bcr-Abl includes the coiled-coil (CC) oligomerization domain, which is the major target throughout this dissertation [25]. Next is the serine/threonine kinase domain (discussed earlier), as well as the Dbl homology/Pleckstrin homology (DH/PH) domain. While the DH/PH domain is present in p210 Bcr-Abl, its absence in p190 Bcr-Abl suggests it plays a role in cellular adhesion, as its absence results in the release of immature lymphocytes from bone marrow [3, 30].

Following the breakpoint are the SH2 and SH3 domains of c-Abl (Figure 1.2c). C-terminal to the SH2 domain is the tyrosine kinase of c-Abl. Beyond the loss of inhibition caused by deletion of the regulatory cap of c-Abl, Bcr-Abl dimerization and subsequent tetramerization further increases the kinase activity. While the CC domain will be discussed in detail later, the following is a brief overview. The N-terminal CC domain enables antiparallel dimerization of 2 Bcr-Abl proteins, which is then followed by the

tetramer formation of a dimer of dimers [31, 32]. This orientation allows for the transautophosphorylation of tyrosine residues in the Bcr and c-Abl portions of the protein [17, 33]. Both the altered location of c-Abl and its tyrosine kinase activity are responsible for the oncogenic activity of Bcr-Abl [29]. The downstream targets of Bcr-Abl are discussed in the next section.

Downstream Targets of Bcr-Abl

The cytoplasmic nature of the fusion protein Bcr-Abl allows it to bind with many proteins not normally recognized by the primarily-nuclear c-Abl. Bcr-Abl requires phosphorylation of Y245 and Y412 for kinase activity [34]. While c-Abl contains the constitutively active tyrosine kinase, much of this kinase activity is targeted towards Bcr [35]. As stated above, phosphorylation Y177 in Bcr creates a Grb2 binding site. This adapter protein is the base of a protein complex including Bcr-Abl, Grb2, GAB2, and SoS [36]. This complex in turn activates many antiapoptotic, progrowth, and prosurvival pathways and proteins, including Ras, AKT, Janus kinase (JAK2 and 1), STAT5/3 and PI3K (Figure 1.2D) [36]. Although the relative importance of each of these pathways to Bcr-Abl oncogenesis is unclear, Ras signaling is a prerequisite to Bcr-Abl-mediated, growth-factor-independent growth and survival [3, 19]. Further, the transcription factor STAT5 is necessary for both initiation and maintenance of oncogenesis in CML, and its activation is mediated via kinase activation of src family kinases (SFC) [19]. Bcr-Abl positive cells have also been shown to have increased levels of the antiapoptotic proteins Bcl-2 and phospho-BAD [3]. Taken together, alterations in these proteins/pathways result in decreased cell adhesion, increased mobility, decreased apoptosis, and increased cell

proliferation [3, 25, 37]. Next, the disease caused by Bcr-Abl – chronic myeloid leukemia—will be discussed.

Chronic Myeloid Leukemia

CML is generally considered a triphasic disease: chronic phase, accelerated phase, and blast crisis. Today, approximately 90% of patients who are diagnosed with CML are in the chronic phase [38]. Patients diagnosed in chronic phase typically present with vague symptoms, such as fatigue, weight loss, abnormal bleeding, splenomegalay, and/or leukocytosis [39]. Diagnosis is confirmed by cytogenic analysis and the presence of the Ph chromosome [38]. The chronic phase is defined by the presence of <10% blastic cells in the peripheral blood or bone marrow [38]. If left untreated, patients will progress into the accelerated disease phase within 2 years, and then rapidly move into the fatal blast crisis [40]. Patients in the accelerated phase have increased basophils and blastic cells in peripheral blood, as well as persistent splenomegaly [38]. Finally, blast crisis is defined by an increase number of blasts (>30%) in bone marrow and extramedullary disease, with typical sites including bone, lymph nodes, skin, and soft tissue [38]. The molecular mechanisms of progression are not fully understood, but are thought to involve genetic instability of Ph+ cells, resulting in gene duplications, mutations, and rearrangements, many of which affect p53 or retinoblastoma (Rb) pathways [41, 42].

An estimated 70,000 people live with CML in the United states [43], with over 8,000 new cases estimated for 2016. [43]. While the median age at diagnosis is 64, 10% of patients are diagnosed before the age of 35, and 35% are diagnosed before 55 [43]. Due almost entirely to the development of tyrosine kinase inhibitors (TKIs) (discussed in the

next section), the 5-year survival rate went from just above 30% in the 1990s to 63% in 2015 [43].

Treatment

Although CML was first characterized in 1845, the first breakthrough TKI was not approved until 2001 [25]. Prior to this, nonspecific anticancer drugs such as the alkylating agent busulfan or the ribonucleotide reductase inhibitor hydroxyurea were given to patients [44]. Hydroxyurea was shown to increase overall survival (OS) compared to either busulfan or placebo, while busulfan showed no improvement in OS compared to placebo controls [44, 45]. Allogenic bone marrow transplant (BMT) was the treatment of choice for healthy individuals, and it is still the only curative treatment for CML [46]. However, due to the risks, today BMT is reserved for patients refractory to TKI therapy [46].

Interferon α, first used to treat myeloid malignancies in the 1970s, was another popular therapy before the development of TKIs [47]. Although it was used extensively throughout the 80s and 90s, it was only approved as a first-line agent for CML in 1995 [47]. Interferon α2A demonstrated increased OS and event-free survival over both busulfan and hydroxyurea [47]. However, adverse effects associated with interferon, such as severe fatigue, neurotoxicity, and liver function abnormalities, curbed its use [47]. This was partially overcome by PEGylated versions of interferon α (Pegasys®, and PegIntron®) which are better tolerated than naked interferon α. Interferon α has many mechanisms of action, and the individual importance of any one of these is unclear [47]. Broadly, interferon α can induce apoptosis through Jak/STAT pathway, arrest cells in G1, suppress angiogenesis, activate immune effector cells, suppress hematopoiesis, and increase cell

adhesion [47]. While largely replaced by TKIs, interferon α is being investigated in combination with these TKIs, as the combination has the potential to cure a subset of patients [47, 48].

Omacetaxine (Synribo®), a protein translation inhibitor, was approved in 2012 for use in refractory CML. While omacetaxine has been shown to marginally benefit those with refractory CML (including those with T315I), the ubiquitous nature of serious adverse events (seen in 99% of patients) curtails its use [49].

Tyrosine Kinase Inhibitors

The breakthrough drug imatinib (Gleevec®), approved in 2001, selectively inhibits the tyrosine kinase of c-Abl and Bcr-Abl [47]. Originally identified in a screen for inhibitors of protein kinase C, whose catalytic site closely resembles that of c-Abl [26], the molecule was then modified to 1) abolish PKC inhibition while maintaining Bcr-Abl inhibition, and 2) improve aqueous solubility and bioavailability [26]. Imatinib is known to interact with the nucleotide binding site of Abl when it is in the inactive, closed formation [26, 50, 51]. In vitro, imatinib inhibits Bcr-Abl autophosphorylation as well as phosphorylation of downstream targets at submicromolar doses [47]. Once shown superior to interferon α in the IRES trial, imatinib was approved and quickly became the first-line therapy of choice [47, 50].

While treatment with imatinib is typically initially effective, resistance may develop, leaving patients in need of alternative therapies. Various mechanisms of resistance will be discussed in the next section, but briefly, it is common that mutations in/near the Abl tyrosine kinase domain can preclude drug binding while leaving the

catalytic activity of the pocket unaltered [51]. For this reason, the second generation TKIs nilotinib (Tasigna®) and dasatinib (Sprycel®) were developed. Nilotinib is based on the imatinib structure, but was designed to be a more potent inhibitor [51]. Dasatinib, originally designed to inhibit Src kinases, is a competitive inhibitor of the ATP binding site, and thus binds Bcr-Abl in the *active* conformation [52, 53]. While these two drugs did much to help those with imatinib-resistant CML, further Bcr-Abl kinase domain mutations often develop, leaving these second generation drugs ineffective, especially against T315I mutants and compound mutants [54]. Bosutinib, another dual Src/Abl1 kinase inhibitor, which binds to Bcr-Abl in a unique manner, has different resistance profiles from all of the previous three TKIs [55]. Ponatinib (Tasigna®) was developed specifically to target the T315I 'gatekeeper' mutation [55]. This mutation both disrupts hydrogen binding of the TKI, and also biases the kinase towards the active state [55]. However, the modifications that allow ponatinib to inhibit T315I Bcr-Abl also cause it to inhibit multiple off-target kinases, such as those in the hedgehog pathways, GFGP, and Src-family kinases [51]. Indeed, ponatinib was temporarily removed from the market due to unacceptable, serious cardiovascular events, likely linked to the nonspecific nature of ponatinib, and has a black box warning [52]. Due to the clonal nature of CML, many researchers believe resistance to all TKIs is inevitable [56] Table 1.1 shows the different TKIs and efficacy against Bcr-Abl tyrosine kinase domain mutations [52, 57, 58].

Nilotinib, dasatinib, and imatinib are now all approved as first-line therapy, leaving clinicians with much to consider. The second-generation drugs produce higher molecular and cellular responses compared to imatinib, but none has shown superior long-term survival [59]. These drugs are generally well tolerated, but they are not without their

Table 1.1 Bcr-Abl mutations and clinical effectiveness of approved TKIs. Warm colors (green) represent sensitivity to the particular TKI, while cold colors (red) denote TKI resistance.

Single Mutants

	imatinib	nilotinib	dasatinib	ponatinib	bosutinib
M244V					
G250E					
Q252H					
Y253H					
E255V					
V299L					
F311I					
T315I					
T315M					
F317L					
M351T					
F359C					
H396R					

Compound mutants with T315I

	imatinib	nilotinib	dasatinib	ponatinib	bosutinib
M244V					
G250E					
Q252H					
Y253H					
E255V					
F311I					
M351T					
F359V					
H396R					
E453K					

Non-T315I Compound mutants

	imatinib	nilotinib	dasatinib	ponatinib	bosutinib
G250E/V299L					
Y253H/E255V					
Y253H/F317L					
E255V/V299L					
V299L/F317L					
V299L/M351T					
V299L/F359V					
F317L/F359V					

adverse events. Indeed, in the initial phase III trial of imatinib, 14.3% of patients discontinued therapy due to adverse drug events [60]. Each TKI has its own unique side effect profile (Table 1.2), and this information is commonly used when starting/changing a patient's TKI [52, 61].

Allosteric Inhibitor

ABL001, currently in clinical trials, binds the pocket in c-Abl normally filled by its own myristoylated N-terminal cap [62]. This causes a conformational change, ablating the Y-kinase activity of c-Abl. In vitro and in vivo, ABL001 is effective against nearly all tested tyrosine kinase mutations, including T315I. However, mutations that preclude ABL001 from binding Bcr-Abl have been discovered. Mice treated with ABL001 alone had complete tumor regression, but relapsed within 60 days of the termination of treatment. However, mice treated with the combination of nilotinib and ABL001 showed no signs of disease relapse, up to 150 days after the end of treatment, thus suggesting these two drugs may be used synergistically (as in this ongoing clinical trial) [62]. Serious ADEs include anemia, neutropenia, and increased lipases, which caused 10% of patients in the phase 1 trial to discontinue therapy (ref). Overall, ABL001 is a promising new therapeutic, although its place in therapy is yet to be determined.

Resistance

It is estimated that up to 1/3 of patients who start on imatinib will not achieve their therapeutic goals, known as 'primary resistance' [63]. However, point mutations were identified in less than half of patients who are nonresponsive to imatinib [64]. This

Table 1.2 Approved TKIs and corresponding adverse reaction profile

Drug Name	Adverse Reactions/Toxicity
imatinib	**Rash, decreased LVEF, CHF, arterial thrombotic events, noninfectious pneumonitis/diffuse alveolar damage/pulmonary fibrosis, mucositis/stomatitis, diarrhea/colitis, neutropenia, thrombocytopenia, transaminase elevations, hyperlipasemia, hypophosphatemia**
nilotinib	**Rash, decreased LVEF, CHF, QT prolongation, arterial thrombotic events, diarrhea/colitis, hyperglycemia, neutropenia, thrombocytopenia, transaminase elevations, hyperlipasemia, hypophosphatemia** **BBW: Life-threatening heart problems, sudden death**
dasatinib	**Rash, decreased LVEF, CHF, QT prolongation, arterial thrombotic events, noninfectious pneumonitis/diffuse alveolar damage/pulmonary fibrosis, pulmonary arterial hypertension, diarrhea/colitis, neutropenia, thrombocytopenia, transaminase elevations, hypophosphatemia**
ponatinib	**Hypertension, peripheral edema, CHF, arterial ischemia, hypophosphatemia, gastrointestinal hemorrhage, neutropenia, leukopenia, thrombocytopenia, anemia, neutropenic fever, hemorrhage, ALT/AST increased, myalgia, peripheral neuropathy, pleural effusion, respiratory tract infection, sepsis** **BBW: Life-threatening blood clots and narrowing of blood vessels**
bosutinib	**Rash, decreased LVEF, CHF, QT prolongation, arterial thrombotic events, diarrhea/colitis, neutropenia, thrombocytopenia, transaminase elevations, hyperlipasemia, hypophosphatemia**

anomalous result is explained by the existence of two types of TKI-resistance – Bcr-Abl-dependent, and Bcr-Abl independent.

Bcr-Abl dependent resistance usually involves a point mutation(s) in the c-Abl portion of Bcr-Abl, specifically in the P-loop, C-helix, SH2 domain, substrate binding site, A-loop, or C-terminal lobe [50]. These mutations interfere with the binding of the TKI, leaving the tyrosine kinase in Bcr-Abl constitutively active [50]. Other mutations may prevent Bcr-Abl from entering its inactive conformation, thus precluding imatinib and nilotinib binding [50]. 'Secondary resistance' occurs when a patient initially responded to a TKI, but the drug has since become ineffective [64]. In these cases, patients are screened for common Bcr-Abl point mutations, and changed to a TKI that is effective against their specific mutation [64]. Ponatinib, the third generation TKI, is effective against most single point mutations, including the gatekeeper T315I [52]. However, even ponatinib is not universally effective against Bcr-Abl mutants, as it has decreased efficacy against the E255V and many T315-containing compound mutants, such as E255V/T315I [52, 61].

Eleven percent of patients who fail TKI therapy have 2 or more mutations in the kinase domain, known as double mutants [52]. There are two types of double mutants – compound and polyclonal mutants [52]. In compound mutants, there are 2 separate mutations in one Bcr-Abl gene. Patients with polyclonal mutations, on the other hand, have 2 different point mutations in 2 different Bcr-Abl genes, either in the same (duplication event) or different cells [52]. Of patients with double mutants, approximately 70% are compound, and 30% are polyclonal [65]. Bcr-Abl duplication has also been correlated with TKI resistance and disease progression, and the duplication may lead to rapid Bcr-Abl mutation [66]. Further, multiple copies of Bcr-Abl are indicative of a poor

prognosis, even in the absence of mutations in the drug binding site [66].

If a TKI is ineffective despite the absence of point mutations, the patient is said to have 'Bcr-Abl independent" resistance [67]. While this is a complicated and progressing area of research, a brief overview of the topic will give the reader the information needed for the remainder of this dissertation. Bcr-Abl independent resistance has been associated with genetic variabilities in drug import and efflux [67-69], low trough drug concentrations [50], epigenetic modifications/upregulation of HDACs [50, 70], growth factors in the bone marrow sustaining CML stem cells [51], and the activation of alternative signaling pathways [50]. Stat3 has recently been implemented as a key mediator of Bcr-Abl independent resistance, and the Deininger group has successfully screened and tested a Stat3 inhibitor + imatinib, a combination that is synthetically lethal to CML progenitor cells that display Bcr-Abl independent resistance [71, 72].

The Coiled-Coil

While TKIs target the kinase domain of the Abl portion of Bcr-Abl, the N-terminal coiled-coil domain is also of therapeutic interest. The coiled-coil (CC) located at the N-terminus of Bcr-Abl acts as an oligomerization domain; specifically, a teteramer of Bcr-Abl proteins is formed through a dimer of antiparallel dimers (Figure 1.3) [31]. Bcr-Abl proteins lacking this CC domain are unable to induce CML in murine models [73, 74]. A brief overview of CCs will give the reader the background needed for an understanding of the experimental works discussed in Chapters 3 and 4.

Coiled-coils are a universal protein structure that commonly mediate protein homo- and heterooligomerization [75]. CCs are present in approximately 10% of all eukaryotic

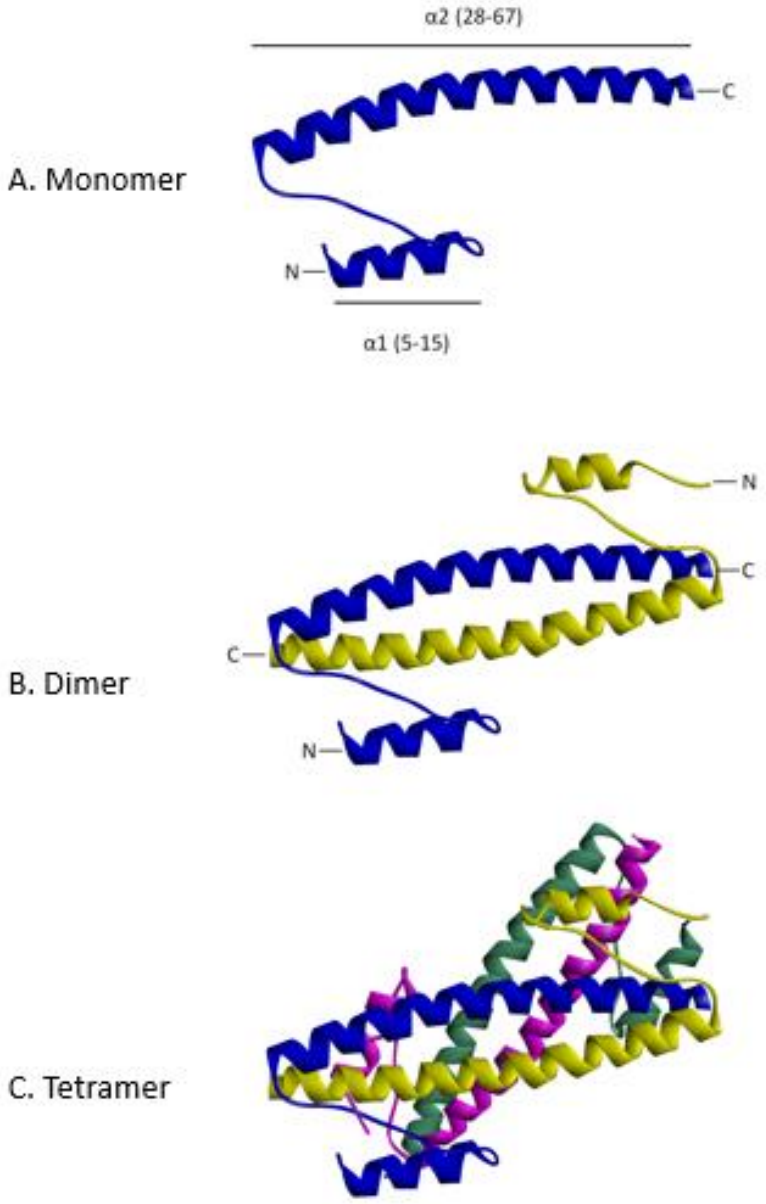

Figure 1.3 Bcr-Abl coiled-coil oligomerization. A) The N-terminal coiled-coil of Bcr and Bcr-Abl consists of 2 α-helices; amino acids 5-15 make up the shorter helix 1, while helix 2 consists of residues 28-67. The coiled-coil can form an antiparallel homodimer (B) and subsequently a tetramer (C), via dimerization of dimers. Diagrams were generated with Discovery Suites with Bcr coiled-coil domain crystal structure (PDB ID: 1K1F).

proteins [31], and it is estimated that 2-5% of all protein residues form CCs [75, 76]. CCs are characterized by 2-5 alpha helices that oligomerize to form a supercoil [31, 75]. The more common left-handed coiled coils generally contain a heptad repeat, HXXHCXC, with H being hydrophobic amino acids (isoleucine, leucine or valine most commonly), C being charged amino acids [31, 75]. Each heptad makes up two turns of the alpha helix, that is, there are 3.5 residues per turn [31, 77]. Coiled-coil oligomerization is driven by hydrophobic interactions, salt bridge formation, and helicity. The hydrophobic residues thermodynamically drive the association of coiled-coils in aqueous environment, with the hydrophobic residues being buried at the interface of the two alpha helices [31, 75, 78]. The charged residues increase complex stability by forming interhelical salt bridges [31].

The CC of Bcr is a 72-amino acid sequence that encodes for two parallel alpha helixes connected by a short linker (Figure 1.3A) [79]. The shorter of the two, helix 1, is near the N-terminus of the protein, composed of aa 5-15. Helix 1 and 2 are connected by a short, flexible linker that allows helix 2 to orient itself parallel to helix 1. The longer helix 2 (aa 28-67) is the major dimerization interface. While the two helices of one Bcr-Abl molecule are oriented parallel, dimerization of two Bcr helix 2s is antiparallel (Figure 1.3B). Helix 1 can wrap around the backside of helix 2, participate in aromatic stacking, and thereby further stabilize the dimer [79]. The coiled coil can then proceed to form a tetramer from two CC dimers (Figure 1.3C). Studies have shown that the CC is required for the oncogenesis of Bcr-Abl; dimerization/tetramerization is a prerequisite to trans autophosphorylation [32].

With this knowledge, the Ruthardt group set out to competitively interfere with Bcr-Abl dimerization by introducing excess copies of the CC into CML cells, with

marginal success [80, 81]. Dr. Andrew Dixon, a graduate from the Lim Lab, pioneered an improvement on this work in combination with Dr. Scott Pendley and Dr. Thomas Cheatham. The antiparallel nature of the dimerization interface allowed for the rational design of a mimetic of Bcr CC that preferentially binds to the CC of Bcr-Abl (and Bcr) while avoiding homodimerization with itself [31]. Careful study of the dimerization interface led Dixon to propose the mutations of CC residues to create CC^{mut2}, which preferentially bound to the wild-type CC (CC^{wt}) of Bcr-Abl, while minimally autodimerizing [31]. The 5 mutations proposed by Dixon were C38A, S41R, L45D, E48R, and Q60E. The mutations S41R and Q60E provides for 2 additional salt bridges between CCwt:CC^{mut3}, L45D and E48R destabilized the mutant homodimer, and C38A was incorporated for crystallographic concerns [31].

This hypothesis was born out by computational modelling in the Cheatham group, and supported by in vitro work, performed by transfecting a gene encoding for CC^{mut2} [31]. CC^{mut2} reduced the transformative ability and induced apoptosis of Bcr-Abl+ (but not negative) cells, and decreased phosphorylation of Bcr-Abl and downstream targets Stat5 and CrkL [31]. An additional mutation, K39E, was proposed to decrease homodimerization of the mutant CC by creating an additional charge-charge repulsion with E60 of the mutant CC, but not the Q60 in CC^{wt} (Figure 1.4A). While decreased homodimerization was supported by in silico modeling and a mammalian two-hybrid assay (1.4b), the new CC^{mut3} was not statistically superior in biologic assays [82]. However, subsequent work utilized CC^{mut3} due to its increased in vitro binding to CC^{wt}.

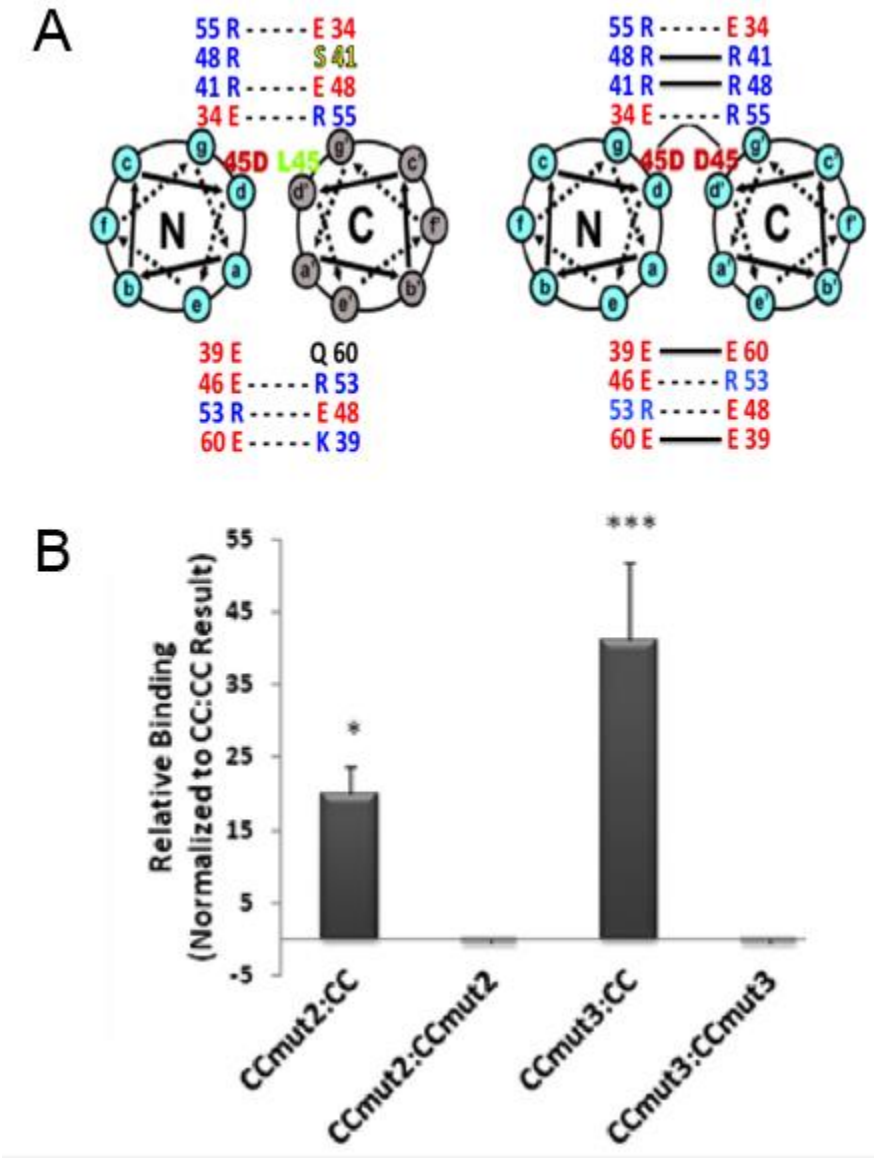

Figure 1.4: CC^{mut3} dimerization with CC^{wt}. A) Helical wheel diagram displaying interactions between CC^{mut3}:CC^{wt}(left) and CC^{mut3}:CC^{mut3} (right)**.** Above and below the helical wheels are individual residues from each domain. Side chains of those residues are color-coded as follows: blue = basic, red = acidic, yellow = serine. Potential ionic interactions are shown with the *dotted lines*, whereas potential charge-charge repulsions are shown with a *solid line*. B) A mammalian two-hybrid assay suggests CC^{mut3} is a stronger binder of CC^{wt} than CC^{mut2}. This figure was adapted from Dixon, Miller et al. (2012).

Statement of Objectives

The shortcomings of currently approved (and future) TKIs necessitate the development of CML therapeutics that target domains other than the tyrosine kinase. The original design and optimization of our oligomerization inhibitor (CC^{mut3}) has been performed. The overall goal of the work in the following studies is to translate the successes seen with gene delivery of CC^{mut} into a clinically-relevant protein therapeutic for CML. Towards this goal, we cloned and purified CC^{mut3} protein with an N-terminal cell-penetrating peptide. This improved the cell permeability and selective delivery of CC^{mut3} to leukemic cells.

The protein we have designed is specific to Bcr-Abl; we expect minimal off-target effects. Further, the dimerization interface has many more contacts than do TKIs with the TK pocket in Bcr-Abl. Therefore, we believe resistance to CCmut would be less likely than what is seen with TKIs. Further, as we are targeting a dimerization interface, it is likely that any mutations in the CC of Bcr-Abl that abrogated CCmut binding would also likely prevent Bcr-Abl CC:CC dimerization, resulting in 'auto-inactivation' of Bcr-Abl. This strategy could therefore result in a therapeutic with greater long-term efficacy and pan-activity against Bcr-Abl mutants.

Research Aims

Research Aim 1

CC^{mut3} was previously delivered via gene delivery, which is not practical for the clinical treatment of CML. Therefore, a CC^{mut3} protein will be purified. An N-terminal cell-penetrating peptide will be included to improve cell penetration.

Research Aim 2

Delivery of the protein CC^{mut3} to leukemia cells will be accomplished by the use of a leukemia-specific cell-penetrating peptide (LS-CPP). Further LS-CPP-CC^{mut3} will induce apoptosis in Bcr-Abl+ cell lines, while being nontoxic to Bcr-Abl- leukemia cell lines.

Research Aim 3

In vivo proteolysis of CPP-CC^{mut3} will limit translatability to the clinic. To remedy this, peptide stapling is implemented to improve the protease resistance of CC^{mut3}. We aim to see if these staples do indeed increase the protease stability of our CC^{mut3} constructs.

Research Aim 4

Stapling of hydrophilic proteins may cause protein misfolding. Future work will investigate the effect staples of varying hydrophobicity have on the conformation of hydrophilic proteins.

References

[1] O.O. Olabisi, G.M. Mahon, E.V. Kostenko, Z. Liu, H.L. Ozer, I.P. Whitehead, Bcr interacts with components of the endosomal sorting complex required for transport-I and is required for epidermal growth factor receptor turnover, Cancer Res 66(12) (2006) 6250-7.

[2] R. Ren, Mechanisms of BCR-ABL in the pathogenesis of chronic myelogenous leukaemia, Nat Rev Cancer 5(3) (2005) 172-83.

[3] E. Laurent, M. Talpaz, H. Kantarjian, R. Kurzrock, The BCR gene and philadelphia chromosome-positive leukemogenesis, Cancer Res 61(6) (2001) 2343-55.

[4] J.D. Alexis, N. Wang, W. Che, N. Lerner-Marmarosh, A. Sahni, V.A. Korshunov, Y. Zou, B. Ding, C. Yan, B.C. Berk, J. Abe, Bcr kinase activation by angiotensin II inhibits peroxisome-proliferator-activated receptor gamma transcriptional activity in vascular smooth muscle cells, Circ Res 104(1) (2009) 69-78.

[5] T. Kato, Molecular genetics of bipolar disorder and depression, Psychiatry Clin Neurosci 61(1) (2007) 3-19.

[6] A.R. Park, D. Oh, S.H. Lim, J. Choi, J. Moon, D.Y. Yu, S.G. Park, N. Heisterkamp, E. Kim, P.K. Myung, J.R. Lee, Regulation of dendritic arborization by BCR Rac1 GTPase-activating protein, a substrate of PTPRT, J Cell Sci 125(Pt 19) (2012) 4518-31.

[7] A.S. Narayanan, S.B. Reyes, K. Um, J.H. McCarty, K.F. Tolias, The Rac-GAP Bcr is a novel regulator of the Par complex that controls cell polarity, Mol Biol Cell 24(24) (2013) 3857-68.

[8] D. Diekmann, S. Brill, M.D. Garrett, N. Totty, J. Hsuan, C. Monfries, C. Hall, L. Lim, A. Hall, Bcr encodes a GTPase-activating protein for p21rac, Nature 351(6325) (1991) 400-2.

[9] S.M. Kweon, Y.J. Cho, P. Minoo, J. Groffen, N. Heisterkamp, Activity of the Bcr GTPase-activating domain is regulated through direct protein/protein interaction with the Rho guanine nucleotide dissociation inhibitor, J Biol Chem 283(6) (2008) 3023-30.

[10] M.W. Deininger, B.J. Druker, Specific targeted therapy of chronic myelogenous leukemia with imatinib, Pharmacol Rev 55(3) (2003) 401-23.

[11] M. Preyer, P. Vigneri, J.Y. Wang, Interplay between kinase domain autophosphorylation and F-actin binding domain in regulating imatinib sensitivity and nuclear import of BCR-ABL, PloS One 6(2) (2011) e17020.

[12] Y. Maru, O.N. Witte, The BCR gene encodes a novel serine/threonine kinase activity within a single exon, Cell 67(3) (1991) 459-68.

[13] H. Modi, L. Li, S. Chu, J. Rossi, J.K. Yee, R. Bhatia, Inhibition of Grb2 expression demonstrates an important role in BCR-ABL-mediated MAPK activation and transformation of primary human hematopoietic cells, Leukemia 25(2) (2011) 305-12.

[14] J.W. Voncken, H. van Schaick, V. Kaartinen, K. Deemer, T. Coates, B. Landing, P. Pattengale, O. Dorseuil, G.M. Bokoch, J. Groffen, et al., Increased neutrophil respiratory burst in bcr-null mutants, Cell 80(5) (1995) 719-28.

[15] Y.J. Cho, J.M. Cunnick, S.J. Yi, V. Kaartinen, J. Groffen, N. Heisterkamp, Abr and Bcr, two homologous Rac GTPase-activating proteins, control multiple cellular functions of murine macrophages, Mol Cell Biol 27(3) (2007) 899-911.

[16] B. Nagar, O. Hantschel, M.A. Young, K. Scheffzek, D. Veach, W. Bornmann, B. Clarkson, G. Superti-Furga, J. Kuriyan, Structural basis for the autoinhibition of c-Abl tyrosine kinase, Cell 112(6) (2003) 859-71.

[17] S.E. Hernandez, M. Krishnaswami, A.L. Miller, A.J. Koleske, How do Abl family kinases regulate cell shape and movement?, Trends Cell Biol 14(1) (2004) 36-44.

[18] A. Sirvent, C. Benistant, S. Roche, Cytoplasmic signalling by the c-Abl tyrosine kinase in normal and cancer cells, Biol Cell 100(11) (2008) 617-31.

[19] O. Hantschel, B. Nagar, S. Guettler, J. Kretzschmar, K. Dorey, J. Kuriyan, G. Superti-Furga, A myristoyl/phosphotyrosine switch regulates c-Abl, Cell 112(6) (2003) 845-57.

[20] J.Y. Wang, Regulation of cell death by the Abl tyrosine kinase, Oncogene 19(49) (2000) 5643-50.

[21] X. Wang, L. Zeng, J. Wang, J.F. Chau, K.P. Lai, D. Jia, A. Poonepalli, M.P. Hande, H. Liu, G. He, L. He, B. Li, A positive role for c-Abl in Atm and Atr activation in DNA damage response, Cell Death Differ 18(1) (2011) 5-15.

[22] C.E. Canman, D.S. Lim, K.A. Cimprich, Y. Taya, K. Tamai, K. Sakaguchi, E. Appella, M.B. Kastan, J.D. Siliciano, Activation of the ATM kinase by ionizing radiation and phosphorylation of p53, Science 281(5383) (1998) 1677-9.

[23] M. Kurokawa, S. Kornbluth, Caspases and kinases in a death grip, Cell 138(5) (2009) 838-54.

[24] M.H. David-Cordonnier, M. Hamdane, C. Bailly, J.C. D'Halluin, The DNA binding domain of the human c-Abl tyrosine kinase preferentially binds to DNA sequences

containing an AAC motif and to distorted DNA structures, Biochemistry 37(17) (1998) 6065-76.

[25] S. Wong, O.N. Witte, The BCR-ABL story: bench to bedside and back, Annu Rev Immunol 22 (2004) 247-306.

[26] R. Capdeville, E. Buchdunger, J. Zimmermann, A. Matter, Glivec (STI571, imatinib), a rationally developed, targeted anticancer drug, Nat Rev Drug Discov 1(7) (2002) 493-502.

[27] N. Heisterkamp, G. Jenster, J. ten Hoeve, D. Zovich, P.K. Pattengale, J. Groffen, Acute leukaemia in bcr/abl transgenic mice, Nature 344(6263) (1990) 251-3.

[28] G.Q. Daley, R.A. Van Etten, D. Baltimore, Induction of chronic myelogenous leukemia in mice by the P210bcr/abl gene of the Philadelphia chromosome, Science 247(4944) (1990) 824-30.

[29] L.A. Hazlehurst, N.N. Bewry, R.R. Nair, J. Pinilla-Ibarz, Signaling networks associated with BCR-ABL-dependent transformation, Cancer Control 16(2) (2009) 100-7.

[30] D. Miroshnychenko, A. Dubrovska, S. Maliuta, G. Telegeev, P. Aspenstrom, Novel role of pleckstrin homology domain of the Bcr-Abl protein: analysis of protein-protein and protein-lipid interactions, Exp Cell Res 316(4) (2010) 530-42.

[31] A.S. Dixon, S.S. Pendley, B.J. Bruno, D.W. Woessner, A.A. Shimpi, T.E. Cheatham, 3rd, C.S. Lim, Disruption of Bcr-Abl coiled coil oligomerization by design, J Biol Chem 286(31) (2011) 27751-60.

[32] J.R. McWhirter, D.L. Galasso, J.Y. Wang, A coiled-coil oligomerization domain of Bcr is essential for the transforming function of Bcr-Abl oncoproteins, Mol Cell Biol 13(12) (1993) 7587-95.

[33] J. Liu, M. Campbell, J.Q. Guo, D. Lu, Y.M. Xian, B.S. Andersson, R.B. Arlinghaus, BCR-ABL tyrosine kinase is autophosphorylated or transphosphorylates P160 BCR on tyrosine predominantly within the first BCR exon, Oncogene 8(1) (1993) 101-9.

[34] H. Pluk, K. Dorey, G. Superti-Furga, Autoinhibition of c-Abl, Cell 108(2) (2002) 247-59.

[35] A.M. Pendergast, L.A. Quilliam, L.D. Cripe, C.H. Bassing, Z. Dai, N. Li, A. Batzer, K.M. Rabun, C.J. Der, J. Schlessinger, et al., BCR-ABL-induced oncogenesis is mediated by direct interaction with the SH2 domain of the GRB-2 adaptor protein, Cell 75(1) (1993) 175-85.

[36] T. O'Hare, M.W. Deininger, C.A. Eide, T. Clackson, B.J. Druker, Targeting the BCR-ABL signaling pathway in therapy-resistant Philadelphia chromosome-positive leukemia, Clin Cancer Res 17(2) (2011) 212-21.

[37] D. Cortez, L. Kadlec, A.M. Pendergast, Structural and signaling requirements for BCR-ABL-mediated transformation and inhibition of apoptosis, Mol Cell Biol 15(10) (1995) 5531-41.

[38] J.E. Cortes, M. Talpaz, S. O'Brien, S. Faderl, G. Garcia-Manero, A. Ferrajoli, S. Verstovsek, M.B. Rios, J. Shan, H.M. Kantarjian, Staging of chronic myeloid leukemia in the imatinib era: an evaluation of the World Health Organization proposal, Cancer 106(6) (2006) 1306-15.

[39] D.G. Savage, R.M. Szydlo, J.M. Goldman, Clinical features at diagnosis in 430 patients with chronic myeloid leukaemia seen at a referral centre over a 16-year period, Br J Haematol 96(1) (1997) 111-6.

[40] U. Bacher, W. Kern, S. Schnittger, W. Hiddemann, C. Schoch, T. Haferlach, Blast count and cytogenetics correlate and are useful parameters for the evaluation of different phases in chronic myeloid leukemia, Leuk Lymphoma 46(3) (2005) 357-66.

[41] C.J. Sherr, F. McCormick, The RB and p53 pathways in cancer, Cancer Cell 2(2) (2002) 103-12.

[42] B. Calabretta, D. Perrotti, The biology of CML blast crisis, Blood 103(11) (2004) 4010-22.

[43] N. Howlander, N. Krapcho, M. Miller, D. Bishop, K. Altekruse, S. Kosary, C. Yu, M. Ruhl, J. Tatalovich, Z. Mariotto, A. Lewis, D. Chen, H. Feuer, E. Cronin. SEER Cancer Statistics, 2015. Online. 2016 July. Availble from URL: http://seer.cancer.gov/statfacts/html/cmyl.html.

[44] R.W. Bolin, W.A. Robinson, J. Sutherland, R.F. Hamman, Busulfan versus hydroxyurea in long-term therapy of chronic myelogenous leukemia, Cancer 50(9) (1982) 1683-6.

[45] R. Hehlmann, H. Heimpel, J. Hasford, H.J. Kolb, H. Pralle, D.K. Hossfeld, W. Queisser, H. Loffler, A. Hochhaus, B. Heinze, et al., Randomized comparison of interferon-alpha with busulfan and hydroxyurea in chronic myelogenous leukemia. The German CML Study Group, Blood 84(12) (1994) 4064-77.

[46] J.F. Zeidner, M. Zahurak, G.L. Rosner, C.D. Gocke, R.J. Jones, B.D. Smith, The evolution of treatment strategies for patients with chronic myeloid leukemia relapsing after allogeneic bone marrow transplant: can tyrosine kinase inhibitors replace donor lymphocyte infusions?, Leuk Lymphoma 56(1) (2015) 128-34.

[47] M. Talpaz, J. Mercer, R. Hehlmann, The interferon-alpha revival in CML, Ann Hematol 94 Suppl 2 (2015) S195-207.

[48] A.M. Cornelison, M.A. Welch, C. Koller, E. Jabbour, Dasatinib combined with interferon-alfa induces a complete cytogenetic response and major molecular response in a patient with chronic myelogenous leukemia harboring the T315I BCR-ABL1 mutation, Clin Lymphoma Myeloma Leuk 11 Suppl 1 (2011) S111-3.

[49] J. Cortes, J.H. Lipton, D. Rea, R. Digumarti, C. Chuah, N. Nanda, A.C. Benichou, A.R. Craig, M. Michallet, F.E. Nicolini, H. Kantarjian, Phase 2 study of subcutaneous omacetaxine mepesuccinate after TKI failure in patients with chronic-phase CML with T315I mutation, Blood 120(13) (2012) 2573-80.

[50] D. Bixby, M. Talpaz, Mechanisms of resistance to tyrosine kinase inhibitors in chronic myeloid leukemia and recent therapeutic strategies to overcome resistance, Hematology Am Soc Hematol Educ Program (2009) 461-76.

[51] K. Yang, L.W. Fu, Mechanisms of resistance to BCR-ABL TKIs and the therapeutic strategies: A review, Crit Rev Oncol Hematol 93(3) (2015) 277-92.

[52] G.D. Miller, B.J. Bruno, C.S. Lim, Resistant mutations in CML and Ph(+)ALL - role of ponatinib, Biologics 8 (2014) 243-54.

[53] D.W. Woessner, C.S. Lim, M.W. Deininger, Development of an effective therapy for chronic myelogenous leukemia, Cancer J 17(6) (2011) 477-86.

[54] A.A. Mian, M. Schull, Z. Zhao, C. Oancea, A. Hundertmark, T. Beissert, O.G. Ottmann, M. Ruthardt, The gatekeeper mutation T315I confers resistance against small molecules by increasing or restoring the ABL-kinase activity accompanied by aberrant transphosphorylation of endogenous BCR, even in loss-of-function mutants of BCR/ABL, Leukemia 23(9) (2009) 1614-21.

[55] T. O'Hare, M.S. Zabriskie, A.M. Eiring, M.W. Deininger, Pushing the limits of targeted therapy in chronic myeloid leukaemia, Nat Rev Cancer 12(8) (2012) 513-26.

[56] M. Azam, G.Q. Daley, Anticipating clinical resistance to target-directed agents : the BCR-ABL paradigm, Mol Diagn Ther 10(2) (2006) 67-76.

[57] S. Redaelli, R. Piazza, R. Rostagno, V. Magistroni, P. Perini, M. Marega, C. Gambacorti-Passerini, F. Boschelli, Activity of bosutinib, dasatinib, and nilotinib against 18 imatinib-resistant BCR/ABL mutants, J Clin Oncol 27(3) (2009) 469-71.

[58] M. Baccarani, Managing children with chronic myeloid leukaemia, Br J Haematol 169(5) (2015) 759-60.

[59] E.a.K. Jabbour, H., How we treat patients with chronic myeloid leukemia, Oncology Times 38(4) (2016) 8-9.

[60] S.G. O'Brien, F. Guilhot, R.A. Larson, I. Gathmann, M. Baccarani, F. Cervantes, J.J. Cornelissen, T. Fischer, A. Hochhaus, T. Hughes, K. Lechner, J.L. Nielsen, P. Rousselot, J. Reiffers, G. Saglio, J. Shepherd, B. Simonsson, A. Gratwohl, J.M. Goldman, H. Kantarjian, K. Taylor, G. Verhoef, A.E. Bolton, R. Capdeville, B.J. Druker, Imatinib compared with interferon and low-dose cytarabine for newly diagnosed chronic-phase chronic myeloid leukemia, N Engl J Med 348(11) (2003) 994-1004.

[61] M.S. Zabriskie, C.A. Eide, S.K. Tantravahi, N.A. Vellore, J. Estrada, F.E. Nicolini, H.J. Khoury, R.A. Larson, M. Konopleva, J.E. Cortes, H. Kantarjian, E.J. Jabbour, S.M. Kornblau, J.H. Lipton, D. Rea, L. Stenke, G. Barbany, T. Lange, J.C. Hernandez-Boluda, G.J. Ossenkoppele, R.D. Press, C. Chuah, S.L. Goldberg, M. Wetzler, F.X. Mahon, G. Etienne, M. Baccarani, S. Soverini, G. Rosti, P. Rousselot, R. Friedman, M. Deininger, K.R. Reynolds, W.L. Heaton, A.M. Eiring, A.D. Pomicter, J.S. Khorashad, T.W. Kelley, R. Baron, B.J. Druker, M.W. Deininger, T. O'Hare, BCR-ABL1 compound mutations combining key kinase domain positions confer clinical resistance to ponatinib in Ph chromosome-positive leukemia, Cancer Cell 26(3) (2014) 428-42.

[62] A. Wylie, J. Schoepfer, G. Berellini, H. Cai, G. Caravatti, S. Cotesta, S. Dodd, J. Donovan, B. Erb, P. Furet, G. Gangal, R. Grotzfeld, Q. Hassan, T. Hood, V. Iyer, S. Jacob, W. Jahnke, F. Lombardo, A. Loo, P.W. Manley, A. Marzinzik, M. Palmer, X. Pelle, B. Salem, S. Sharma, S. Thohan, S. Zhu, N. Keen, L. Petruzzelli, K.G. Vanasse, W.R. Sellers, ABL001, a potent allosteric inhibitor of BCR-ABL, prevents emergence of resistant disease when administered in combination with nilotinib in an in vivo murine model of chronic myeloid leukemia, Blood 124(21) (2014) 398.

[63] P.K. Bhamidipati, H. Kantarjian, J. Cortes, A.M. Cornelison, E. Jabbour, Management of imatinib-resistant patients with chronic myeloid leukemia, Ther Adv Hematol 4(2) (2013) 103-17.

[64] M. Baccarani, J. Cortes, F. Pane, D. Niederwieser, G. Saglio, J. Apperley, F. Cervantes, M. Deininger, A. Gratwohl, F. Guilhot, A. Hochhaus, M. Horowitz, T. Hughes, H. Kantarjian, R. Larson, J. Radich, B. Simonsson, R.T. Silver, J. Goldman, R. Hehlmann, Chronic myeloid leukemia: an update of concepts and management recommendations of European LeukemiaNet, J Clin Oncol 27(35) (2009) 6041-51.

[65] J.S. Khorashad, T.W. Kelley, P. Szankasi, C.C. Mason, S. Soverini, L.T. Adrian, C.A. Eide, M.S. Zabriskie, T. Lange, J.C. Estrada, A.D. Pomicter, A.M. Eiring, I.L. Kraft, D.J. Anderson, Z. Gu, M. Alikian, A.G. Reid, L. Foroni, D. Marin, B.J. Druker, T. O'Hare, M.W. Deininger, BCR-ABL1 compound mutations in tyrosine

kinase inhibitor-resistant CML: frequency and clonal relationships, Blood 121(3) (2013) 489-98.

[66] W. Al-Achkar, A. Wafa, F. Moassass, E. Klein, T. Liehr, Multiple copies of BCR-ABL fusion gene on two isodicentric Philadelphia chromosomes in an imatinib mesylate-resistant chronic myeloid leukemia patient, Oncol Lett 5(5) (2013) 1579-1582.

[67] S. Dulucq, S. Bouchet, B. Turcq, E. Lippert, G. Etienne, J. Reiffers, M. Molimard, M. Krajinovic, F.X. Mahon, Multidrug resistance gene (MDR1) polymorphisms are associated with major molecular responses to standard-dose imatinib in chronic myeloid leukemia, Blood 112(5) (2008) 2024-7.

[68] L.C. Crossman, B.J. Druker, M.W. Deininger, M. Pirmohamed, L. Wang, R.E. Clark, hOCT 1 and resistance to imatinib, Blood 106(3) (2005) 1133-4; author reply 1134.

[69] L. Wang, A. Giannoudis, S. Lane, P. Williamson, M. Pirmohamed, R.E. Clark, Expression of the uptake drug transporter hOCT1 is an important clinical determinant of the response to imatinib in chronic myeloid leukemia, Clin Pharmacol Ther 83(2) (2008) 258-64.

[70] W. Fiskus, M. Pranpat, P. Bali, M. Balasis, S. Kumaraswamy, S. Boyapalle, K. Rocha, J. Wu, F. Giles, P.W. Manley, P. Atadja, K. Bhalla, Combined effects of novel tyrosine kinase inhibitor AMN107 and histone deacetylase inhibitor LBH589 against Bcr-Abl-expressing human leukemia cells, Blood 108(2) (2006) 645-52.

[71] A.M. Eiring, B.D. Page, I.L. Kraft, C.C. Mason, N.A. Vellore, D. Resetca, M.S. Zabriskie, T.Y. Zhang, J.S. Khorashad, A.J. Engar, K.R. Reynolds, D.J. Anderson, A. Senina, A.D. Pomicter, C.C. Arpin, S. Ahmad, W.L. Heaton, S.K. Tantravahi, A. Todic, R. Colaguori, R. Moriggl, D.J. Wilson, R. Baron, T. O'Hare, P.T. Gunning, M.W. Deininger, Combined STAT3 and BCR-ABL1 inhibition induces synthetic lethality in therapy-resistant chronic myeloid leukemia, Leukemia 29(3) (2015) 586-97.

[72] A.M. Eiring, I.L. Kraft, B.D. Page, T. O'Hare, P.T. Gunning, M.W. Deininger, STAT3 as a mediator of BCR-ABL1-independent resistance in chronic myeloid leukemia, Leukemia supplements 3(Suppl 1) (2014) S5-6.

[73] X. Zhang, R. Subrahmanyam, R. Wong, A.W. Gross, R. Ren, The NH(2)-terminal coiled-coil domain and tyrosine 177 play important roles in induction of a myeloproliferative disease in mice by Bcr-Abl, Mol Cell Biol 21(3) (2001) 840-53.

[74] Y. He, J.A. Wertheim, L. Xu, J.P. Miller, F.G. Karnell, J.K. Choi, R. Ren, W.S. Pear, The coiled-coil domain and Tyr177 of bcr are required to induce a murine

chronic myelogenous leukemia-like disease by bcr/abl, Blood 99(8) (2002) 2957-68.

[75] P. Burkhard, J. Stetefeld, S.V. Strelkov, Coiled coils: a highly versatile protein folding motif, Trends Cell Biol 11(2) (2001) 82-8.

[76] E. Wolf, P.S. Kim, B. Berger, MultiCoil: a program for predicting two- and three-stranded coiled coils, Protein Sci 6(6) (1997) 1179-89.

[77] A. Lupas, Coiled coils: new structures and new functions, Trends Biochem Sci 21(10) (1996) 375-82.

[78] D.N. Woolfson, The design of coiled-coil structures and assemblies, Adv Protein Chem 70 (2005) 79-112.

[79] X. Zhao, S. Ghaffari, H. Lodish, V.N. Malashkevich, P.S. Kim, Structure of the Bcr-Abl oncoprotein oligomerization domain, Nat Struct Biol 9(2) (2002) 117-20.

[80] T. Beissert, A. Hundertmark, V. Kaburova, L. Travaglini, A.A. Mian, C. Nervi, M. Ruthardt, Targeting of the N-terminal coiled coil oligomerization interface by a helix-2 peptide inhibits unmutated and imatinib-resistant BCR/ABL, Int J Cancer 122(12) (2008) 2744-52.

[81] T. Beissert, E. Puccetti, A. Bianchini, S. Guller, S. Boehrer, D. Hoelzer, O.G. Ottmann, C. Nervi, M. Ruthardt, Targeting of the N-terminal coiled coil oligomerization interface of BCR interferes with the transformation potential of BCR-ABL and increases sensitivity to STI571, Blood 102(8) (2003) 2985-93.

[82] A.S. Dixon, G.D. Miller, B.J. Bruno, J.E. Constance, D.W. Woessner, T.P. Fidler, J.C. Robertson, T.E. Cheatham, 3rd, C.S. Lim, Improved coiled-coil design enhances interaction with Bcr-Abl and induces apoptosis, Mol Pharm 9(1) (2012) 187-95.

CHAPTER 2

BASICS AND RECENT ADVANCES IN PEPTIDE AND PROTEIN DRUG DELIVERY

Abstract

While the peptide and protein therapeutic market has developed significantly in the past decades, delivery has limited their use. While oral delivery is preferred, most are currently delivered intravenously or subcutaneously due to degradation and limited absorption in the GI tract. Therefore, absorption enhancers, enzyme inhibitors, carrier systems, and stability enhancers are being studied to facilitate oral peptide delivery. Additionally, transdermal peptide delivery avoids the issues of the GI tract, but also faces absorption limitations. Due to proteases, opsonization, and agglutination, free peptides are not systemically stable without modifications. This review discusses oral and transdermal peptide drug delivery, focusing on barriers and solutions to absorption and stability issues. Methods to increase systemic stability and site-specific delivery are also discussed.

Introduction

Peptides and proteins have great potential as therapeutics. Currently, the market for peptide and protein drugs is estimated to be greater than $40 billion/year, or 10% of the

---

Reprinted with permission from Molecular Pharmaceutics 2013; **4**(11):1443-67. Benjamin J. Bruno, Geoffrey D. Miller and Carol S. Lim.

pharmaceutical market [1]. This market is growing much faster than that of small molecules, and will make up an even larger proportion of the market in the future [1]. At present there over 100 approved peptide-based therapeutics on the market, with the majority being smaller than 20 amino acids [1]. Compared to the typical small molecule drugs which currently make up the majority of the pharmaceutical market, peptides and proteins can be highly selective as they have multiple points of contact with their targets [1]. Increased selectivity may also result in decreased side effects and toxicity. Peptides can be designed to target a broad range of molecules, giving them almost limitless possibilities in fields such as oncology, immunology, infectious disease, and endocrinology. For an overview of some popular therapeutic peptides/proteins, see Table 2.1.

These peptide and protein therapeutics have disadvantages as well such as low bioavailability and metabolic labiality. Oral bioavailability of peptides is limited by degradation in the GI tract as well as their inability to cross the epithelial barrier. These therapeutics tend to have high molecular weights, low lipophilicity, and charged functional groups which hamper their absorption [2]. These characteristics lead to the low bioavailability of most orally administered peptides (<2%) and short half-lives (<30 minutes) [3]. Intravenous (IV) or subcutaneous (SubQ) delivery of these therapeutics overcomes the issue of absorption, but other factors limit the bioavailability of peptide and protein therapeutics: systemic proteases, rapid metabolism, opsonization, conformational changes, dissociation of subunit proteins, noncovalent complexation with blood products, and destruction of labile side-groups [1, 4].

As oral delivery improves patient compliance, there is great interest in the

Table 2.1. Overview of a selection of currently available peptide/protein therapeutics. RA: Rheumatoid Arthritis; AA: Amino acids; D-AA: D-amino acids; DM: Diabetes Mellitus; GLP-1: Glucagon-like peptide 1; SubQ: Subcutaneous

DRUG NAME	SIZE	INDICATIONS[5]	RECENT SALES NUMBERS	ROUTE DELIVERED[5]
ETANERCEPT	150 kDa	RA, psoriatic arthritis, Plaque Psoriasis, Ankylosing Spondylitis	$7.9 Billion (2012) [6]	SubQ
INSULIN GLARGINE	53 AA, 6.1 kDa	Type 1 and 2 DM	$6.6 Billion (2012) [6]	SubQ
PEGFILGRASTIM	39 kDa	Neutropenia	$4.1 Billion (2012) [6]	SubQ
SALMON CALCITONIN	32 AA	Osteoporosis	$1,700,000 Units (2011) [7]	IM, SubQ, Intranasal
CYCLOSPORINE	Cyclic, 11 AA	Prophylaxis, solid organ rejection	$579 Million (2012) [8]	Oral, IV
OCTREOTIDE	8 AA	Acromegaly, gigantism, carcinoid syndrome	Est. $1.5 Billion (2011) [9]	IV, SubQ, IM (Depot)
LIRAGLUTIDE	31 AA, 3.8 kDa	Type 2 DM (GLP-1 agonist)	Est. $843 Million (Q3 2012-Q2 2013) [10]	SubQ
BIVALIRUDIN	2.2 kDa	Anticoagulant	$481 Million (2011) [11]	IV
DESMOPRESSIN	9AA (8 D-AA)	Nocturnal Enuresis	610,000 Rx US in 2009 [12]	IV, IM, SubQ, Intranasal

development of systems which allow for the oral delivery of peptide and protein therapeutics [13]. This review will summarize the barriers to various noninvasive delivery methods with a focus on oral and transdermal delivery. Additionally, current methods to overcome these delivery barriers will be discussed. The final portion of this paper will cover schemes designed to overcome the problems of therapeutic targeting and systemic stability.

Oral Delivery

Barriers to Oral Delivery

Oral delivery is the preferred route of drug administration, as the majority of patients see it as the most convenient way to take their drugs[14]. Drugs taken by the oral route have the highest level of patient compliance due to the ease and simplicity of taking medications [14, 15]. Despite the large number of protein therapeutics being discovered each year, oral delivery continues to be a barrier. As a whole, protein and peptide drugs have low bioavailability when administered orally due to problematic barriers including gastrointestinal proteases, the epithelial barrier, and efflux pumps. Common routes of administration for the systemic delivery of peptide and protein therapeutics are summarized in Figure 2.1. Table 2.2 provides an overview of the delivery enhancers discussed in this paper with regard to where they act.

Proteins are degraded via enzymes and hydrolysis in the acidic environment in the stomach and in the GI tract by a number of proteases and peptidases [16-18]. The human degradome, a complete list of proteases in human cells, consists of at least 569 proteases [19]. There are 5 broad classes of proteases, including serine, cysteine, threonine, aspartic,

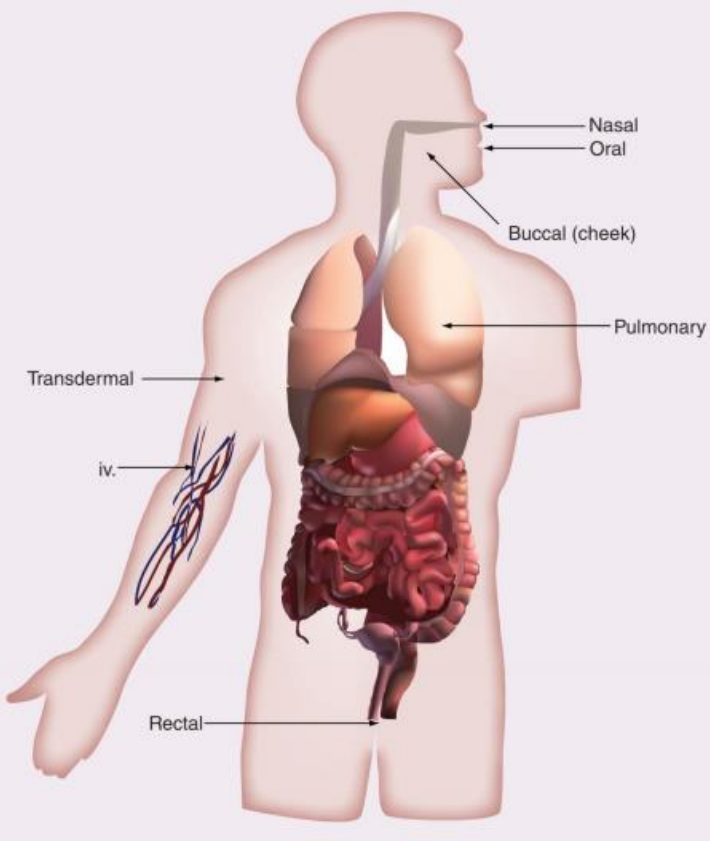

Figure 2.1. Routes of administration for systemic delivery of peptides and proteins. Numbering on figure refers to Table 2.2, where 1 = stomach, 2 = small intestine, 3 = circulation

Table 2.2 Overview of peptide modifications and delivery systems. CPP: Cell-penetrating peptide; SLN: Solid lipid nanoparticle; ZOT: Zonula occludens toxin.

Goal of modification	Peptide
Stomach	
Increased Stability	PEG, D-amino acids, nanoparticles, SLN
Small intestine	
Increased Stability	Cyclization, PEG, lipidization, D-amino acids, polymer matrices, nanoparticles, esterification, *N*-acetylation
Enzyme Inhibitors	Soybean trypsin inhibitor, aprotinin, puromycin, bacitracin
Absorption Enhancers	Chitosans, fatty acids, lectins, ZOT, CPP, liposomes, nanoemulsions, mucoadhesive polymers, nanoparticles, SLN
Circulation	
Increased Stability	PEG, hyperglycosylation, liposomes, nanoparticles
Targeting	Antibody CPP

and metalloproteinases [20]. These proteases play roles in DNA replication, transcription, cell proliferation, fertility, stem cell mobilization, hemostasis, inflammation, senescence, apoptosis, and many other vital cellular and regulatory processes [20]. Trypsin, carboxypeptidase, and chymotrypsin are secreted from the pancreas into the small intestine, mostly in the duodenum, where they are present in gram quantities. These enzymes are responsible for 20% of the enzymatic degradation of ingested proteins and peptides [16, 21, 22]. The causes of the remaining 80% of enzymatic degradation are discussed below.

While peptide degradation is one obstacle to oral protein therapeutic delivery, the epithelial barrier of the small intestine poses an even greater challenge. This barrier consists of a single layer of columnar epithelial cells supported by lamina propria and muscularis mucosa [21]. Molecules can cross the epithelium by either transcellular or paracellular routes as depicted in Figure 2.2. Apical to the epithelial cell barrier is the mucosal layer, which contains glycocalyx, a layer of sulfated mucopolysaccharides [21], glycoproteins, enzymes, electrolytes, and water [21, 23]. Additionally, most mucosal surfaces are coated by a hydrated gel consisting of mucins, which are high molecular weight, heavily glycosylated proteins [24]. Bulk flow to the epithelial cells is limited, creating an unstirred layer near the epithelial surface [24]. This unstirred layer is protected from convective mixing forces, slowing the absorption of small molecules and ions. Once a molecule passes the mucosal layer, however, the unstirred layer may act as an absorption enhancer by allowing the particle more time exposed to the epithelial barrier [24].

The brush border membrane (Figure 2.2) is where the majority of peptide degradation occurs [21]. The brush border is the microvilli-covered surface of cells found in the small intestine, and the microvilli play a major role in nutrient digestion and

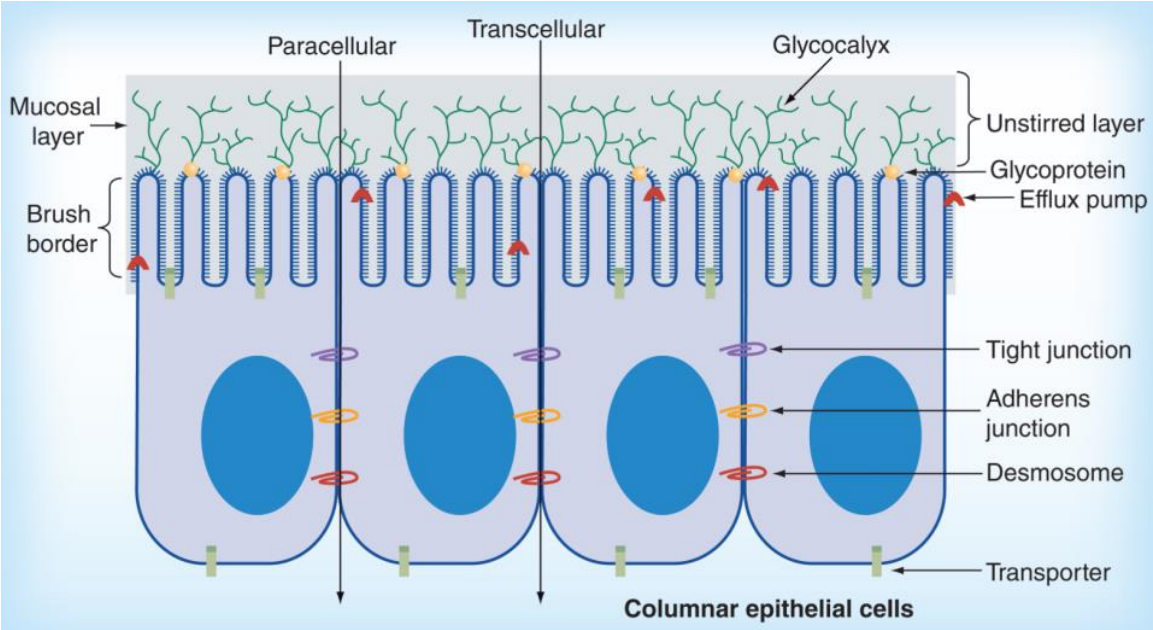

Figure 2.2. **Intestinal barriers to peptide delivery.** Epithelial intestinal barrier is made up of a single layer of columnar epithelial cells. The apical side of the barrier contains the mucosal layer. Drugs may penetrate the epithelial barrier either through the transcellular route (across the cell) or the paracellular route (between tight junctions). See text for other term explanations.

absorption [3]. Tight junctions (TJs) mediate the paracellular pathway of absorption in intact membranes (Figure 2.2) [24]. TJs are the rate limiting step in transepithelial transport [24]. Adherin junctions, which are required for the assembly of TJs, are a multi-protein complex made of transmembrane proteins, peripheral membrane proteins, and regulatory molecules including kinases [24]. Adherin junctions work with desmosomes to provide the adhesive bonds that maintain cellular proximity and intercellular communication [24]. Both adherin junctions and TJs are supported by dense perijunctional rings of actin and myocin. The most important proteins to tight junction assembly and maintenance are zonula occludens 1 and 2 along with transmembrane proteins in the claudin family [24, 25].

A final barrier to protein drug absorption is efflux pumps, depicted in Figure 2.2. These are proteins belonging to the ATP binding cassette (ABC) superfamily which sit on the apical side of mature epithelial cells and mediate multidrug resistance (MDR) in humans [26]. Forty-nine ABC proteins have been Identified, many of which are overexpressed in MDR cell lines [27]. One specific example of an efflux pump is P-glycoprotein-I, or PGP-I (also known as MDR1) [28]. After peptides are absorbed in the GI, PGP-I can pump the drug or peptide back into the GI lumen [16]. It is known that linear lipophilic and cyclic peptides (including cyclosporine) are substrates of PGP-I [16, 29].

Even after the drug is absorbed, first-pass metabolism can greatly reduce the fraction of drug which reaches systemic circulation. The first-pass effect, as it is known, is the phenomenon which accounts for the decreased fraction of drug systemically available compared to the fraction of drug that is absorbed. Once a drug is absorbed after oral

administration it enters the hepatic portal system. It is then carried via the portal vein to the liver prior to reaching the rest of the body. The liver then metabolizes the drug, reducing the amount of the active, parent compound which enters systemic circulation [30]. Intravenous (IV), intramuscular (IM), subcutaneous (SubQ), sublingual (SL), intrarectal, transdermal, and pulmonary routes of administration avoid or minimize the first-pass effect [31].

While these barriers to absorption are large, much work has been done in order to overcome them. Methods to improve the bioavailability of protein therapeutics can be broadly classified into the following categories: structural modifications, enzyme inhibitors, absorption enhancers, and carrier systems.

Strategies for Oral Delivery of Peptides

Direct Structural Modification

One class of structural modifications under study is cyclization. The benefits of cyclization to oral peptide/protein therapy are evidenced by cyclosporine (CSA). CSA is a fungal-derived, nonribosomal 11-amino acid peptide with a cyclic backbone and a single D-amino acid [1]. While most naturally occurring proteins and peptides are composed of L-amino acids, D-amino acids are found in some naturally occurring nonribosomally synthesized peptides [32]. Cyclosporine is used most frequently as an immune system modulator for the prevention of solid organ rejection [33]. This cyclic peptide is resistant to proteolytic degradation and also has higher than expected absorption after oral administration [1]. The superior oral bioavailability is thought to be due to a number of properties including decreased flexibility and hydrogen bonding characteristics. The cyclic

nature of CSA incorporates 7 n-methyl groups that reduce the number of hydrogen bond donors, and the remaining 4 hydrogens bond intramolecularly . This reduction in intermolecular bonding reduces hydrophilicity. CSA has lipophilic side chain amino acids which further raise its lipophilicity and allow it to cross the gut wall [1]. Other peptides such as somatostatin and encephalin have shown similar characteristics and improved oral absorption after cyclization [34, 35]. Generically, cyclization is usually carried out between side chains or ends of the peptide sequences through disulfide bonds, lanthionine, dicarba, hydrazine, or lactam bridges [1]. While cyclization is an option for some peptides, its widespread use is limited when larger peptides and proteins are needed for therapy.

PEGylation is a modification option for some peptides not amenable to cyclization. Polyethylene glycol, or PEG, is an amphipathic molecule that dissolves in organic solvents as well as in water [36]. Both PEG and its metabolites are nontoxic and US-FDA approved [37, 38]. PEG has been shown to be toxic at high parenteral doses, much higher than the amount of PEG a patient would be exposed to with current PEGylated therapies [39]. If PEG toxicity is seen it usually presents in the kidney, as unmodified PEG is mainly cleared through the kidneys. Interesting, even when pathological changes were seen, no functional deficits resulted [39]. Case studies exist which demonstrate high doses of PEG can induce acute tubular necrosis, and the use of PEG in colonoscopy bowel preparation is associated with an increased risk of acute renal failure in patients over 50 [40, 41]. There is also evidence that repeat administration of PEGylated particles can lead to increased clearance rate, likely related to anti-PEG IgG and IgM antibodies [42, 43]. The structure of the PEG molecules, properties of the molecule being PEGylated, and method of PEGylation all play a role in determining immunogenicity [43].

Direct PEGylation confers benefits in both protein absorption and systemic stability (described later in this paper). As an example, insulin PEGylated with a 750 Da version of PEG was formulated into a mucoadhesive tablet. After oral administration, insulin activity was demonstrated by the observed drop in blood glucose levels of approximately 50% 3 hours after administration. Additionally, some activity of the orally administered insulin was seen up to 30 hours after administration [44]. PEGylation of another peptide, salmon calcitonin (sCT), resulted in resistance to intestinal enzymes, a nearly 6-fold increase in intestinal absorption, and slowed systemic clearance compared to the unmodified version of sCT [45].

Vitamin B12 has been used to increase the oral absorption of a number of therapeutic proteins including G-CSF, EPO, insulin, and LHRH [46]. By fusing therapeutic proteins to vitamin B12, it is possible to take advantage of the binding of vitamin B12 to intrinsic factor (IF), followed by the receptor-mediated absorption of the vitamin B12-IF conjugate. However, this system is limited by the quantity of B12 that can be absorbed, GI degradation, decreased activity of the protein therapeutic due to steric hindrances, and loss of IF affinity for conjugated vitamin B12 [46]. For more information on the use of B12 to improve the oral delivery of protein and peptides, see the review by Petrus et al. [47].

Protein lipidization is another method which increases the bioavailability of orally administered proteins. Fatty acid conjugates of polypeptides show improved transport across biological membranes, higher stability, and longer plasma half-lives [48, 49]. Salmon calcitonin was lipidized using reversible aqueous lipidization (REAL), and thus it is categorized as a prodrug in this case [49]. Compared to the free sCT, the REAL-sCT

showed increased absorption and a 19 times higher AUC value [49]. Caprates, medium-chain fatty acids, promote paracellular diffusion of Class III (highly soluble, low permeability) molecules such as peptides [50]. In addition, triglycerides can be used to evade first-pass metabolism [50]. While irreversible methods of lipidization allow for increased membrane permeability, the activity of such modified proteins may be diminished due to steric issues with the fatty acid chain [50].

Recently, stapled peptides have garnered interest due to their enhanced biochemical properties in the context of drug delivery. More specifically, these are alpha helical peptides which contain a synthetic, hydrocarbon backbone linking various residues [51]. This backbone, known as the staple, locks the conformation of the peptide, increasing its helicity and stability in solution [52]. As an example, Walensky et al. have shown the ability of a hydrocarbon-stapled BH3 helix to increase apoptosis in vivo [53]. The enhanced stability of these peptides, along with increased cellular penetration capabilities, makes these molecules ideal candidates for future study in peptide delivery.

A final method of peptide modification to increase oral bioavailability is the substitution of natural L-amino acids with D-amino acids. One study showed that a variety of peptides cleaved by chymotrypsin, elastase, papain (a cysteine protease found in papaya), pepsin, trypsin, and carboxypeptidases are cleaved minimally or not at all by these enzymes when certain residues were replaced with D-amino acids [32, 54]. Tugyi et al. investigated D-amino acid substitutions in MUC2, a mucin glycoprotein [55]. The authors noted that the substituted peptide demonstrated high resistance to proteolytic degradation in vitro in both human serum and lysosomal preparations. Their work demonstrated that simultaneously modifying both N- and C-terminal regions with D-amino acids conferred

the greatest stability increases [55].

The above mentioned direct modifications of peptides and proteins are key strategies that have been implemented to increase stability and oral bioavailability. Many other direct modifications have been carried out, including certain prodrug methods, in Table 2.3.

In addition to direct modifications, another method to increase oral peptide bioavailability is to coadminister with enzyme inhibitors. These enzyme inhibitors are usually more effective in the large intestine than the small intestine due to the large quantity and variety of proteases in the small intestine [56]. A leading enzyme inhibitor is soybean trypsin inhibitor, FT-448, a potent and specific inhibitor of chymotrypsin [56]. When coadministered with insulin to rats and dogs, levels of immunoreactive insulin rose proportionally to a decrease in blood glucose levels. Further, it is thought to play some role in increasing peptide absorption [56].

Enzyme Inhibitors

Aprotinin, originally branded as Trasylol™ and used to reduce bleeding during complex surgeries, is another enzyme inhibitor used [57]. When administered with insulin intraileally, blood glucose decreased by 30% over the next 3 hours compared to administration of insulin alone [57]. Other enzyme inhibitors are summarized in Table 2.4. An alternative method to inhibit enzymes is to alter the pH at the site of action of the enzymes [58]. Most enzymes in the stomach, including pepsin, are only active at low pH (around 2) [59]. Therefore, if the pH in the stomach is increased, the enzymes are no longer able to degrade the peptides. Conversely, enzymes in the intestines often work at a higher

Table 2.3. Direct modifications of peptides and proteins. Overview of direct modifications made to peptides and the resulting change in bioavailability. PEG: Polyethylene glycol; AA: Amino acid; CSA: Cyclosporine; IFN: Interferon; MUC2: Mucin 2; IgG: Immunoglobulin G; G-CSF: granulocyte colony stimulating fator; EPO: erythropoietin; LHRH: lutenizing hormone releasing hormone; DP3: octapeptide (Glu-Ala-Ser-Ala-Ser-Tyr-Ser-Ala); AUC: Area under the curve

Modification	Subtype of modification	Modified Compounds	Outcome
Cyclization		CSA, somatostatin, encephalin	Reduced hydrophilicity, decreased conformational flexibility, enhanced membrane permeability, and resistance to proteolysis [3, 34, 35]
PEG	Direct, permanent modification	Insulin, salmon calcitonin	Resistance to intestinal enzymes, slowed systemic clearance, increased intestinal absorption, [44, 45]
	Prodrug	IFN-B-1b	Prolonged activity, dimished IgG response, improved protection from enzymatic degradation [44, 60]
B12 Conjugation	ε position on the Corrin ring		Albumin, G-CSF, EPO, LHRH and analogues, DP3, dextran nanoparticles [47]
	5'-hydroxy on α tail		IFN, insulin [47]
	Phosphate unit of the α tail		Albumin, γG-globulin [47]
Lipidization	REAL with n-palmitoyl cysteinyl 2-pyridyl disulfide	Salmon calcitonin	AUC 19x higher than unmodified, marker for bone resorption reduced [48]
N-acetylation	α	Salmon calcitonin	Improved oral bioavailability, improved resistance to trypsin and leucine aminopeptidase, enhanced membrane permeability [61]
D-amino acids	6 out of 11 L-AA substituted for D-AA	MUC2	Resistance to chymotrypsin proteolysis, elastase, papain, pepsin, trypsin, and carboxypeptidase [55]
Prodrug	Esterification	Desmopressin	Increased permeation of Caco-2 cell layer; active in plasma [62]
	Perbuytrylation	Glycovir	Increased bioavailability [63]
Stapling	Hydrocarbon		Increased bioavailability, resistance to GI proteases [64]

Table 2.4. Enzyme inhibitors, their targets, and effects on peptide delivery. An overview of potentially clinically relevant enzyme inhibitors.
Ala: Alanine; Leu: Leucine

ENZYME INHIBITOR	MOLECULES INHIBITED	EFFECT ON PEPTIDE DRUGS
SOYBEAN TRYPSIN INHIBITOR FK-448	Chymotrypsin	Enhanced intestinal absorption of insulin in rats and dogs Suppressed digestion of insulin by pancreatic enzymes [56]
APROTININ	Serine proteases, specifically trypsin, chymotrypsin, and plasmin	Intraileally administered insulin with aprotinin led to decrease in blood glucose of 30% compared to controls [57]
PUROMYCIN	Serine and metallopeptidases	Improved stability of leucine encephalin and stability, permeability of D-Ala2, D-Leu5 enkephalin (DADLE) [65-67]
N-ACETYLCYSTEINE	Inhibits aminopeptidase N and had mucolytic properties[68, 69]	
BACITRACIN	Trypsin and pepsin, aminopeptidase N[69, 70]	Used to increase delivery of insulin, met-kephamid, and buserelin [68]

pH; therefore, lowering the pH can decrease the activity of these enzymes [71, 72]. These protease inhibitors do have shortcomings. First, they can disrupt the normal absorption of dietary peptides and may induce toxic shock after prolonged therapy [73, 74]. It is believed this may cause the body to increase production of these proteases, which may lead to hypertrophy and hyperplasia of the pancreas [68]. The inhibitors themselves may also be toxic and damaging to the GI tract after prolonged administration [68]. Indeed, the majority of enzyme inhibitors are highly toxic. Table 2.4 summarizes enzyme inhibitors with some promise of therapeutic translatability.

Absorption Enhancers

The optimal absorption enhancer should be reversible, nontoxic at the effective concentration, and provide a rapid permeation enhancing effect on the intestinal cell membrane. One such compound class of absorption enhancers is chitosans. Chitosans are nontoxic, biocompatible, US-FDA approved polymer derivatives of chitin which enhance the absorption of hydrophilic macromolecule drugs [75]. Additionally, due to their high molecular weight, they are minimally absorbed from the gut, limiting the possibility of systemic side effects [76]. It is thought that varying degrees of deacetylation of chitin confer different amounts of absorption enhancement, with >80% deacetylation affording the greatest promoter effect in cell culture [77]. Chitosans have been used to enhance the absorption of such molecules as atenolol, insulin, and 8-R-vasopressin [76]. Further, chitosans appear to be quite safe at their effective concentration [75, 78]. Chitosans work by increasing paracellular permeability. By binding tightly to the epithelium via positive charges, chitosans cause redistribution of cytoskeletal F-actin and the zonula occludens 1

[79]. Chitosans are limited by their ability to diffuse across the mucous layer, as evidenced by their decreased activity on mucus-producing cells [80]. In vivo studies with chitosans demonstrated a three-fold increase in octreotide absorption when the two were coadministered into the duodenum [76]. Another study with trimethyl chitosan chloride (TMC), a chitosan derivative, had many favorable characteristics. TMC was able to reversibly interact with TJs, leading to widening of the paracellular route and at the same time did not damage cell membrane or alter the viability of intestinal epithelial cells. In vivo studies in rats showed that it was able to increase the oral bioavailability of a peptide when the two were coadministered [75]. Overall, chitosans and their derivatives are a promising class of absorption enhancers.

Another class of absorption enhancers showing potential includes the medium chain fatty acids [81]. C8, C10, and C12 fatty acids (caprylate, caprate, and laurate, respectively) can enhance paracellular permeability of hydrophilic compounds. First, caprate is thought to work by inducing dilation of TJs [82]. Interestingly, the lowest concentration which enhanced absorption was near the critical micelle concentration (CMC) of each fatty acid [81]. The order of increased absorption in vivo is caprate>laurate>caprylate. Sodium caprate (C10) is the most studied of the medium chain fatty acids. It is thought to increase absorption of hydrophobic molecules via the paracellular and transcellular route [83]. Unfortunately, a study showed that it can only significantly increase absorption for molecules up to 1200g/mol, or 1.2 kDa (such as octreotide) [84]. At the effective dose of 13mM, sodium caprate is nontoxic to epithelial cells [84].

Lectins are another type of absorption enhancers which have many of the

characteristics of the ideal absorption enhancer. Lectins are proteins that specifically recognize and bind to sugar complexes attached to proteins and lipids [85]. Lectins are also naturally resistant to proteolytic breakdown, making inactivity before reaching their site of action unlikely [86]. They can be used to target luminal surfaces of the small intestine and trigger vesicular transport into or across epithelial cells [85]. Lectins are also mucoadhesive which further leads to increased absorption [18].

Toxins can also be used for absorption enhancement, so long as they do not cause permanent cellular damage. ZOT, or zonula occludens toxin, is one such compound. ZOT, a 45 kDa toxin made by *Vibrio cholerae,* has been shown to increase the permeability of small intestine mucosa by reversibly affecting the structure of TJs [87, 88]. ZOT binds to ZOT receptors on the luminal surface of the intestine and causes cytoskeletal rearrangement related to changes in protein kinase C and binding to β-tubulin [88, 89]. TJs can be perturbed enough to allow the transport of agents across the intestinal mucosa, although the increased bioavailability of insulin was only 20% [90]. In a study with Caco-2 cells, incubation with 4μg/mL ZOT for 30 minutes increased the permeability to insulin by 6.3-fold. [90] Mediation of TJs may not be the only method by which ZOT works; a study demonstrated that a fragment of ZOT was able to increase the bioavailability of hydrophobic drugs by interacting with PGP [91]. Additional work has been done to determine the smallest portion of ZOT which maintains activity [92].

Recently, coadministration of cell-penetrating peptides (CPPs - described later in more detail) with therapeutic peptides has been attempted in order to increase absorption of the therapeutic. In one study, insulin coadministered with CPPs consisting of 6-10 repeats of arginine led to increased GI uptake of insulin [93]. Interestingly, the study

investigated both D- and L-arginine-based CPPs, and the D-based CPPs allowed for greater increases in insulin absorption, assumed to be due resistance of D-amino acids to proteases [93]. It is important to note that the CPP was not fused to insulin; rather, they were coadministered. A follow-up study demonstrated that electrostatic interactions between insulin and the CPP were responsible for the enhanced absorption of insulin [94]. Another study revealed that the CPP penetratin was best able to increase ileal insulin absorption [95]. Penetratin consists of basic amino acids (lys, arg) along with some hydrophobic regions. Use of CPPs as absorption enhancers represents a relatively new area of research which have the potential to add weapons to the absorptive enhancement arsenal.

Other classes of absorption enhancers have lost favor in recent years due to irreversible epithelial damage [96]. Surfactants such as SDS were shown to cause increased permeability of the GI tract to hydrophilic compounds, but also cause altered cell morphology and cell membrane damage [97]. SDS shortened microvilli of cells and produced actin disbandment, structural separation of the TJs, and damage to the apical cell membrane with even limited exposure [98]. Certain in vivo rat studies support the increase in absorption and revealed the damage caused to be reversible [99]. Bile salts such as sodium cholate and deoxycholate were originally seen as safe and effective at increasing drug absorption. However, it is now understood that these particles are damaging after long-term use [100].

Carrier Systems

Many drug carrier systems are currently being developed in an attempt to increase the oral bioavailability of peptide drugs. Some of these systems contain a combination of

components listed above, while others have novel mechanisms.

The first group of carrier systems consists of hydrophilic mucoadhesive polymers(polyacrylates, cellulose, chitosan), which can be altered to suit the needs of the peptide/protein being delivered [101]. While chitosan has already been discussed under the absorption enhancers category, it has also been combined with EDTA in order to create a resin which binds bivalent cations [102]. It is thought that bivalent cations are essential for the activity of proteolytic enzymes; in fact, zinc proteases, carboxypeptidases, and aminopeptidases were strongly inhibited by this system, but serine proteases, trypsin, alpha chymotrypsin, and elastase were not inhibited [102].

Thiomers, thiolated polymers, have also been used as drug carrier systems. These mucoadhesive polymers display thiol-bearing side chains; disulfide bonds form between the polymer and cysteine rich protein domains in the mucous glycoprotein layer. These polymers are available in both cationic and anionic varieties and can increase mucoadhesive properties of gels by up to 140-fold [103]. When adhered in the small intestine, mucoadhesion allows for a steeper concentration gradient across the epithelial barrier, which may lead to increased passive drug uptake and prolonged therapeutic effect [103].

Next, polymer matrices can be used to protect proteins from proteolysis and antibody neutralization, resulting in increased protein activity in vivo [104]. It is very important that interaction between the protein and matrix be optimized; too little attraction and the protein will not be immobilized on the gel; too great an attraction will cause the protein to remain in the gel and thus not become systemically available. A sustained release system which protects the protein in the GI tract can be developed by tuning the cross-

linkage and electrostatic interactions between matrix and protein [104].

Nanoemulsions are another carrier system for oral protein therapeutics. Nanoemulsions are defined as oil in water (o/w) or water in oil (w/o) emulsions with mean droplet diameter ranging from 50 to 1000 nm. The average droplet size is usually between 100 and 500 nm [105]. Generally, these emulsions are made from surfactants approved for human consumption and are generally recognized as safe. Nanoemulsions have a much higher surface area and free energy than macroemulsions, thus making them an effective transport system. Further, nanoemulsions do not cream, flocculate, coalesce, or sediment. One such system in development is the "Self-Nanoemulsifying Drug Delivery System ," or SNEDDS. To test the concept, FITC-labeled β-lactamase (BLM) was loaded into SNEDDS through solid dispersion. After an O/W emulsion was formed via addition of water, the nanoemulsion was able to increase transport of FITC-BLM across MDCK monolayer of cells [106]. In vivo studies showed a significant increase in SNEDDS-BLM absorption compared to free BLM [106].

Hydrogels are a network of cross-linked water-soluble polymer chains which are insoluble in water but have water as their dispersion medium. The porous nature of hydrogels can be finely tuned to allow for drug loading into the hydrogel. Further, pharmacokinetic properties for release of the loaded drug can be adjusted to the requirements of individual drugs [107]. Hydrogels can designed to deliver drugs to four sites after oral ingestion: mouth, stomach, small intestine, or colon [107]. Newly developed homo- and copolymeric hydrogels are capable of protecting and delivering peptides and protein therapeutics [107]. For an overview on hydrogels, see Bindu Sri et al., and for more detail on the use of hydrogels for the oral peptide drug delivery, the review by Peppas

et al. is helpful [107, 108].

While liposomes system have potential as oral drug delivery, there is a concern with stability of the vesicles under the physiologic conditions of the GI tract [109]. Adding to the problem, mucus may act as a barrier by blocking the diffusion oPf liposomes to the epithelial layer [110]. Despite this, orally administered liposomes have demonstrated some successes. Calcitonin was administered in a chitosan-aprotinin coated liposome and showed an increased pharmacological effect compared to free calcitonin [111]. Cyclosporine has also been delivered in liposomes; the egg lectin-cremophore-lactose liposome containing CSA had 9 times the bioavailability of free CSA and 4 times that of the microemulsion on the market [112]. PEG, coating, enteric encapsulation, and the use of archaeosomes have been proposed to decrease degradation of the liposome in the GI tract [113].

Nanoparticles are solid particles with sizes in the range of 10-1000 nm [114]. Nanoparticles allow for the encapsulation of proteins inside a polymeric matrix, thus protecting them against hydrolysis and enzymatic degradation [114]. These systems can be tuned in order to maximize encapsulation efficiency, bioavailability, and retention time [115]. Nanoparticles, however, have a difficult time being absorbed from the GI tract; studies have shown that cells lacking mucus (including M cells and Peyer's patches in general) are best at absorbing nanoparticles [114]. Particles of 50 and 100 nm demonstrated the greatest absorption and detection in intestinal mucosa [116]. Further, nanoparticles smaller than 100nm show higher extents of uptake by absorptive enterocytes while those over 500 nm will rarely be taken up by absorptive enterocytes [114]. Nanoparticles are often made from poly(lactic acid) (PLA), poly(lactic-co-glyclic acid)

(PLGA), chitosan, gelatin, and poly-alkyl-acyanoacrylate, all of which are nontoxic, nonthrombogenic, nonimmunogenic, noninflammatory, stable in blood, biodegradable, avoid the reticuloendothelial system (RES), and are applicable to various biologics such as protein, peptides, and nucleotides [115]. While there is minimal scientific data on the toxicity of nanoparticles, their size makes exposure during manufacturing almost guaranteed [117]. Impaired lung function and other respiratory symptoms have been seen in workers who were exposed to nanoparticles [117]. Intravenous administration of nanoparticles is followed by increased synthesis and release of cytokines. Further, nanoparticles passively target the liver through uptake by Kupfer cells, again followed by an inflammatory response [117]. Generally, the toxic effects of nanoparticles are not fully understood, and care must be taken with the manufacturing and use of nanoparticles as therapeutic agents. Table 2.5 provides some details regarding the various polymers used to make nanoparticles.

Nanoparticles (NPs) can be targeted to certain sites based on particle size, surface charge, surface modification, and hydrophobicity [115]. Surface charge is particularly important for cell internalization, as cationic surfaces increase the rate and extent of nanoparticle internalization [115]. Carboxylated polystyrene NPs show decreased affinity to intestinal epithelia and M cells compared to neutral and positively charged polystyrene nanoparticles [118]. While hydrophobic polymer-based nanoparticles are better absorbed than their hydrophilic counterparts [114], in order to avoid opsonization and the mononuclear phagocytic system (MPS), the use of hydrophilic surfaced nanoparticles is preferred over traditional hydrophobic-surfaced nanoparticles [115, 119]. Interestingly, negatively charged, hydrophilic NPs have increased bioadhesive properties and are

Table 2.5. Polymer carrier systems. Commonly used polymers for construction of nanoparticles, their biocompatibility, and use in peptide delivery
BSA: Bovine serum albumin; OGTT: Oral glucose tolerance test; AmB: Amphotericin B; PLGA: Poly(lactic-co-glyclic acid); PLA: Poly(lactic acid)

POLYMER	BIOCOMPATIBLE?[115]	EXAMPLE OF USE
PLA	Biocompatible and biodegradable	BSA loaded with 71% efficiency, BSA was stable after release [120]
PCL **POLY(E-CAPROLACTONE)**	Degraded by hydrolysis	Preparation of long-term implantable device, Insulin loaded with 96% efficiency, improved response to oral glucose tolerance test (OGTT) Has mucoadhesive properties Amphotericin B loaded PCL nanoparticles 2-3x more effective than free AmB [121, 122]
CHITOSAN	Nontoxic, biocompatible	Insulin loaded chitosan nanoparticles enhanced intestinal absorption of insulin through a combination of insulin internalization in enterocytes and insulin-loaded particle uptake by Peyer's patches [123]
GELATIN	Nontoxic, biodegradable,	Encapsulated paclitaxel, oligonucleotides, and chloroquine[124-126]
PAC **POLY(ALKYL-CYANO-ACRYLATES)**	Biodegradable and biocompatible, degraded by esterases. Produce some toxic metabolites, not suitable for human use	Encapsulated doxorubicin, ampicillin, indomethacin [115]
PLGA	Biodegradable, excellent toxicological profile	PLGA nanoparticles with influenza HA incorporated throughout the matrix, increased uptake via M cells[127]

uptaken by absorptive enterocytes and M cells [114, 128].

Surface modifications such as PEG can create a steric barrier and reduce clearance by circulating macrophages in the liver as well as by the MPS [115]. PEG-coating of nanoparticles increases blood circulation half-life as well as reducing interactions between the nanoparticles and digestive enzymes [129]. Lectins have been conjugated to nanoparticles which led to increased transport across intestinal mucosa, especially via M cells of Peyer's patches [114, 115]. Finally, higher molecular weight polymers will release the peptide more slowly than lower molecular weight polymers [115].

Solid lipid nanoparticles (SLN) are solid lipids which are stabilized with an emulsifying layer in an aqueous dispersion (Figure 2.3). The colloidal size ranges between 50 and 1000nm [109]. This system avoids the use of organic solvents and has the capacity to allow fast, effective, large-scale manufacturing of high-concentration suspensions. This system can be used to encapsulate peptides and proteins and thereby protect them against enzymatic degradation [130]. Another benefit of SLNs is that the drug can be incorporated into the matrix, onto the shell, or into the core of the particle [109]. A lectin-modified and insulin-coated SLN was able to deliver insulin to the system after administration to the small intestine [131]. SLNs have also been used for controlled release of sCT [132]. The systemic stability and GI absorption of SLNs and nanoparticles as a whole make them a promising protein carrier system; research in this field continues to enhance the likelihood for oral delivery of systemically-active peptides. Many companies are attempting to develop carrier systems which will be able to deliver a wide variety of therapeutics with minimal modification [73]. Examples include Emisphere's Eligen ™ system which has the potential to deliver therapeutics form 0.5-150 kDa. The drug-carrier system known as

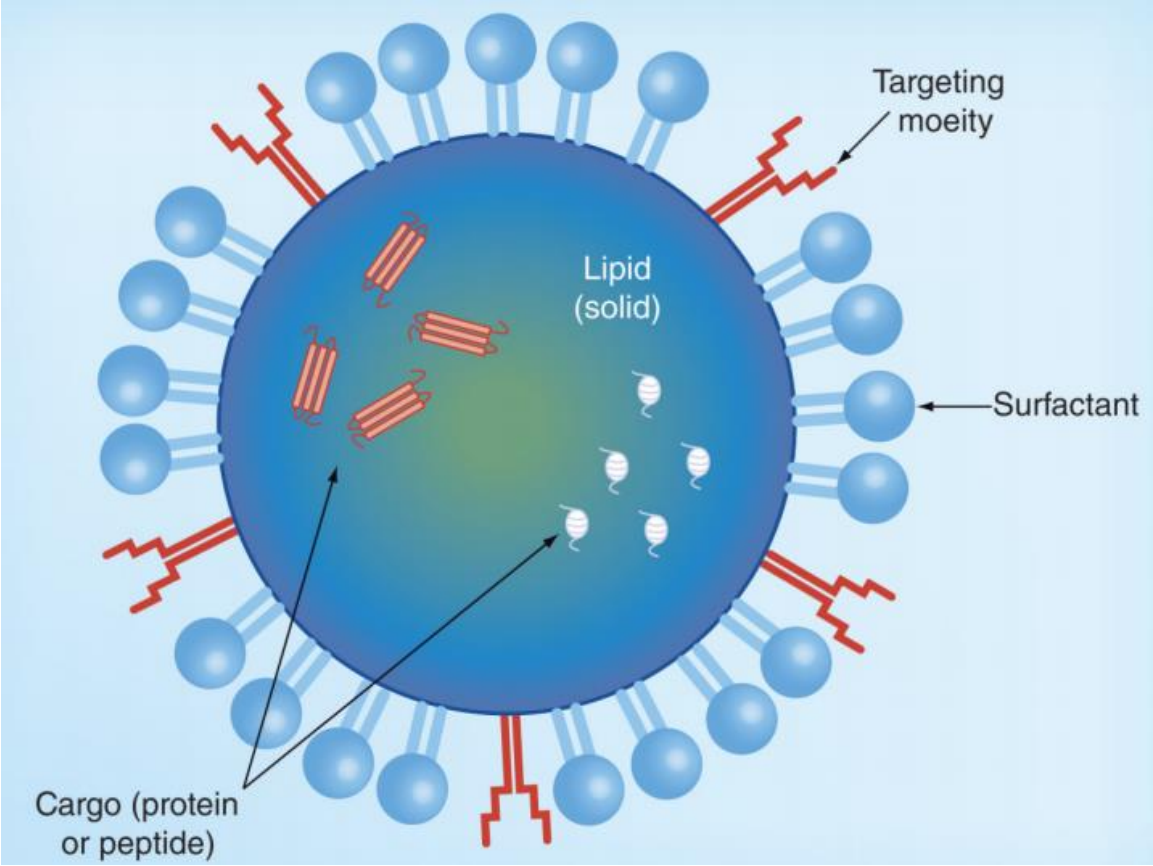

Figure 2.3. **Solid lipid nanoparticles (SLN).** SLN has a solid lipid core and is coated with surfactant. Targeting moieties may be added to decorate the surface of the SLN. Cargo for SLN shown as peptides or proteins, but may also include siRNA or small molecule drugs.

SNAC (*n*-(8-[2-hydroxylbenzoyl]amino)caprylic acid) can be used to orally deliver active peptides into circulation [133, 134]. The peptide/protein therapeutic is mixed with SNAC which creates a noncovalently linked drug-carrier complex. The complex is highly lipophilic and is proposed to be able to directly cross the epithelial membrane. After absorption, the complex dissociates by simple dilution, and the therapeutic is released, unchanged and in its active conformation [73, 133]. This system has shown promise in both human and animal models for the oral delivery of insulin, human growth hormone (hGH), and sCT [134].

A second such system is the "gastrointestional mucoadhesive patch system" or GI-MAPS, depicted in Figure 2.4. The GI-MAPS system is composed of four layers contained in an enteric capsule, which combined result in protection of the protein in the GI tract as well as increased absorption. The backing is made of ethyl cellulose, while the surface layer is made of an enteric, pH sensitive polymer, in this case Eudragit L100. The middle layer is a cellulose membrane which contains both the drug and absorption enhancers. The surface layer is attached to the middle layer via an adhesive layer made of Hiviswako 103 polymer [135].

When the capsule is swallowed, the enteric coating dissolves in the small intestine. Once this layer dissolves, the mucoadhesive layer of the patch is exposed. The patch therefore adsorbs to the mucus membrane of the small intestine, exposing the drug and absorption enhancer to the epithelial surface. When the patch attaches, it provides increased contact time, allowing more of the drug to be absorbed. Additionally, a large concentration gradient is created across the epithelial cells, increasing the amount of drug absorbed [135]. While these are two examples of systems, Table 2.6 has a more complete

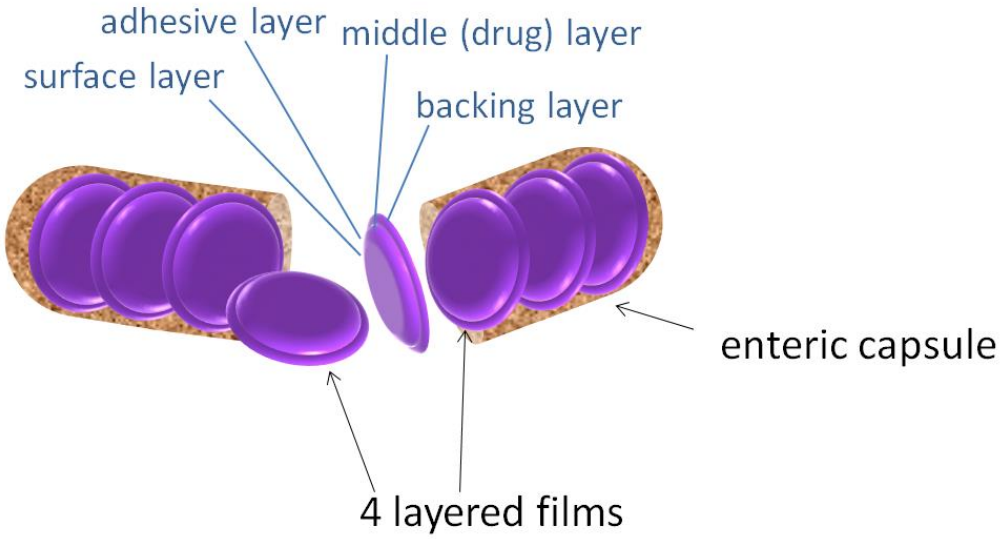

Figure 2.4: GI-MAPS system. The system contains 4 layered films in an enteric capsule. Layer 1 is the backing layer; layer 2 is the middle or drug layer; layer 3 is the adhesive layer; layer 4 is the surface layer.

Table 2.6. Multicomponent carrier systems. These systems are composed of multiple parts and chemicals. They are designed to allow for the delivery of a variety of peptides and proteins. GI-MAPS: Gastrointestinal mucoadhesive patch system; SNAC: *n*-(8-[2-hydroxylbenzoyl]amino)caprylic acid; GLP-1: Glucagon like peptide 1; sCT: Salmon calcitonin

SYSTEM	PRODUCT NAME	EFFECT ON ABSORPTION	THERAPEUTICS TESTED WITH THE SYSTEM
GI-MAPS	Eudragit L100, Eudragit S100, HP-55	Protection of peptide, increased exposure to GI tract	Granulocyte colony-stimulating factor
SNAC CARRIER MOLECULE	Emisphere ™	Increased membrane permeability	Insulin, calcitonin, growth hormone, GLP-1
AMPHIPHILIC OLIGOMERS	HIM2	Resists GI enzyme degradation and increases membrane permeability	Insulin, calcitonin, enkephalin, parathyroid hormone
LIPID-BASED MICROEMULSION	Macrulin ™	Protects peptide against acidic and proteolytic degradation; increased GI absorption	Insulin, sCT
PROTEIN CRYSTALLIZATION	CLEC ™	Increased stability against proteolysis	Calcitonin, lipases, polypeptides

list of similarly functional systems (adapted from [73]).

The above has been a broad overview of the issues associated with oral administration of peptide and protein therapeutics. Many systems which increase stability and absorption of these therapeutics have been described. Until a more widely applicable system is developed, every protein therapeutic will require a unique system made of combinations of the above if the drug is to be orally bioavailable. While the oral route is a preferred method of administration, other routes, too, have their benefits. The next section will address the issues with transdermal peptide and protein delivery.

Transdermal Delivery

Delivering peptides transdermally allows the avoidance of both GI degradation and hepatic first-pass metabolism of short half-life drugs while still allowing administration via an easily accessible, noninvasive route. This not only diminishes the amount of potential drug-drug interactions with combined therapies, but can also lead to better patient compliance (compared to IV injection) due to the ease of use, self-administration, and less frequent dosing characterized by the prolonged, continuous and rate-controlled drug release unique to these systems [136-140].

First and foremost, the most important barrier for transdermal delivery is the skin itself [136]. Drugs that have been delivered transdermally for some time now, namely nicotine, estrogen, and scopolamine, among others, are all small, highly hydrophobic molecules. Historically, it has been shown that the skin tends to keep out drug molecules greater than 500 Da [141], especially those molecules of hydrophilic nature [142]. After all, the main biological function of the skin is to deny entry to foreign objects. Therefore,

bypassing skin for drug entry is a necessary step to successful transdermal delivery [143].

Anatomically, the skin is made up of three major layers. The outermost portion, and first line of defense to drug entry, is the stratum corneum [144]. This layer, mainly comprised of dead cells (keratinocytes), is approximately 10-15 μm thick and surrounded by a lipid extracellular matrix. Below the stratum corneum lies an avascular layer, approximately 50-100 μm thick, known as the viable epidermis. Taken together, these two layers are known as the full epidermis. Below the full epidermis is the first sign of vasculature, present in a layer known simply as the dermis [140]. A fibrous layer, approximately 1-2mm thick, the dermis is comprised of large capillary beds which are the site of drug entry into the circulation [145].

Due to these obstacles provided by the skin, successful transdermal delivery of large, potentially hydrophilic peptides requires some type of physical and/or chemical enhancement. Conventional enhancements in transdermal delivery generally aim to bypass the main physical barrier, the stratum corneum [138, 146-150]. Direct entry into the dermis, despite being the most direct way to get the drug into circulation, is often avoided as penetration of this layer would lead to patient bleeding and possible disruption of nerve endings [148].

Because the traditional transdermal patch is used solely to deliver small, hydrophobic drugs, and not peptides, it will not be discussed in this section. Instead, many of the currently "in-development" transdermal enhancement methods will be briefly described, including microneedle technology, electroporation, iontophoresis, sonophoresis, thermal ablation, and chemical enhancement.

Microneedle Technology

Microneedle technology involves the use of small needles which create small pores in the skin, allowing drug passage across the outermost physical barrier [138]. Because one of the overall goals of transdermal delivery is to increase efficiency while still maintaining an easy, noninvasive technique, these microneedles are designed to breach only the stratum corneum [148]. By not reaching as far as the viable dermis, both the capillaries and nerve endings are avoided, leading to a painless feeling for the patient. These needles have been created using a number of materials, including silicon, various metals, or biodegradable materials such as some polymers and sugars [145].

As described by Herwadker and Banga [137], multiple microneedle designs and drug introduction routes have been tested for efficient delivery . One such method involves a two-step approach, where the needles are used to puncture the skin to create pores, followed by topical administration of the drug. Another method includes coating the microneedles themselves with drugs, thus allowing the drug to then enter the body as the skin is treated with the needle. A third method includes encapsulating the drug in biodegradable microneedles, slowly releasing the drug as the needles degrade. Lastly, a final method includes creating hollow needles, through which drug can be infused following puncturing of the skin. Microneedles can be introduced via physical injection on the skin or in the form of a patch. One example utilizing this technology comes from Zosano Pharma, who have developed a patch containing drug-coated microneedles capable of delivering a variety of drugs including peptides and vaccines [145].

Thermal Ablation

Like microneedle technology, thermal ablation aims to permeabilize only the stratum corneum, avoiding a breach of the deeper capillary and nerve-containing tissue layers [150]. However, instead of using needles to perforate the skin, this technique relies on short pulses of high heat (around 100°C) to create small, reversible channels in the micron size-range [151]. Following the short bursts of heat, drug can be applied to the treated area for entry into the circulation. Multiple systems have been designed to successfully deliver drugs via thermal ablation, including PassPort® (Nitto Denko) and ViaDor® (Syneron Medical Ltd). While these systems have shown success with smaller drugs, delivery of peptides is still under study [145].

Electroporation

Electroporation utilizes very short pulses of high voltages (between 10 and 100 V) to perforate the skin. Similar to microneedles and iontophoresis, application of electroporation breaches only the stratum corneum, characterizing it as another noninvasive method for drug introduction [152]. Instead of simply targeting the layer of dead cells, this method targets the surrounding lipid bilayers which are spread out throughout this layer. Application of electric current disrupts the structure of these lipids, allowing molecules to penetrate the skin. In addition, delivery of drug can be increased using this method by increasing the voltage, number of pulses, and duration of pulses to levels still viewed as safe for the patient [137]. Due to the high complexity of these systems, no peptides have been FDA approved for delivery by electroporation. However, multiple DNA-based vaccines are in clinical trials, which, if successful, could pave the way

for other peptide-based vaccines.

Sonophoresis

Sonophoresis, also referred to as cavitational ultrasound, relies on the application of sound waves to the skin to increase its permeability. Like electroporation, sonophoresis achieves this task by targeting the lipid bilayers imbedded in the stratum corneum [137]. Sound waves, generally between 20-100 kHz, are believed to cause an increase in pore sizes on the skin (increased fluidity in these lipid bilayers), thus allowing drug penetration transcellularly through stratum corneum [151]. Though nothing is currently FDA approved, delivery of insulin for Type I diabetes using the U-Strip system (Transdermal Specialties, Inc.) is presently in clinical trials, parts of which are expected to be completed within a year [153].

Iontophoresis

Not all methods utilized for transdermal peptide delivery require physical disruption of the skin's outer barrier. Iontophoresis is one of those methods, which instead uses principles of both electrorepulsion (for charged peptides) and electroosmosis (uncharged peptides) to act on the drug molecules themselves rather than the skin [137]. Generally speaking, iontophoresis utilizes a device placed on the skin capable of generating an electric current, similar to a battery. When delivering charged peptides (negatively charged peptides for instance), the battery builds up a strong negative charge at the anode, which would be placed on the same portion of the skin as the drug molecules. Utilizing charge-charge repulsion, this anode will drive the negatively-charged peptide into the skin

[136, 154]. Using this method, the rate of drug release can be controlled as the release (entry into the body) is directly proportional to the current being administered on the skin [151]. Although peptides have yet to see FDA-approval for delivery via iontophoresis, the system has been fine-tuned to deliver smaller molecules such as lidocaine (LidoSite®, Vyteris). In addition, iontophoretic peptide delivery, including delivery of gonadotropin releasing hormone and insulin, has reached clinical trials on multiple occasions [145].

Biochemical Enhancement

A final method involves the use of biochemical molecules to enhance permeation of peptide drugs across the skin. The ultimate goal in using biochemical enhancers is to increase the permeability of the skin, which provides a path for peptide drug delivery into the circulation [151], while remaining nontoxic, nonirritating, and nonallergenic [144]. One such peptide used to enhance skin permeability is magainin, a 23 amino acid peptide known to form pores in bacterial cell membranes [155, 156]. While previously shown to increase the permeability of small molecules, its use for peptide delivery enhancement still requires optimization [157]. In addition, recently, work by Ruan et al. showed the ability of a small peptide known as TD1 to increase the transdermal penetration capability of human epidermal growth factor (hEGF) when fused together [142, 158]. This fusion system involving TD1 could have major implications in the near future for delivering hydrophilic peptides transdermally.

To summarize, all of the methods described above aim to make the drug delivery process as easy and as painless as possible. Painless, in these cases, requires avoiding a breach of the viable dermis layer of the skin, which includes vasculature and nerve endings.

However, other barriers still exist, making this delivery process more efficient. Despite moderate success seen using the previously described physical and chemical enhancement methods, a recent study suggests that bypassing more than simply the stratum corneum is necessary for the most efficient transdermal delivery [140]. In addition, despite displaying low activity compared to other locations in the body, proteases do exist on the skin, adding another challenge to transdermal delivery of peptides.

Other Delivery Routes

While this review has focused on delivery of peptides by oral and transdermal routes, delivery by other routes is also currently being researched. The next section of the review will give a brief overview and recommendations for readings on intranasal, buccal, pulmonary, and rectal administration of peptide therapeutics. These routes of administration are shown in Figure 2.1.

The intranasal route for peptide drug delivery is an area which has already had some successes. For instance, desmopressin, calcitonin, and the seasonal influenza vaccine are already available via the intranasal route [159], [160]. Advantages of the nasal route over injected medications include increased patient convenience and comfort, elimination of needle-stick related injuries and infections, and decreased syringe-related medical waste [160]. Disadvantages include nasal irritation, limitations on volume and milligram amount of drug that can be delivered nasally, the rapid renewal of nasal epithelium, acidic pH, endo- and exopeptidases, and large interpatient variability in absorption [160]. While the nasal route has traditionally been thought to be an option only for small molecules, highly effective and nonirritating absorption enhancers have been developed [161]. For a more

thorough review on intranasal peptide delivery, see Illum et al. [159].

The buccal route, administration of drug through the mucosal membranes lining the cheeks, is another option for peptide delivery [162]. Drugs delivered by the buccal route are placed in the mouth between the gums and cheek [163]. Buccal delivery has many advantages including bypassing of the GI tract and possibly first-pass metabolism, ease of use, rapid onset, large contact surface area, and is generally amenable to the delivery of hydrophilic macromolecules [163, 164]. There are limitations to buccal delivery and patient adherence such as irritation of the mucosa, low permeability to peptides, and bitter taste of many buccal drugs [163]. Absorption enhancers and bioadhesive polymers are being used to resolve these problems. Oxytocin, insulin, sCT, and GLP-1 have all been successfully delivered via the buccal route [163, 164]. For further reading on buccal peptide delivery, see Mujoriya et al. [164].

Rectal administration of drugs, while not patients' top choice, is sometimes necessary if other routes of administration (such as oral and IV) are not possible. The rectum is comprised of a one layer thick epithelium complete with mucus and tight junctions [165]. While there are no villi, the surface area for drug absorption is approximately 200-400 cm^2 [165]. Rectal administration is useful due to the minimal amount of proteases and avoidance of the first-pass effect. However, the bioavailability of peptides is low without the use of absorption enhancers [165]. Both insulin and pentagastrin have been successfully delivered via the rectal route. See Lakshmi et al. for a more in-depth discussion of rectal peptide delivery [165].

The pulmonary route can be utilized for the systemic delivery of peptide therapeutics. However, the anatomy of the lung creates many barriers to delivery including

respiratory mucus, mucociliary clearance, alveolar epithelium with TJs, pulmonary enzymes, and macrophages which secrete peroxidases and proteases [166]. The alveolar epithelium and capillary endothelium have high permeability to many lipophilic substances, but passage of large hydrophilic molecules is limited [166]. Many absorption enhancers and enzyme inhibitors that have been used to increase peptide absorption have been shown to be damaging to lung tissue [166]. Pulmonary delivery of insulin has been extensively studied and was US-FDA approved in 2006, but Pfizer discontinued production in 2007 due to poor sales [166, 167]. Calcitonin, hGH, parathyroid hormone (PTH), and desmopressin have also successfully delivered via inhalation [166, 168]. A complete review of pulmonary peptide delivery can be found in the paper by Agu et al. [168].

Systemic Peptide Stability and Site-Specific Delivery

Unfortunately, once the peptide has gained entrance to the systemic circulatory system, the task is only halfway complete. The protein must still reach its target site, and as many of the targets for protein drugs are intraceullular, this means transport through the circulation to the appropriate site, uptake by the appropriate cells, and activity of the protein inside these cells. Therefore, the goals for the protein in the circulatory system include: avoidance of enzymatic degradation; opsonization and the RES; nonselective accumulation of the protein; maintenance of protein solubility and activity; distribution to the site of action with targeting to certain cell types; cellular uptake and release of the active protein. This portion of the paper will discuss many of the systems and methods mentioned earlier, but now focusing on issues within systemic circulation. Some of the systems discussed are not amenable to oral or transdermal delivery and would necessitate IV delivery. Strategies

discussed here include: stability enhancers, drug carriers, endosomal escape, and targeting moieties.

Systemic Stability Enhancement

Many of the stability enhancers discussed in the first portion of this review have a role in increasing the systemic stability of protein therapeutics as well. For example, fatty acid conjugation leads to extended plasma half-lives, site specific delivery, and sustained release upon IV administration [50]. As these drugs are lipophilic, they will likely be solubilized and stabilized by albumin and other serum lipoproteins [50]. Furthermore, these fatty acids can be removed from the protein via chemistry based on pH, reduction, peptidases, or esterases [50]. Nonreversible lipidization is also an option, and has been shown to increase internalization and activity over nonlipidized counterparts [169].

PEGylation

PEGylation has also been used as a systemic stability enhancer. Direct PEGylation can aid in the stability of proteins for delivery, leading mainly to an increase in circulation time. PEG molecules are highly hydrated, and this increased size leads to decreased glomerular filtration [37]. Moreover, PEGylation of proteins is thought to reduce proteolysis and opsonization [170]. PEGylation also reduces uptake by the RES, decreases the formation of antibodies against the protein, and decreases the apparent volume of distribution [37]. PEGylation, however, does have drawbacks. Due to the size of PEG, steric hindrance may decrease the activity of the protein. Also, increased protein aggregation after PEGylation has been noted [37]. Chronic IV administration of PEG

proteins has unintended consequences such as vacuolation of the renal cortical tubular epithelium in lab animals. However, these side effects were noted only after exposure to toxic, supratherapeutic doses of PEG. Newer PEGylation methods such as living radical polymerization (LRP), free radical polymerization (FRP), atom transfer radical polymerization (ATRP) and reversible addition fragment transfer (RAFT) have allowed PEGylation with greater specificity and purity while making modification with PEG a simpler task [171].

Hyperglycosylation

Hyperglycosylation has many of the same benefits as PEGylation, namely increased half-life, improved solubility, and reduced immunogenicity [37]. An additional benefit is that the oligosaccharides added via glycosylation are natural and biodegradable, thus skirting the possible problem of PEG accumulation with chronic administration. The increased stability of hyperglycosylated peptides may be due to masking hydrophobic sites on the protein surface involved in noncovalent interactions that lead to aggregation, loss of activity, and/or increased immunogenicity [172]. Hyperglycosylated therapeutic proteins may however see decreased activity due to steric hindrances [37].

Liposomes

Liposomes show great potential as a carrier system for systemically administered protein therapeutics. If constructed from biocompatible and biodegradable materials, liposomes cause very little to no antigenic, pyrogenic, allergic, or toxic reactions [173]. Further, liposomes can be nonimmunogenic and have already shown delivery of a variety

of active protein therapies to cells in vivo [4]. Liposomes have been used to cross the blood brain barrier to deliver an active enzyme when injected in the tail vein of a rat [4, 174]. While first generation liposomes are easily cleared from the bloodstream and accumulate in Kupfer cells of the liver and macrophages in the spleen, advances have begun to reduce these problems [173]. To start, PEG-grafted liposomes have increased circulation time, reduced aggregation, and decreased capture by the RES. PEGylated liposomes, or Steath ™ liposomes, have been used to deliver the anthracycline chemotherapeutic doxorubicin and were able to deliver preferentially to the tumor site, likely via the enhanced permeability and retention (EPR) effect [175].

Fusogenic Modifications to Liposomes

Many modifications have been made to liposomes to increase intracellular delivery of proteins. When liposomes enter the cell they are contained in an endosome. Particles smaller than 300 nm usually do not enter cells through the endosomal pathway, but particles of size 500-700 nm are often taken up by endocytosis [176]. If the liposome or the contents of the liposome do not escape the endosome, the endosome will deliver its contents to the lysosome, where the therapeutic peptide will be digested. One method of facilitating endosomal escape is to include a pH-sensitive element into the liposome. The pH in the endosome is around 5, and many systems take advantage of this relatively low pH to allow liposomes to escape the endosome [176]. Methods for endosomal escape include pore formation in the endosomal membrane, the proton sponge effect, and fusion with the endosomal membrane [176].

Pore formation is based on a pore-forming or pore-enlarging molecule binding to

the rim of a pore in the endosome. Once bound, the pore-forming agent reduces tension in the membrane, which then keeps the pore radius stable.[176]. Therefore, these agents act to stabilize naturally forming pores rather than to form pores *de novo* [177]. Pore forming compounds include penton base, cholera toxin, melittin (the major ingredient in bee venom), and Shiga toxin [178-181]. The pH buffering effect, also known as the proton sponge effect, occurs when the low pH in the endosome leads to the protonation of molecules contained inside the endosome. If the molecule has a high buffering capacity, protonation leads to an influx of H^+, Cl^-, and H_2O, resulting in osmotic swelling and eventual endosomal rupture [176]. Examples of molecules causing the proton sponge effect include gp41 with polyethyleneimine, poly (l-histidine), and chloroquine [182-185]. Fusion within the endosome requires fusogenic peptides which undergo conformational changes with the lowered pH, allowing fusion with the lipid bilayer of the endosome [176]. For example, a decrease in pH converts hemagglutinin, a protein in the capsid of the influenza virus, from an anionic hydrophilic coil to a hydrophobic helical conformation, followed by fusion of the viral membrane to the endosomal membrane. Fusogenic peptides used in liposomes include the HA-2 subunit of hemagglutinin, influenza-derived diINF-7, the major envelope protein E of the West Nile Virus, glycoprotein H from Herpes Simplex Virus, and KALA based on HA-2 subunit of influenza hemagglutinin [176, 178, 186-189]. For a complete discussion of endosomal escape pathways, please see Varkouhi et al. [176].

One more fusogenic agent worth mentioning in detail is dioleylphosphoethanolamine, or DOPE. This peptide exhibits a conical shape due to its small and minimally hydrated headgroup compared to its highly lipophilic tail [173]. It can be used as a stabilizer in cationic liposomal membranes, but its major activity concerns

endosomal escape [173]. As the pH drops in the endosome containing a DOPE-liposome, it is hypothesized that DOPE displays an inverted hexagonal phase, which in turn destabilizes the endosomal membrane [190]. DOPE has been used to deliver Print3G, a hydrophilic 25-amino acid antagonist of an oncoprotein involved in breast cancer. Print3G was enveloped in a Stealth ™ pH-sensitive liposome and was able to deliver the peptide to the cytoplasm of cancerous cells [173]. While PEGylation reduced the pH dependent release, it did not hinder the cytoplasmic delivery of the liposomal cargo [191].

Micelles

Due to their large size, liposomes may have difficulty reaching the desired site of action, as the liposome may be larger than the vascular cutoff size in certain tumors [192]. If this is the case, micelles may be a better alternative. A study by Weissig et al. demonstrated this by comparing micelle and liposome protein delivery side-by-side in a Lewis lung carcinoma mouse model. The PEG-micelle delivered more of the therapeutic protein at the desired site than did the long-circulating PEG-liposome [193]. Micelles, however, have inherent problems that may prevent them from being used in the delivery of therapeutic proteins including low drug loading capacity, low stability in water (especially when diluted), short half-life in biological environments, and possible in vivo toxicity [194].

Nanoparticles

Nanoparticles play a role in the protection and delivery of peptides in systemic circulation as well. One example, the carbon nanotube, is well-studied and has been used

to deliver proteins [195]. A 2005 study by Wong and colleagues allowed for the pro-apoptotic protein cytochrome c (cyt-c) to spontaneously adsorb onto carbon nanotubes. The nanotubes were then incubated with a variety of cell lines, and the nanotubes were taken up via energy-dependent endocytosis. Once in the cell, cyt-c was released from the nanotube and caused increased apoptosis over the empty control nanotube [195]. It has been consistently reported that "well processed, water-soluble nanotubes exhibit no apparent cytotoxicity to all living cell lines investigated thus far, at least in the timeframe of days" [196]. In general, carbon nanotubes have a high propensity to cross cell membrane with the apparent mechanism being passive and endocytosis independent [197, 198]. A proposed mechanism for cell entry is similar to that of nanoneedles, where the nanoparticles perforate and diffuse through the lipid bilayer without causing damage or death to the cells [198]. However, nanoparticle targeting is not optimal, and nanoparticles often have poor tumor and tissue penetration. The EPR effect may also be overstated; thus passive targeting of nanoparticles is not as good as once thought [199].

Functionalized nanoparticles have been used to deliver antibodies, active proteins, and epitope peptides to the immune system [198, 200]. A recent study revealed new details on the mechanism of protein release from protein-loaded nanoparticle systems. The release of protein from an aliphatic polyester-based nanoparticle system was caused by bulk degradation of the nanoparticle. Moreover, intramolecular transesterification was followed by hydrolysis of the polymers, which caused the degradation [201]. Further, lyophilizing nanoparticles lead to a higher burst release of protein (40-50%) compared to nonlyophilized nanoparticles (10-20%). The authors concluded therefore that freeze-drying forms pores in the nanoparticles, thus facilitating burst release of encapsulated

protein [201].

Many types of nanoparticles other than carbon nanotubes have been used in systemic drug delivery. A type of nanoparticle made of a PCL-PEO combination was able to demonstrate increased accumulation at the tumor site as well as reduced clearance by macrophages of the liver, thus increasing the possibility of the nanoparticle taking advantage of the EPR effect [202].

Cell-Penetrating Peptides

While increased systemic circulation time and cargo stability are important factors, all of this is futile if the therapeutic is not internalized into the cells of interest. A promising and adaptable system for increased internalization is cell penetrating peptides (CPP). CPPs are short, water soluble, polybasic peptides with a net positive charge at physiological pH [203]. CPPs are able to penetrate cell membranes at low micromolar concentrations while not causing significant membrane damage [203]. The internalization method of these CPPs and their covalently attached cargo is still being debated; there is evidence of both energy independent internalization and endocytosis as the mechanism of internalization. It is currently believed that endocytotic entry followed by endosomal escape is the most common entry pathway [204, 205]. The endocytotic pathway is further broken down to include macropinocytosis and receptor-mediated endocytosis [204]. While receptor mediated endocytosis relies on clathrin, caveolin, or both for internalization, macropinocytois may be internalized regardless of cell receptor status [204].

CPPs do have a number of pitfalls, one of which is their stability in serum-containing media [206-209]. Serum proteases may inactivate the cell-penetrating peptide

itself, or the attached cargo before the complex is able to reach its target and cross the cell membrane [209]. Further, the cationic nature of most CPPs results in aggregation with negatively-charged serum proteins [206, 207]. The use of nonnatural amino acids and cyclization of the CPP have been utilized to improve the stability of the CPP [208, 210], but stability in serum and in vivo models is still problematic. Details on preclinical and clinical trials using CPPs will be discussed in Chapter 5.

Hydrocarbon Stapling

As mentioned in the introductory chapter, α-helices are common protein secondary structures that have important roles in protein-protein binding [211]. However, α-helices tend to lose their structure when in isolation, which can affect their binding affinity [212]. One of the earliest attempts to stabilize α-helices utilized lactamization between lysine and glutamic or aspartic acid to create an intramolecular amide bond [211]. Indeed, this so-called 'lactam staple' resulted in increased helicity of a model hydrophobic peptide [213]. Blackwell and Grubbs were the first to implement ruthenium-catalyzed ring closing metathesis (RCM) stapling to stabilize peptides (Figure 2.5a)[214, 215]; briefly, Blackwell and Grubbs substituted two O-allyl serine at i, i+4 spacing into a hydrophobic heptapeptide, and covalently joined these UAAs via RCM [214]. With this proof-of-concept study in hand, Schafmeister and Verdine created the first all-hydrocarbon stapled peptide utilizing Blackwell and Grubbs's ruthenium- catalyzed ring-closing metathesis (RCM) [216]. After incorporating α,α disubstituted unnatural amino acids (UAAs) one (i,i+3 or i,i+4) or two (i,i+7) (Figure 2.5b) helical turns apart, the Verdine group optimized the stereochemistries of the UAAs as well as the length of the hydrocarbon linkers [216]. The resulting stapled

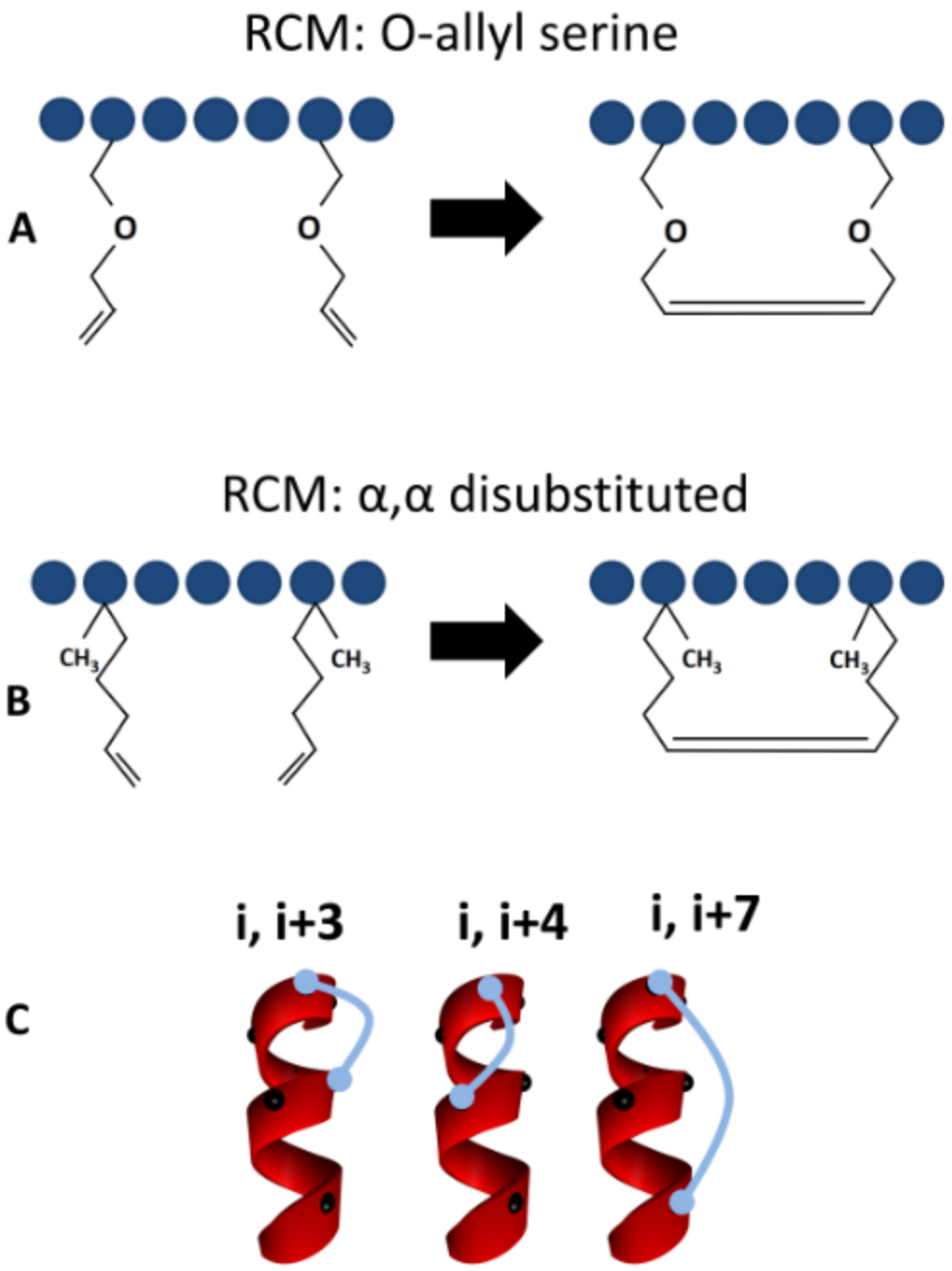

Figure 2.5. Innovative peptide stapling chemistries. A) Peptide stapling scheme implemented by Grubbs and Blackwell. B) First all-hydrocarbon peptide staple. C) Representation of common staple lengths. Adapted from [217]

peptides demonstrated increased helicity and up to 50 times greater proteolytic resistance over unmodified peptides [216].

Since this work was first published in 2000, the annual number of papers on stapled peptides continues to grow, with 35 stapled peptide studies published in 2015 (Figure 2.6). Hydrocarbon stapling has been shown to increase target affinity (5-5000 fold), improve cell permeability via pinocytotic uptake, and grant strong protection against proteolysis [51, 53, 217]. To date, stapled peptides have been investigated for targeting both intra- and extracellular targets. Some notable intracellular stapled peptide targets under investigation include p53/MDM2, BH3 domains/MCL-1, axin/β-catenin, and E1/CD81 in hepatitis C [218] [219-223]. Extracellularly, stapled peptides have been utilized to target and inhibit ABC transporters, estrogen receptors, and have even been utilized in the creation of a long-acting growth hormone-releasing hormone (GHRH) analogue, which underwent a Phase 1 clinical trial in 2013 (results not disclosed). [217, 222, 224].

Beyond a variety of targets, the field of stapled peptides has also expanded the chemistry of stapling techniques. Many early adaptions to stapling chemistry are considered 'one component' staples. One component staples usually require nonnative amino acids which bear functional groups which are joined to create the staple (Figure 2.7a) [211]. The requirement of UAAs means these peptides must be synthesized, which practically limits production to peptides of a maximum 30-50aa in length [225]. While the length and chemical identity of the staple can be altered, this must be done by altering the UAAs, which can be challenging [211, 217]. Two-component systems involve a bifunctional linker compound which is ligated to the peptide and itself becomes the staple (Figure 2.7b). Two-component systems grant researchers great flexibility in staple choice,

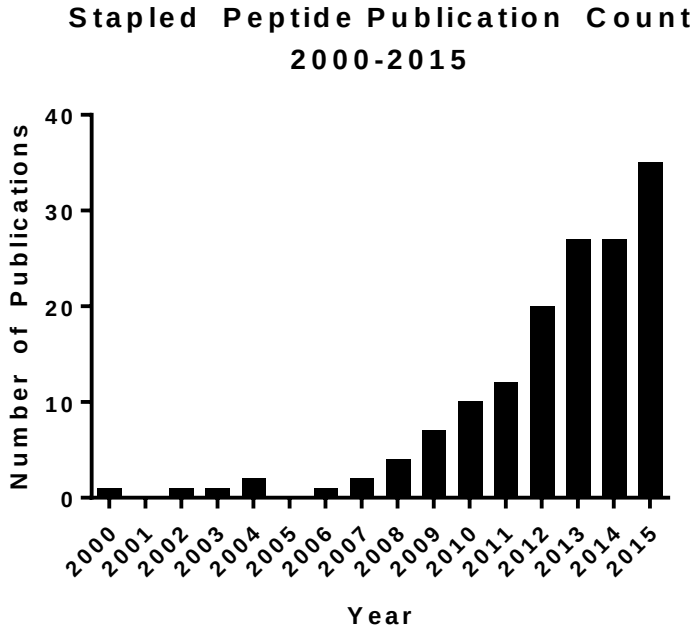

Figure 2.6. Stapled peptide annual publication count. Number of annual 'stapled peptide' research publications, as reported by MEDLINE.

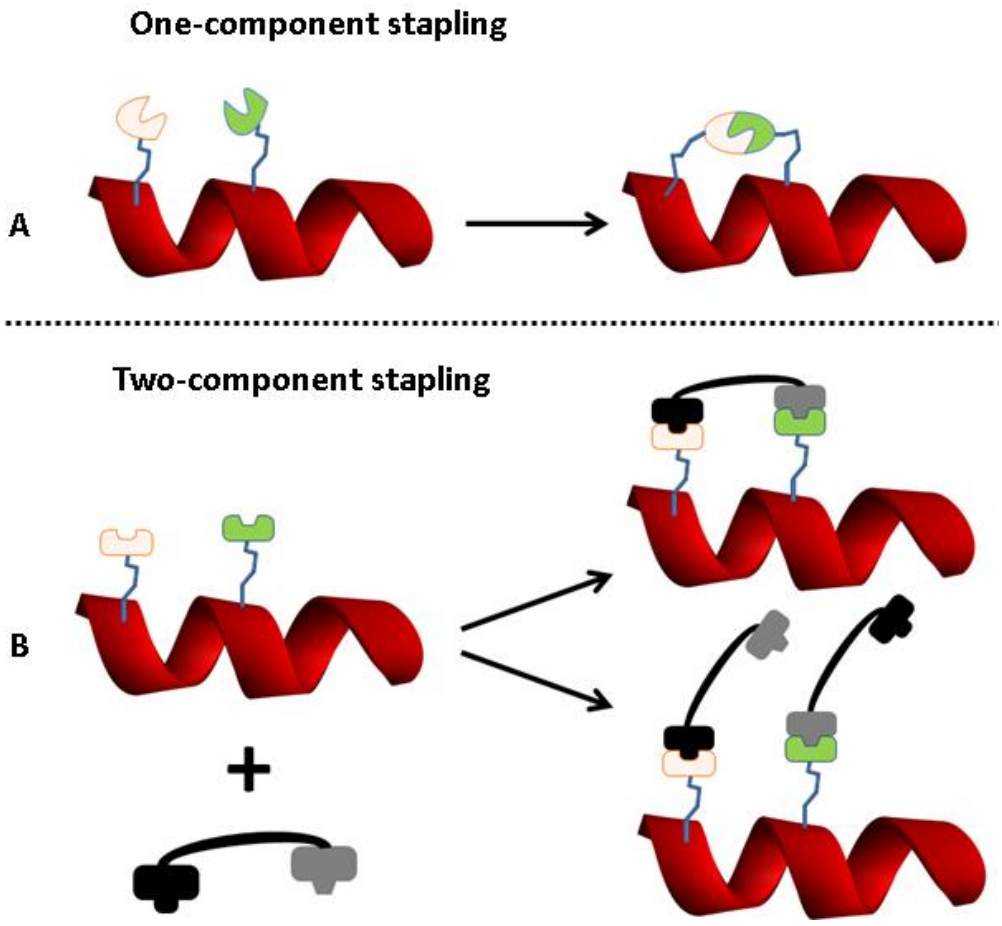

Figure 2.7. One- and two-component peptide stapling. Representation of one-component (A) and two-component (B) peptide stapling. 2B shows the favorable, stapled outcome (top) as well as the disfavored (tethered, unstapled) outcome (bottom).

and can allow for rapid screens to optimize staple chemical makeup and length without needing to alter the peptide itself [211]. However, it is also possible for the peptide to react with two separate staple molecules at the staple sites (Figure 2.7b), a side-reaction that is not possible in one-component systems. Table 2.7 includes the characteristics of some of the most commonly used stapling techniques.

Thiol-ene peptide stapling, first published by Wang and Chou in 2015, utilizes the well-known thiol-ene click reaction (Figure 2.8) to staple cysteine-containing peptides [225, 226]. Importantly, as the stapling can be done off the thiol groups of cysteines, this method does not require UAAs. Stapling off cysteines theoretically allows for the stapling of recombinant (rather than synthesized) peptides, which opens the door to stapling larger peptides and proteins. In this work, the researchers tested various reaction conditions, staple length, and chemical makeup and the resulting peptide helicity, proteolytic resistance, and in vitro activity [225]. Importantly, this reaction was shown to be specific for thiol groups, even when other functional groups (such as amines, alcohols, and carboxylic acids) are present [225]. Further, Wang and Chou created a thiol-ene stapled version of Walensky and Verdine's p53-MDM2/MDMX inhibitor that was able to recapitulate everything seen with the RCM stapled peptide (helicity, proteolytic resistance, cell internalization, inhibition of p53-MDM2/MDMX interaction, and apoptosis induction) [225]. The relatively long length of CC^{mut3} (72aa) protein meant it was 'un-stapleable' with older techniques. However, as this thiol-ene stapling does not require UAAs and SPSS, it is now possible to staple recombinant CC^{mut3}.

Table 2.7. Stapled peptide chemistries and characteristics.[211, 218-221, 225, 227, 228]

	Modification	Natural AAs	Chemical Stability	Structural Versatility
One-Component	Lactamization	-	+	+
	RCM	-	+	++
	Click Chemistry	-	+	+++
	Disulfide Bridges	+	-	-
	O-N Acyl Transfer	-	+	+
Two-Component	Photoswitchable Linkers	-	+	+
	2-Component Click Chemistry	-	+	+++
	Phe Derivatives	+/-	+	-
	Thiol-ene	+	+	+++
	Photoswitchable Linkers	-	+	+

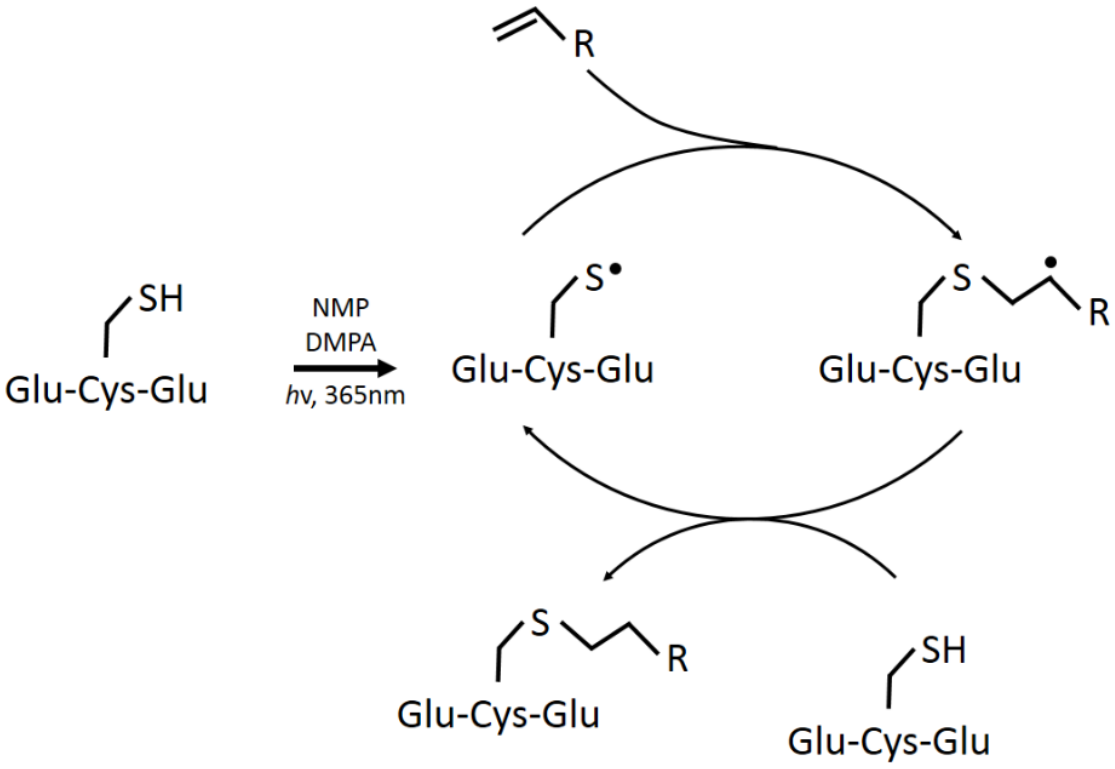

Figure 2.8. Thiol-ene stapling reaction scheme. A peptide containing two cysteines is combined with the radical initiator 2,2 dimethoxy-2-phenylacetophenone (DMPA) in the organic solvent N-methyl-2-pyrrolidone (NMP). Irradiation results in radicalization of the sulfur in cysteine. This radical reacts with the alkene-containing staple, and the free radical is then transferred to another cysteine, allowing the reaction to continue.

Design Principles

To date, there exist no 'hard and fast' rules regarding stapled peptide design; researchers are regularly surprised, often unpleasantly, by the helicity, permeability, and/or binding affinity of their stapled peptides. However, certain guidelines on design have been developed over the last 15 years. First, the staple should either be opposite (fully solvent exposed) or adjacent (partially solvent exposed) to the binding interface, as to not sterically interfere with binding [229]. Interestingly, some partially exposed staples have been shown to themselves participate in target binding via van der Waals contacts, as seen with some of the BH3 mimetics [229]. Adjacent stapling also decreases the entropic penalty of solvation for the hydrocarbon, which may aid in aqueous solubility [229, 230].

Second, as all stapling reactions to date require specific amino acids at stapling sites, critical interacting residues should not be replaced. The goal is to decrease the entropic cost of binding by locking the peptide in its α-helical conformation without negatively affecting the enthalpy of binding. Towards this same goal, UAA selection, stereochemistry, and linker length have been optimized for RCM. For i,i+7 staples, R,S or S,R stereochemistries for the UAAs are most commonly used along with an 11-carbon linker [229]. Staple length will have to be optimized independently for each of the staples to be used in two-step reactions, although the size of the linkers is generally comparable to those in RCM reactions [211, 217, 225, 229]. The Verdine group recently published a new technique known as 'peptide stitching', which creates a stapled peptide i, i+7, i+11 – that is, there are two hydrocarbon staples, both sharing an anchor point on a disubstituted UAA at the i+7 position. Optimal UAA stereochemistry and hydrocarbon linker lengths for peptide stitching are similar to those of standard peptide stapling [231, 232].

Computational modeling is commonly utilized in the design of stapled peptides. As it can be expensive (in time and money) to synthesize, staple, and test the activity of stapled peptides, any method that can reduce the frequency of inactive peptides is useful. Energy minimization, the simplest and fastest of the commonly used computational techniques, can determine comparative energy minima of different stapled peptides. However, this method requires *a priori* knowledge of the peptide's structure in solution. Further, the simulations cannot calculate energy minima for conformations grossly different from the starting conformation, another limitation [229]. Monte Carlo simulations work similarly, but they generate an ensemble of conformations by making *random* changes to the positions of atoms at each step, which allows this simulation to sample conformations that are quite different from the starting conformation [229]. Finally, Molecular dynamics (MD) simulations integrate Newton's equations of motion to describe the "temporal evolution of a set of interacting atoms"[229] . MD is quite accurate at predicting peptide helicity, which is extremely useful at the early stages of a project [229, 233, 234].

As the majority of stapled peptides have been designed to inhibit intracellular protein:protein interactions, cell penetration of stapled peptides is prerequisite to their function. Although much work has been done to determine the exact mechanism of cell permeation by stapled peptides, it is not yet known [230, 232]. The process is known to be clathrin- and caveolin-independent endocytosis, although the peptides appear to exploit an as-of-yet uncharacterized pathway [235]. However, cell surface proteoglycans are thought to be involved [232]. Certain characteristics such as α-helicity, overall charge, hydrophobicity, staple composition and placement affect stapled peptide internalization

have been understood to play a role in stapled peptide internalization, but until recently, the exact contribution and importance of each was unknown. The Verdine group recently tested over 200 stapled peptides which cover a large range of all of the aforementioned characteristics [232]. They found that a formal charge between 0 and +2 was optimal for nondamaging cell penetration. Although larger positive formal charges corresponded with greater peptide internalization, they also are linked to membrane damage [232]. The Walensky group carried out their own analysis and found that staple location (partially solvent-exposed), and helical content are the best predictors of stapled peptide membrane penetration sans membrane disruption as tested by electron microscopy and lactate dehydgogenase assays [217, 230]. Stapled peptides with approximately 60-90% helicity and pIs between 8.8 and 9.3 demonstrated optimal cellular uptake. However, Walensky et al. found little correlation between formal charge and cell penetration for stapled peptides, and found that large positive charge and higher pI (greater than 9.7) are associated with membrane damage [230]. Further, these peptides cross the cell membrane without damage and efficiently escape the endosome [231] . This may not be surprising, as the first stapled peptide against an intracellular target that has made it to clinical trials has a net charge of -1 [236]. A clearer picture of the pro-internalization characteristics may become clearer as more stapled peptides are created with variations in all of the aforementioned characteristics.

Targeting and Membrane Permeation

CPPs are a versatile tool which can be used for increased internalization of liposomes, nanoparticles, or proteins themselves [237-239]. CPPs have been extensively

researched as supplements to liposomes, and a few issues have been uncovered. First, CPPs like Trans-activating transcriptional activator, TAT, are susceptible to enzymatic cleavage by plasma enzymes when they are on the surface of liposomes [237]. Also, CPP-modified liposomes can cause severe toxicity and are rapidly cleared from the blood and accumulate in the kidney and liver; therefore, PEG modification is often necessary when using CPPs with liposomes [240-243]. Unfortunately, PEGylation of CPP-modified liposomes appears to decrease the effectiveness of the CPP [244]. TAT and arginine-rich CPPs have been used to target the kidney and spleen, respectively [245, 246]. One study demonstrated that R8 (8 arginine repeat) modified lipid nanoparticles were able to efficiently deliver cargo (in this case siRNA) to the cytosol of cells in the liver [247]. Further, hydrocarbon stapling of CPPs increases their stability and cell permeability [232].

CPPs have also been directly conjugated to proteins for delivery in vivo and in vitro [248-253]. One successful example of in vivo use delivered a single chain antibody Fv fragment to tumors, resulting in a decrease in tumor volume and neovascularization *[251]*. Targeted CPPs have also been discovered and designed. The specificity is often gained via activation of the CPP in the tumor environment or by conjugating a targeting moiety to the CPP [254-256]. Selectivity can also be obtained by having a homing motif in the CPP sequence; Nishimura et al. have discovered a CPP screened by phage display that selectively transduces leukemia cells [257]. The CPP consists of a lymph-node homing motif (CAY) and the CPP motif (RLRR), with the full sequence being CAYHRLRRC [257]. This CPP is currently being utilized in our lab to deliver a protein therapeutic for CML therapy. CPPs are appealing, as they may be able to increase the delivery of protein therapeutics through the cell membrane, escape from endosomes, and get into the

cytoplasm of the desired cells. Table 2.8 provides a representative example from a variety of CPP classes.

Antibodies are another modification strategy which has been implemented to increase the targeting ability of liposomes and nanoparticles. One study by Kirpotin and colleagues demonstrated that monoclonal antibodies (MAb) directed against the HER2 receptor increased the cytoplasmic delivery of the liposomes contents [258]. Interestingly, in this study the MAb did not alter the biodistribution of the liposome, but rather increased MAb-mediated endocytosis which increased drug delivery to the cytoplasm. Similar methods have been used with PLGA nanoparticles [259]. Researchers were able to demonstrate in vitro selectivity and increased internalization of the MAb-adsorbed nanoparticles [258]. As both liposomes and nanoparticles can be loaded and/or coated with therapeutic peptides, targeting via antibodies can lead to increased peptide delivery to a specific site or cell type. The conjugation and adsorption of antibodies to liposomes and nanoparticles is a promising field; further research will likely produce translatable results which will aid in the targeting of therapeutics.

Conclusions and Future Perspective

While proteins and peptides have immense therapeutic potential, delivery and systemic stability currently limit their clinical use. The oral route is appealing, as it is a simple and often cheap route of delivery. Couple this with reduced consumption of the supplies needed for invasive delivery (IV, IM, SubQ, etc.), and it is easy to see why patient compliance is highest for orally delivered drugs. Peptides and proteins are readily metabolized in the GI tract, and the hydrophilic nature of most natural peptides restricts

Table 2.8. Sample CPPs and their applications in peptide delivery. This table contains representative CPPs which represent the major classes of targeted and untargeted CPPs. TAT and Penetratin are generally untargeted, although their biodistribution may cause site-selective accumulation. LS-CPP is a leukemia-specific CPP. The tumor prodrug CPP is cleaved at the "/" when in the tumor environment, thus separating the negatively charged amino acids from the positively charged CPP-cargo conjugate. Antibody-targeted CPPs can be used to selectively deliver a CPP-cargo conjugate to desired cell types.
CPP: Cell-penetrating Peptide; Tat: trans-activating transcriptional activator; LS-CPP: Leukemia-Specific Cell-penetrating Peptide; MAb: Monoclonal Antibody; HIV: Human Immunodeficiency Virus

	SEQUENCE	CATEGORY	OUTCOMES OF INTEREST
TAT	CGRKKRRQRRRPPQC	Protein Derived CPP from HIV-1	Able to deliver peptides, proteins, nanoparticles, and oligonucleotides intracellularly [260]
PENETRATIN	RQIKIWFQNRRMKWKK	Protein Derived CPP from *Drosophila* antennapedia domain	Able to deliver a variety of cargoes to many cell types[261]
LS-CPP	CAYHRLRRC	Dual-motif CPP	Specific delivery to leukemia cells[257]
TUMOR PRODRUG CPP	EEEEEDDDDK/ARRRRRRRRR	Prodrug with tumor-environment activation	Proteases in the tumor environment cleave the sequence, removing the acidic (negative) amino acid residues[254]
ANTIBODY-CPP CONJUGATE	Penetratin+MAb CC49	MAb targeted CPP	Increased tumor: normal tissue delivery ratio[252]

movement across the epithelial barrier. Advances in the oral delivery of proteins and peptides have been made by the use of absorption enhancers, enzyme inhibitors, and direct structural modification of the therapeutic. Mucoadhesive polymers, nanoemulsions, and nanoparticles have been utilized to increase the stability of peptides as well as increase their absorption. However, as of yet no generalizable strategy for the delivery of peptide and protein therapeutics has been found; many of the strategies in this paper were customized to the peptide being delivered, as the complex nature and variety of peptides and proteins makes this difficult. Work on generalizable peptide delivery systems is ongoing; both the GI-MAPS and SNAC systems show encouraging data and appear to be well suited to deliver a large range of peptides. With all of these systems, however, safety and efficacy questions loom large. Long-term safety has not been studied, and safety issues have arisen even with the short-term use of some of the compounds discussed in this review.

By delivering drugs transdermally, issues with GI stability can be avoided, but absorption still poses problems. Systems developed to overcome the barriers posed by the skin include microneedle technology, thermal ablation, electroporation, sonophoresis, and iontophoresis. Each of these systems was designed with patient comfort and ease of use in mind. Despite some successes with transdermal delivery, most of the systems above have not been used to deliver therapeutic peptides or proteins to humans; further development and study in this area is necessary. While peptide delivery by other noninvasive routes (pulmonary, intranasal, buccal, rectal) is being studied, other reviews provide a more complete coverage of these topics.

After a peptide therapeutic enters the systemic circulation, it must remain active

and reach the correct site/cell type in the body. Direct peptide modifications, liposomes, and nanoparticles are used to increase stability while the addition of antibodies and CPPs are used for targeting and to supplement cellular delivery. Endosomal escape, which threatens to inactivate the therapeutic peptide at the last stage, has also had some promising advances. It is important to note that some of the methods which increase systemic stability are not currently amenable to oral delivery (e.g., liposomes).

Peptide and protein therapeutics, with their high target specificity and broad applicability, have the potential to revolutionize medical therapy. Clearly, there are still challenges to overcome in each of the areas discussed. Optimally, in the future there will be a system that can be used for the oral delivery and systemic stability of a variety of peptides and proteins. As delivery and systemic stability are two overarching issues with protein and peptide therapeutics, overcoming these would likely lead to even further development of peptide and protein therapeutics with great therapeutic potential.

Funding and Acknowledgements

This work was funded by NIH R01-CA129528, NIH R01-CA151847, and by an AFPE Pre-Doctoral Fellowship . We would like to thank Natalie Cheatham for assistance with figure illustration. The authors have no other relevant affiliations or financial involvement with any organization or entity with a financial interest in or financial conflict with the subject matter or materials disclosed in the manuscript apart from those disclosed.

References

[1] D.J. Craik, D.P. Fairlie, S. Liras, D. Price, The future of peptide-based drugs, Chem Biol Drug Des 81(1) (2013) 136-47.

[2] B. Aungst, Saitoh, H., Burcham, D., Huand, S., Mousa, S., Hussain, M., Enhancement of the intestinal absorption of peptides and non-peptides, J Control Release 41(1) (1996) 19-31.

[3] T. Borchardt, J. Aube, T.J. Siahaan, S. Gangwar, G.M. Pauletti, Improvement of oral peptide bioavailability: peptidomimetics and prodrug strategies, Adv Drug Deliv Rev 27(2-3) (1997) 235-256.

[4] V. Torchilin, Intracellular delivery of protein and peptide therapeutics, Drug Discov Today Technol (2009).

[5] UpToDate - Drug Overviews. May 2013. Available from URL: uptodate.com/drugoverviews

[6] Top 20 Best-Selling Drugs of 2012, 2013. March 2014. Available from URL: http://www.genengnews.com/insight-and-intelligence/top-20-best-selling-drugs-of-2012/77899775/?page=2.

[7] P.H.S. Department of Health and Human Services, Food and Drug Administration, Center for Drug Evaluation and Research, Office of Surveillance and Epidemilogy, Background Document for Meeting of Advisory Committee for Reproductiove Health Drugs and Drug Safety and Risk Management Advisory Committee, 2013, p. 113.

[8] Novartis Annual Report, 2013. March 2014. Available from URL: https://www.novartis.com/sites/www.novartis.../novartis-annual-report-2013-en.pdf

[9] Novartis Annual Report, 2011. June 2013. Available from URL: https://www.novartis.com/sites/www.novartis.com/files/novartis-annual-report-2011-en.pdf

[10] Victoza Sales Data. July 2013. Available from URL: http://www.drugs.com/stats/victoza

[11] M. Mitchell, The Medicines Company Reports Full Year and Fourth Quarter 2011 Financial Results. July 2013. Available from URL: http://www.themedicinescompany.com/investors/news/medicines-company-reports-full-year-and-fourth-quarter-2011-financial-results

[12] R. Gill, Desmopressin acetate drug use review in pediatric population. July 2013.

Available from URL: https://www.fda.gov/downloads/AdvisoryCommittees/CommitteesMeetingMaterials/PediatricAdvisoryCommittee/UCM214422.pdf

[13] S. Maher, D. Brayden, Overcoming poor permeability: translating permeation enhancers for oral peptide delivery, Drug Discov Today Technol 9(2) (2012) e113-e119.

[14] J.H. Hamman, G.M. Enslin, A.F. Kotze, Oral delivery of peptide drugs: barriers and developments, BioDrugs 19(3) (2005) 165-77.

[15] J. Shaji, V. Patole, Protein and peptide drug delivery: oral approaches, Indian J Pharm Sci 70(3) (2008) 269-77.

[16] R.I. Mahato, A.S. Narang, L. Thoma, D.D. Miller, Emerging trends in oral delivery of peptide and protein drugs, Crit Rev Ther Drug Carrier Syst 20(2-3) (2003) 153-214.

[17] J.S. Fruton, A history of pepsin and related enzymes, Q Rev Biol 77(2) (2002) 127-47.

[18] Y.J. Yamanaka, K.W. Leong, Engineering strategies to enhance nanoparticle-mediated oral delivery, J Biomater Sci Polym Ed 19(12) (2008) 1549-70.

[19] C. Lopez-Otin, L.H. Palavalli, Y. Samuels, Protective roles of matrix metalloproteinases: from mouse models to human cancer, Cell Cycle 8(22) (2009) 3657-62.

[20] K.Y. Choi, M. Swierczewska, S. Lee, X. Chen, Protease-activated drug development, Theranostics 2(2) (2012) 156-78.

[21] G.P. Carino, E. Mathiowitz, Oral insulin delivery, Adv Drug Deliv Rev 35(2-3) (1999) 249-257.

[22] G. Pauletti, Structural requirements for intestinal absorption of peptide drugs, J Control Release 41 (1996) 3-17.

[23] S. Khafagy el, M. Morishita, Oral biodrug delivery using cell-penetrating peptide, Adv Drug Deliv Rev 64(6) (2012) 531-9.

[24] J.R. Turner, Intestinal mucosal barrier function in health and disease, Nat Rev Immunol 9(11) (2009) 799-809.

[25] J.D. Schulzke, M. Fromm, Tight junctions: molecular structure meets function, Ann N Y Acad Sci 1165 (2009) 1-6.

[26] P.D. Eckford, F.J. Sharom, ABC efflux pump-based resistance to chemotherapy drugs, Chem Rev 109(7) (2009) 2989-3011.

[27] C. Kourtesi, A.R. Ball, Y.Y. Huang, S.M. Jachak, D.M. Vera, P. Khondkar, S. Gibbons, M.R. Hamblin, G.P. Tegos, Microbial efflux systems and inhibitors: approaches to drug discovery and the challenge of clinical implementation, Open Microbiol J 7 (2013) 34-52.

[28] S.F. Zhou, Structure, function and regulation of P-glycoprotein and its clinical relevance in drug disposition, Xenobiotica 38(7-8) (2008) 802-32.

[29] F.J. Sharom, G. DiDiodato, X. Yu, K.J. Ashbourne, Interaction of the P-glycoprotein multidrug transporter with peptides and ionophores, J Biol Chem 270(17) (1995) 10334-41.

[30] S.M. Pond, T.N. Tozer, First-pass elimination. Basic concepts and clinical consequences, Clin Pharmacokinet 9(1) (1984) 1-25.

[31] I. Buxton, Pharmacokinetics and Pharmacodynamics: The Dynamics of Drug Absorption, Distribution, Action, and Elimination, in: L. Brunton, Lazo, J., Parker, K. (Ed.), Goodman & Gilman's The Pharmacological Basis of Therapeutics, McGraw-Hill Medical Publishing Division, 2006, pp. 1-40.

[32] R.M. Balaram, The use of D amino acids in peptide design, in: H.B. Ryuichi Konno, A. D'Aniello, G. H. Fisher, N. Fujii, H. Homma, D Amino Acids: A New Frontier in Amino Acid and Protein Research - Practical Methods and Protocols, Nova Biomedica Books, 2007, pp. 415-430.

[33] H. Kaminski, Cyclosporine is derived from a fungus and is a cyclic undecapeptide with actions directed exclusively on T cells, in: H. Kaminski, Myasthenia Gravis and Related Disorders, Blackwell Publishing, 2008, pp. 393-405.

[34] C. McMartin, L.E. Hutchinson, R. Hyde, G.E. Peters, Analysis of structural requirements for the absorption of drugs and macromolecules from the nasal cavity, J Pharm Sci 76(7) (1987) 535-40.

[35] P. Vlieghe, V. Lisowski, J. Martinez, M. Khrestchatisky, Synthetic therapeutic peptides: science and market, Drug Discov Today 15(1-2) (2010) 40-56.

[36] R.B. Greenwald, Y.H. Choe, J. McGuire, C.D. Conover, Effective drug delivery by PEGylated drug conjugates, Adv Drug Deliv Rev 55(2) (2003) 217-50.

[37] D.S. Pisal, M.P. Kosloski, S.V. Balu-Iyer, Delivery of therapeutic proteins, J Pharm Sci 99(6) (2010) 2557-75.

[38] F.M. Veronese, J.M. Harris, Introduction and overview of peptide and protein

pegylation, Adv Drug Deliv Rev 54(4) (2002) 453-6.

[39] R. Webster, V. Elliot, B. Park, D. Walker, M. Hankin, P. Taupin, PEG and PEG conjugates toxicity: towards an understanding of the toxicity of PEG and its relevance to PEGylated biologicals, in: F. Veronese, PEGylated Protein Drugs: Basic Science and Clinical Applications, Birkhauser, 2009, pp. 127-146.

[40] G.A. Laine, S.M. Hossain, R.T. Solis, S.C. Adams, Polyethylene glycol nephrotoxicity secondary to prolonged high-dose intravenous lorazepam, Ann Pharmacother 29(11) (1995) 1110-4.

[41] N. Choi, J. Lee, Y. Chang, S. Jung, Y. Kim, S. Lee, J. Lee, J. Kim, H. Song, and B. Park, Polyethylene Glycol Increases the Risk of Acute Renal Failure: A Population-based Case-Crossover Study, 27th ICPE, Chicago, IL, 2011. May 2013. Available from: https://www.pharmacoepi.org/meetings/27thconf/presentations/aj_oral_presentations_key.cfm

[42] T. Ishida, M. Ichihara, X. Wang, H. Kiwada, Spleen plays an important role in the induction of accelerated blood clearance of PEGylated liposomes, J Control Release 115(3) (2006) 243-50.

[43] K. Park, To PEGylate or not to PEGylate, that is not the question, J Control Release 142(2) (2010) 147-8.

[44] P. Calceti, S. Salmaso, G. Walker, A. Bernkop-Schnurch, Development and in vivo evaluation of an oral insulin-PEG delivery system, Eur J Pharm Sci 22(4) (2004) 315-23.

[45] Y.S. Youn, J.Y. Jung, S.H. Oh, S.D. Yoo, K.C. Lee, Improved intestinal delivery of salmon calcitonin by Lys18-amine specific PEGylation: stability, permeability, pharmacokinetic behavior and in vivo hypocalcemic efficacy, J Control Release 114(3) (2006) 334-42.

[46] K.B. Chalasani, G.J. Russell-Jones, S.K. Yandrapu, P.V. Diwan, S.K. Jain, A novel vitamin B12-nanosphere conjugate carrier system for peroral delivery of insulin, J Control Release 117(3) (2007) 421-9.

[47] A.K. Petrus, T.J. Fairchild, R.P. Doyle, Traveling the vitamin B12 pathway: oral delivery of protein and peptide drugs, Angew Chem Int Ed 48(6) (2009) 1022-8.

[48] J. Wang, D. Wu, W.C. Shen, Structure-activity relationship of reversibly lipidized peptides: studies of fatty acid-desmopressin conjugates, Pharm Res 19(5) (2002) 609-14.

[49] J. Wang, D. Chow, H. Heiati, W.C. Shen, Reversible lipidization for the oral

delivery of salmon calcitonin, J Control Release 88(3) (2003) 369-80.

[50] M.J. Hackett, J.L. Zaro, W.C. Shen, P.C. Guley, M.J. Cho, Fatty acids as therapeutic auxiliaries for oral and parenteral formulations, Adv Drug Deliv Rev 65(10) (2012) 1331-9.

[51] G.L. Verdine, G.J. Hilinski, Stapled peptides for intracellular drug targets, Methods Enzymol 503 (2012) 3-33.

[52] C.E. Schafmeister, J. Po, G.L. Verdine, An all-hydrocarbon cross-linking system for enhancing the helicity and metabolic stability of peptides, J Am Chem Soc 122(24) (2000) 5891-5892.

[53] L.D. Walensky, A.L. Kung, I. Escher, T.J. Malia, S. Barbuto, R.D. Wright, G. Wagner, G.L. Verdine, S.J. Korsmeyer, Activation of apoptosis in vivo by a hydrocarbon-stapled BH3 helix, Science 305(5689) (2004) 1466-70.

[54] S. Miller, Reyna, J., Ng, S., Zuckermann, R., Kerr, J., Moos, W., Comparison of the proteolytic susceptibilities of homologous L-amino acid, D-amino acid, and N-substituted glycine peptide and peptoid oligomers, Drug Dev Res 35(1) (2004) 20-32.

[55] R. Tugyi, K. Uray, D. Ivan, E. Fellinger, A. Perkins, F. Hudecz, Partial D-amino acid substitution: Improved enzymatic stability and preserved Ab recognition of a MUC2 epitope peptide, Proc Natl Acad Sci U S A 102(2) (2005) 413-8.

[56] S. Fujii, T. Yokoyama, K. Ikegaya, F. Sato, N. Yokoo, Promoting effect of the new chymotrypsin inhibitor FK-448 on the intestinal absorption of insulin in rats and dogs, J Pharm Pharmacol 37(8) (1985) 545-9.

[57] E. Ziv, O. Lior, M. Kidron, Absorption of protein via the intestinal wall. A quantitative model, Biochem Pharmacol 36(7) (1987) 1035-9.

[58] T. Bass, Thacker, P., Impact of gastric pH on dietary enzyme activity and survivability in swine fed β-glucanase supplemented diets, Can J Anim Sci 76(2) (1996) 245-252.

[59] D.W. Piper, B.H. Fenton, pH stability and activity curves of pepsin with special reference to their clinical importance, Gut 6(5) (1965) 506-8.

[60] A. Basu, K. Yang, M. Wang, S. Liu, R. Chintala, T. Palm, H. Zhao, P. Peng, D. Wu, Z. Zhang, J. Hua, M.C. Hsieh, J. Zhou, G. Petti, X. Li, A. Janjua, M. Mendez, J. Liu, C. Longley, M. Mehlig, V. Borowski, M. Viswanathan, D. Filpula, Structure-function engineering of interferon-beta-1b for improving stability, solubility, potency, immunogenicity, and pharmacokinetic properties by site-selective mono-PEGylation, Bioconjug Chem 17(3) (2006) 618-30.

[61] A. Leone-Bay, N. Santiago, D. Achan, K. Chaudhary, F. DeMorin, L. Falzarano, S. Haas, S. Kalbag, D. Kaplan, H. Leipold, et al., N-acylated alpha-amino acids as novel oral delivery agents for proteins, J Med Chem 38(21) (1995) 4263-9.

[62] A.H. Kahns, A. Buur, H. Bundgaard, Prodrugs of peptides. 18. Synthesis and evaluation of various esters of desmopressin (dDAVP), Pharm Res 10(1) (1993) 68-74.

[63] C.S. Cook, P.J. Karabatsos, G.L. Schoenhard, A. Karim, Species dependent esterase activities for hydrolysis of an anti-HIV prodrug glycovir and bioavailability of active SC-48334, Pharm Res 12(8) (1995) 1158-64.

[64] G.H. Bird, N. Madani, A.F. Perry, A.M. Princiotto, J.G. Supko, X. He, E. Gavathiotis, J.G. Sodroski, L.D. Walensky, Hydrocarbon double-stapling remedies the proteolytic instability of a lengthy peptide therapeutic, Proc Natl Acad Sci U S A 107(32) (2010) 14093-8.

[65] T. Uchiyama, A. Kotani, T. Kishida, H. Tatsumi, A. Okamoto, T. Fujita, M. Murakami, S. Muranishi, A. Yamamoto, Effects of various protease inhibitors on the stability and permeability of [D-Ala2,D-Leu5]enkephalin in the rat intestine: comparison with leucine enkephalin, J Pharm Sci 87(4) (1998) 448-52.

[66] J.M. Chen, P.M. Dando, N.D. Rawlings, M.A. Brown, N.E. Young, R.A. Stevens, E. Hewitt, C. Watts, A.J. Barrett, Cloning, isolation, and characterization of mammalian legumain, an asparaginyl endopeptidase, J Biol Chem 272(12) (1997) 8090-8.

[67] J.K. McDonald, T.J. Reilly, B.B. Zeitman, S. Ellis, Dipeptidyl arylamidase II of the pituitary. Properties of lysylalanyl-beta-naphthylamide hydrolysis: inhibition by cations, distribution in tissues, and subcellular localization, J Biol Chem 243(8) (1968) 2028-37.

[68] A. Bernkop-Schnurch, The use of inhibitory agents to overcome the enzymatic barrier to perorally administered therapeutic peptides and proteins, J Control Release 52(1-2) (1998) 1-16.

[69] A. Bernkop-Schnurch, M.K. Marschutz, Development and in vitro evaluation of systems to protect peptide drugs from aminopeptidase N, Pharm Res 14(2) (1997) 181-5.

[70] R.J. Hickey, Bacitracin, its manufacture and uses, Prog Ind Microbiol 5 (1964) 93-150.

[71] A. Knarreborg, S.K. Jensen, R.M. Engberg, Pancreatic lipase activity as influenced by unconjugated bile acids and pH, measured in vitro and in vivo, J Nutr Biochem 14(5) (2003) 259-65.

[72] H.H. Hyun, J.G. Zeikus, General biochemical characterization of thermostable extracellular beta-amylase from clostridium thermosulfurogenes, Appl Environ Microbiol 49(5) (1985) 1162-7.

[73] K. Park, Kwon, I., Park, Ki., Oral protein delivery: current status and future prospects, Reactive and Functional Polymers 71(3) (2011) 280-287.

[74] J. Renukuntla, A.D. Vadlapudi, A. Patel, S.H. Boddu, A.K. Mitra, Approaches for enhancing oral bioavailability of peptides and proteins, Int J Pharm 447(1-2) (2013) 75-93.

[75] M. Thanou, J.C. Verhoef, H.E. Junginger, Chitosan and its derivatives as intestinal absorption enhancers, Adv Drug Deliv Rev 50 Suppl 1 (2001) S91-101.

[76] M. Cano-Cebrian, Zornoza, T., Granero, L., Polache, A., Intestinal absorption enhancement via the paracellular route by fatty acids, chitosans, and others: a target for drug delivery, Current Drug Delivery 2(1) (2005) 9-22.

[77] J. Smith, E. Wood, M. Dornish, Effect of chitosan on epithelial cell tight junctions, Pharm Res 21(1) (2004) 43-9.

[78] A. Bernkop-Schnurch, Chitosan and its derivatives: potential excipients for peroral peptide delivery systems, Int J Pharm 194(1) (2000) 1-13.

[79] N.G. Schipper, K.M. Varum, P. Artursson, Chitosans as absorption enhancers for poorly absorbable drugs. 1: Influence of molecular weight and degree of acetylation on drug transport across human intestinal epithelial (Caco-2) cells, Pharm Res 13(11) (1996) 1686-92.

[80] N.G. Schipper, K.M. Varum, P. Stenberg, G. Ocklind, H. Lennernas, P. Artursson, Chitosans as absorption enhancers of poorly absorbable drugs. 3: Influence of mucus on absorption enhancement, Eur J Pharm Sci 8(4) (1999) 335-43.

[81] T. Lindmark, T. Nikkila, P. Artursson, Mechanisms of absorption enhancement by medium chain fatty acids in intestinal epithelial Caco-2 cell monolayers, J Pharmacol Exp Ther 275(2) (1995) 958-64.

[82] T. Sawada, T. Ogawa, M. Tomita, M. Hayashi, S. Awazu, Role of paracellular pathway in nonelectrolyte permeation across rat colon epithelium enhanced by sodium caprate and sodium caprylate, Pharm Res 8(11) (1991) 1365-71.

[83] M. Sakai, T. Imai, H. Ohtake, H. Azuma, M. Otagiri, Effects of absorption enhancers on the transport of model compounds in Caco-2 cell monolayers: assessment by confocal laser scanning microscopy, J Pharm Sci 86(7) (1997) 779-85.

[84] P. Artursson, J. Karlsson, Correlation between oral drug absorption in humans and apparent drug permeability coefficients in human intestinal epithelial (Caco-2) cells, Biochem Biophys Res Commun 175(3) (1991) 880-5.

[85] C. Bies, C.M. Lehr, J.F. Woodley, Lectin-mediated drug targeting: history and applications, Adv Drug Deliv Rev 56(4) (2004) 425-35.

[86] J. Haas, C.M. Lehr, Developments in the area of bioadhesive drug delivery systems, Expert Opin Biol Ther 2(3) (2002) 287-98.

[87] A. Fasano, B. Baudry, D.W. Pumplin, S.S. Wasserman, B.D. Tall, J.M. Ketley, J.B. Kaper, Vibrio cholerae produces a second enterotoxin, which affects intestinal tight junctions, Proc Natl Acad Sci U S A 88(12) (1991) 5242-6.

[88] A. Fasano, C. Fiorentini, G. Donelli, S. Uzzau, J.B. Kaper, K. Margaretten, X. Ding, S. Guandalini, L. Comstock, S.E. Goldblum, Zonula occludens toxin modulates tight junctions through protein kinase C-dependent actin reorganization, in vitro, J Clin Invest 96(2) (1995) 710-20.

[89] W.L. Wang, R.L. Lu, M. DiPierro, A. Fasano, Zonula occludin toxin, a microtubule binding protein, World J Gastroenterol 6(3) (2000) 330-334.

[90] A. Fasano, S. Uzzau, Modulation of intestinal tight junctions by Zonula occludens toxin permits enteral administration of insulin and other macromolecules in an animal model, J Clin Invest 99(6) (1997) 1158-64.

[91] N.N. Salama, A. Fasano, M. Thakar, N.D. Eddington, The impact of DeltaG on the oral bioavailability of low bioavailable therapeutic agents, J Pharmacol Exp Ther 312(1) (2005) 199-205.

[92] K.H. Song, A. Fasano, N.D. Eddington, Effect of the six-mer synthetic peptide (AT1002) fragment of zonula occludens toxin on the intestinal absorption of cyclosporin A, Int J Pharm 351(1-2) (2008) 8-14.

[93] M. Morishita, N. Kamei, J. Ehara, K. Isowa, K. Takayama, A novel approach using functional peptides for efficient intestinal absorption of insulin, J Control Release 118(2) (2007) 177-84.

[94] N. Kamei, M. Morishita, K. Takayama, Importance of intermolecular interaction on the improvement of intestinal therapeutic peptide/protein absorption using cell-penetrating peptides, J Control Release 136(3) (2009) 179-86.

[95] N. Kamei, M. Morishita, Y. Eda, N. Ida, R. Nishio, K. Takayama, Usefulness of cell-penetrating peptides to improve intestinal insulin absorption, J Control Release 132(1) (2008) 21-5.

[96] J. Hochman, Artursson, P., Mechanisms of absorption enhancement and tight junction regulation, J Control Release 1(29) (1994) 253-257.

[97] E.K. Anderberg, P. Artursson, Epithelial transport of drugs in cell culture. VIII: Effects of sodium dodecyl sulfate on cell membrane and tight junction permeability in human intestinal epithelial (Caco-2) cells, J Pharm Sci 82(4) (1993) 392-8.

[98] E.K. Anderberg, C. Nystrom, P. Artursson, Epithelial transport of drugs in cell culture. VII: Effects of pharmaceutical surfactant excipients and bile acids on transepithelial permeability in monolayers of human intestinal epithelial (Caco-2) cells, J Pharm Sci 81(9) (1992) 879-87.

[99] E.S. Swenson, W.B. Milisen, W. Curatolo, Intestinal permeability enhancement: efficacy, acute local toxicity, and reversibility, Pharm Res 11(8) (1994) 1132-42.

[100] S.S. Davis, L. Illum, Absorption enhancers for nasal drug delivery, Clin Pharmacokinet 42(13) (2003) 1107-28.

[101] G.S. Asane, S.A. Nirmal, K.B. Rasal, A.A. Naik, M.S. Mahadik, Y.M. Rao, Polymers for mucoadhesive drug delivery system: a current status, Drug Dev Ind Pharm 34(11) (2008) 1246-66.

[102] A. Bernkop-Schnurch, M.E. Krajicek, Mucoadhesive polymers as platforms for peroral peptide delivery and absorption: synthesis and evaluation of different chitosan-EDTA conjugates, J Control Release 50(1-3) (1998) 215-23.

[103] A. Bernkop-Schnurch, Thiomers: a new generation of mucoadhesive polymers, Adv Drug Deliv Rev 57(11) (2005) 1569-82.

[104] K. Lee, and Yuk, S., Polymeric protein delivery systems, Prog Polym Sci 1(32) (2007) 669-697.

[105] B.D. Shah P, Shelat P., Nanoemulsion: a pharmaceutical review, Sys Rev Pharm 1(1) (2010) 24-32.

[106] S.V. Rao, P. Agarwal, J. Shao, Self-nanoemulsifying drug delivery systems (SNEDDS) for oral delivery of protein drugs: II. In vitro transport study, Int J Pharm 362(1-2) (2008) 10-5.

[107] M. Bindu Sri, Ashok, V., and Arkendu C., As a review on hydrogels as drug delivery in the pharmaceutical field, Int J Pharm Chem Sci 1(2) (2012) 642-661.

[108] N.A. Peppas, K.M. Wood, J.O. Blanchette, Hydrogels for oral delivery of therapeutic proteins, Expert Opin Biol Ther 4(6) (2004) 881-7.

[109] G. Fricker, T. Kromp, A. Wendel, A. Blume, J. Zirkel, H. Rebmann, C. Setzer, R.O. Quinkert, F. Martin, C. Muller-Goymann, Phospholipids and lipid-based formulations in oral drug delivery, Pharm Res 27(8) (2010) 1469-86.

[110] Y. Chen, Q. Ping, J. Guo, W. Lv, J. Gao, The absorption behavior of cyclosporin A lecithin vesicles in rat intestinal tissue, Int J Pharm 261(1-2) (2003) 21-6.

[111] M. Werle, H. Takeuchi, Chitosan-aprotinin coated liposomes for oral peptide delivery: development, characterisation and in vivo evaluation, Int J Pharm 370(1-2) (2009) 26-32.

[112] N.M. Shah, J. Parikh, A. Namdeo, N. Subramanian, S. Bhowmick, Preparation, characterization and in vivo studies of proliposomes containing Cyclosporine A, J Nanosci Nanotechnol 6(9-10) (2006) 2967-73.

[113] K. Iwanaga, S. Ono, K. Narioka, M. Kakemi, K. Morimoto, S. Yamashita, Y. Namba, N. Oku, Application of surface-coated liposomes for oral delivery of peptide: effects of coating the liposome's surface on the GI transit of insulin, J Pharm Sci 88(2) (1999) 248-52.

[114] T. Jung, W. Kamm, A. Breitenbach, E. Kaiserling, J.X. Xiao, T. Kissel, Biodegradable nanoparticles for oral delivery of peptides: is there a role for polymers to affect mucosal uptake?, Eur J Pharm Biopharm 50(1) (2000) 147-60.

[115] A. Kumari, S.K. Yadav, S.C. Yadav, Biodegradable polymeric nanoparticles based drug delivery systems, Colloids Surf B Biointerfaces 75(1) (2010) 1-18.

[116] P. Jani, G.W. Halbert, J. Langridge, A.T. Florence, Nanoparticle uptake by the rat gastrointestinal mucosa: quantitation and particle size dependency, J Pharm Pharmacol 42(12) (1990) 821-6.

[117] C.S. Yah, G.S. Simate, S.E. Iyuke, Nanoparticles toxicity and their routes of exposures, Pak J Pharm Sci 25(2) (2012) 477-91.

[118] P. Jani, G.W. Halbert, J. Langridge, A.T. Florence, The uptake and translocation of latex nanospheres and microspheres after oral administration to rats, J Pharm Pharmacol 41(12) (1989) 809-12.

[119] G. Storma, Belliota, SO, Lasicc, T., Surface modification of nanoparticles to oppose uptake by the mononuclear phagocyte system, Adv Drug Deliv Rev 1(17) (1995) 31.

[120] H. Gao, Y.N. Wang, Y.G. Fan, J.B. Ma, Synthesis of a biodegradable tadpole-shaped polymer via the coupling reaction of polylactide onto mono(6-(2-aminoethyl)amino-6-deoxy)-beta-cyclodextrin and its properties as the new carrier of protein delivery system, J Control Release 107(1) (2005) 158-73.

[121] C. Damge, P. Maincent, N. Ubrich, Oral delivery of insulin associated to polymeric nanoparticles in diabetic rats, J Control Release 117(2) (2007) 163-70.

[122] M.S. Espuelas, P. Legrand, P.M. Loiseau, C. Bories, G. Barratt, J.M. Irache, In vitro antileishmanial activity of amphotericin B loaded in poly(epsilon-caprolactone) nanospheres, J Drug Target 10(8) (2002) 593-9.

[123] B. Sarmento, A. Ribeiro, F. Veiga, P. Sampaio, R. Neufeld, D. Ferreira, Alginate/chitosan nanoparticles are effective for oral insulin delivery, Pharm Res 24(12) (2007) 2198-206.

[124] Z. Lu, T.K. Yeh, M. Tsai, J.L. Au, M.G. Wientjes, Paclitaxel-loaded gelatin nanoparticles for intravesical bladder cancer therapy, Clin Cancer Res 10(22) (2004) 7677-84.

[125] J. Zillies, C. Coester, Evaluating gelatin based nanoparticles as a carrier system for double stranded oligonucleotides, J Pharm Pharm Sci 7(4) (2005) 17-21.

[126] A.K. Bajpai, J. Choubey, Design of gelatin nanoparticles as swelling controlled delivery system for chloroquine phosphate, J Mater Sci Mater Med 17(4) (2006) 345-58.

[127] T.E. Rajapaksa, M. Stover-Hamer, X. Fernandez, H.A. Eckelhoefer, D.D. Lo, Claudin 4-targeted protein incorporated into PLGA nanoparticles can mediate M cell targeted delivery, J Control Release 142(2) (2010) 196-205.

[128] E. Mathiowitz, J.S. Jacob, Y.S. Jong, G.P. Carino, D.E. Chickering, P. Chaturvedi, C.A. Santos, K. Vijayaraghavan, S. Montgomery, M. Bassett, C. Morrell, Biologically erodable microspheres as potential oral drug delivery systems, Nature 386(6623) (1997) 410-4.

[129] M. Tobio, A. Sanchez, A. Vila, I.I. Soriano, C. Evora, J.L. Vila-Jato, M.J. Alonso, The role of PEG on the stability in digestive fluids and in vivo fate of PEG-PLA nanoparticles following oral administration, Colloids Surf B Biointerfaces 18(3-4) (2000) 315-323.

[130] M. Morishita, N.A. Peppas, Is the oral route possible for peptide and protein drug delivery?, Drug Discov Today 11(19-20) (2006) 905-10.

[131] N. Zhang, Q. Ping, G. Huang, X. Han, Y. Cheng, W. Xu, Transport characteristics of wheat germ agglutinin-modified insulin-liposomes and solid lipid nanoparticles in a perfused rat intestinal model, J Nanosci Nanotechnol 6(9-10) (2006) 2959-66.

[132] M. Garcia-Fuentes, D. Torres, M.J. Alonso, New surface-modified lipid nanoparticles as delivery vehicles for salmon calcitonin, Int J Pharm 296(1-2) (2005) 122-32.

[133] R.E. Steinert, B. Poller, M.C. Castelli, K. Friedman, A.R. Huber, J. Drewe, C. Beglinger, Orally administered glucagon-like peptide-1 affects glucose homeostasis following an oral glucose tolerance test in healthy male subjects, Clin Pharmacol Ther 86(6) (2009) 644-50.

[134] J. Chin, Mahmud, K., Kim, S., Park, K., and Byun, Y., Insight of current technologies for oral delivery of proteins and peptides, Drug Discov Today Technol 9(2) (2012) e105-e112.

[135] S. Eiamtrakarn, Y. Itoh, J. Kishimoto, Y. Yoshikawa, N. Shibata, M. Murakami, K. Takada, Gastrointestinal mucoadhesive patch system (GI-MAPS) for oral administration of G-CSF, a model protein, Biomaterials 23(1) (2002) 145-52.

[136] H. Kalluri, A.K. Banga, Transdermal delivery of proteins, AAPS PharmSciTech 12(1) (2011) 431-41.

[137] A. Herwadkar, A.K. Banga, Peptide and protein transdermal drug delivery, Drug Discov Today Technol 9(2) (2012) e147-e154.

[138] A. Arora, M.R. Prausnitz, S. Mitragotri, Micro-scale devices for transdermal drug delivery, Int J Pharm 364(2) (2008) 227-36.

[139] K. Saroha, B. Sharma, B. Yadav, Sonophoresis: an advanced tool in transdermal drug delivery system, Int J Cur Pharm Res 3(3) (2011) 89-97.

[140] S.N. Andrews, E. Jeong, M.R. Prausnitz, Transdermal delivery of molecules is limited by full epidermis, not just stratum corneum, Pharm Res 30(4) (2013) 1099-109.

[141] J.D. Bos, M.M. Meinardi, The 500 Dalton rule for the skin penetration of chemical compounds and drugs, Exp Dermatol (3) (2000) 165-9.

[142] R.Q. Ruan, S.S. Wang, C.L. Wang, L. Zhang, Y.J. Zhang, W. Zhou, W.P. Ding, P.P. Jin, P.F. Wei, N. Man, L.P. Wen, Transdermal delivery of human epidermal growth factor facilitated by a peptide chaperon, Eur J Med Chem 62 (2013) 405-9.

[143] Jitendra, P.K. Sharma, S. Bansal, A. Banik, Noninvasive routes of proteins and peptides drug delivery, Indian J Pharm Sci 73(4) (2011) 367-75.

[144] I.B. Pathan, C.M. Setty, Chemical penetration enhancers for transdermal drug delivery systems, Tropical Journal of Pharm Res 8(2) (2009) 173-179.

[145] E.J. Wilson, Three Generations: The Past, Present, and Future of Transdermal Drug Delivery Systems, PharmCon Continuing Pharmacy Education (2011).

[146] A.V. Badkar, A.M. Smith, J.A. Eppstein, A.K. Banga, Transdermal delivery of interferon alpha-2B using microporation and iontophoresis in hairless rats, Pharm Res 24(7) (2007) 1389-95.

[147] B.S. Bloom, J.A. Brauer, R.G. Geronemus, Ablative fractional resurfacing in topical drug delivery: an update and outlook, Dermatologic Surgery : Official Publication For American Society for Dermatologic Surgery [et al.] (2013).

[148] M.J. Garland, E. Caffarel-Salvador, K. Migalska, A.D. Woolfson, R.F. Donnelly, Dissolving polymeric microneedle arrays for electrically assisted transdermal drug delivery, J Control Release 159(1) (2012) 52-9.

[149] T. Gratieri, I. Alberti, M. Lapteva, Y.N. Kalia, Next generation intra- and transdermal therapeutic systems: Using non- and minimally-invasive technologies to increase drug delivery into and across the skin, Eur J Pharm Sci (2013).

[150] J.W. Lee, P. Gadiraju, J.H. Park, M.G. Allen, M.R. Prausnitz, Microsecond thermal ablation of skin for transdermal drug delivery, J Control Release 154(1) (2011) 58-68.

[151] M.R. Prausnitz, R. Langer, Transdermal drug delivery, Nat Biotechnol 26(11) (2008) 1261-8.

[152] A.R. Denet, R. Vanbever, V. Preat, Skin electroporation for transdermal and topical delivery, Adv Drug Deliv Rev (5) (2004) 659-74.

[153] Transdermal Specialties, Inc., U-Strip Insulin Program: HPT-7 Clinical Trial Scheduled for 2013, (2012).

[154] B. Ghosh, D. Iyer, A.B. Nair, H.N. Sree, Prospects of iontophoresis in cardiovascular drug delivery, J Basic Clin Pharm 4(1) (2013) 25-30.

[155] Y.C. Kim, S. Late, A.K. Banga, P.J. Ludovice, M.R. Prausnitz, Biochemical enhancement of transdermal delivery with magainin peptide: modification of electrostatic interactions by changing pH, Int J Pharm 362(1-2) (2008) 20-8.

[156] Y.C. Kim, P.J. Ludovice, M.R. Prausnitz, Transdermal delivery enhanced by magainin pore-forming peptide, J Control Release 122(3) (2007) 375-83.

[157] Y.C. Kim, P.J. Ludovice, M.R. Prausnitz, Optimization of transdermal delivery using magainin pore-forming peptide, J Phys Chem Solids 69(5-6) (2008) 1560-1563.

[158] Y. Chen, Y. Shen, X. Guo, C. Zhang, W. Yang, M. Ma, S. Liu, M. Zhang, L.P. Wen, Transdermal protein delivery by a coadministered peptide identified via phage display, Nat Biotechnol 24(4) (2006) 455-60.

[159] L. Illum, Nasal drug delivery: new developments and strategies, Drug Discov Today 7(23) (2002) 1184-9.

[160] E.T. Maggio, Intravail: highly effective intranasal delivery of peptide and protein drugs, Expert Opin Drug Deliv 3(4) (2006) 529-39.

[161] D.J. Pillion, S. Hosmer, E. Meezan, Dodecylmaltoside-mediated nasal and ocular absorption of lyspro-insulin: independence of surfactant action from multimer dissociation, Pharm Res 15(10) (1998) 1637-9.

[162] A.H. Shojaei, Buccal mucosa as a route for systemic drug delivery: a review, J Pharm Pharm Sci 1(1) (1998) 15-30.

[163] P. Gandhi, Patel, K., A review article on mucoadhesive buccal drug delivery system, Int J Pharm Res 3(5) (2011) 159-173.

[164] R. Mujoriya, Dhamande, K., Wankhede, U., Angure, S., A review on study of buccal drug delivery system, ISDE 2(3) (2011).

[165] P. Lakshmi, Deepthi, B., Rama, N., Rectal drug delivery: A promising route for enhancing drug absorption, Asian J Res Pharm Sci 2(4) (2012) 143-149.

[166] R.W. Niven, Delivery of biotherapeutics by inhalation aerosol, Crit Rev Ther Drug Carrier Syst 12(2-3) (1995) 151-231.

[167] C. Bailey, Why is Exubera being withdrawn?, BMJ 335(7630) (2007) 1156.

[168] R. Agu, Ugwoke, M., Armand, M., Kinget, R., The lung as a route for systemic delivery of therapeutic proteins and peptides, Respir Res 2(4) (2001) 198-209.

[169] N. Kocevar, N. Obermajer, B. Strukelj, J. Kos, S. Kreft, Improved acylation method enables efficient delivery of functional palmitoylated cystatin into epithelial cells, Chem Biol Drug Des 69(2) (2007) 124-31.

[170] B.W. Bailon P, Polyethylene glycol-conjugated pharmaceutical proteins, Pharm Sci Technol Today 1 (1998) 352-356.

[171] J. Magnusson, S. Aram, F. Fernandez-Trillo, C. Alexander, Synthetic polymers for biopharmaceutical delivery, Polym. Chem. 2 (2010) 48-59.

[172] R.S. Rajan, T. Li, M. Aras, C. Sloey, W. Sutherland, H. Arai, R. Briddell, O. Kinstler, A.M. Lueras, Y. Zhang, H. Yeghnazar, M. Treuheit, D.N. Brems, Modulation of protein aggregation by polyethylene glycol conjugation: GCSF as a case study, Protein Sci 15(5) (2006) 1063-75.

[173] E. Ducat, J. Deprez, A. Gillet, A. Noel, B. Evrard, O. Peulen, G. Piel, Nuclear

delivery of a therapeutic peptide by long circulating pH-sensitive liposomes: benefits over classical vesicles, Int J Pharm 420(2) (2011) 319-32.

[174] M.Naoi, K. Yagi, Incorporation of enzyme through blood-brain barrier into the brain by means of liposomes, Biochem. Intl 1(6) (1980) 591-596.

[175] A. Gabizon, F. Martin, Polyethylene glycol-coated (pegylated) liposomal doxorubicin. Rationale for use in solid tumours, Drugs 54 Suppl 4 (1997) 15-21.

[176] A.K. Varkouhi, M. Scholte, G. Storm, H.J. Haisma, Endosomal escape pathways for delivery of biologicals, J Control Release 151(3) (2011) 220-8.

[177] G. Fuertes, D. Gimenez, S. Esteban-Martin, O.L. Sanchez-Munoz, J. Salgado, A lipocentric view of peptide-induced pores, Eur Biophys J 40(4) (2011) 399-415.

[178] E. Prchla, C. Plank, E. Wagner, D. Blaas, R. Fuchs, Virus-mediated release of endosomal content in vitro: different behavior of adenovirus and rhinovirus serotype 2, J Cell Biol 131(1) (1995) 111-23.

[179] J. Sun, E.E. Pohl, O.O. Krylova, E. Krause, Agapov, II, A.G. Tonevitsky, P. Pohl, Membrane destabilization by ricin, Eur Biophys J 33(7) (2004) 572-9.

[180] M. Ogris, R.C. Carlisle, T. Bettinger, L.W. Seymour, Melittin enables efficient vesicular escape and enhanced nuclear access of nonviral gene delivery vectors, J Biol Chem 276(50) (2001) 47550-5.

[181] K. Sandvig, B. Spilsberg, S.U. Lauvrak, M.L. Torgersen, T.G. Iversen, B. van Deurs, Pathways followed by protein toxins into cells, Int J Med Microbiol 293(7-8) (2004) 483-90.

[182] E.J. Kwon, J.M. Bergen, S.H. Pun, Application of an HIV gp41-derived peptide for enhanced intracellular trafficking of synthetic gene and siRNA delivery vehicles, Bioconjug Chem 19(4) (2008) 920-7.

[183] R.S. Singh, C. Goncalves, P. Sandrin, C. Pichon, P. Midoux, A. Chaudhuri, On the gene delivery efficacies of pH-sensitive cationic lipids via endosomal protonation: a chemical biology investigation, Chem Biol 11(5) (2004) 713-23.

[184] O. Boussif, F. Lezoualch, M.A. Zanta, M.D. Mergny, D. Scherman, B. Demeneix, J.P. Behr, A versatile vector for gene and oligonucleotide transfer into cells in culture and in vivo: polyethylenimine, Proc Natl Acad Sci U S A 92(16) (1995) 7297-301.

[185] I. Mellman, R. Fuchs, A. Helenius, Acidification of the endocytic and exocytic pathways, Annu Rev Biochem 55 (1986) 663-700.

[186] T. Kimura, A. Ohyama, Association between the pH-dependent conformational change of West Nile flavivirus E protein and virus-mediated membrane fusion, J Gen Virol 69 (Pt 6) (1988) 1247-54.

[187] E. Mastrobattista, G.A. Koning, L. van Bloois, A.C. Filipe, W. Jiskoot, G. Storm, Functional characterization of an endosome-disruptive peptide and its application in cytosolic delivery of immunoliposome-entrapped proteins, J Biol Chem 277(30) (2002) 27135-43.

[188] Y. Tu, J.S. Kim, A fusogenic segment of glycoprotein H from herpes simplex virus enhances transfection efficiency of cationic liposomes, J Gene Med 10(6) (2008) 646-54.

[189] T.B. Wyman, F. Nicol, O. Zelphati, P.V. Scaria, C. Plank, F.C. Szoka, Jr., Design, synthesis, and characterization of a cationic peptide that binds to nucleic acids and permeabilizes bilayers, Biochemistry 36(10) (1997) 3008-17.

[190] W.L.a.J.K.W. Lam, Endosomal escape pathways for non-viral nucleic acid delivery systems, in: D.B. Ceresa (Ed.), Molecular Regulation of Endocytosis 2012, p. 465.

[191] S. Simoes, J.N. Moreira, C. Fonseca, N. Duzgunes, M.C. de Lima, On the formulation of pH-sensitive liposomes with long circulation times, Adv Drug Deliv Rev 56(7) (2004) 947-65.

[192] V.P. Torchilin, A.N. Lukyanov, Peptide and protein drug delivery to and into tumors: challenges and solutions, Drug Discov Today 8(6) (2003) 259-66.

[193] V. Weissig, K.R. Whiteman, V.P. Torchilin, Accumulation of protein-loaded long-circulating micelles and liposomes in subcutaneous Lewis lung carcinoma in mice, Pharm Res 15(10) (1998) 1552-6.

[194] S. Kim, Y. Shi, J.Y. Kim, K. Park, J.X. Cheng, Overcoming the barriers in micellar drug delivery: loading efficiency, in vivo stability, and micelle-cell interaction, Expert Opin Drug Deliv 7(1) (2010) 49-62.

[195] K.S. Wong N, and Dai H, Carbon nanotubes as intracellular protein transporters: generality and biological functionality, J Am Chem Soc 127 (2005) 6021-6026.

[196] G. Caocci, M.A. Maioli, S. Atzeni, R. Piras, N. Carboni, G. La Nasa, Absence of histological myopathy in chronic myeloid leukemia patients complaining of muscle spasms and myalgia during treatment with nilotinib, Leuk Res 36(9) (2012) e206-8.

[197] D. Pantarotto, J.P. Briand, M. Prato, A. Bianco, Translocation of bioactive peptides across cell membranes by carbon nanotubes, Chem Commun (Camb) (1)

(2004) 16-7.

[198] A. Bianco, K. Kostarelos, M. Prato, Applications of carbon nanotubes in drug delivery, Curr Opin Chem Biol 9(6) (2005) 674-9.

[199] T. Lammers, F. Kiessling, W.E. Hennink, G. Storm, Drug targeting to tumors: principles, pitfalls and (pre-) clinical progress, J Control Release 161(2) (2012) 175-87.

[200] S.S. Bale, S.J. Kwon, D.A. Shah, A. Banerjee, J.S. Dordick, R.S. Kane, Nanoparticle-mediated cytoplasmic delivery of proteins to target cellular machinery, ACS Nano 4(3) (2010) 1493-500.

[201] N. Samadi, C.F. van Nostrum, T. Vermonden, M. Amidi, W.E. Hennink, Mechanistic studies on the degradation and protein release characteristics of poly(lactic-co-glycolic-co-hydroxymethylglycolic acid) nanospheres, Biomacromolecules 14(4) (2013) 1044-53.

[202] D.B. Shenoy, M.M. Amiji, Poly(ethylene oxide)-modified poly(epsilon-caprolactone) nanoparticles for targeted delivery of tamoxifen in breast cancer, Int J Pharm 293(1-2) (2005) 261-70.

[203] P. Jarver, U. Langel, Cell-penetrating peptides--a brief introduction, Biochim Biophys Acta 1758(3) (2006) 260-3.

[204] F. Madani, S. Lindberg, U. Langel, S. Futaki, A. Graslund, Mechanisms of cellular uptake of cell-penetrating peptides, J Biophys 2011 (2011) 414729.

[205] S. El-Andaloussi, T. Holm, U. Langel, Cell-penetrating peptides: mechanisms and applications, Curr Pharm Des 11(28) (2005) 3597-611.

[206] D.M. Copolovici, K. Langel, E. Eriste, U. Langel, Cell-penetrating peptides: design, synthesis, and applications, ACS Nano 8(3) (2014) 1972-94.

[207] P. Boisguerin, S. Deshayes, M.J. Gait, L. O'Donovan, C. Godfrey, C.A. Betts, M.J. Wood, B. Lebleu, Delivery of therapeutic oligonucleotides with cell penetrating peptides, Adv Drug Deliv Rev 87 (2015) 52-67.

[208] G. Guidotti, L. Brambilla, D. Rossi, Cell-penetrating peptides: from basic research to clinics, Trends Pharmacol Sci 38(4) (2017) 406-424.

[209] S. Reissmann, Cell penetration: scope and limitations by the application of cell-penetrating peptides, J Peptide Sci 20(10) (2014) 760-84.

[210] F. Reichart, M. Horn, I. Neundorf, Cyclization of a cell-penetrating peptide via click-chemistry increases proteolytic resistance and improves drug delivery, J

Peptide Sci 22(6) (2016) 421-6.

[211] Y.H. Lau, P. de Andrade, Y. Wu, D.R. Spring, Peptide stapling techniques based on different macrocyclisation chemistries, Chem Soc Rev 44(1) (2015) 91-102.

[212] Z. Wang, J.C. Zhao, H.Z. Lian, H.Y. Chen, Aptamer-based organic-silica hybrid affinity monolith prepared via "thiol-ene" click reaction for extraction of thrombin, Talanta 138 (2015) 52-8.

[213] S.N. Phelan JC, Braisted AC, and Mcdowell RS, A general method for constraining short peptides to an alpha-helical conformation, J Am Chem Soc 119(3) (1997) 6.

[214] a.G.R. Blackwell HE, Highly Efficient synthesis of covalently cross-linked peptide helices by ring-closing metathesis, Angew Chem 37(23) (1998) 4.

[215] S.J. Miller, H.E. Blackwell, R. H. Grubbs, Application of ring-closing metathesis to the synthesis of rigidified amino acids and peptides, J Am Chem Soc 118 (40) (1996) 9606-9614.

[216] C. Schafmeister, J. Po, G.L. Verdine, An all-hydrocarbon cross-linking system for enhancing the helicity and metabolic stability of peptides, J Am Chem Soc 122 (40) (2000) 5891-5892.

[217] L.D. Walensky, G.H. Bird, Hydrocarbon-stapled peptides: principles, practice, and progress, J Med Chem 57(15) (2014) 6275-88.

[218] J.L. LaBelle, S.G. Katz, G.H. Bird, E. Gavathiotis, M.L. Stewart, C. Lawrence, J.K. Fisher, M. Godes, K. Pitter, A.L. Kung, L.D. Walensky, A stapled BIM peptide overcomes apoptotic resistance in hematologic cancers, J Clin Invest 122(6) (2012) 2018-31.

[219] M.L. Stewart, E. Fire, A.E. Keating, L.D. Walensky, The MCL-1 BH3 helix is an exclusive MCL-1 inhibitor and apoptosis sensitizer, Nat Chem Biol 6(8) (2010) 595-601.

[220] F. Bernal, M. Wade, M. Godes, T.N. Davis, D.G. Whitehead, A.L. Kung, G.M. Wahl, L.D. Walensky, A stapled p53 helix overcomes HDMX-mediated suppression of p53, Cancer Cell 18(5) (2010) 411-22.

[221] T.N. Grossmann, J.T. Yeh, B.R. Bowman, Q. Chu, R.E. Moellering, G.L. Verdine, Inhibition of oncogenic Wnt signaling through direct targeting of beta-catenin, Proc Natl Acad Sci U S A 109(44) (2012) 17942-7.

[222] A.P. Higueruelo, H. Jubb, T.L. Blundell, Protein-protein interactions as druggable targets: recent technological advances, Curr Opin Pharmacol 13(5) (2013) 791-6.

[223] H.K. Cui, J. Qing, Y. Guo, Y.J. Wang, L.J. Cui, T.H. He, L. Zhang, L. Liu, Stapled peptide-based membrane fusion inhibitors of hepatitis C virus, Bioorg Med Chem 21(12) (2013) 3547-54.

[224] C.S. Higman, J.A. Lummiss, D.E. Fogg, Olefin Metathesis at the dawn of implementation in pharmaceutical and specialty-chemicals manufacturing, Angew Chem Int Ed 55(11) (2016) 3552-65.

[225] Y. Wang, D.H. Chou, A thiol-ene coupling approach to native peptide stapling and macrocyclization, Angew Chem Int Ed 54(37) (2015) 10931-4.

[226] C.E. Hoyle, C.N. Bowman, Thiol-ene click chemistry, Angew Chem Int Ed 49(9) (2010) 1540-73.

[227] Y.H. Lau, Y. Wu, P. de Andrade, W.R. Galloway, D.R. Spring, A two-component 'double-click' approach to peptide stapling, Nat Protoc 10(4) (2015) 585-94.

[228] L. Mendive-Tapia, S. Preciado, J. Garcia, R. Ramon, N. Kielland, F. Albericio, R. Lavilla, New peptide architectures through C-H activation stapling between tryptophan-phenylalanine/tyrosine residues, Nat Commun 6 (2015) 7160.

[229] Y.S. Tan, D.P. Lane, C.S. Verma, Stapled peptide design: principles and roles of computation, Drug Discov Today (2016).

[230] G.H. Bird, E. Mazzola, K. Opoku-Nsiah, M.A. Lammert, M. Godes, D.S. Neuberg, L.D. Walensky, Biophysical determinants for cellular uptake of hydrocarbon-stapled peptide helices, Nat Chem Biol (2016).

[231] G.J. Hilinski, Y.W. Kim, J. Hong, P.S. Kutchukian, C.M. Crenshaw, S.S. Berkovitch, A. Chang, S. Ham, G.L. Verdine, Stitched alpha-helical peptides via bis ring-closing metathesis, J Am Chem Soc 136(35) (2014) 12314-22.

[232] Q. Chu, R.E. Mollering, G.J. Hilinski, Y.W. Kim, T.N. Grossmann, J.T.H. Yeh, G.L. Verdine, Towards understanding cell penetration by stapled peptides, Med Chem Commun 6 (2015) 111-119.

[233] Z. Guo, U. Mohanty, J. Noehre, T.K. Sawyer, W. Sherman, G. Krilov, Probing the alpha-helical structural stability of stapled p53 peptides: molecular dynamics simulations and analysis, Chem Biol Drug Des 75(4) (2010) 348-59.

[234] S.A. Kawamoto, A. Coleska, X. Ran, H. Yi, C.Y. Yang, S. Wang, Design of triazole-stapled BCL9 alpha-helical peptides to target the beta-catenin/B-cell CLL/lymphoma 9 (BCL9) protein-protein interaction, J Med Chem 55(3) (2012) 1137-46.

[235] A.M. White, D.J. Clark, Discovery and optimization of peptide macrocycles, Ex

Op on Drug Delivery, 11(12) (2016) 1151-63

[236] Y.S. Chang, B. Graves, V. Guerlavais, C. Tovar, K. Packman, K.H. To, K.A. Olson, K. Kesavan, P. Gangurde, A. Mukherjee, T. Baker, K. Darlak, C. Elkin, Z. Filipovic, F.Z. Qureshi, H. Cai, P. Berry, E. Feyfant, X.E. Shi, J. Horstick, D.A. Annis, A.M. Manning, N. Fotouhi, H. Nash, L.T. Vassilev, T.K. Sawyer, Stapled alpha-helical peptide drug development: a potent dual inhibitor of MDM2 and MDMX for p53-dependent cancer therapy, Proc Natl Acad Sci 110(36) (2013) E3445-54.

[237] E. Koren, A. Apte, R.R. Sawant, J. Grunwald, V.P. Torchilin, Cell-penetrating TAT peptide in drug delivery systems: proteolytic stability requirements, Drug Deliv 18(5) (2011) 377-84.

[238] V.P. Torchilin, T.S. Levchenko, R. Rammohan, N. Volodina, B. Papahadjopoulos-Sternberg, G.G. D'Souza, Cell transfection in vitro and in vivo with nontoxic TAT peptide-liposome-DNA complexes, Proc Natl Acad Sci 100(4) (2003) 1972-7.

[239] A. Ziegler, P. Nervi, M. Durrenberger, J. Seelig, The cationic cell-penetrating peptide CPP(TAT) derived from the HIV-1 protein TAT is rapidly transported into living fibroblasts: optical, biophysical, and metabolic evidence, Biochemistry 44(1) (2005) 138-48.

[240] D. Fischer, Y. Li, B. Ahlemeyer, J. Krieglstein, T. Kissel, In vitro cytotoxicity testing of polycations: influence of polymer structure on cell viability and hemolysis, Biomaterials 24(7) (2003) 1121-31.

[241] W.C. Tseng, F.R. Haselton, T.D. Giorgio, Mitosis enhances transgene expression of plasmid delivered by cationic liposomes, Biochim Biophys Acta 1445(1) (1999) 53-64.

[242] E. Koren, A. Apte, A. Jani, V.P. Torchilin, Multifunctional PEGylated 2C5-immunoliposomes containing pH-sensitive bonds and TAT peptide for enhanced tumor cell internalization and cytotoxicity, J Control Release 160(2) (2012) 264-73.

[243] D. Sarko, B. Beijer, R. Garcia Boy, E.M. Nothelfer, K. Leotta, M. Eisenhut, A. Altmann, U. Haberkorn, W. Mier, The pharmacokinetics of cell-penetrating peptides, Molecular Pharm 7(6) (2010) 2224-31.

[244] V.P. Torchilin, R. Rammohan, V. Weissig, T.S. Levchenko, TAT peptide on the surface of liposomes affords their efficient intracellular delivery even at low temperature and in the presence of metabolic inhibitors, Proc Natl Acad Sci 98(15) (2001) 8786-91.

[245] Y. Nakamura, K. Kogure, S. Futaki, H. Harashima, Octaarginine-modified multifunctional envelope-type nano device for siRNA, J Control Release 119(3) (2007) 360-7.

[246] H. Akita, K. Kogure, R. Moriguchi, Y. Nakamura, T. Higashi, T. Nakamura, S. Serada, M. Fujimoto, T. Naka, S. Futaki, H. Harashima, Nanoparticles for ex vivo siRNA delivery to dendritic cells for cancer vaccines: programmed endosomal escape and dissociation, J Control Release 143(3) (2010) 311-7.

[247] Y. Hayashi, J. Yamauchi, I.A. Khalil, K. Kajimoto, H. Akita, H. Harashima, Cell penetrating peptide-mediated systemic siRNA delivery to the liver, Int J Pharm 419(1-2) (2011) 308-13.

[248] J.S. Wadia, R.V. Stan, S.F. Dowdy, Transducible TAT-HA fusogenic peptide enhances escape of TAT-fusion proteins after lipid raft macropinocytosis, Nat Med 10(3) (2004) 310-5.

[249] I.N. Shokolenko, M.F. Alexeyev, S.P. LeDoux, G.L. Wilson, TAT-mediated protein transduction and targeted delivery of fusion proteins into mitochondria of breast cancer cells, DNA Repair (Amst) 4(4) (2005) 511-8.

[250] D. Jo, D. Liu, S. Yao, R.D. Collins, J. Hawiger, Intracellular protein therapy with SOCS3 inhibits inflammation and apoptosis, Nat Med 11(8) (2005) 892-8.

[251] I. Shin, J. Edl, S. Biswas, P.C. Lin, R. Mernaugh, C.L. Arteaga, Proapoptotic activity of cell-permeable anti-Akt single-chain antibodies, Cancer Res 65(7) (2005) 2815-24.

[252] M. Jain, S.C. Chauhan, A.P. Singh, G. Venkatraman, D. Colcher, S.K. Batra, Penetratin improves tumor retention of single-chain antibodies: a novel step toward optimization of radioimmunotherapy of solid tumors, Cancer Res 65(17) (2005) 7840-6.

[253] M. Mae, U. Langel, Cell-penetrating peptides as vectors for peptide, protein and oligonucleotide delivery, Curr Opin Pharmacol 6(5) (2006) 509-14.

[254] T. Jiang, E.S. Olson, Q.T. Nguyen, M. Roy, P.A. Jennings, R.Y. Tsien, Tumor imaging by means of proteolytic activation of cell-penetrating peptides, Proc Natl Acad Sci U S A 101(51) (2004) 17867-72.

[255] M. Hallbrink, K. Kilk, A. Elmquist, P. Lundberg, M. Lindgren, Y. Jiang, M. Pooga, U. Soomets, U. Langel, Prediction of cell-penetratin peptides, Int J Peptide Res and Ther, 11(4) (2005) 249-59.

[256] A.M. D'Ursi, L. Giusti, S. Albrizio, F. Porchia, C. Esposito, G. Caliendo, C. Gargini, E. Novellino, A. Lucacchini, P. Rovero, M.R. Mazzoni, A membrane-

permeable peptide containing the last 21 residues of the G alpha(s) carboxyl terminus inhibits G(s)-coupled receptor signaling in intact cells: correlations between peptide structure and biological activity, Mol Pharmacol 69(3) (2006) 727-36.

[257] S. Nishimura, S. Takahashi, H. Kamikatahira, Y. Kuroki, D.E. Jaalouk, S. O'Brien, E. Koivunen, W. Arap, R. Pasqualini, H. Nakayama, A. Kuniyasu, Combinatorial targeting of the macropinocytotic pathway in leukemia and lymphoma cells, J Biol Chem 283(17) (2008) 11752-62.

[258] D.B. Kirpotin, D.C. Drummond, Y. Shao, M.R. Shalaby, K. Hong, U.B. Nielsen, J.D. Marks, C.C. Benz, J.W. Park, Antibody targeting of long-circulating lipidic nanoparticles does not increase tumor localization but does increase internalization in animal models, Cancer Res 66(13) (2006) 6732-40.

[259] P. Kocbek, N. Obermajer, M. Cegnar, J. Kos, J. Kristl, Targeting cancer cells using PLGA nanoparticles surface modified with monoclonal antibody, J Control Release 120(1-2) (2007) 18-26.

[260] M. Silhol, M. Tyagi, M. Giacca, B. Lebleu, E. Vives, Different mechanisms for cellular internalization of the HIV-1 Tat-derived cell penetrating peptide and recombinant proteins fused to Tat, Eur J Biochem 269(2) (2002) 494-501.

[261] M. Zorko, U. Langel, Cell-penetrating peptides: mechanism and kinetics of cargo delivery, Adv Drug Deliv Rev 57(4) (2005) 529-45.

CHAPTER 3

INHIBITION OF BCR-ABL IN HUMAN LEUKEMIC CELLS WITH A COILED-COIL PROTEIN DELIVERED BY A LEUKEMIA-SPECIFIC CELL-PENETRATING PEPTIDE

Reprinted with permission from Molecular Pharmaceutics 2015; **12**(5):1412-21. Benjamin J. Bruno and Carol S. Lim

molecular pharmaceutics

Article

pubs.acs.org/molecularpharmaceutics

Inhibition of Bcr-Abl in Human Leukemic Cells with a Coiled-Coil Protein Delivered by a Leukemia-Specific Cell-Penetrating Peptide

Benjamin J. Bruno and Carol S. Lim*

Department of Pharmaceutics and Pharmaceutical Chemistry, College of Pharmacy, University of Utah, Salt Lake City, Utah 84112, United States

ABSTRACT: The oncoprotein Bcr-Abl is the cause of chronic myeloid leukemia (CML).[1] Current therapies target the tyrosine kinase domain of Bcr-Abl, but resistance to these drugs is common.[2] Bcr-Abl homo-oligomerization via its N-terminal coiled-coil (CC) domain is required for tyrosine kinase activity.[3] Our previous work has shown that it is possible to inhibit Bcr-Abl activity by targeting the CC domain with a peptidomemetic known as CC^{mut3}, delivered as a plasmid.[4] In this study, CC^{mut3} is delivered to cells as a protein by utilizing a leukemia-specific cell-penetrating peptide (CPP).[5] Here, recombinant CPP-CC^{mut3} was expressed, purified, and tested for its antioncogenic activity. CPP-CC^{mut3} was able to enter two leukemic cell lines (K562 and Ba/F3−P210) and inhibit Bcr-Abl activity as shown by induction of necrosis/apoptosis via 7-AAD/Annexin V staining, reduction of oncogenic potential in colony forming assays, reduction of cell proliferation, and inhibition of Bcr-Abl phosphorylation (kinase activity). Further, CPP-CC^{mut3} did not enter nonleukemic cell lines (HEK293 and MCF-7). While CPP-CC^{mut3} was able to enter the parental, nonleukemic Bcr-Abl$^-$ Ba/F3 pro-B cell line, it revealed no signs of activity in the assays performed, as expected. These results indicate the feasibility of using CPP-CC^{mut3} as a therapeutic against CML.

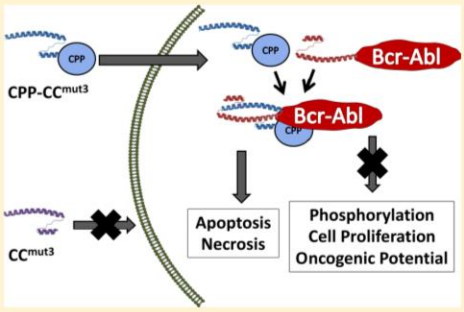

KEYWORDS: *CML, cell-penetrating peptide, Bcr-Abl, coiled-coil, CC^{mut3}*

INTRODUCTION

Chronic myeloid leukemia (CML) is a myeloproliverative disorder characterized by the presence of the Philadelphia chromosome (Ph^+). This truncated version of chromosome 22 is formed by a reciprocal translocation between the Abelson (Abl) tyrosine kinase gene of chromosome 9 with the breakpoint cluster (Bcr) gene of chromosome 22, resulting in the formation of the Bcr-Abl fusion gene.[6] The product of this translation, the Bcr-Abl protein, is the causative agent of CML.[7] Bcr-Abl is a constitutively active tyrosine kinase that alters many cellular processes including the JAK-STAT, PI3K/AKT, RAS, and MAPK signaling pathways.[1]

Bcr-Abl is active as a tetramer; the N-terminus of Bcr contains a coiled-coil domain (CC), which allows for dimerization and further tetramerization of Bcr-Abl molecules.[8,9] Once tetramerized, Bcr-Abl trans-autophosphorylates the tyrosine kinase domain present in the Abl portion of the protein, which is responsible for the constitutive kinase activity of Bcr-Abl.[3] Most currently approved therapies target this tyrosine kinase domain, known as tyrosine kinase inhibitors, or TKIs. Treatment with TKIs has transformed CML from a disease with a poor long-term prognosis into a chronic, treatable condition.[7,10,11] However, with continued treatment, many patients become resistant to these TKIs mainly due to point mutations in the tyrosine kinase domain that prevent TKI binding.[12−14] Second and third generation TKIs have been developed specifically to treat those whose disease is resistant to the breakthrough first generation inhibitor, imatinib (Gleevec).[7,15] Nevertheless, clinical resistance to all second and third generation TKIs, including the most recently approved TKI ponatinib (Iclusig), has already been seen.[2,16,17] It is believed that, with continued treatment, patients will inevitably develop point mutations in the tyrosine kinase domain that abrogate TKI effectiveness.[13,18−20]

While current agents target the tyrosine kinase domain, another possible target is the CC at the N-terminus of the protein.[21−23] Our lab has created a mutant version of the CC present in Bcr (CC^{mut3}), which preferentially binds to the CC of Bcr-Abl while avoiding autodimerization with itself.[24] CC^{mut3} prevents dimerization (and therefore tetramerization) of Bcr-Abl and thereby halts trans-autophosphorylation.[4,24] Additionally, CC^{mut3} inhibits both wild-type Bcr-Abl[24,25] and a clinically relevant mutant form Bcr-Abl (Bcr-Abl T315I),[25] while it is nontoxic to Bcr-Abl$^-$ cells.[4,24,25] Additionally, CC^{mut3} acts additively with ponatinib to further decrease the oncogenicity of Bcr-Abl T315I, the "gatekeeper" mutation.[25]

All of this previous work with CC^{mut3} was performed via transfection of plasmid DNA[4,24−26] or lentiviral infection (patient samples[27]) as proof of concept in vitro and ex vivo.

Received: October 17, 2014
Revised: March 27, 2015
Accepted: April 9, 2015
Published: April 9, 2015

DOI: 10.1021/mp500701u
Mol. Pharmaceutics 2015, 12, 1412−1421

However, transfection or viral delivery is not currently clinically feasible for CML. The aim of this study is to translate these findings by delivering CC^{mut3} as a protein.

Peptide and protein therapeutics are growing in popularity and commercial use,[28,29] and cell-penetrating peptides (CPPs) are a promising way to internalize proteins, thus enhancing intracellular activity.[30,31] CPPs are short, often positively charged peptides that are able to translocate across cell membranes.[32] These peptides are capable of carrying attached DNA, peptides, and proteins across cell membranes,[33] and some are currently being tested in clinical trials.[28,30,33] For this study, a leukemia-specific CPP was utilized for delivery of CC^{mut3} preferentially (if not specifically) to leukemia cells.[5] This CPP has the amino acid sequence CAYHRLRRC and contains two motifs, a lymph node-homing motif (CAY) and a cell-penetrating motif (RLRR), which give it a positive charge at physiologic pH.[5] It was discovered by phage display[5] and has shown to be nontoxic to leukemia cells by itself. Further, the CPP entered patient-derived leukemia cells but not non-leukemic patient-derived blood cells.[5]

The studies in this paper aim to test if CC^{mut3} can be an effective treatment for CML when delivered as a protein. CPP-CC^{mut3} and controls were encoded in plasmids, and corresponding proteins were expressed in *E. coli* and purified. After identity verification, these recombinant proteins were tested for their ability to enter leukemic and nonleukemic cells. 7-AAD/Annexin V staining, colony forming assays, cell proliferation assays, and kinase activity Western blots were then performed to test the antioncogenic activity of CPP-CC^{mut3}.

MATERIALS AND METHODS

Plasmid Construction. Plasmids encoding wild-type CC (CC^{wt}) and CC^{mut3} were created as previously described.[4,24] The DNA encoding the CPP was added with the primers 5′-TAACATTGTACACAACTGCGCGTATCATCGCCTGCG-CCGCTGCATGGTGGACCCGGTGGGCTTCGC-3′ and 5′-ACTGAATAAGCTTTTAGCAGCAGCCCGGGCAGCACC-GGTCATAGCTCTTCTTTTCCTTGGCCAGCAACG-3′, and resulting constructs were subcloned into the ELP-Intein vector (Qiagen, Valencia, CA, USA) using *Bsr*GI and *Hind*III restriction sites. An N-terminal 6x histidine tag and HRV-3C (PreScission) protease site (LEVLFQ/GP) were then added with the forward primers 5′-CGCAAGGGAGCT-CCCATCATCATCATCATCATCTTGAAGTTCTTTTTC-AAGGTCCTTGCGCGTATCATCGCCTGCG-3′ and 5′-CGCAAGGGAGCTCCCATCATCATCATCATCTTG-AAGTTCTTTTTCAAGGTCCTATGGTGGACCCGGTGG-GCTT-3′ for the constructs with and without the LS-CPP, respectively. The back primer 5′-TATGCTGGATCC-TTACCGGTCATAGCTCTTC-3′ was used for all constructs. The inserts were subcloned into the protein expression vector, pMal-C2x (New England Biolabs) using *Sac*I and *Bam*HI restriction sites. In this way, the final constructs encoding maltose binding protein (M)-6x histidine tag (H)-HRV-3C protease site (P)-leukemia-specific CPP-CC^{mut3} (MHP-CPP-CC^{mut3}), MHP-CPP-CC^{wt}, and MHP-CC^{mut3} were created.

Protein Expression and Purification. BL21(DE3) *E. coli* cells (Invitrogen, Carlsbad, CA, USA) were transformed with the plasmids described above per the manufacturer's protocol. Five milliliters of Rich Medium [10 g of tryptone (Sigma-Aldrich, St, Louis, MO, USA), 5 g of yeast extract (Sigma-Aldrich), 5 g of NaCl (ThermoFisher, Waltham, MA, USA), and 2 g of glucose (Sigma-Aldrich) per liter] was supplemented with carbenecillin (Invitrogen) to a final concentration of 50 μg/mL. This was seeded with freshly transfected BL21(DE3) cells and grown overnight. Sixteen hours later, 1 L of rich medium was inoculated with the 5 mL overnight culture and grown at 37 °C until the desired optical density @600 nm (0.4, 0.6, 0.8, 1.0) was reached (Varian Cary 100, Agilent Technologies, Santa Clara, CA, USA). A sample of 0.2 μm filtered (Acrodisc nylon filter, Life Sciences, St. Petersburg, FL, USA) isopropyl β-D-1-thiogalactopyranoside (IPTG) (GoldBio, St. Louis, MO, USA) was added to the culture to a final concentration of 0.5 or 1.0 mM to induce protein expression. Cultures were then grown for 4 or 16 h at 27 or 37 °C.

After expression, the culture was transferred to 500 mL centrifuge containers and centrifuged at 4000*g* for 20 min. The supernatant was discarded, and the pellet was resuspended in 45 mL of amylose binding buffer (ABB) [20 mL of 1.0 M Tris-HCl, pH 7.4 (Sigma-Aldrich), 11.7 g of NaCl (Fisher), 2.0 mL of 0.5 M EDTA (Fisher), 154 mg of DTT (GoldBio), with a sufficient quantity of Milli-Q water to make 1 L, filtered with a 0.4 μm nylon vacuum filter (VWR)], transferred to a 50 mL tube, and frozen at −20 °C overnight.

The following morning, the sample was thawed on ice and transferred to a 100 mL beaker. Approximately 5 mg of egg-white lysozyme (Sigma-Aldrich) was added, and the sample was incubated on ice for 1 h with occasional stirring. After the hour, the sample was sonicated for six cycles of 10 s on, 15 s off at 20% amplitude with the Sonic Dismembrator Model 500 (Fisher Scientific). Fifty microliters of 10% poly(ethylenimine) (Sigma-Aldrich) was added to the sample to precipitate the DNA. The samples were transferred to centrifuge tubes and spun at 15 000*g* for 30 min. The supernatant was transferred into a fresh 50 mL tube, and the pellet was saved for analysis. Samples were stored at 4 °C with 0.1% sodium azide (Sigma-Aldrich).

The supernatant was then purified on amylose resin (New England Biolabs). After elution with ABB+20% v/v maltose (Sigma-Aldrich), the protein was diluted with ABB to a concentration of 0.9 mg/mL to prevent precipitation during the next step. The proteins were incubated with the HRV-3C (PreScission) protease (a kind gift from Katherine Ferrell, laboratory of Dr. Chris Hill, University of Utah) overnight at 4 °C. Next, samples were dialyzed into cobalt binding buffer [7 g of sodium phosphate (Sigma-Aldrich), 17.5 g of NaCl (Fisher) per liter, 0.4 μm filtered] using SnakeSkin dialysis tubing, 3.5 kDa molecular weight cutoff (MWCO) (ThermoFisher). The maltose binding protein and protease site were then removed by running the sample over cobalt resin (GoldBio Technologies). Since the HRV-3C protease also had a His tag, it was removed along with the maltose binding protein. Proteins were concentrated to 0.5 mg/mL using a 9 kDa MWCO centrifugal protein concentrator (ThermoFisher), lyophilized, and stored in a desiccant container.

Protein Preparation for Experiments. Proteins were resuspended in DPBS (Gibco by Life Technologies, Grand Island, NY, USA) at a concentration of 1 mg/mL. Resuspended proteins were then run over a polyacrylamide desalting column (Fisher Scientific, Hanover Park, IL, USA). CPP-His, which was ordered from LifeTein (South Plainfield, NJ, USA), was run over a column with a MWCO of 1.8 kDa, while the other three constructs (CPP-CC^{mut3}, CPP-CC^{wt}, and CC^{mut3}) were run over columns with a 7 kDa MWCO. The samples were then sterile filtered through a 0.22 μm PVDF filter (EMD Millipore,

DOI: 10.1021/mp500701u
Mol. Pharmaceutics 2015, 12, 1412−1421

Billerica, MA, USA) into sterile tubes. The proteins concentrations were found using absorption at 280 nm with extinction coefficients and molecular weight on the Nanodrop 2000 spectrophotometer (Thermo Scientific). These values were corroborated by BCA assays (Thermo Scientific).

Cell Lines. Cell lines were maintained at 37 °C and 5% CO_2 in a humidity controlled incubator. K562 human leukemia, Bcr-Abl$^+$ cells (a gift from Kojo Elenitoba-Johnson, University of Michigan) were cultured in RPMI 1640 (Invitrogen) with 10% FBS (HyClone Laboratories, Logan, UT, USA), 1% penicillin/streptomycin (Invitrogen), 1% L-glutamine (Invitrogen), and 0.1% gentamycin (Invitrogen), referred to as complete RPMI. Cells were passaged every 2−3 days and seeded at 50 000 cells/mL.

Ba/F3 murine pro-B cells (a gift from Michael Deininger, University of Utah) were transformed to stably express P210 Bcr-Abl, as previously described,[34] and grown in complete RPMI. Nontransformed (parental, Bcr-Abl$^-$) Ba/F3 cells were grown in complete RPMI supplemented with 15% WEHI-3B conditioned media as a source of murine IL-3 required for proliferation.[35] Parental Ba/F3 cells are commonly used as a control cell to the Bcr-Abl$^+$ Ba/F3 P210 cell line.[25,36−38] Cells were split every 2−3 days and seeded at 100 000 cells/mL. The parental Ba/F3 cell media always contained 15% WEHI-3B conditioned media, regardless of what other supplements the experiment required to be omitted (FBS, penicillin, streptomycin, gentamicin).

The nonleukemia cell lines HEK-293 (human embryonic kidney cells, a kind gift from Hamid Ghandehari, University of Utah) and MCF7 (human breast cancer cells, ATCC) were grown as monolayers cultured in DMEM (Invitrogen) with 10% FBS, 1% penicillin/streptomycin, 1% L-glutamine, and 0.1% gentamycin, referred to as complete DMEM. Cells were split 1:5 every 2−3 days when they were 80−90% confluent.

Mass Spectrometry. *Intact Protein Analysis by ESI/MS.* CPP-CC^{mut3}, CPP-CC^{wt}, and CC^{mut3} were analyzed via electrospray ionization mass spectrometry (ESI/MS). For ESI/MS of intact proteins, samples were purified using the C18 Ziptip (Millipore). ESI/MS analysis of the intact proteins was performed using a Quattro-II mass spectrometer (Micromass, Inc., Milford, MA, USA). The eluent from Ziptip purification was infused into the instrument at 3 μL/min. Data were acquired with a cone voltage of 50 eV, spray voltage of 2.8 kV, and the instrument was scanned from 800−1400 m/z in 4 s. Scans were accumulated for about 1 min. Spectra were combined, and multiply charged molecular ions were deconvoluted into molecular-mass spectrum (i.e., processed into neutral molecular weight) using MaxEnt software (Micromass, Inc.).

MALDI/MS Analysis. CPP-His was analyzed by matrix-assisted laser desorption ionization/mass spectrometry (MALDI/MS). The mass spectral data shown were collected using delayed ion extraction mode on a Bruker's ultrafleXtrem MALDI-time-of-flight (TOF)/TOF mass spectrometer (Bruker Corp., Billerica, MA, USA). Peptide sample was spotted using dried-droplet method. Fresh solution of saturated α-cyano-4-hydroxy cinnamic acid matrix (CHCA) in a solvent system of 50:50 water/acetonitrile 0.1% TFA was prepared by thoroughly mixing the matrix powder with 0.5 mL of solvent in a 1.7 mL Eppendorf tube, and then any undissolved matrix was centrifuged to pellet. The supernatant of this matrix solution was used for sample preparation for MALDI analysis. Peptide samples (0.5 μL of 1 pmol/μL) were loaded onto a target plate and mixed on the target with 0.5 μL of supernatant of saturated matrix solution. The sample spot was air-dried followed by cocrystallization of the mixture. The spot was then ablated with a 1 kHz smartbeam-II laser technology (Bruker) from the plate, while the sample was simultaneously desorbed and ionized, then accelerated into a flight tube. The MALDI spectrum was acquired in reflector mode, which was operated at around 30 000 resolving power over a mass range from 500−5000 Da.

Peptide Internalization and Kinase Activity Western Blots. Samples of 1.0×10^6 cells resuspended in RPMI (K562 or Ba/F3) or DMEM (HEK-293 or MCF7) were seeded in a CellStar six-well plate (Sigma-Aldrich). Cells were then treated with the peptides (CPP-CC^{mut3}, CPP-CC^{wt}, CC^{mut3}, and CPP-His) at a final concentration 30 μM. This is a standard concentration used in cell-penetrating peptide studies. For the kinase activity Western blot, cells were treated with peptides for 16 h.

For the internalization experiment, cells were treated with peptides for 1.5 h followed by washes with heparin sulfate and trypsin, which has been shown to remove over 95% of membrane-associated (noninternalized) proteins.[39] Cells were first washed with a 15 min incubation at 37 °C with heparin sulfate, 0.5 mg/mL (a gift from Kuby Balagurunathan, University of Utah). Cells were centrifuged and resuspended in 1 mL of plain RPMI. Trypsin was added to a final concentration of 0.1% w/v, and the cells were incubated at 37 °C for 10 min. At that time, 1 mL of FBS was added to neutralize the trypsin. Cells were then centrifuged at 500g for 10 min, followed by three rounds of washes with 5 mL of cold PBS.

For both kinase activity and internalization Western blots, cells were resuspended in 100 μL of RIPA lysis buffer (Cell Signaling, Danvers, MA, USA) with 100x protease/phosphatase inhibitor added (Cell Signaling) and transferred into a prechilled microcentrifuge tube. Cells were then sonicated, centrifuged at 12 000g for 15 min, and then the supernatant was transferred into a fresh, prechilled microcentrifuge tube. A BCA assay (Thermo Scientific) was run per manufacturer's protocol to calculate protein concentrations, and 10 μg of total protein was loaded for each sample.

Following gel electrophoresis on a 10% Bis-Tris gel (Life Technologies) and transfer onto a PVDF membrane (Life Technologies), the membranes were blocked for 1 h with TBST + 5% milk, washed, and probed for the desired proteins. For the kinase activity Western blot, the Cell Signaling PathScan Bcr/Abl activity assay antibody, (CS5300s, Cell Signaling 1:250 dilution) which probes for phospho-Bcr-Abl, phospho-STAT5, phospho-CrkL, and the loading control Rab11, was used.

To analyze internalization, primary antibodies against the N-terminal 20 amino acids of the CC (BCR-N-20 sc-885, Santa Cruz Biotechnology, Santa Cruz, CA, USA, 1:500 dilution), 6x histidine tag (ab18184, Abcam, Cambridge, CA, USA, 1:1000 dilution), and actin (ab1801, Abcam, 1:1000 dilution) were used. All primary antibodies were diluted in TBST + 5% bovine serum albumin (Sigma-Aldrich) and incubated at 4 °C for 16 h. After three 5 min TBST washes, secondary antibodies were added and incubated at room temperature for 1 h. Antirabbit (CS7074s, Cell Signaling, 1:3000) and antimouse (ab6814, Abcam, 1:5000) were diluted in TBST + 5% milk. Following washes and the addition of the Westernbright chemiluminescent reagent (Bioexpress, Kaysville, UT, USA), the blots were imaged on a FluorChem FC2 imager (AlphaInnotech, San

DOI: 10.1021/mp500701u
Mol. Pharmaceutics 2015, 12, 1412−1421

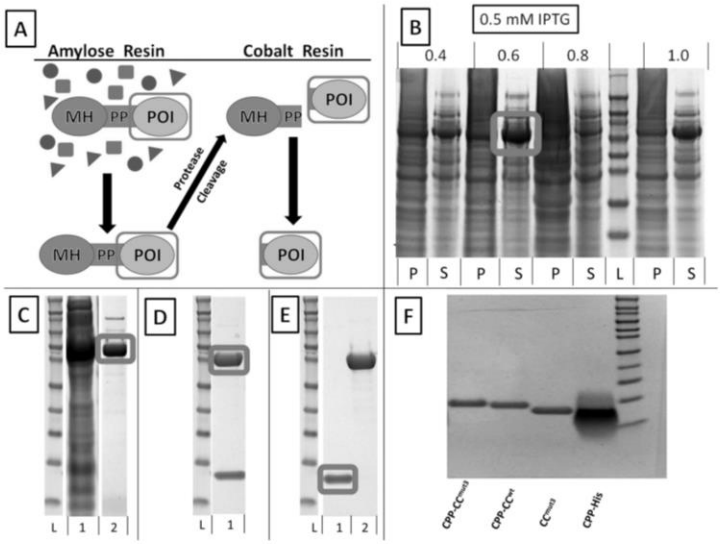

Figure 1. Expression and purification of proteins. POI is boxed in all figures. (A) Overview of the purification scheme. (B) Expression of fusion proteins was found to be optimal when induced at OD = 0.6 at 600 nm with 0.5 mM IPTG and then grown for 4 h at 37 °C. Lanes alternate between pellets (P) and supernatants (S), taken after lysis and centrifugation. Samples were then (C) purified on amylose resin (Lane 1 is pre amylose purification, lane 2 is post amylose purification), (D) cleaved with the HRV-3C protease, and (E) the affinity/solubility tags were separated from proteins of interest in a cobalt column (Lane 1 is the flow through, lane 2 is the eluate). (F) Purity was tested via SDS-PAGE gel. MH = Maltose Binding Protein and 6x Histidine tag. PP = PreScission Protease site; POI = Protein of interest; IPTG = isopropyl β-D-1-thiogalactopyranoside.

Leandro, CA, USA). Western blots were performed three times with samples from three different cell treatments (n = 3).

Treatment of Cells for Activity Experiments (Colony Forming, Cell Proliferation, 7-AAD/Annexin V, Western Blot Kinase Activity). Samples of 6 ×10^4 cells (K562, parental Ba/F3, or Ba/F3 P210) were seeded in a six-well CellStar plate in RPMI. Proteins (30 μM) or imatinib (standard dosing of 1.0 or 2.5 μM) (a gift from Novartis) were added, and PBS was added to a final volume of 1 mL. Sixteen hours after the treatment, 1 mL of complete RPMI was added to the wells.

7-AAD and Annexin V Staining. Forty-eight or 72 h after treatment with the proteins (30 μM) or imatinib (2.5 μM), 1.0 mL of cells from each treatment was pelleted and resuspended in 0.5 mL of 1x Annexin Binding Buffer (Invitrogen). A 0.5 μL sample of 1 mM 7-AAD (Invitrogen) was added to each sample, followed by a 45 min incubation on ice. Five minutes before analysis via flow cytometry, 1.0 μL of Annexin V (APC) (Invitrogen) was added to each sample. Analysis was performed using the FACS Canto-II (BD BioSciences, University of Utah Core Facility) with FACS Diva software. 7-AAD and APC were excited at 488 and 635 nm wavelengths, and emissions were detected at 660 nm. Percentage of apoptosis/necrosis was calculated by the percentage of cells that stained positive for 7-AAD or APC. Independent treatments were tested three times (n = 3).

Colony Forming Assay. This experiment was carried out as before[4,24,25] with the modifications noted below. Sixteen hours after treatment with proteins (30 μM) or imatinib (1.0 μM), 1.0 × 10^4 cells were transferred to 1 mL of IMDM (Iscove's modified Dulbecco's media) with 2% FBS, and from this, 3.0 × 10^3 cells were taken and seeded in 3 mL of Methocult media in the absence of cytokines (H4230 media for K562, M3234 media for Ba/F3−P210) or in the presence of cytokines (GF M3434 media for parental Ba/F3 cells). Imatinib, but not proteins, was added again to the Methocult media for the imatinib-treated cells to a final concentration of 1.0 μM. Cells (1 × 10^3 in 1.1 mL) were seeded in a six-well plate (CellStar) in duplicate for each treatment. Seven days after seeding cells, colonies were counted in a 100 μm^2 area per well. Independent treatments were tested three times in duplicate (n = 3). All reagents for the CFA were purchased from Stem Cell Technologies, Vancouver, BC, Canada.

Cell Proliferation. Sixteen hours following treatment, cells were transferred to a 25 cm^2 flask, where 4 mL of complete RPMI was added. At 48, 72, and 96 h post-treatment, trypan blue (Life Technologies) was used to determine cell viability as done previously.[4,24,25] Cell counts were performed using both a standard light microscope and Countess automated cell counter (Invitrogen). Independent treatments were tested three times (n = 3).

■ RESULTS

Protein Constructs Were Expressed and Purified. A graphical overview of the protein purification scheme can be found in Figure 1, panel A. Constructs were successfully cloned and then transformed into BL21(DE3) *E. coli* cells, and this was followed by optimization of fusion protein expression. After lysis, DNA precipitation, and centrifugation, the supernatant containing the protein of interest (POI) was collected and run on a sodium dodecyl sulfate polyacrylamide gel electrophoresis (SDS-PAGE) gel and stained with Simply Blue SafeStain (Invitrogen). Optimal expression was achieved when the cultures were induced at a 0.6 OD at 600 nm with 0.5 mM IPTG and then grown for 4 h at 37 °C (Figure 1B, lane 4, boxed).

The supernatants (containing the POI) collected after lysis were then loaded onto an amylose resin column and washed with amylose binding buffer ABB until <0.1 mg/mL of protein

DOI: 10.1021/mp500701u
Mol. Pharmaceutics 2015, 12, 1412−1421

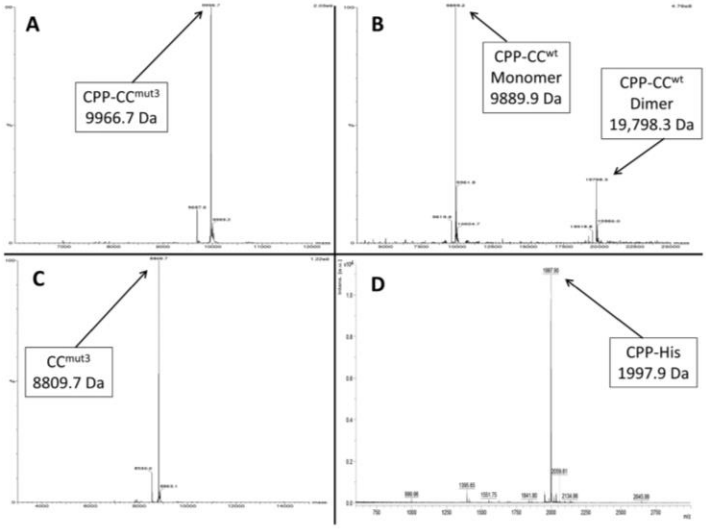

Figure 2. MS supports the identity and purity of constructs. (A) The sole major peak for CPP-CC^{mut3} agrees with theory (theoretical MW 9969.6 Da, experimental MW 9966.7 Da) and supports the presence of a disulfide bond leading to cyclization of the CPP. (B) CPP-CC^{wt} has two major peaks, the first representative of a monomer and the second of a covalent CC:CC dimer (theoretical MW 9901.7 Da, experimental MW 9889.9 Da, 19 798.3 Da). (C) The major peak from CC^{mut3} agrees with theory (theoretical 8810.2 Da, experimental 8809.7 Da). (D) CPP-His's only major peak agrees with the theoretical MW and belies the presence of a cyclizing disulfide bridge in the CPP (theoretical 2000.3 Da, experimental 1997.9 Da).

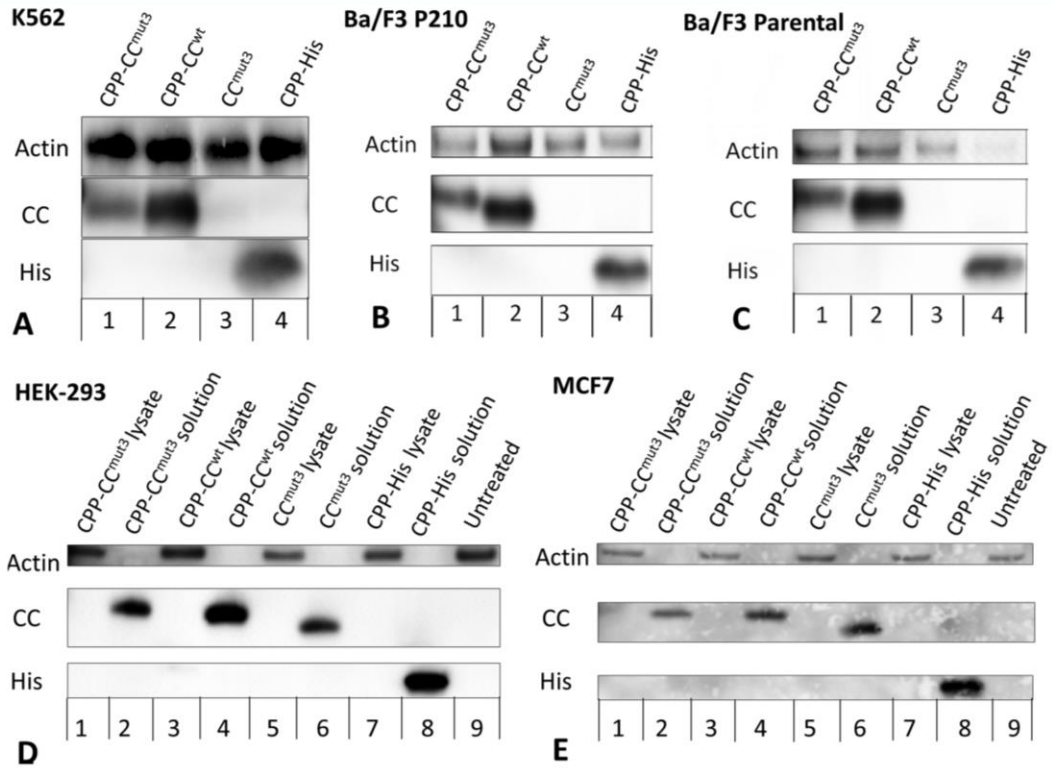

Figure 3. Internalization Western Blots. (A) In leukemic K562 cells, constructs with the cell-penetrating peptide were able to enter, while CC^{mut3} without the CPP was unable to enter the cells. (B, C) In Ba/F3−P210 and parental Ba/F3 cells, only those proteins with the CPP were internalized. (D, E) In nonleukemic HEK-293 and MCF7 cells, none of the proteins were able to enter the cells. For panels D and E, lanes alternate between cell lysates (odd lanes) and purified protein solutions (even lanes, run as a control for the antibody). For all, representative images shown, $n = 3$.

DOI: 10.1021/mp500701u
Mol. Pharmaceutics 2015, 12, 1412−1421

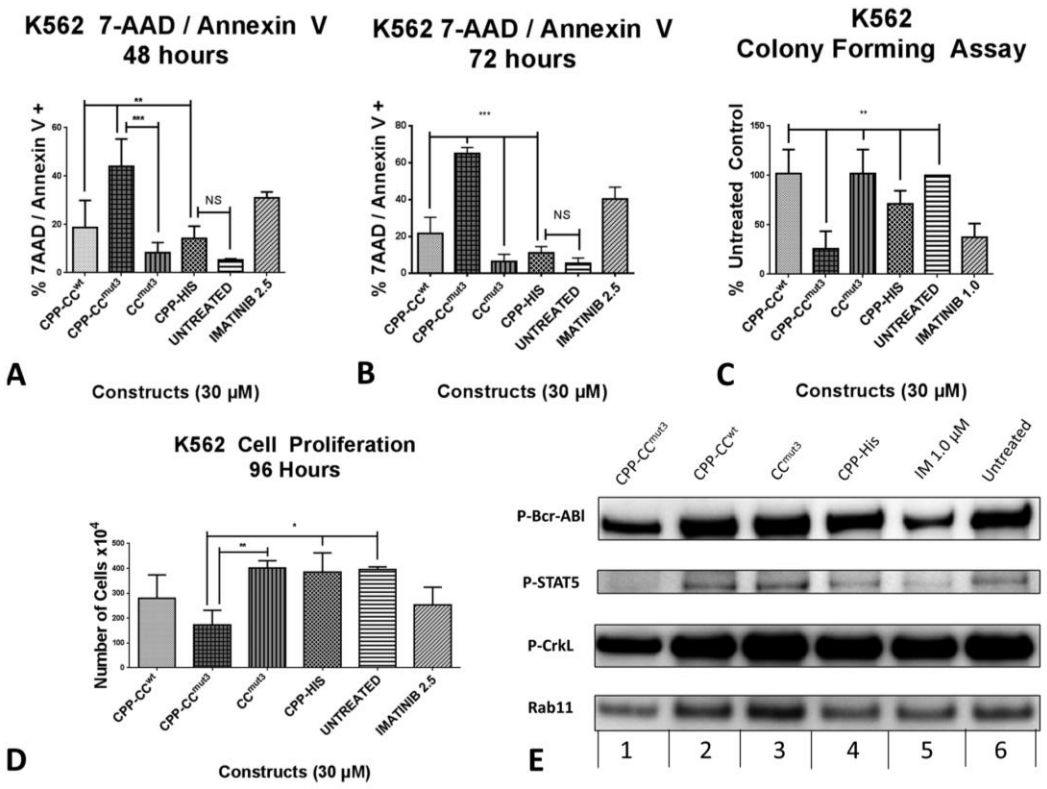

Figure 4. Internalized CPP-CC^{mut3} induces apoptosis/necrosis, reduces proliferation, inhibits colony forming, and reduces phosphorylation of Bcr-Abl in K562 cells. (A, B) In the 7-AAD/Annexin V assay, CPP-CC^{mut3} was superior at inducing apoptosis and necrosis compared to all treatments except imatinib at both 48 and 72 h post-treatment. (C) In a test of transformative ability, CPP-CC^{mut3} reduced colony forming. (D) In this cell proliferation assay, CPP-CC^{mut3} decreased the proliferation of K562 cells. (E) In kinase activity Western blots, CPP-CC^{mut3} qualitatively deceased phosphorylation of Bcr-Abl as well as its downstream targets CrkL and STAT5 (representative blot shown). Rab11 is a loading control. For all experiments, $n = 3$. Values reported as overall means ± SD; one-way ANOVA with Tukey's post-test, $* p < 0.05$, $** p < 0.01$, $*** p < 0.001$.

was flowing off the column. At this point, the POI was eluted with ABB + 20% v/v maltose (Figure 1C, lane 2). To remove the maltose binding protein, the recombinant protein was cleaved with HRV-3C protease (Figure 1D, lane 1). The proteins were diluted to 0.9 mg/mL prior to cleavage to prevent precipitation upon cleavage. After dialysis into cobalt binding buffer, the POIs were loaded onto a cobalt resin. The POIs flow through the column (Figure 1E, lane 1), while the histidine tags of the maltose binding protein and HRV-3C protease adhere to the column (Figure 1E, lane 2). Samples were tested for purity by SDS-PAGE and all found to be >95% purity (Figure 1F). Proteins were then lyophilized and stored desiccated at −20 °C.

To verify the identity of the purified proteins, their sequences were analyzed using MS (Figure 2). A 2 Da difference between predicted and experimental masses of CPP-CC^{mut3} suggests an intramolecular disulfide bond (Figure 2A, theoretical MW 9969.6 Da, experimental MW 9966.7 Da). Since there are only two cysteine residues in the protein, the disulfide bridge must be formed within the CPP, thus cyclizing it. This is known to be required for internalization for this leukemia-specific CPP.[5] A portion of CPP-CC^{wt} appeared to be present as a dimer (Figure 2B, theoretical MW 9901.7 Da, experimental MW 9889.9 Da, 19 798.3 Da). CPP-CC^{mut3} did not exhibit this dimerization, which implies that mutations introduced into the CC[24] inhibited homo-oligemerization of CC^{mut3}. Results for CC^{mut3} without the cell-penetrating peptide as well as CPP-His matched theoretical molecular weights and support cyclization of the CPP in CPP-His (Figure 2C, theoretical 8810.2 Da, experimental 8809.7 Da; Figure 2D, theoretical 2000.3 Da, experimental 1997.9 Da). Minor peaks were seen for CPP-CC^{mut3}, CPP-CC^{wt}, and CC^{mut3} with a mass shift of approximately 279.7. The major peak in each of the MS combined with SDS-PAGE showed construct purity of >95%.

LS-CPP Delivers Proteins Specifically to Blood cells. Proteins were added to 1×10^6 K562 cells at a final concentration of 30 μM, a dose that was chosen based on the original doses used by Nishimura et al. as well as a pilot dosing 7-AAD performed with CPP-CC^{mut3} (data not shown).[5] Western blots with antibodies against the CC and His tag were used (Figure 3). The Western blot in Figure 3 shows that all constructs with the CPP were internalized by K562 cells (Figure 3A, lanes 1, 2, and 4), while CC^{mut3} without the CPP was not internalized (Figure 3A, lane 3).

The same internalization study was carried out with Ba/F3 pro-B mouse cells in both unmodified Ba/F3 cells and Ba/F3 cells engineered to stably express the 210 kDa variant of Bcr-Abl (Ba/F3−P210), thus giving it a CML phenotype. All of the

DOI: 10.1021/mp500701u
Mol. Pharmaceutics 2015, 12, 1412−1421

constructs with the CPP were internalized into both cell lines (Figure 3B,C, lanes 1, 2, and 4). Since the only modification between these cells is the presence of Bcr-Abl, differences between these cell lines in activity assays can allow us to understand if the activity of CPP-CC^{mut3} is Bcr-Abl dependent.

Two nonleukemic cell lines previously shown by Nishimura et al. to not internalize this CPP[5] were tested to determine if the CPP is indeed leukemia-specific. HEK-293 human embryonic kidney cells and MCF7 human breast cancer cells were treated with the proteins and peptide, and cell lysates were probed for the presence of the CC and His motifs. Figure 3, panels D (Hek-293) and E (MCF7) are representative Western blots showing that none of the constructs entered these nonleukemic cells. The odd lanes are the cell lysates of the treated cells, while the even lanes are a solution of the purified proteins, as a positive control for the antibodies. The absence of bands in the cell lysate lanes (odd numbered lanes) indicates the lack of entry of these proteins into the cells (Figures 3D,E). While only two cell lines were tested here, the original study by Nishimura et al. demonstrated the specificity of the LS-CPP in a variety of leukemic and nonleukemic cell lines and patient samples.[5]

Activity in K562 Cells. After these studies showed protein delivery to leukemic cells, experiments were performed to investigate if CPP-CC^{mut3} is active in Bcr-Abl$^+$ K562 leukemia cells. To this end, the first experiment carried out utilized 7-AAD and Annexin V staining, a flow cytometry assay testing for induction of necrosis and apoptosis, respectively. Cells were prepared for flow cytometry, and percentages of 7-AAD or Annexin V positive cells were calculated at 48 h (Figure 4A) and 72 h (Figure 4B) after treatment. CPP-CC^{mut3} was superior in inducing apoptosis compared to CPP-CC^{wt} as well as the negative controls CC^{mut3} and CPP-His (Figures 4A,B, bar 2 vs bars 1, 3, and 4). While CPP-His was internalized into K562 cells (Figure 3A, lane 4), it did not induce apoptosis/necrosis compared to untreated cells (Figure 4A,B, bar 4 vs bar 5). CC^{mut3} without the cell-penetrating peptide did not induce apoptosis (Figures 4A,B, bar 3), presumably because it did not enter K562 cells (Figure 3A, lane 3).

CPP-CC^{mut3} was then tested for its ability to inhibit transformative ability and oncogenic potential in K562 cells via the colony forming assay (Figure 4C) and cell proliferation (trypan blue cell proliferation assay, Figure 4D). Both of these experiments concur with the apoptosis/necrosis assays; CPP-CC^{mut3} was more effective at reducing cell proliferation and transformative ability of K562 cells than CPP-His and CC^{mut3} (Figures 4C,D, bar 2 vs bars 3 and 4), but was not statistically different from imatinib (Figures 4C,D, bar 2 vs bar 6). CPP-CC^{mut3} was superior to CPP-CC^{wt} in the colony forming assay but not in the cell proliferation assay (Figures 4C,D, bar 2 vs bar 1). CPP-His and CC^{mut3} were ineffective at reducing cell proliferation and colony forming compared to untreated cells, which suggests that the effect is specific to internalized CC^{mut3}.

Finally, a kinase activity Western blot was performed using antibodies probing for phospho-Bcr-Abl as well as its known downstream phosphorylation targets STAT5 (phospho-STAT5) and CrkL (phospho-CrkL) (Figure 4E).[4] CPP-CC^{mut3} (Figure 4E, lane 1) and imatinib (Figure 4E, lane 5) both qualitatively decreased phosphorylation of Bcr-Abl (1st row) as well as its downstream targets STAT5 (2nd row) and CrkL (3rd row) (Figure 4E, compare CPP-CCmut3, lane 1, 1st−3rd rows to untreated, lane 6, 1st−3rd rows).

Activity in Ba/F3 Cells. To further study the effects of CPP-CC^{mut3}, apoptosis/necrosis, colony forming, and cell proliferation, assays were carried out in both Bcr-Abl$^+$ and Bcr-Abl$^-$ Ba/F3 lineages. As previous experiments demonstrated, CPP-CC^{mut3} entered both cell types; these assays were performed to determine if CPP-CC^{mut3} was active *only* in the Bcr-Abl$^+$ Ba/F3−P210 cells and not the Bcr-Abl$^-$ Ba/F3 parental cells. 7-AAD/Annexin V experiments were carried out in these two cell lines at 48 h post-treatment (Figure 5A,B). In Ba/F3−P210 cells, CPP-CC^{mut3} was again superior to CPP-CC^{wt}, CC^{mut3}, and CPP-His in inducing apoptosis/necrosis (Figure 5A, bar 2 vs bars 1, 3, and 4) but was not statistically different from imatinib (Figure 5A, bar 2 vs bar 6). Further,

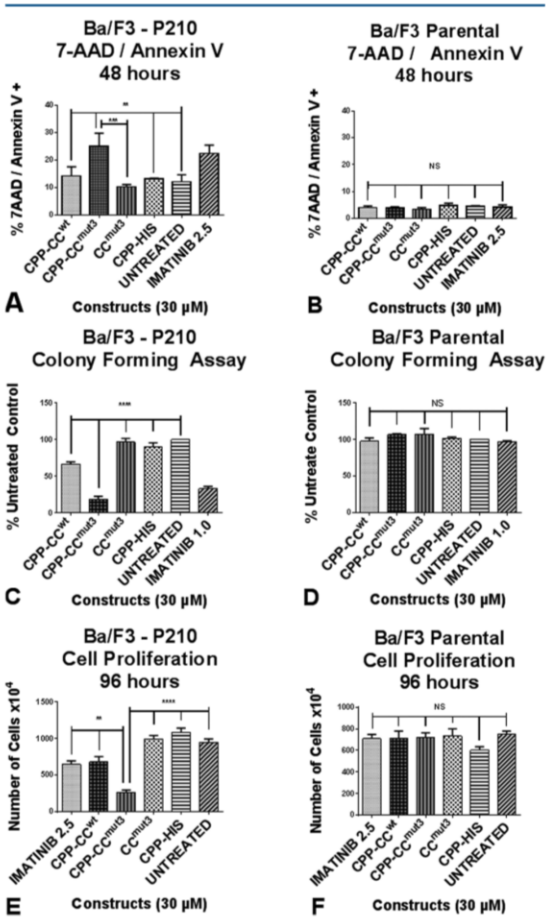

Figure 5. CPP-CC^{mut3} is active in Bcr-Abl$^+$ Ba/F3−P210 cells but not parental, Bcr-Abl$^-$ Ba/F3 Parental cells. (A, B) CPP-CC^{mut3} induced apoptosis and necrosis in (A) Bcr-Abl$^+$ Ba/F3−P210 cells, while it caused no effect on (B) parental, Bcr-Abl$^-$ Ba/F3 cells. (C, D) CPP-CC^{mut3} decrease colony formation in (C) Ba/F3−P210 cells, while it had no effect on (D) parental Ba/F3 cells. (E, F) Similarly, in the cell proliferation assay, CPP-CC^{mut3} inhibited cell proliferation in (E) Ba/F3−P210 cells, while none of the treatments had an effect on the proliferation of (F) parental Ba/F3 cells. For all experiments, $n = 3$. Values reported as overall means ± SD; one-way ANOVA with Tukey's post-test, $* p < 0.05$, $** p < 0.01$, $*** p < 0.001$, $**** p < 0.0001$.

DOI: 10.1021/mp500701u

CPP-His and CC^{mut3} lacking the CPP were not statistically different from the untreated control (Figure 5A, bars 3, 4, and 5). In the parental, Bcr-Abl$^-$ cells, no treatment (protein or imatinib) induced apoptosis/necrosis over the control, as expected (Figure 5B). These results therefore suggest that the activity of CPP-CC^{mut3} requires the presence of Bcr-Abl to induce apoptosis/necrosis, as anticipated.

The results of the colony forming (Figures 5C,D) and cell proliferation assays (Figures 5E,F) agree with the flow cytometry results (Figures 5A,B). In Ba/F3−P210 cells, CPP-CC^{mut3} was superior at inhibiting colony formation over all other treatments except imatinib 1.0 μM (Figure 5C, bar 2 vs bars 1, 3, and 4), whereas none of the treatments caused a difference in colony formation in the parental Ba/F3 cells (Figure 5D), as expected. The same trend was seen in the cell proliferation assay; at 96 h, CPP-CC^{mut3} inhibited cell proliferation to a greater extent that all other treatments in Ba/F3−P210 cells (Figure 5E, bar 3), and no treatment effects were seen from either imatinib or proteins in parental Ba/F3 cells, as expected (Figure 5F).

■ DISCUSSION

Previous work in our lab has shown that CC^{mut3} inhibits Bcr-Abl phosphorylation, induces apoptosis, and inhibits proliferation and transformative ability of CML cells.[4,24,25] Further, CC constructs were nontoxic to six Bcr-Abl negative cell lines, including THP-1, an acute monocytic leukemia cell line[40,41] (unpublished data). The work was performed using gene delivery methods where cells were either transfected or virally infected. Since these transfection methods are currently not clinically achievable for blood cancers, the purpose of this work was to deliver CC^{mut3} as a protein. To accomplish this, a leukemia-specific cell-penetrating peptide previously discovered by phage display was fused to CC^{mut3}.[5] CPP-CC^{mut3}, as well as controls CPP-CC^{wt} and CC^{mut3} (lacking the CPP), was cloned, expressed, and purified, while the 15 amino acid peptide control CPP-His was purchased.

CPP-CC^{mut3} entered K562 human leukemia cells (Figure 3A, lane 1) as well as two variants of Ba/F3 pro-B mouse cells, one of which expresses Bcr-Abl (Ba/F3−P210) (Figure 3B,C, lane 1). In addition to penetrating the cells, CPP-CC^{mut3} caused apoptosis/necrosis, reduced cell proliferation, and reduced transformative ability in K562 and Ba/F3−P210 cells, while it had no toxic effects on parental, Bcr-Abl$^-$ Ba/F3 cells (Figures 4A−D, bars 2, 5A−D, bar 2; Figure 5E−F, bar 3). Further, a Western blot of K562 cells demonstrated that CPP-CC^{mut3} decreases phosphorylation of Bcr-Abl as well as its downstream targets CrkL and STAT5 (Figure 4E, lane 1).

Since constructs containing the CPP did not internalize into MCF7 or HEK-293 cells, activity assays were not conducted for these non-blood cell lines. The activity experiments in the leukemia cells demonstrated that only internalized proteins were active (see CPP-CC^{mut3} vs CC^{mut3}), and since none of the proteins were taken up by MCF7 or HEK-293 cells, none should be active against the nonleukemic cells. This is supported by experiments from Nishimura et al., where a mitochondrial-toxic peptide was conjugated to the LS-CPP and was only toxic to the cells that internalized the construct.[5] Further, previous work in our lab has shown that CC^{mut3} is nontoxic to Bcr-Abl$^-$ cell lines, which thus demonstrates the specificity of CC^{mut3} for Bcr-Abl.[4,24]

CPP-CC^{mut3} has two built-in safeguards against nonspecific toxicity. The first safeguard is the leukemia-specific CPP, which preferentially delivers the construct to leukemia cells. The second is the Bcr-Abl specificity of CC^{mut3}. It has previously been shown that not only does CC^{mut3} induce apoptosis in Bcr-Abl$^+$ cells, but also is also nontoxic to Bcr-Abl$^-$ cells.[4,24,25] We also show here that CPP-CC^{mut3} enters but is nontoxic to the parental, Bcr-Abl$^-$ Ba/F3 cells (Figures 3C and 5B,D,F), which further supports this claim. To verify the leukemic-specificity of the CPP, internalization experiments testing if CPP-CC^{mut3} enters two nonleukemic cell lines (MCF7 and HEK-293) were carried out. In agreement with the original paper that discovered the LS-CPP,[5] no internalization of proteins was observed in these cell lines (Figures 3D,E). Further, Nishmura et al. showed lack of internalization correlated with the lack of induction of apoptosis of a mitochondrial-toxic peptide in six other cell lines including U251MG, A549, PC-9, PC-3, HepG2, and WM115 as well as patient-derived normal blood cells including T-lymphocytes, monocytes, and macrophages, demonstrating leukemia cell specificity.[5] Therefore, no activity experiments were carried out in these nonleukemic cells.

Others have attempted to use CC^{wt} to inhibit Bcr-Abl, however with limited efficacy compared to CC^{mut3}.[24,42−44] Further, only nonspecific CPPs have been used to deliver CC^{wt}.[41,45−47] Therefore, CPP-CC^{mut3} has added specificity and potency against Bcr-Abl$^+$ cells via the optimized CC^{mut3} and the leukemia-specific CPP.

Although TKIs have revolutionized CML treatment, patients often become resistant, which led to the development of second and third generation TKIs. It is thought that resistance to any (even future) generation of TKI is inevitable, as Bcr-Abl can mutate to avoid TKI binding, known as mutational escape.[2,22] Indeed, compound mutants (two point mutations in one molecule of Bcr-Abl) that confer resistance to ponatinib, a third generation agent, are already therapeutically problematic.[2,16] CC^{mut3} has many contact points with the CC of Bcr-Abl; therefore, it is unlikely that any single point mutation would be sufficient to prevent binding of CC^{mut3}. Further, any combination of mutations that disrupts CC:CC^{mut3} binding would likely also prevent two CC motifs from Bcr-Abl molecules from forming a dimer. To clarify, any mutation or mutations that allowed the native CC of Bcr-Abl to avoid binding by CC^{mut3} would also inhibit Bcr-Abl dimerization, thereby resulting in autoinactivation. Thus, CC^{mut3} may be able to avoid "mutational escape" by Bcr-Abl.[22]

Although CC^{mut3} may be resistant to mutational escape, it is important that CC^{mut3} be effective in patients who are already resistant to TKIs. Derivatives of the Ba/F3 cells, which express Bcr-Abl with clinically relevant point mutations in the tyrosine kinase domain, have been developed.[48,49] We have evidence that CC^{mut3}, when delivered as a plasmid, is effective against Bcr-Abl point mutations T315I,[25] E255V, and compound mutant E255V/T315I.[27] Further, CC^{mut3} is effective against primary patient samples with mutant Bcr-Abl (including Bcr-Abl T315I) when delivered lentivirally.[27]

CC^{mut3} and TKIs target different domains of Bcr-Abl, and combination therapy with CC^{mut3} and ponatinib resulted in additive effects.[25] Further, the combination allows for a dose reduction of ponatinib, which may be clinically relevant as ponatinib has severe toxic effects that are thought to be dose-dependent.[50,51]

This work provides critical evidence supporting the feasibility of delivering CC^{mut3} as a protein. However, CC^{mut3} may be further modified to improve translation potential. To that end, stability-enhancing modifications such as PEGylation or

DOI: 10.1021/mp500701u
Mol. Pharmaceutics 2015, 12, 1412−1421

hyperglycosylation may be implemented in future work.[28,52] Another possible modification is hydrocarbon stapling, which has been shown to increase helicity, enhance serum stability, and improve cell penetration.[52] A truncated, hydrocarbon stapled version of CC^{mut3} is currently being modeled and developed in our lab. Combining the CPP and a truncated, stapled CC^{mut3} has the potential to maximize stability, specificity, and membrane permeability. This stapled peptide could pave the way to translation to therapy. With the effectiveness of CC^{mut3} against compound mutants and additive effects with TKIs, CC^{mut3} may play an important role in the future of CML treatment.

■ AUTHOR INFORMATION

Corresponding Author

*Fax 801-585-3614. E-mail: carol.lim@pharm.utah.edu.

Author Contributions

The manuscript was written through contributions of both authors. Both authors have given approval to the final version of the manuscript.

Notes

The authors declare no competing financial interest.

■ ACKNOWLEDGMENTS

The authors acknowledge the use of DNA/Peptide Core, Flow Cytometry Core, and Mass Spectrometry and Proteomics Core (use of core facilities supported by P30 CA042014, awarded to the Huntsman Cancer Institute). We acknowledge support of funds in conjunction with NCI Cancer Center Support Grant No. P30 CA042014 awarded to Huntsman Cancer Institute. Research reported in this publication was also supported by the National Cancer Institute of the National Institutes of Health under Award No. NIH R01 CA129528. We thank Drs. Krishna Parsawar and Chad Nelson of the Mass Spectrometry and Proteomics Core Facility for valuable discussions regarding MS analysis. We would also like to thank Katherine Ferrell (Chris Hill lab, University of Utah) for producing the HRV3C protease used in this study. We would like to thank Thomas Cheatham, Geoffrey Miller, Andrew Dixon, Karina Matissek, Abood Okal, Phong Lu, David Woessner, Shixian Wang, Janice Muehle, and Connor Helgeson for collaborative work and scientific discussion.

■ REFERENCES

(1) Cilloni, D.; Saglio, G. Molecular pathways: BCR-ABL. *Clin. Cancer Res.* **2012**, *18* (4), 930−7.

(2) Zabriskie, M. S.; Eide, C. A.; Tantravahi, S. K.; Vellore, N. A.; Estrada, J.; Nicolini, F. E.; Khoury, H. J.; Larson, R. A.; Konopleva, M.; Cortes, J. E.; Kantarjian, H.; Jabbour, E. J.; Kornblau, S. M.; Lipton, J. H.; Rea, D.; Stenke, L.; Barbany, G.; Lange, T.; Hernandez-Boluda, J. C.; Ossenkoppele, G. J.; Press, R. D.; Chuah, C.; Goldberg, S. L.; Wetzler, M.; Mahon, F. X.; Etienne, G.; Baccarani, M.; Soverini, S.; Rosti, G.; Rousselot, P.; Friedman, R.; Deininger, M.; Reynolds, K. R.; Heaton, W. L.; Eiring, A. M.; Pomicter, A. D.; Khorashad, J. S.; Kelley, T. W.; Baron, R.; Druker, B. J.; Deininger, M. W.; O'Hare, T. BCR-ABL1 compound mutations combining key kinase domain positions confer clinical resistance to ponatinib in Ph chromosome-positive leukemia. *Cancer Cell* **2014**, *26* (3), 428−42.

(3) Liu, J.; Campbell, M.; Guo, J. Q.; Lu, D.; Xian, Y. M.; Andersson, B. S.; Arlinghaus, R. B. BCR-ABL tyrosine kinase is autophosphorylated or transphosphorylates P160 BCR on tyrosine predominantly within the first BCR exon. *Oncogene* **1993**, *8* (1), 101−9.

(4) Dixon, A. S.; Pendley, S. S.; Bruno, B. J.; Woessner, D. W.; Shimpi, A. A.; Cheatham, T. E., 3rd; Lim, C. S. Disruption of Bcr-Abl coiled-coil oligomerization by design. *J. Biol. Chem.* **2011**, *286* (31), 27751−60.

(5) Nishimura, S.; Takahashi, S.; Kamikatahira, H.; Kuroki, Y.; Jaalouk, D. E.; O'Brien, S.; Koivunen, E.; Arap, W.; Pasqualini, R.; Nakayama, H.; Kuniyasu, A. Combinatorial targeting of the macropinocytotic pathway in leukemia and lymphoma cells. *J. Biol. Chem.* **2008**, *283* (17), 11752−62.

(6) Bartram, C. R.; de Klein, A.; Hagemeijer, A.; van Agthoven, T.; Geurts van Kessel, A.; Bootsma, D.; Grosveld, G.; Ferguson-Smith, M. A.; Davies, T.; Stone, M.; et al. Translocation of c-ab1 oncogene correlates with the presence of a Philadelphia chromosome in chronic myelocytic leukaemia. *Nature* **1983**, *306* (5940), 277−80.

(7) Woessner, D. W.; Lim, C. S.; Deininger, M. W. Development of an effective therapy for chronic myelogenous leukemia. *Cancer J.* **2011**, *17* (6), 477−86.

(8) McWhirter, J. R.; Galasso, D. L.; Wang, J. Y. A coiled-coil oligomerization domain of Bcr is essential for the transforming function of Bcr-Abl oncoproteins. *Mol. Cell. Biol.* **1993**, *13* (12), 7587−95.

(9) Zhao, X.; Ghaffari, S.; Lodish, H.; Malashkevich, V. N.; Kim, P. S. Structure of the Bcr-Abl oncoprotein oligomerization domain. *Nat. Struct. Biol.* **2002**, *9* (2), 117−20.

(10) Hochhaus, A.; Druker, B.; Sawyers, C.; Guilhot, F.; Schiffer, C. A.; Cortes, J.; Niederwieser, D. W.; Gambacorti-Passerini, C.; Stone, R. M.; Goldman, J.; Fischer, T.; O'Brien, S. G.; Reiffers, J. J.; Mone, M.; Krahnke, T.; Talpaz, M.; Kantarjian, H. M. Favorable long-term follow-up results over six years for response, survival, and safety with imatinib mesylate therapy in chronic-phase chronic myeloid leukemia after failure of interferon-alpha treatment. *Blood* **2008**, *111* (3), 1039−43.

(11) Hunter, T. Treatment for chronic myelogenous leukemia: The long road to imatinib. *J. Clin. Invest.* **2007**, *117* (8), 2036−43.

(12) Branford, S.; Rudzki, Z.; Walsh, S.; Parkinson, I.; Grigg, A.; Szer, J.; Taylor, K.; Herrmann, R.; Seymour, J. F.; Arthur, C.; Joske, D.; Lynch, K.; Hughes, T. Detection of BCR-ABL mutations in patients with CML treated with imatinib is virtually always accompanied by clinical resistance, and mutations in the ATP phosphate-binding loop (P-loop) are associated with a poor prognosis. *Blood* **2003**, *102* (1), 276−83.

(13) Sierra, J. R.; Cepero, V.; Giordano, S. Molecular mechanisms of acquired resistance to tyrosine kinase targeted therapy. *Mol. Cancer* **2010**, *9*, 75.

(14) Radich, J. Structure, function, and resistance in chronic myeloid leukemia. *Cancer Cell* **2014**, *26* (3), 305−6.

(15) Cortes, J.; Radich, J.; Mauro, M. J. Clinical roundtable monograph: Emerging treatment options for TKI-resistant chronic myelogenous leukemia. *Clin. Adv. Hematol. Oncol.* **2012**, *10* (Suppl. 19), 1−16.

(16) Kimura, S.; Ando, T.; Kojima, K. BCR-ABL point mutations and TKI treatment in CML patients. *J. Hematol. Transfus.* **2014**, *2* (3), 1022−34.

(17) Bauer, R. C.; Sanger, J.; Peschel, C.; Duyster, J.; von Bubnoff, N. Sequential inhibitor therapy in CML: In vitro simulation elucidates the pattern of resistance mutations after second- and third-line treatment. *Clin. Cancer Res.* **2013**, *19* (11), 2962−72.

(18) Gorbunova, A.; Porozov, Y. *Structural Modeling of BCR-ABL Drug Resistance Mutations*; Moscow Conference on Computational Molecular Biology: Moscow, Russia, 2011; pp 291−2.

(19) Storey, S. Chronic myelogenous leukaemia market. *Nat. Rev. Drug Discovery* **2009**, *8* (6), 447.

(20) Lovly, C. M.; Shaw, A. T. Molecular pathways: Resistance to kinase inhibitors and implications for therapeutic strategies. *Clin. Cancer Res.* **2014**, *20* (9), 2249−56.

(21) Zhang, J.; Yang, P. L.; Gray, N. S. Targeting cancer with small molecule kinase inhibitors. *Nat. Rev. Cancer* **2009**, *9* (1), 28−39.

(22) O'Hare, T.; Zabriskie, M. S.; Eiring, A. M.; Deininger, M. W. Pushing the limits of targeted therapy in chronic myeloid leukaemia. *Nat. Rev. Cancer* **2012**, *12* (8), 513−26.

DOI: 10.1021/mp500701u
Mol. Pharmaceutics 2015, 12, 1412−1421

(23) Woessner, D. W.; Lim, C. S. Disrupting BCR-ABL in combination with secondary leukemia-specific pathways in CML cells leads to enhanced apoptosis and decreased proliferation. *Mol. Pharmaceutics* **2013**, *10* (1), 270−7.
(24) Dixon, A. S.; Miller, G. D.; Bruno, B. J.; Constance, J. E.; Woessner, D. W.; Fidler, T. P.; Robertson, J. C.; Cheatham, T. E., 3rd; Lim, C. S. Improved coiled-coil design enhances interaction with Bcr-Abl and induces apoptosis. *Mol. Pharmaceutics* **2012**, *9* (1), 187−95.
(25) Miller, G. D.; Woessner, D. W.; Sirch, M. J.; Lim, C. S. Multidomain targeting of Bcr-Abl by disruption of oligomerization and tyrosine kinase inhibition: Toward eradication of CML. *Mol. Pharmaceutics* **2013**, *10* (9), 3475−83.
(26) Dixon, A. S.; Constance, J. E.; Tanaka, T.; Rabbitts, T. H.; Lim, C. S. Changing the subcellular location of the oncoprotein Bcr-Abl using rationally designed capture motifs. *Pharm. Res.* **2012**, *29* (4), 1098−109.
(27) Woessner, D. W.; Eiring, A. M.; Bruno, B. J.; Zabriskie, M. S.; Reynolds, K. R.; Miller, G. D.; O'Hare, T.; Deininger, M. W.; Lim, C. S. A coiled-coil mimetic intercepts BCR-ABL1 dimerization in native and kinase-mutant chronic myeloid leukemia. *Leukemia* **2015**, DOI: 10.1038/leu.2015.53.
(28) Bruno, B. J.; Miller, G. D.; Lim, C. S. Basics and recent advances in peptide and protein drug delivery. *Ther. Delivery* **2013**, *4* (11), 1443−67.
(29) Carter, P. J. Introduction to current and future protein therapeutics: A protein engineering perspective. *Exp. Cell Res.* **2011**, *317* (9), 1261−9.
(30) Koren, E.; Torchilin, V. P. Cell-penetrating peptides: Breaking through to the other side. *Trends Mol. Med.* **2012**, *18* (7), 385−93.
(31) Copolovici, D. M.; Langel, K.; Eriste, E.; Langel, U. Cell-penetrating peptides: Design, synthesis, and applications. *ACS Nano* **2014**, *8* (3), 1972−94.
(32) Madani, F.; Lindberg, S.; Langel, U.; Futaki, S.; Graslund, A. Mechanisms of cellular uptake of cell-penetrating peptides. *J. Biophys.* **2011**, *2011*, 414729.
(33) Vasconcelos, L.; Parn, K.; Langel, U. Therapeutic potential of cell-penetrating peptides. *Ther. Delivery* **2013**, *4* (5), 573−91.
(34) Deng, M.; Daley, G. Q. Expression of interferon consensus sequence binding protein induces potent immunity against BCR/ABL-induced leukemia. *Blood* **2001**, *97* (11), 3491−7.
(35) Bunce, C. M.; French, P. J.; Allen, P.; Mountford, J. C.; Moor, B.; Greaves, M. F.; Michell, R. H.; Brown, G. Comparison of the levels of inositol metabolites in transformed haemopoietic cells and their normal counterparts. *Biochem. J.* **1993**, *289* (Part 3), 667−73.
(36) O'Hare, T.; Walters, D. K.; Stoffregen, E. P.; Jia, T.; Manley, P. W.; Mestan, J.; Cowan-Jacob, S. W.; Lee, F. Y.; Heinrich, M. C.; Deininger, M. W.; Druker, B. J. In vitro activity of Bcr-Abl inhibitors AMN107 and BMS-354825 against clinically relevant imatinib-resistant Abl kinase domain mutants. *Cancer Res.* **2005**, *65* (11), 4500−5.
(37) Wagner, M. C.; Dziadosz, M.; Melo, J. V.; Heidel, F.; Fischer, T.; Lipka, D. B. Nilotinib shows prolonged intracellular accumulation upon pulse-exposure: A novel mechanism for induction of apoptosis in CML cells. *Leukemia* **2013**, *27* (7), 1567−70.
(38) O'Hare, T.; Shakespeare, W. C.; Zhu, X.; Eide, C. A.; Rivera, V. M.; Wang, F.; Adrian, L. T.; Zhou, T.; Huang, W. S.; Xu, Q.; Metcalf, C. A., 3rd; Tyner, J. W.; Loriaux, M. M.; Corbin, A. S.; Wardwell, S.; Ning, Y.; Keats, J. A.; Wang, Y.; Sundaramoorthi, R.; Thomas, M.; Zhou, D.; Snodgrass, J.; Commodore, L.; Sawyer, T. K.; Dalgarno, D. C.; Deininger, M. W.; Druker, B. J.; Clackson, T. AP24534, a pan-BCR-ABL inhibitor for chronic myeloid leukemia, potently inhibits the T315I mutant and overcomes mutation-based resistance. *Cancer Cell* **2009**, *16* (5), 401−12.
(39) Kaplan, I. M.; Wadia, J. S.; Dowdy, S. F. Cationic TAT peptide transduction domain enters cells by macropinocytosis. *J. Controlled Release* **2005**, *102* (1), 247−53.
(40) Okal, A.; Cornillie, S.; Matissek, S. J.; Matissek, K. J.; Cheatham, T. E., 3rd; Lim, C. S. Re-engineered p53 chimera with enhanced homo-oligomerization that maintains tumor suppressor activity. *Mol. Pharmaceutics* **2014**, *11* (7), 2442−52.
(41) Wang, H. X.; Xiao, H.; Zhong, L.; Tao, K.; Li, Y. J.; Huang, S. F.; Wen, J. P.; Feng, W. L. Cell-penetrating fusion peptides OD1 and OD2 interact with Bcr-Abl and influence the growth and apoptosis of K562 cells. *Mol. Cell. Biochem.* **2014**, *385* (1−2), 311−8.
(42) Mian, A. A.; Oancea, C.; Zhao, Z.; Ottmann, O. G.; Ruthardt, M. Oligomerization inhibition, combined with allosteric inhibition, abrogates the transformation potential of T315I-positive BCR-ABL. *Leukemia* **2009**, *23* (12), 2242−7.
(43) Beissert, T.; Puccetti, E.; Bianchini, A.; Guller, S.; Boehrer, S.; Hoelzer, D.; Ottmann, O. G.; Nervi, C.; Ruthardt, M. Targeting of the N-terminal coiled-coil oligomerization interface of BCR interferes with the transformation potential of BCR-ABL and increases sensitivity to STI571. *Blood* **2003**, *102* (8), 2985−93.
(44) Guo, X. Y.; Cuillerot, J. M.; Wang, T.; Wu, Y.; Arlinghaus, R.; Claxton, D.; Bachier, C.; Greenberger, J.; Colombowala, I.; Deisseroth, A. B. Peptide containing the BCR oligomerization domain (AA 1−160) reverses the transformed phenotype of p210bcr-abl positive 32D myeloid leukemia cells. *Oncogene* **1998**, *17* (7), 825−33.
(45) Huang, Z. L.; Gao, M.; Ji, M. S.; Tao, K.; Xiao, Q.; Zhong, L.; Zeng, J. M.; Feng, W. L. TAT-CC fusion protein depresses the oncogenicity of BCR-ABL in vitro and in vivo through interrupting its oligomerization. *Amino Acids* **2013**, *44* (2), 461−72.
(46) Huang, Z.; Ji, M.; Peng, Z.; Huang, S.; Xiao, Q.; Li, C.; Zeng, J.; Gao, M.; Feng, W. Purification of TAT-CC-HA protein under native condition and its transduction analysis and biological effects on BCR-ABL positive cells. *Biomed. Pharmacother.* **2011**, *65* (3), 183−92.
(47) Beissert, T.; Hundertmark, A.; Kaburova, V.; Travaglini, L.; Mian, A. A.; Nervi, C.; Ruthardt, M. Targeting of the N-terminal coiled-coil oligomerization interface by a helix-2 peptide inhibits unmutated and imatinib-resistant BCR-ABL. *Int. J. Cancer* **2008**, *122* (12), 2744−52.
(48) La Rosee, P.; Corbin, A. S.; Stoffregen, E. P.; Deininger, M. W.; Druker, B. J. Activity of the Bcr-Abl kinase inhibitor PD180970 against clinically relevant Bcr-Abl isoforms that cause resistance to imatinib mesylate (Gleevec, STI571). *Cancer Res.* **2002**, *62* (24), 7149−53.
(49) O'Hare, T.; Pollock, R.; Stoffregen, E. P.; Keats, J. A.; Abdullah, O. M.; Moseson, E. M.; Rivera, V. M.; Tang, H.; Metcalf, C. A., 3rd; Bohacek, R. S.; Wang, Y.; Sundaramoorthi, R.; Shakespeare, W. C.; Dalgarno, D.; Clackson, T.; Sawyer, T. K.; Deininger, M. W.; Druker, B. J. Inhibition of wild-type and mutant Bcr-Abl by AP23464, a potent ATP-based oncogenic protein kinase inhibitor: Implications for CML. *Blood* **2004**, *104* (8), 2532−9.
(50) Cortes, J. E.; Kantarjian, H.; Shah, N. P.; Bixby, D.; Mauro, M. J.; Flinn, I.; O'Hare, T.; Hu, S.; Narasimhan, N. I.; Rivera, V. M.; Clackson, T.; Turner, C. D.; Haluska, F. G.; Druker, B. J.; Deininger, M. W.; Talpaz, M. Ponatinib in refractory Philadelphia chromosome-positive leukemias. *N. Engl. J. Med.* **2012**, *367* (22), 2075−88.
(51) Razzak, M. Haematology: Ponatinib—The next TKI challenge. *Nat. Rev. Clin. Oncol.* **2013**, *10* (2), 65.
(52) Verdine, G. L.; Hilinski, G. J. Stapled peptides for intracellular drug targets. *Methods Enzymol.* **2012**, *503*, 3−33.

DOI: 10.1021/mp500701u
Mol. Pharmaceutics 2015, 12, 1412−1421

CHAPTER 4

APPLICATION OF THIOL-YNE/THIOL-ENE REACTION FOR PEPTIDE AND PROTEIN MACROCYCLIZATION

Reprinted with permission from Chemistry, a European Journal 2017. **23**(29): p. 7087-7092. Yuanxiang Wang, Benjamin J. Bruno, Sean Cornillie, Jason M. Nogieira, Diao Chen, Thomas E. Cheatham III, Carol S. Lim, and Danny HC Chou.

ChemPubSoc Europe

DOI: 10.1002/chem.201700572

CHEMISTRY A European Journal Full Paper

Peptide Macrocyclization

Application of Thiol–yne/Thiol–ene Reactions for Peptide and Protein Macrocyclizations

Yuanxiang Wang[+],[a] Benjamin J. Bruno[+],*[b] Sean Cornillie,[c] Jason M. Nogieira,[a] Diao Chen,[a] Thomas E. Cheatham, III,[c] Carol S. Lim,*[b] and Danny Hung-Chieh Chou*[a]

Abstract: The application of thiol–yne/thiol–ene reactions to synthesize mono- and bicyclic-stapled peptides and proteins is reported. First, a thiol–ene-based peptide-stapling method in aqueous conditions was developed. This method enabled the efficient stapling of recombinantly expressed coil-coiled proteins. The resulting stapled protein demonstrated higher stability in its secondary structure than the unstapled version. Furthermore, a thiol–yne coupling was performed by using an α,ω-diyne to react with two cysteine residues to synthesize a stapled peptide with two vinyl sulfide groups. The stapled peptide could further react with another biscysteine peptide to yield a bicyclic stapled peptide with enhanced properties. For example, the cell permeability of a stapled peptide was further increased by appending an oligoarginine cell-penetrating peptide. The robustness and versatility of thiol–yne/thiol–ene reactions that can be applied to both synthetic and expressed peptides and proteins were demonstrated.

Introduction

The application of chemical modification tools to peptides and proteins has enabled the elegant study of biological targets and development of first-in-class biological therapeutics.[1,2] One example, macrocyclic peptides, and in particular "stapled" peptides, have been used to inhibit a variety of protein–protein interactions (PPIs) that are generally "undruggable" by small molecules.[3,4] Although a variety of bio-orthogonal reactions have been used to circumvent the selectivity challenges associated with the many functional groups in native biomolecules,[5–12] these techniques depend upon the incorporation of unnatural amino acids. Alternatively, various chemoselective bioconjugation methods have been used to modify native amino acid residues for stapled-peptide synthesis.[13–20] Cysteine-based stapling has received great attention owing to the chemical reactivity of cysteine and its relatively low frequency in native proteins. We recently reported a thiol–ene-based strategy for native peptide stapling with high conversion and broad substrate scope in polar aprotic solvents.[21] In this article, we expand the reaction scope into the aqueous solvent system, which enables macrocyclization of recombinantly expressed proteins. Additionally, we further develop a consecutive thiol–yne/thiol–ene combination to synthesize bicyclic stapled peptides. This new method enables the addition of external groups that confer enhanced properties such as cell permeability.

Results and Discussion

In our previously reported work,[21] the thiol–ene-based peptide-stapling reaction had to be conducted in organic solvents owing to two reasons: 1) the pure hydrocarbon dienes are not water-soluble, and 2) the radical initiator, 2,2-dimethoxy-2 phenylacetophenone (DMPA), is not water-soluble. To expand the reaction scope into aqueous conditions, we used water-soluble 1,3-diallylurea (**2**) and a water-soluble, photo-inducible radical initiator 2,2′-azobis[2-(2-imidazolin-2-yl)propane]-dihydrochloride (VA044, **3**). Irradiation of peptide **1** under 365 nm wavelength in the presence of **2** and **3** in double-distilled water, with an overall pH value of 4, led to 53% conversion to product **5** (Scheme 1). Inspired by the results reported by Liu and co-workers[22] and Brimble and co-workers,[23] in which addition of a reducing agent improved the peptide-based thiol–ene reaction, we screened various reducing agents as additives. Unfortunately, when we added reduced glutathione (**4a**) to the reaction, the conversion was lowered to 37% after 15 min. A similar result was observed in the reaction using dithiothreitol (DTT, **4b**) as an additive. However, when

[a] Dr. Y. Wang,[+] Dr. J. M. Nogieira, Dr. D. Chen, Prof. Dr. D. H.-C. Chou
Department of Biochemistry
University of Utah
15 N, Medical Drive East 4100, Salt Lake City, UT 84112 (USA)
E-mail: dchou@biochem.utah.edu

[b] Dr. B. J. Bruno,[+] Prof. Dr. C. S. Lim
Department of Pharmaceutics and Pharmaceutical Chemistry
University of Utah
30 S 2000 E, Rm 2916, Salt Lake City, UT 84112 (USA)
E-mail: benjamin.bruno@pharm.utah.edu
carol.lim@pharm.utah.edu

[c] Dr. S. Cornillie, Prof. Dr. T. E. Cheatham, III
Department of Medicinal Chemistry
University of Utah
30 S 2000 E, Rm 4914, Salt Lake City, UT 84112 (USA)

[+] These authors contributed equally to this work.

Supporting Information and the ORCID identification number(s) for the author(s) of this article can be found under https://doi.org/10.1002/chem.201700572.

ChemPubSoc Europe

CHEMISTRY A European Journal Full Paper

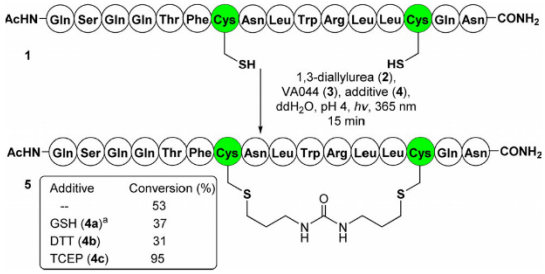

Scheme 1. Peptide-based thiol–ene reaction in aqueous solution. Reactions were performed with **1** (5 μmol), **2** (5 μmol), **3** (5 μmol), and **4** (5 μmol) in double-distilled water (ddH_2O, 0.5 mL) under 365 nm wavelength irradiation for 15 min. Conversions were calculated based on HPLC and LC–MS analysis. [a] 10 μmol of **2** was added.

tris(2-carboxyethyl)phosphine hydrochloride (TCEP, **4c**) was added to the reaction mixture, the yield increased to 95%.

With optimized aqueous conditions in hand, we investigated the utility of this method for water-only soluble proteins. Protein **6** is based on the coiled-coil dimerization domain present at the N-terminus of the Bcr-Abl oncoprotein and was designed to preferentially bind to and inhibit Bcr-Abl activity.[24–26] We chose to examine the stapling of recombinantly expressed coiled-coil protein **7**, a variant of protein **6** that has been mutated to contain two cysteine residues at sites that have minimal effect on activity, with **2**. Using **4c** as the reducing agent, we observed desulfurization of the protein as the major product (see the Supporting Information). This was not surprising because Liu and co-workers also observed this similar transformation in their previous study.[22] When we switched the reducing agent from **4c** to **4a** under the same conditions, the desulfurization product was not observed; however, oxidation of **7** was the major product (M + 16 Da, see the Supporting Information). It has been reported that a weakly acidic pH buffer can prevent the oxidation of the starting material,[22] so an acetate buffer at pH 4 was used as the aqueous solvent to run the reaction. This led to decreased formation of the oxidation product; however, conversion to the thiol–ene product was only 15%. We reasoned that this may be owing to the poor solubility of the coiled-coil protein **7** in the buffer solution. To remedy this, we added 6 N guanidine·HCl (Gdn·HCl) to increase the protein solubility. Gratifyingly, the conversion to **8** was improved to 90% by using the acetate buffer and 6 N Gdn·HCl as a co-solvent (Scheme 2).

Having established a protocol for the single stapling of **7** with **2**, we turned our attention to the double-stapling of **9** with **2,** which could potentially further improve proteolytic stability and helical structures. This protein has been mutated to contain four cysteine residues. By increasing the equivalents of the **2** and **3**, we were able to successfully double-staple to produce **10** in 80% conversion (Scheme 3).

To evaluate proteolytic stability, stapled proteins (**8**, **10**) and unstapled controls (**6**, **7**, **9**) were incubated with chymotrypsin (Figure 1), trypsin (Figure S10 in the Supporting Information)

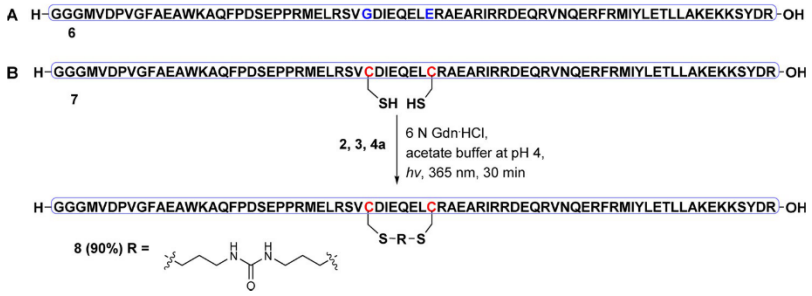

Scheme 2. (A) Sequence of **6**; (B) single-stapling of a coiled-coil protein in aqueous solution. Reactions were performed with **7** (0.5 μmol), **2** (1.0 μmol), **3** (0.5 μmol), and **4a** (0.5 μmol) in an acetate buffer (pH 4, 0.1 mL) and 6 N Gdn·HCl (0.1 mL) under 365 nm wavelength irradiation for 15 min. Conversion was calculated based on HPLC and LC–MS analysis.

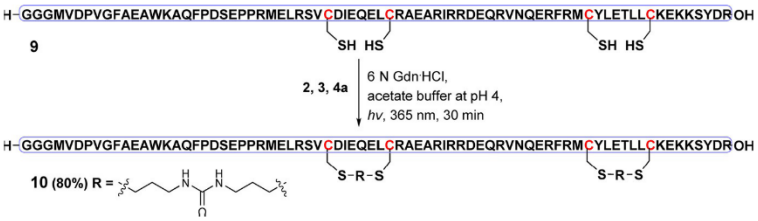

Scheme 3. Double-stapling of a coiled-coil protein in aqueous solution. Reactions were performed with **9** (0.5 μmol), **2** (1.5 μmol), **3** (1.0 μmol), and **4a** (0.5 μmol) in acetate buffer (pH 4, 0.1 mL) and 6 N Gdn·HCl (0.1 mL) under 365 nm wavelength irradiation for 15 min. Conversion was calculated based on HPLC and LC–MS analysis.

ChemPubSoc Europe

CHEMISTRY A European Journal Full Paper

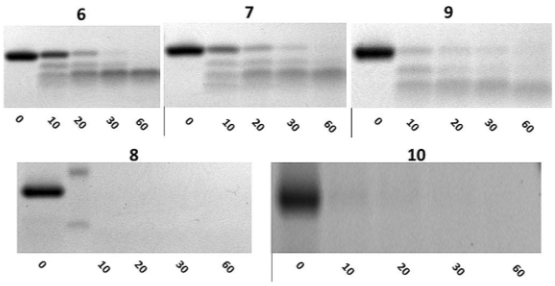

Figure 1. Stapled proteins (**8**, **10**) and unstapled controls (**6**, **7**, **9**) were treated with chymotrypsin, and reactions were terminated at the given time-points [min]. Although some parent protein is present at 30 min for the three unstapled proteins, none of the parent stapled proteins were identified after even 10 min digestion.

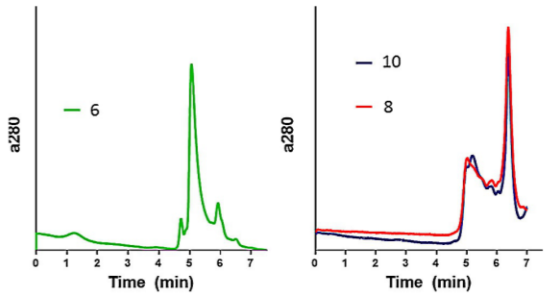

Figure 2. SEC analysis of stapled proteins and controls. **6** (unstapled) eluted as one major peak at 5 min, whereas stapled proteins (**8** and **10**) eluted as two major peaks at 5 and 7 min, suggesting two conformations present in the solution for the stapled proteins.

and endoproteinase Glu-C (Figure S11 in the Supporting Information). Surprisingly, the stapled proteins **8** and **10** were more rapidly degraded than their unstapled protein controls **6**, **7**, and **10**. MS analysis of digested proteins indicates that the staples did protect the underlying region from digestion, whereas the non-stapled regions were rapidly degraded.

One reason for this result could be incomplete stapling; it is possible that the staple only reacted with one of the two cysteines in the protein, which means that there is no true staple, but rather the staple is added to one cysteine and remains a free diene on the other end. The resulting "hemi-stapled" protein would have the same molecular weight as a fully-stapled protein. Iodoacetic acid (IAA), which alkylates free thiols, was used to investigate the completeness of stapling. Each free thiol and subsequent alkylation results in a mass shift of +58 Da. As would be expected for complete stapling, the two stapled proteins saw no mass shift upon incubation with IAA, whereas the unstapled proteins underwent mass increases of +116 and +232 for **7** and **9**, respectively, confirming that there are no free cysteines in the stapled proteins (see the Supporting Information).

One possible explanation for the proteolytic sensitivity may be related to alterations in protein conformation caused by stapling. To investigate this, stapled proteins (**8**, **10**) and unstapled control (**6**) were analyzed by size-exclusion chromatography (SEC, Figure 2). **6** (9 kDa) had a retention time comparable to myoglobin (17 kDa), which is not surprising because myoglobin is quite structured and globular, whereas **6** is more linear and flexible. The stapled proteins (**8**, **10**), however, showed two major peaks, one of which eluted at the same time as **6**. The other eluted later, suggesting the presence of a more compact conformation of the stapled proteins. This second peak had retention times between that of myoglobin and B12 (1.35 kDa, Figure S12 in the Supporting Information). Further, the elution profiles of the two stapled proteins were quite similar. This data supports the presence of (at least) two structural conformations present in solution.

To further probe the possibility of a staple-induced conformational change, molecular dynamics (MD) simulations were performed with an unstapled (**6**), single-stapled (**8**), and double-stapled (**10**) protein. Simulation results were analyzed using the CPPTRAJ toolset[27] to identify the most highly-sampled peptide conformations and assess the structural variance between said conformations. Following over 500 ns of MD simulation, the unstapled and stapled proteins were found to exhibit two very different behaviors. The unstapled variant **6** (Figure 3 A) was found to adopt a single, extended conformation, whereas the single-stapled and double-stapled variants were found to adopt a two-state model: each of the stapled variants adopt a "collapsed" conformation (Figure 3 B and C) in addition to an initial extended conformation similar to that observed in Figure 3 A, further supporting the SEC data and the hypothesis that two or more structural conformations exist in solution. See the Supporting Information for a more comprehensive analysis (Figures S12 and S13, Table S2).

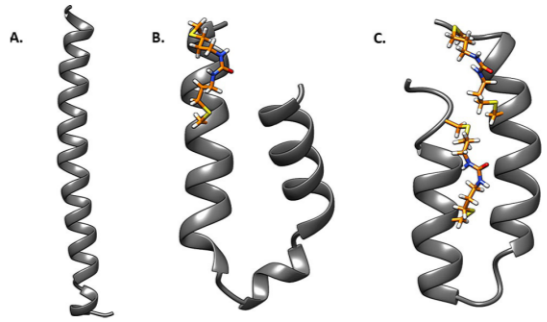

Figure 3. Highly-populated conformations for helix 2 of **6** (A), **8** (B), and **10** (C) observed throughout MD simulation.

We were next interested in utilizing dialkynes as substrate for the thiol–yne coupling reaction. We envisioned that the product of the thiol–yne reaction would then be able to react through a subsequent thiol–ene reaction, allowing for further functionalization of the starting peptide. With our optimized reaction conditions from our previous work,[21] the thiol–ene reaction between peptide **1** and 1,8-nonadiene (**11 a**) was conducted in *N*-methylpyrrolidinone (NMP) with radical

ChemPubSoc Europe

CHEMISTRY A European Journal Full Paper

initiator DMPA (**12**) to afford the stapled peptide **13a** in 92% conversion to be used as a circular dichroism (CD) spectra control. The reaction was repeated using 1,8-nonadiyne (**11b**) to run the thiol–yne reaction. The reaction between **1** and **11b** afforded the stapled dialkene product **13b** in near quantitative conversion (Scheme 4). Owing to the two double bonds in the

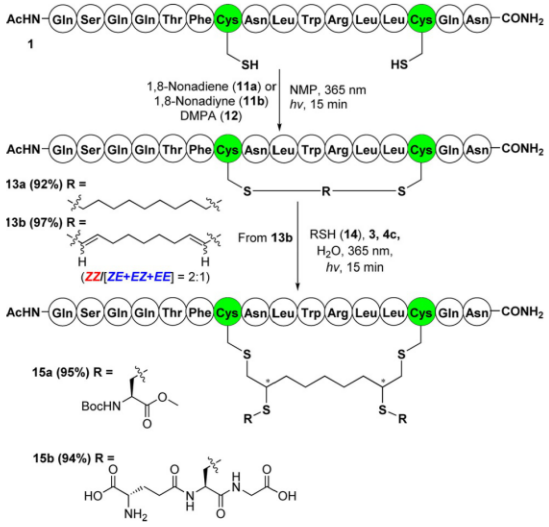

Scheme 4. Thiol–yne reaction between peptide **1** and diyne and the model reaction.

linkage, four different isomers could result from the reaction. The HPLC trace showed two major peaks with retention times of 19.303 and 20.339 min for **13b**, and the proportion of the two peaks was 2:1 (Figure S1 in the Supporting Information). We further characterized the product peaks through ^{1}H NMR and correlation spectroscopy (COSY). It was found that the earlier and major peak (19.303 min) was for the *ZZ* isomer with *J* values of 9.5, 9.5 Hz (Figures S2 and S3 in the Supporting Information). The second peak showed a mixture in the NMR spectrum, correlating with the remaining isomers (Figure S4 in the Supporting Information). With peptide **13b** in hand, we wanted to test the possibility of introducing two sulfur-containing small molecules to the linker of **13b** through a subsequent thiol–ene reaction. Using a L-cysteine derivative (**14a**) and glutathione (**14b**) as sulfur-containing small molecules, the thiol–ene reactions under aqueous conditions with **4c** as an additive were able to provide the corresponding products **15a** and **15b** in excellent conversions.

To further expand on the utility of the intermediate dialkene stapled product **13b**, we chose to staple the small peptide **16**, a water-solubilizing motif containing a CRRRRC amino acid sequence. It is hypothesized that functionalizing the stapled peptide with **16** endows it with improved cell permeability. With the same reaction conditions that were optimized for the thiol–ene reaction in aqueous solution (Scheme 1), product **17** was obtained in 91% conversion (Scheme 5).

Scheme 5. Introducing **16** to a stapled peptide. Reactions were performed with **13b** (3 μmol), peptide **16** (3 μmol), **3** (3 μmol), and **4c** (3 μmol) in water (0.5 mL) under 365 nm wavelength irradiation for 15 min. Conversion was calculated based on HPLC and LC–MS analysis.

To evaluate cell uptake of our functionalized peptide, we synthesized the N-terminal FITC-labeled peptide **18**. Both the thiol–ene and thiol–yne reactions were conducted in NMP to afford **19a** and **19b** in 92 and 96% conversion, respectively. The dialkene product **19b** was then modified by a subsequent thiol–ene reaction in aqueous conditions, yielding the CRRRRC-modified stapled peptide **20** in 93% conversion (Scheme 6).

Scheme 6. Derivatives of peptides.

With stapled peptides in hand, we tested the internalization of **18**, **19a**, **19b**, and **20** by K562 cells (Figure 4). At 1 μM concentrations, all four peptide analogues showed no significant internalization by the cell lines. At 10 and 30 μM concentrations, modified peptide **20** was internalized far better than the others. Both stapled peptides **19a** and **19b** had improved internalization compared to unstapled peptide **18**; however, the difference between the two was not significant.

ChemPubSoc Europe

CHEMISTRY A European Journal Full Paper

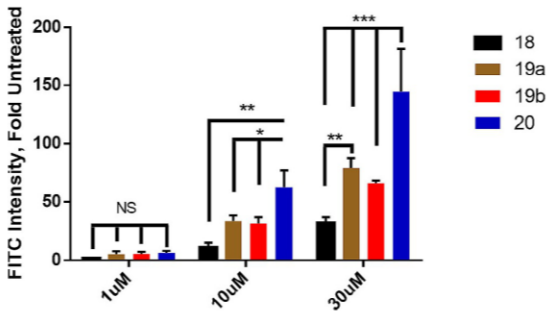

Figure 4. Stapled-peptide internalization in K562 cells. Bicyclic stapled peptide (**20**) demonstrated superior internalization compared to all other peptides at 10 and 30 μM doses 2-way ANOVA with Tukey's multiple comparison test; $n=3$; $^{*}p<0.05$; $^{**}p<0.001$; $^{***}p<0.0001$.

Conclusion

In this work, we modified the thiol–ene stapling technique we previously reported[21] for use in aqueous systems. To accomplish this, the water-soluble radical initiator VA044 (**3**) and diallylurea staple (**2**) were used. After initial success with aqueous peptide stapling, these methods were utilized for the single- and double-stapling of recombinant proteins. Once the stapling reaction was completed, the resulting stapled protein demonstrated increased proteolytic sensitivity (in regions outside of the staples) compared to unstapled controls. SEC and computational modeling suggest that stapling alters the conformation of the proteins, which may be resolved in future studies by using more hydrophilic staples that avoid the entropic penalty of solvation the DAU staple faces. Finally, thiol–yne stapling of a peptide was successful and allowed for the addition of a second, cell-penetrating peptide motif to the staple. Taken together, these techniques provide a foundation for the aqueous stapling of both recombinant and hydrophilic peptides and proteins with improved stability and cell penetration.

Experimental Section

Experimental details as well as compound characterization data and copies of liquid chromatography–mass spectrometry (LC–MS) and HPLC spectra are available in the Supporting Information.

Acknowledgements

We acknowledge funding support from NIH RO1 CA129528, the Utah Science Technology and Research Initiative, and pilot funding 170303 from Huntsman Cancer Institute Experimental Therapeutics Program. The authors acknowledge the use of DNA/Peptide core, flow cytometry core, and mass spectrometry and proteomics core. Mass spectrometry equipment was obtained through NCRR Shared Instrumentation Grant 1 S10 RR020883-01 and 1 S10 RR025532-01A1. The flow cytometry was supported by National Cancer Institute through Award Number 5P30CA042014-24. We thank Dr. Krishna Parsawar of the Mass Spectrometry and Proteomics Core Facility for invaluable discussions regarding MS analysis, and Dr. Jack Skalicky for assistance with NMR spectroscopy. We would also like to thank Katherine Ferrell (Chris Hill lab, University of Utah) for producing the TEV protease used in this study.

Conflict of interest

The authors declare no conflict of interest.

Keywords: peptide macrocyclization · peptide stapling · thiol–ene coupling · thiol–yne coupling

[1] G. L. Verdine, G. J. Hilinski, *Drug Discovery Today Technol.* **2012**, *9*, e41–e47.
[2] K. Fosgerau, T. Hoffmann, *Drug Discovery Today* **2015**, *20*, 122–128.
[3] A. D. Cox, S. W. Fesik, A. C. Kimmelman, J. Luo, C. J. Der, *Nat. Rev. Drug Discovery* **2014**, *13*, 828–851.
[4] T. L. Nero, C. J. Morton, J. K. Holien, J. Wielens, M. W. Parker, *Nat. Rev. Cancer* **2014**, *14*, 248–262.
[5] Y. H. Lau, P. de Andrade, S.-T. Quah, M. Rossmann, L. Laraia, N. Skold, T. J. Sum, P. J. E. Rowling, T. L. Joseph, C. Verma, M. Hyvonen, L. S. Itzhaki, A. R. Venkitaraman, C. J. Brown, D. P. Lane, D. R. Spring, *Chem. Sci.* **2014**, *5*, 1804–1809.
[6] C. M. Haney, M. T. Loch, W. S. Horne, *Chem. Commun.* **2011**, *47*, 10915–10917.
[7] Y. W. Kim, T. N. Grossmann, G. L. Verdine, *Nat. Protoc.* **2011**, *6*, 761–771.
[8] T. N. Grossmann, J. T. Yeh, B. R. Bowman, Q. Chu, R. E. Moellering, G. L. Verdine, *Proc. Natl. Acad. Sci. USA* **2012**, *109*, 17942–17947.
[9] F. Bernal, A. F. Tyler, S. J. Korsmeyer, L. D. Walensky, G. L. Verdine, *J. Am. Chem. Soc.* **2007**, *129*, 2456–2457.
[10] F. Bernal, M. Wade, M. Godes, T. N. Davis, D. G. Whitehead, A. L. Kung, G. M. Wahl, L. D. Walensky, *Cancer Cell* **2010**, *18*, 411–422.
[11] P. Y. Yang, H. Zou, E. Chao, L. Sherwood, V. Nunez, M. Keeney, E. Ghartey-Tagoe, Z. Ding, H. Quirino, X. Luo, G. Welzel, G. Chen, P. Singh, A. K. Woods, P. G. Schultz, W. Shen, *Proc. Natl. Acad. Sci. USA* **2016**, *113*, 4140–4145.
[12] A. Muppidi, H. Zou, P. Y. Yang, E. Chao, L. Sherwood, V. Nunez, A. K. Woods, P. G. Schultz, Q. Lin, W. Shen, *ACS Chem. Biol.* **2016**, *11*, 324–328.
[13] A. D. de Araujo, H. N. Hoang, W. M. Kok, F. Diness, P. Gupta, T. A. Hill, R. W. Driver, D. A. Price, S. Liras, D. P. Fairlie, *Angew. Chem. Int. Ed.* **2014**, *53*, 6965–6969; *Angew. Chem.* **2014**, *126*, 7085–7089.
[14] H. Jo, N. Meinhardt, Y. Wu, S. Kulkarni, X. Hu, K. E. Low, P. L. Davies, W. F. DeGrado, D. C. Greenbaum, *J. Am. Chem. Soc.* **2012**, *134*, 17704–17713.
[15] P. Timmerman, J. Beld, W. C. Puijk, R. H. Meloen, *Chembiochem* **2005**, *6*, 821–824.
[16] P. Timmerman, W. C. Puijk, R. H. Meloen, *J. Mol. Recognit.* **2007**, *20*, 283–299.
[17] A. M. Spokoyny, Y. Zou, J. J. Ling, H. Yu, Y. S. Lin, B. L. Pentelute, *J. Am. Chem. Soc.* **2013**, *135*, 5946–5949.
[18] S. P. Brown, A. B. Smith 3rd, *J. Am. Chem. Soc.* **2015**, *137*, 4034–4037.
[19] Y. Tian, J. Li, H. Zhao, X. Zeng, D. Wang, Q. Liu, X. Niu, X. Huang, N. Xu, Z. Li, *Chem. Sci.* **2016**, *7*, 3325–3330.
[20] M. M. Wiedmann, Y. S. Tan, Y. Wu, S. Aibara, W. Xu, H. F. Sore, C. S. Verma, L. Itzhaki, M. Stewart, J. D. Brenton, D. R. Spring, *Angew. Chem. Int. Ed.* **2017**, *56*, 524–529; *Angew. Chem.* **2017**, *129*, 539–544.
[21] Y. Wang, D. H. Chou, *Angew. Chem. Int. Ed.* **2015**, *54*, 10931–10934; *Angew. Chem.* **2015**, *127*, 11081–11084.
[22] F. Li, A. Allahverdi, R. Yang, G. B. Lua, X. Zhang, Y. Cao, N. Korolev, L. Nordenskiold, C. F. Liu, *Angew. Chem. Int. Ed.* **2011**, *50*, 9611–9614; *Angew. Chem.* **2011**, *123*, 9785–9788.
[23] T. H. Wright, A. E. Brooks, A. J. Didsbury, J. D. MacIntosh, G. M. Williams, P. W. Harris, P. R. Dunbar, M. A. Brimble, *Angew. Chem. Int. Ed.* **2013**, *52*, 10616–10619; *Angew. Chem.* **2013**, *125*, 10810–10813.

ChemPubSoc Europe

CHEMISTRY
A European Journal
Full Paper

[24] A. S. Dixon, G. D. Miller, B. J. Bruno, J. E. Constance, D. W. Woessner, T. P. Fidler, J. C. Robertson, T. E. Cheatham 3rd, C. S. Lim, *Mol. Pharm.* **2012**, *9*, 187 – 195.
[25] B. J. Bruno, C. S. Lim, *Mol. Pharm.* **2015**, *12*, 1412 – 1421.
[26] D. W. Woessner, A. M. Eiring, B. J. Bruno, M. S. Zabriskie, K. R. Reynolds, G. D. Miller, T. O'Hare, M. W. Deininger, C. S. Lim, *Leukemia* **2015**, *29*, 1668 – 1675.
[27] D. R. Roe, T. E. Cheatham, *J. Chem. Theory Comput.* **2013**, *9*, 3084 – 3095.

Manuscript received: February 7, 2017
Accepted Article published: March 26, 2017
Final Article published: April 26, 2017

Supporting Information

Application of Thiol-yne/Thiol-ene Reactions for Peptide and Protein Macrocyclization

Yuanxiang Wang[#,%], Benjamin J Bruno[*,%], Sean Cornillie[†], Jason M. Nogueira[#], Diao Chen[#],Thomas E. Cheatham III[†], Carol Lim*, Danny Hung-Chieh Chou[#].

[#]Department of Biochemistry, University of Utah, Salt Lake City, Utah, USA 84112
[†]Department of Medicinal Chemistry, University of Utah, Salt Lake City, Utah 84112, United States
[*]Department of Pharmaceutics and Pharmaceutical Chemistry, University of Utah, Salt Lake City, Utah, USA 84112.
[%]These authors contributed equally

Table of Contents

General information

1,8-nonadiene, 1,8-octadiyne,N-(tert-Butoxycarbonyl)-L-cysteine methyl ester, 2,2-dimethoxy-2-phenyl-acetophenone (DMAP), piperidine, triisopropylsilane (TIS), 1.2-ethanedithiol (EDT), 2,2'-Azobis[2-(2-imidazolin-2-yl)propane]dihydrochloride (VA044) reduced L-glutathione, and Fluorescein isothiocyanate isomer I, were purchased from Sigma-Aldrich. Tris(2-carboxyethyl)phosphine hydrochloride (TCEP) was purchased from Gold Bio Technology. Fmoc-protected amino acids were obtained from Protein Technologies Inc. O-(Benzotriazol-1-yl)-N,N,N',N'-tetramethyluronium (HBTU) and 1-[Bis(dimethylamino)methylene]-1H-1,2,3-triazolo[4,5-b]pyridinium 3-oxid hexafluorophosphate (HATU) were purchased from ChemPep. Rink Amide MBHA resin HL was obtained from Novabiochem and H-Rink Amide ChemMatrix was provided by Biotage. Dimethylformamide (DMF), N-methylpyrrolidinone (NMP), trifluoroacetic acid (TFA), acetonitrile and ethyl ether were purchased from Fisher Scientific and used as supplied. NMR samples were prepared by dissolving dried peptide in DMSO-d6 at 298K. NMR data were collected on a Varian Inova instrument (600 MHz) with shifts reported in ppm and coupling constants reported in hertz.

Peptide synthesis

Peptides were synthesized via Fmoc solid phase peptide synthesis on a commercial peptide synthesizer (Alstra; Biotage, Inc). Automated peptide synthesis was carried out in a 10 mL reactor vial with the following protocols (for 0.1 mmol scale). For Fmoc deprotection: (i) 4.5 mL of 20% piperidine in DMF; (ii) mix 2 × 3 min (new solvent delivered for each mixing cycle). For amino acid coupling: (i) 1.25 mL of 0.4 M Fmoc-protected amino acid in DMF; (ii) 1.225 mL of 0.4 M HBTU or HATU (HBTU and Rink Amide MBHA resin HL were used for peptides **16**; HATU and H-Rink Amide ChemMatrix for peptides **1** and **18**) in DMF; (iii) 1.0 mL of 1.0 M DIPEA in DMF; and (iv) mix for 5 min at 75 °C (for cysteine coupling: mix for 10 min at 50°C). For DMF washing (performed between deprotection and coupling steps): (i) 4.5 mL of DMF; (ii) mix 45 s. For acetylation at the N-terminus (performed between the last deprotection and precleavage wash with DCM steps): (i) 1.0 mL of 5.0 M acetic anhydride in DMF; (ii) 5.5 mL of 1.0 M DIPEA in DMF; and (iv) mix for 10 min at 25 °C. Upon completion of the peptide chain, resins were washed with DCM and dried (using vacuum) for 20 min. Then peptide was cleaved from the resin by exposure to cleavage cocktail for 2.5 h, which were prepared with 12.5 mL TFA, 330 μL water, 330 μL TIS, and 330 μL EDT. The peptide was precipitated with ethyl ether at 4°C and lyophilized.

The sequences of Cys-containing peptides are as follows:

Peptide **1**: Ac-*Gln-Ser-Gln-Gln-Thr-Phe-Cys-Asn-Leu-Trp-Arg-Leu-Leu-Cys-Gln-Asn*-NH_2

Peptide **16**: Ac-*Cys-Arg-Arg-Arg-Arg-Cys*-NH_2

Peptide **18**: FITC-*bA-Gln-Ser-Gln-Gln-Thr-Phe-Cys-Asn-Leu-Trp-Arg-Leu-Leu-Cys-Gln-Asn*-NH_2 (*b*A = beta-alanine)

HPLC and LC/MS

Preparative reverse-phase HPLC of crude peptides was performed on Luna 5u C8 100 Å (250 × 10 mm) at 3 mL/min with a water/acetonitrile gradient in 0.1% TFA on an Agilent 1260 HPLC system. Fractions collected from preparative were analyzed by LC/MS on a XBridge C18 5-µm (50 × 2.1 mm) column at 0.4 mL/min with a water/acetonitrile gradient in 0.1% formic acid on an Agilent 6120 Quadrupole LC/MS system. Fractions containing targeted product (based on LC/MS) were collected and lyophilized.

Plasmid construction

Protein **6** was cloned into the pMal-C2x vector (New England Biolabs) as previously described .[1] Stapling sites were mutated to cysteines using the QuikChange II site-directed mutagenesis kit (Agilent Technologies). Mutations were made in sequential reactions, starting with the N-terminal residue. The primers used for the mutagenesis of G29C, E36C, I57C, and A64C were 5'-gctgcgctcagtgtgcgacatcgagca-3', 5'-gagcaggagctgtgtcgcgccgaggccc-3', 5'-gcgcttccgcatgtgctacctggagacg-3', and 5'-cctggagacgttgctgtgcaaggaaaagaagagc-3' and each of their reverse complements. The HRV3C protease site was then changed to a TEV protease site in a three step reaction, again using site-directed mutagenesis. First, a valine was changed to an asparagine, then a tyrosine was inserted between the leucine and phenylalanine of the HRV3C site, and finally, the proline of the HRV3C site was mutated to a glycine, and an additional glycine was inserted C-terminal to the cleavage site. The forward primers used for each step respectively were 5'-catcatcatcatcatcttgaaaatctttttcaaggtcctatggtg-3', 5'-catcatcatcttgaaaatctttactttcaaggtcctatggtggac-3', and 5'-ctttactttcaaggtggtggcatggtggacccggtg-3', along with their reverse complements. The final constructs encoding maltose binding protein (M)-6x histidine tag (H)-TEV protease site (TEV) – Protein **6** and cysteine-substituted variants were created.

Protein expression and purification was performed as before with the following alterations. Prior to cleavage with His-tagged TEV (a kind gift from Katherine Ferrell, laboratory of Dr. Chris Hill, University of Utah), fresh DTT (GoldBio) was added to the samples to a final concentration of 1mM. For cleavage of affinity tags, proteins were incubated at room temperature overnight. Prior to purification on Nickel-NTA resin (GoldBio), ETDA (Fisher Biotech) was neutralized with excess $MgCl_2$ (ISC BioExpress). Protein purity was analyzed by SDS-PAGE/band densitometry, and samples ≥95% pure were combined. Samples were then dialyzed against Milli-Q water with/without TCEP using SnakeSkin dialysis tubing, 3.5 kDa molecular weight cutoff (ThermoFisher). In order to prevent intermolecular disulfide bond formation, 1 mM equivalence of TCEP was used for each cysteine in the protein being purified; 0mM for protein **6**, 2mM for protein **7**, and 4mM for protein **9**. Samples were then lyophilized and stored desiccated.

Optimization of the thiol-ene reaction between 1 and 2 in aqueous solution

A solution of peptide **1** (5 µmol), 1,3-diallylurea **2** (5 µmol), and 2,2'-Azobis[2-(2-imidazolin-2-yl)propane]dihydrochloride (VA044, **3,** 5 µmol) in 0.5 mL of distilled deionized water was irradiated at 365 nm. After 15 minutes of stirring, the conversion to stapled peptide **5** was found to be 53% based on LCMS.

A solution of peptide **1** (10 µmol), 1,3-diallylurea **2** (5 µmol), **3** (5 µmol) and additive **4a** (5 µmol) in 0.5 mL of distilled deionized water was irradiated at 365 nm. After 15 minutes of stirring, the conversion to stapled peptide **5** was found to be 37% based on LCMS.

A solution of peptide **1** (5 µmol), 1,3-diallylurea **2** (5 µmol), **3** (5 µmol) and additive **4b** (5 µmol) in 0.5 mL of distilled deionized water was irradiated at 365 nm. After 15 minutes of stirring, the conversion to stapled peptide **5** was found to be 31% based on LCMS.

A solution of peptide **1** (5 µmol), 1,3-diallylurea **2** (5 µmol), **3** (5 µmol) and additive **4c** (5 µmol) in 0.5 mL of distilled deionized water was irradiated at 365 nm. After 15 minutes of stirring, the conversion to stapled peptide **5** was found to be 95% based on LCMS.

Optimization of the thiol-ene reaction between 7 and 2 in aqueous solution

A solution of protein **7** (0.5 µmol), 1,3-diallylurea **2** (0.5 µmol), **3** (0.5 µmol) and additive **4c** (0.5 µmol) in a 0.2 mL of distilled deionized water was irradiated at 365 nm. After 15 minutes of stirring, minimal conversion to the product was observed via LCMS. Instead desulfurization of the protein was the major product (M-64 Da).

MS-spectrum for desulfurization of 7 (8848.308 - 64 Da)

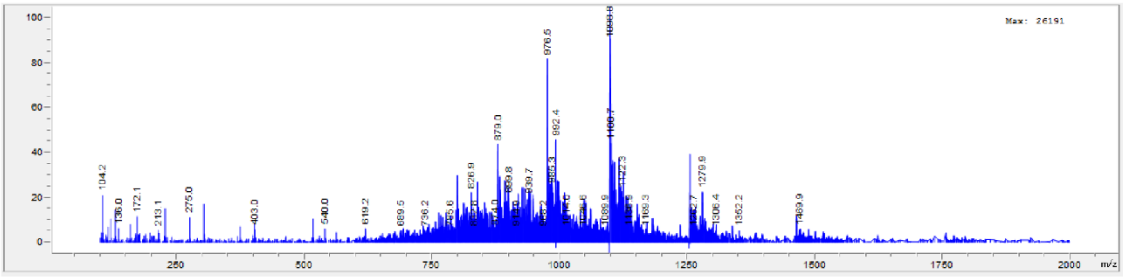

A solution of protein **7** (0.5 µmol), 1,3-diallylurea **2** (1.0 µmol), **3** (0.5 µmol) and additive **4a** (0.5 µmol) in 0.2 mL of distilled deionized water was irradiated at 365 nm. After 15 minutes of stirring, minimal conversion to the product was observed via LCMS. Oxidation of the protein **7** was the major product (M+16 Da.)

MS-spectrum for oxidation of 7 (8848.308 + 16 Da)

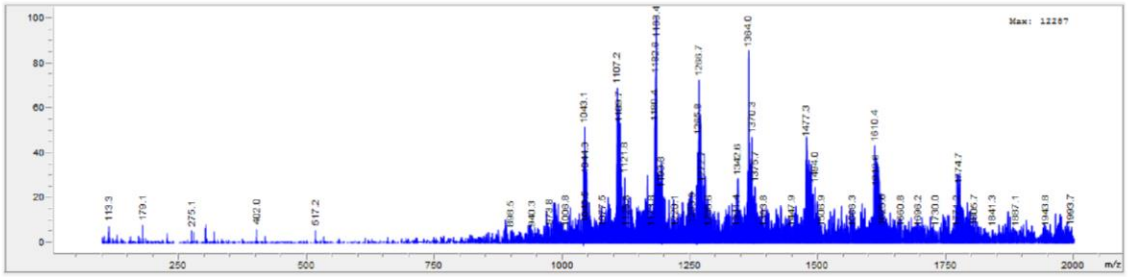

Optimized conditions for the stapling of protein 7 was as follows: A solution of protein **7** (0.5 µmol), 1,3-diallylurea **2** (1.0 µmol), **3** (0.5 µmol) and additive **4a** (0.5 µmol) in a mixture of 0.1 mL of a pH 4 acetate buffer and 0.1 mL of 6N Gdn·HCl was irradiated at 365 nm. After 15 minutes of stirring, the mixture was subjected to HPLC purification. The conversion to stapled protein **8** was found to be 90% based on LCMS.

Procedure for the thiol-ene reaction between 9 and 2:

A solution of protein **9** (0.5 µmol), 1,3-diallylurea **2** (1.5 µmol), **3** (1.0 µmol) and additive **4a** (0.5 µmol) in a mixture of 0.1 mL of a pH 4 acetate buffer and 0.1 mL of 6N Gdn·HCl was irradiated at 365 nm. After 15 minutes of stirring, the mixture was subjected to HPLC purification. The conversion to double-stapled protein **10** was found to be 80% based on LCMS.

General procedure for the thiol-ene reaction between 1 and 11a

A solution of peptide **1** (5 µmol), diene **11a** (5 µmol), and DMPA **12** (5 µmol) in 0.5 mL of NMP was irradiated at 365 nm. After 15 minutes of stirring, the mixture was diluted with 1.5 mL of water and washed with 4 mL of ethyl acetate. The aqueous layer was separated and purified through HPLC to yield stapled peptide **13a** in 92% conversion based on LCMS.

General procedure for the thiol-yne reaction between 1 and 11b

A solution of peptide **1** (5 µmol), diyne **11b** (5 µmol), and DMPA **12** (5 µmol) in 0.5 mL of NMP was irradiated at 365 nm. After 15 minutes of stirring, the mixture was diluted with 1.5 mL of water and washed with 4 mL of ethyl acetate. The aqueous layer was separated and purified through HPLC to yield stapled peptide **13b** in 97% conversion based on LCMS. LCMS signal showed two peaks (19.303 and 20.339) for **13b**, and the proportion of the two peaks is 2:1 (Figure S1). ^{1}H-NMR spectra and COSY spectra were obtained to identify the isomers. It was found that the earlier peak (19.303) was for the ZZ isomer with the *J* value of 9.5, 9.5 Hz (Figure S2 and S3), and the second peak is for the left isomer (Figure S4).

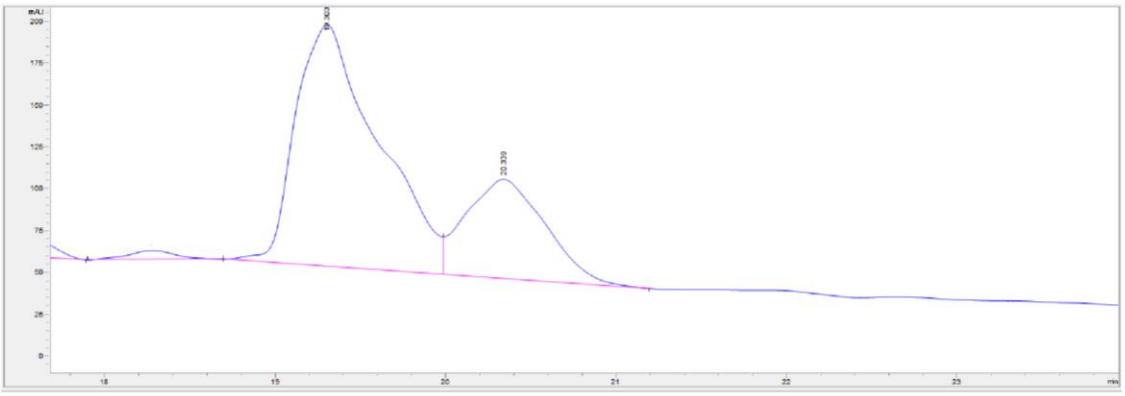

Figure S1. HPLC trace of the reaction mixture after 15 minutes of irradiation.

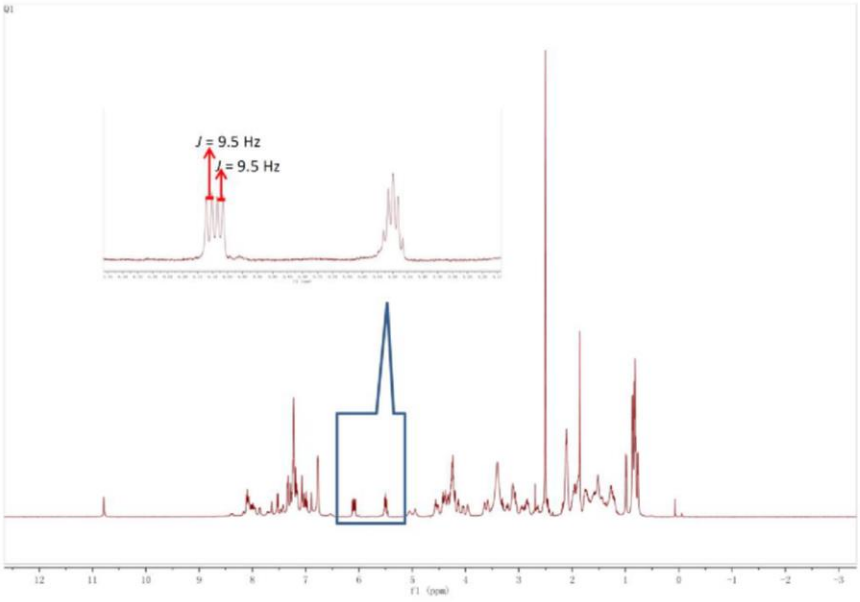

Figure S2. ^{1}H-NMR spectrum of ZZ isomer (at 500 MHz in DMSO-d_6)

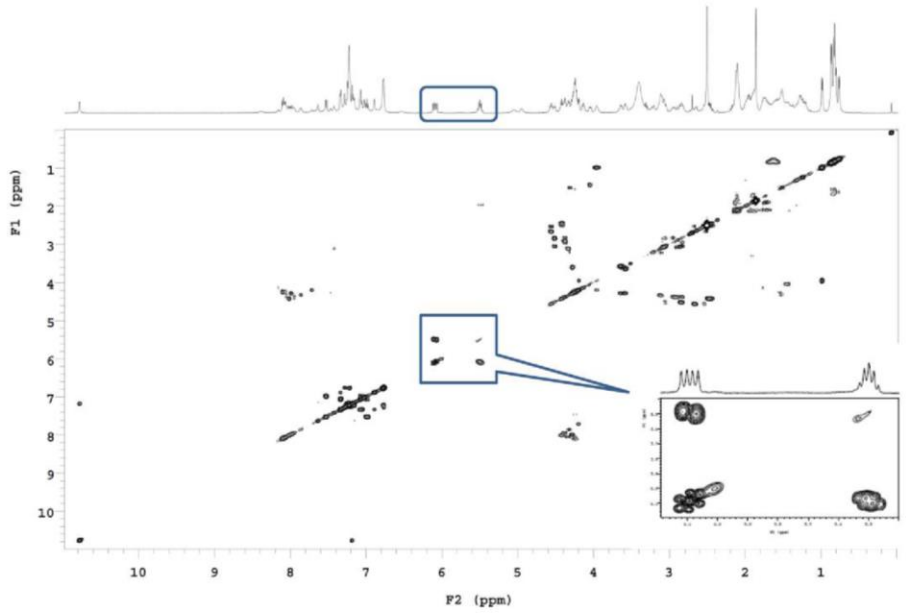

Figure S3. COSY spectrum of ZZ isomer (at 500 MHz in DMSO-d_6)

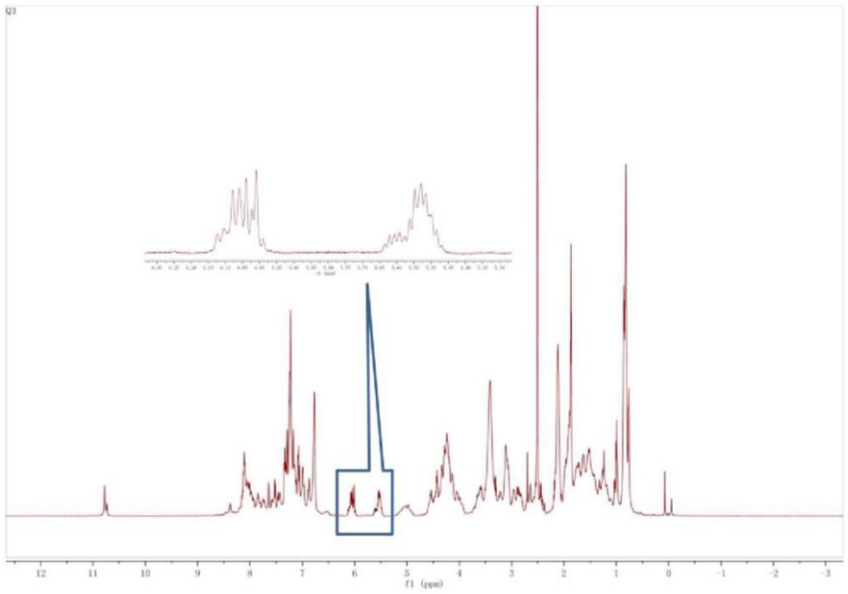

Figure S4. ^{1}H-NMR spectrum of left isomer (at 500 MHz in DMSO-d_6)

General procedure for the thiol-ene reaction between 13b and sulfur containing compounds 14a and 14 b

A solution of stapled peptide **13b** (2 µmol), **14a** (2 µmol), **3** (2 µmol) and **4c** (2 µmol) in 0.5 mL of distilled deionized water was irradiated at 365 nm. After 15 minutes of stirring, the mixture was purified through HPLC to yield peptide **15a** in 95% conversion based on LCMS.

A solution of stapled peptide **13b** (2 µmol), **14b** (2 µmol), **3** (2 µmol) and **4c** (2 µmol) in 0.5 mL of distilled deionized water was irradiated at 365 nm. After 15 minutes of stirring, the mixture was purified through HPLC to yield peptide **15b** in 94% conversion based on LCMS.

General procedure for the thiol-ene reaction between 13b and 16

A solution of stapled peptide **13b** (2 µmol), peptide **16** (2 µmol), **3** (2 µmol) and **4c** (2 µmol) in 0.5 mL of distilled deionized water was irradiated at 365 nm. After 15 minutes of stirring, the mixture was purified through HPLC to yield peptide **17** in 91% conversion based on LCMS.

General procedure for the thiol-ene reaction between 18 and 11a

A solution of FITC-labeled peptide **18** (5 µmol), diene **11a** (5 µmol), and DMPA **12** (5 µmol) in 0.5 mL of NMP was irradiated at 365 nm. After 15 minutes of stirring, the mixture was diluted with 1.5 mL of water and washed with 4 mL of ethyl acetate. The aqueous layer was separated and purified through HPLC to yield stapled peptide **19a** in 92% conversion based on LCMS.

General procedure for the thiol-yne reaction between 18 and 11b

A solution of FITC-labeled peptide **18** (5 µmol), diyne **11b** (5 µmol), and DMPA **12** (5 µmol) in 0.5 mL of NMP was irradiated at 365 nm. After 15 minutes of stirring, the mixture was diluted with 1.5 mL of water and washed with 4 mL of ethyl acetate. The aqueous layer was separated and purified through HPLC to yield stapled peptide **19b** in 96% conversion based on LCMS.

General procedure for the thiol-ene reaction between 19b and 16

A solution of stapled peptide **19b** (2 µmol), peptide **16** (2 µmol), **3** (2 µmol) and **4c** (2 µmol) in 0.5 mL of distilled deionized water was irradiated at 365 nm. After 15 minutes of stirring, the mixture was purified through HPLC to yield peptide **20** in 93% conversion based on LCMS.

Circular dichroism

All CD spectra were recorded on an AVIV Model 410 spectrophotometer (AVIV) in water in a 1 mm QS quartz cuvette (Starna) at 25°C. Wavelength scans were performed at 1-nm resolution with 1-s averaging time. Data from double scans were averaged, blank subtracted, and normalized to mean residue ellipticity by the following equation: $[\theta] = 100 \times \theta/C \times l \times (n - 1)$, where C is concentration of protein in mM, l is path length in centimeters, and n is the number of residues in the protein. The concentrations of the protein samples used for CD experiments were 100 µM. The percentage helicity was calculated from the absorbance at 222 nm using helical models as previously reported.[4]

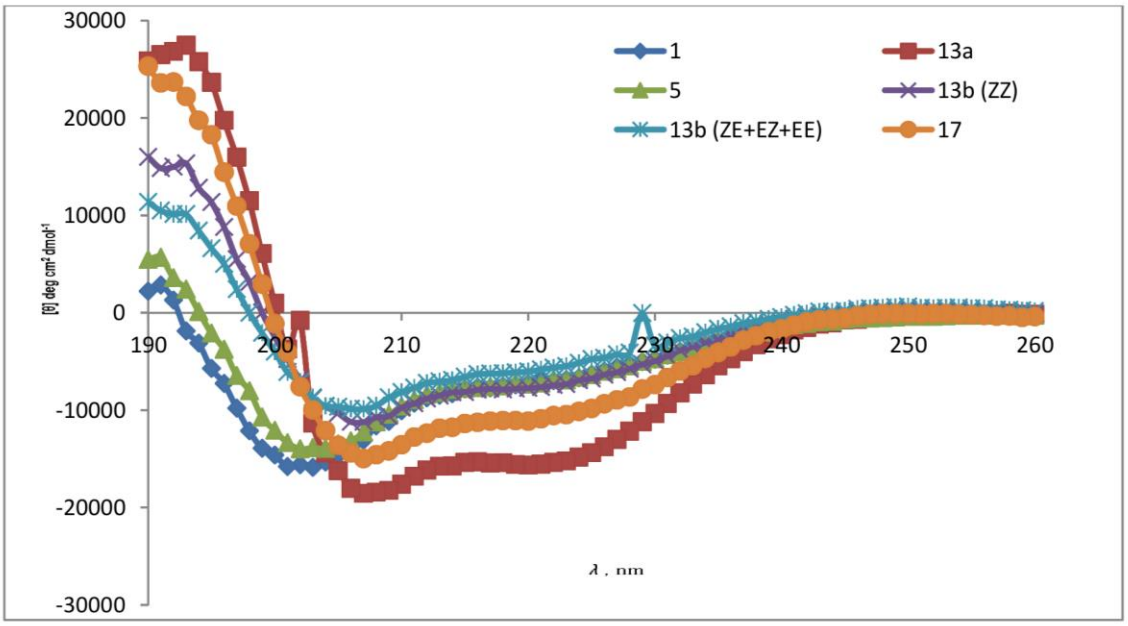

Figure S5. CD spectra for the peptide **1** and its analogs.

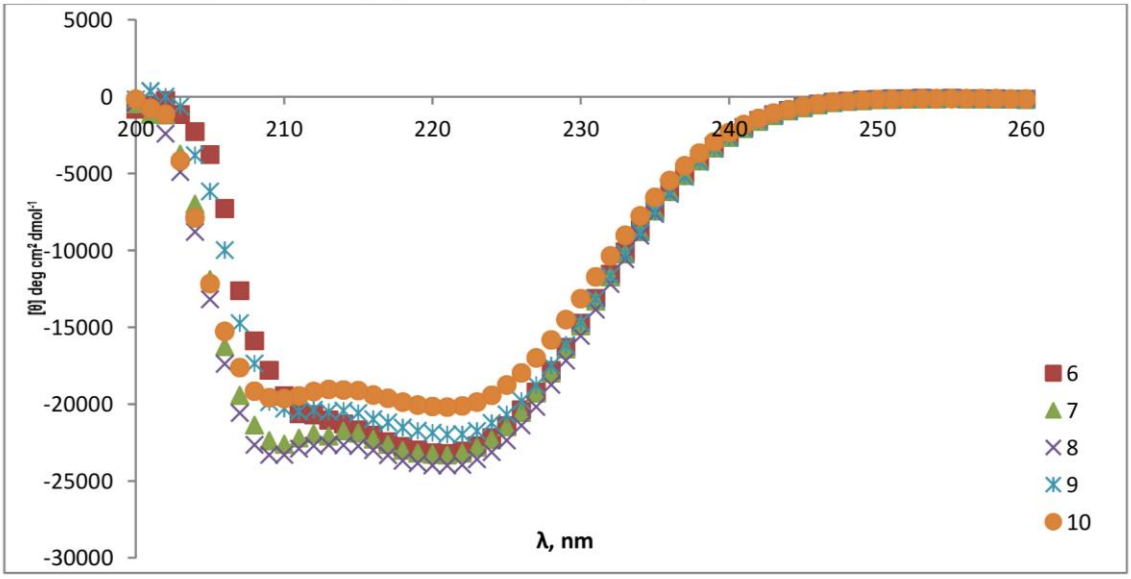

Figure S6. CD spectra for the coil-coil peptide and their stapled analogs.

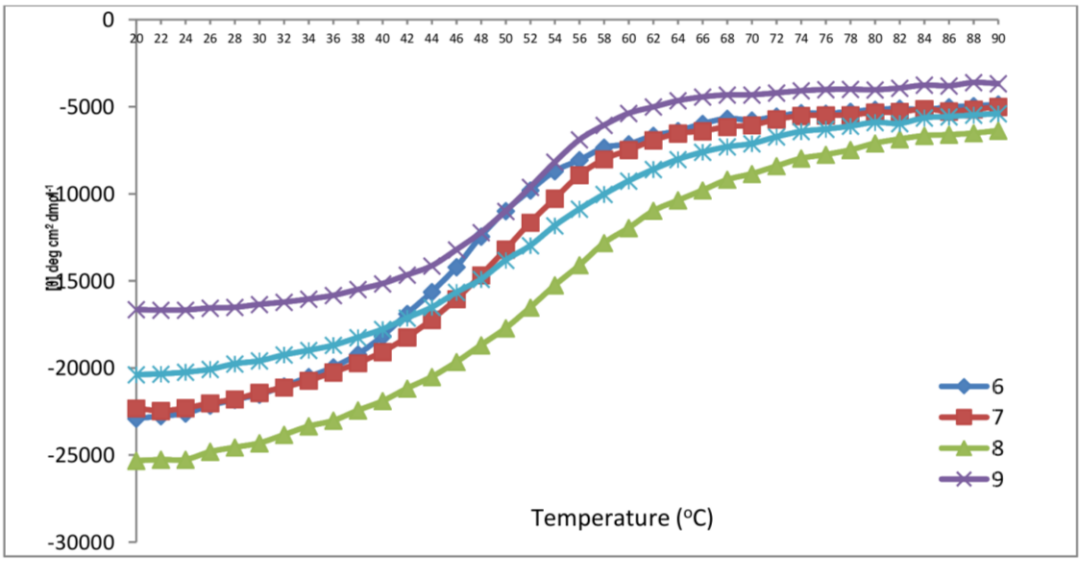

Figure S7. Thermal stability monitored using CD signal at 222 nm

Biological experiments

Protein Constructs Were Expressed and Purified

Recombinant protein **6**, **7**, and **9** were successfully cloned, expressed, and purified (Figure S8). Protein **7** and **9** were stapled, resulting in proteins **8** and **10**, respectively. Identity of the constructs was verified by mass spectroscopy. The major peak in each of the MS, HPLC data, and SDS-PAGE analysis demonstrates construct purity of >95%.

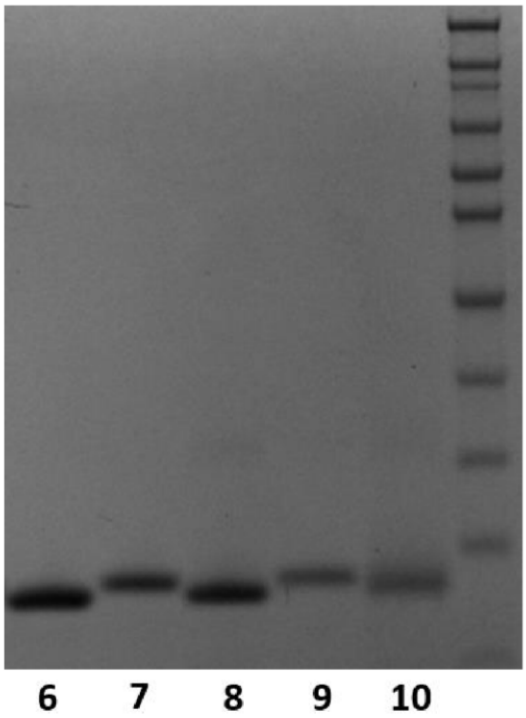

Figure S8. SDS-PAGE analysis of stapled proteins (8 and 10) and unstapled controls (6, 7, and 9) **Iodoacetic acid** alkylates the –SH groups of free cysteines. Proteins were reconstituted to a concentration of 10uM in 8M urea (Qiagen) in 100mM Tris-HCl (Sigma), pH 8. 1.2uL of 0.1M TECP (GoldBio) was added to 40uL of protein (5mM final concentration), and samples were shaken for 20 minutes at room temperature. Next, 0.88uL of a 500mM IAA (Sigma Aldrich) in Milli-Q water was added, and the sample was shaken in the dark for 15 minutes. Samples were analyzed by mass spectroscopy and a mass-shift of +58 Da represents the alkylation of one IAA molecule, and thus one free cysteine.

MS-Spectrum for 7+ 116Da

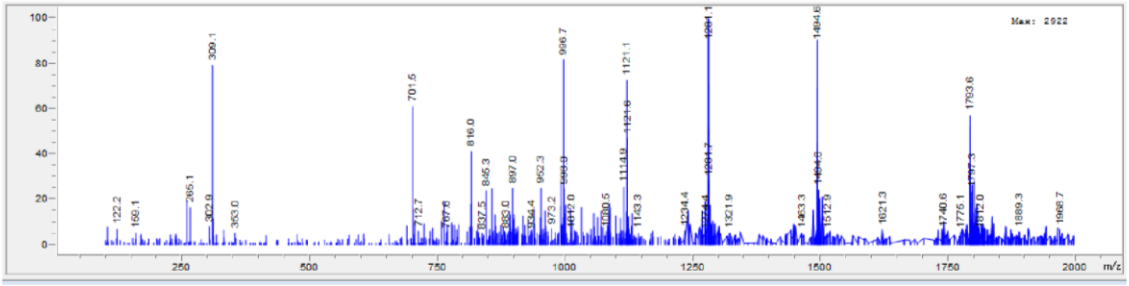

MS-Spectrum for 8

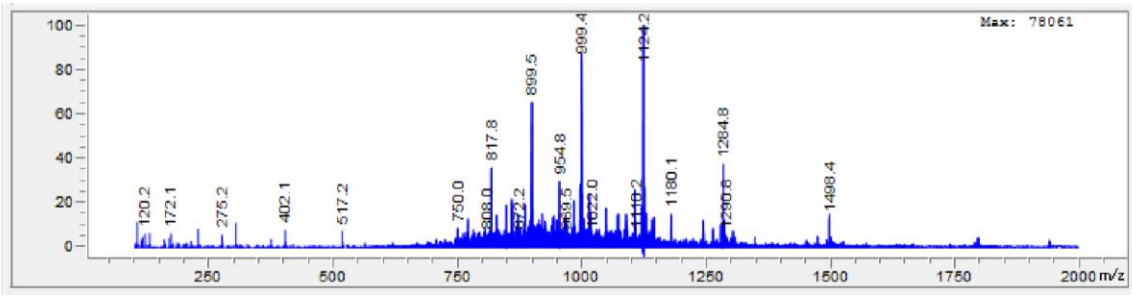

MS-Spectrum for 9+ 232Da

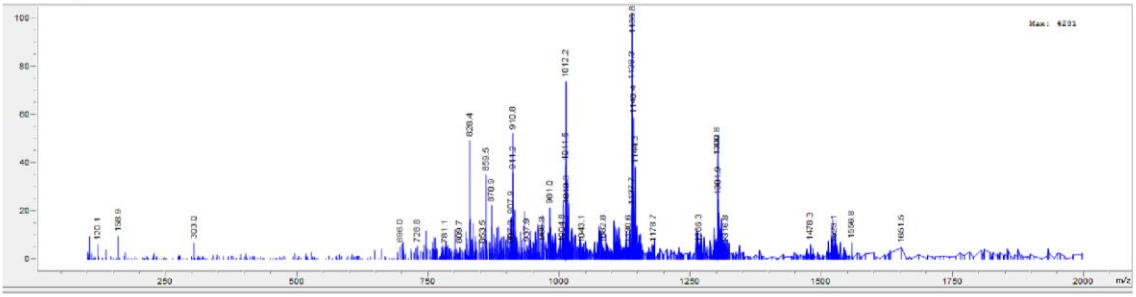

MS-Spectrum for 10

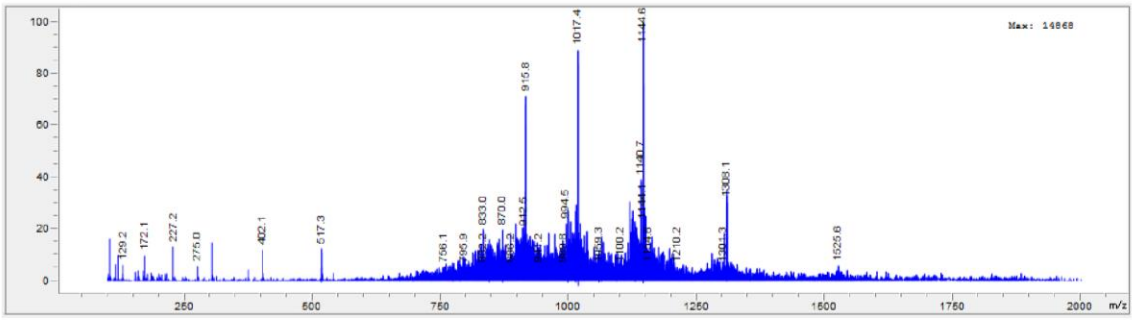

Protease stability assays

Proteins were resuspended in 100mM Tris-HCl, pH 7.8, 10mM CaCl2, 1mM MgCl2, and sequence-grade chymotrypsin (Life Technologies) was resuspended per the manufacturer's protocol. Samples and chymotrypsin were preheated to 30° C, and chymotrypsin was added to the proteins at a 1:100 w/w ratio. Aliquots were removed at the indicated time, and the reaction was halted by the addition of TFA, lowering the pH to below 2. Any remaining chymotrypsin activity was eliminated by immediately boiling the samples. Aliquots were analyzed by SDS PAGE, with Coomassie blue staining. Similar assays were carried out with sequence grade trypsin (Promega) and endoproteinase GluC (New England Biolabs) following manufacturer's protocols, and the stapled peptides were universally less stable to proteolysis than the unstapled controls.

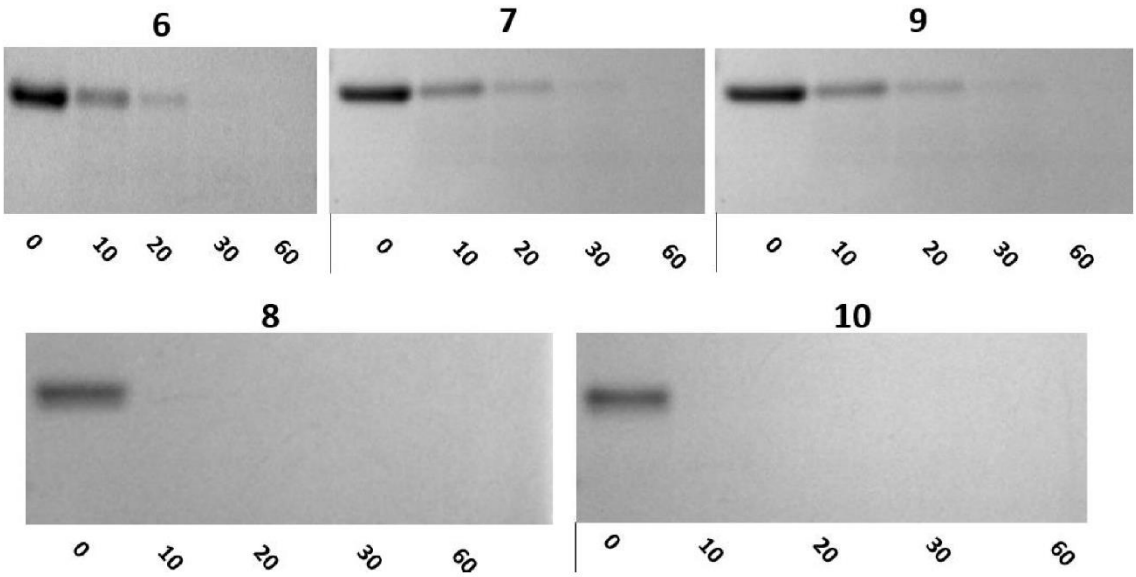

Figure S9. Trypsin digestion of stapled (**8** and **10**) and unstapled proteins (**6, 7,** and **9**) incubated at a 1:1000 w/w ratio of protease:protein.

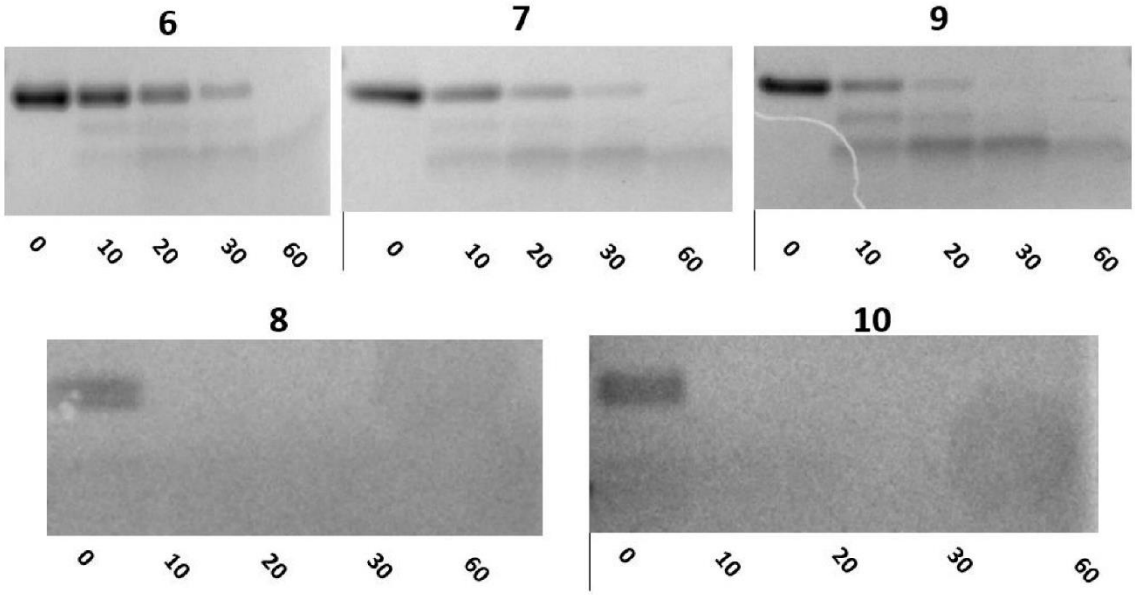

Figure S10. Endoproteinase GluC (V8) digestion of stapled (**8** and **10**) and unstapled proteins (**6**, **7**, and **9**) incubated at a 1:200 w/w ratio of protease:protein.

LC/MS/MS analysis of digested peptides

Digested peptides were analyzed using a nano-LC/MS/MS system equipped with a nano-HPLC pump (2D-ultra, Eksigent) and a maXis II ETD mass spectrometer (Bruker Daltonics, Bremen, Germany). The maXis II ETD mass spectrometer was equipped with a captive spray ion source.

Approximately 5 µL of peptide samples were injected onto a dC18 nanobore LC column. The nanobore column was made in house using dC18 (Atlantis, Waters Corp); 3 µm particle; column: 100µm ID x 100 mm length. A linear gradient LC profile was used to separate and eluted peptides with a constant total flow rate of 400 nL/minute. The gradient consisted of 5 to 96% solvent B in 78 minutes (solvent B:100% acetonitrile with 0.1% formic acid; solvent A: 100% water with 0.1% formic acid) was used for the analyses.

Size-exclusion chromatography

Proteins were centrifuged at 21,000xg for 1 hour, and then diluted to 50uM in 100mM phosphate (Sigma), pH 7.4, 50mM NaCl (Fisher Scientific), followed by another round of centrifugation. 1uL of each sample was run on a Yarra 1.8 µm SEC-X150, at a flow rate of 0.3mL/min, and analyzed by a280. Protein standards (Bio-Rad, 151-1901) were run as well, to determine elution times of known proteins.

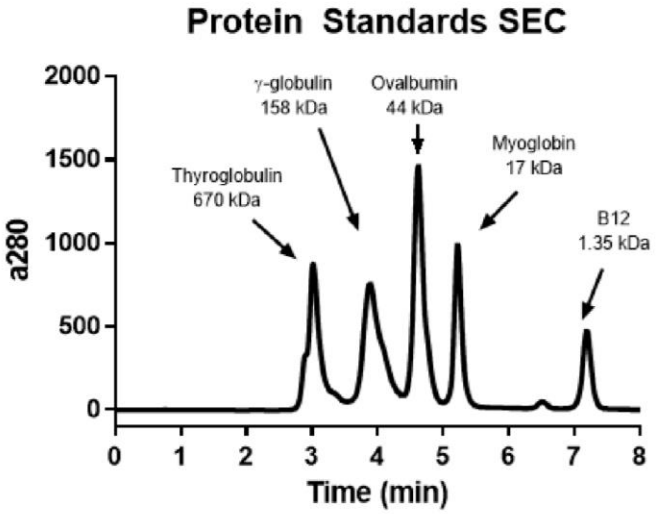

Figure S11. Size-exclusion chromatography of gel filtration standards

Internalization of fluorescein isothiocyanate (FITC)-labeled peptides was carried out as before [1] with the following alterations. Peptides were resuspended in 50% v/v isopropyl alcohol in Milli-Q water. Cells were treated 1, 10, or 30uM concentrations of the peptides. Following washes, K562 cells were resuspended in 500uL PBS (Life Technologies), and analyzed for FITC intensity by flow cytometry using the FACS Canto-II (BD BioSciences, University of Utah Core Facility). FITC was excited with a488nm laser, and a 530/30 fluorescence detector was used, and mean FITC intensity was calculated, and intensity was normalized as a fold increase over untreated cells.

Computational modeling

Models of unstapled protein **6** and stapled versions **8** and **10** were built on the foundation of the crystal structure of the N-terminal oligomerization domain of Bcr-Abl (Protein Data Bank code

1K1F, utilizing Chain A. Using the *swapaa* tool within the Chimera modelling software, [5] selenomethionine residues were reverted back to methionine and residue 38 was mutated to cysteine, as consistent with the wild type. The *swapaa* tool facilitates the accurate replacement of modelled residues by sourcing the Dunbrack backbone-dependent rotamer library to predict the most accurate side-chain rotamers.[6] To build the modified protein 6, the mutations C38A, S41R, L45D, E48R and Q60E were sequentially implemented within Chain A using the *swapaa* tool within Chimera. To build the stapled proteins (8 and 10), non-standard amino acid residue libraries were created and parameterized which contain the molecular staples: Atom coordinates for the non-standard residues were developed using Gaussview 5.0[7] Geometry and partial charges of said residues were assigned using the *RESP ESP charge Derive Server* (RED) server, in which the geometries of the stapled residues were optimized at a HF 6-31G* level of theory and assigned partial charges based on restrained electrostatic potential (RESP) methodology.[8-10] *Antechamber* (AmberTools15) was used to assign AMBER atom types and generate library files to define the non-standard amino acid residues within the ff14SB force field. The modified, staple-containing residues were incorporated into protein 6 by residue replacement within the PDB file.
Models were built using AMBER ff14SB force field parameters [11,12] and explicitly solvated in a truncated octahedron with at least a 10 Å surrounding buffer of TIP3P water.[13] Net neutralizing counter-ions (Na+/Cl-) were incorporated using the Joung and Cheatham ion parameters, and 50 additional Na^+ / Cl^- atoms were added to reach a biologically-representative ion concentration of 200 mM.[14] All solute hydrogen masses were repartitioned to a mass of 3.024 Da to allow for a doubling of the MD time integration step.[15]

All models were subjected to an extensive minimization and equilibration protocol to relax and steer systems towards energetically favorable conformations prior to production molecular dynamics (MD). An initial minimization was performed (500 steps of steepest descent, 500 steps of conjugate gradient) prior to heating the system to 300 K. A 25 kcal/(mol $Å^2$) restraint was placed upon backbone C_α atoms throughout the initial minimization and heating step. Following the initial minimization and heating, systems were subjected to five cycles of minimization (500 steps of steepest descent each, 500 steps of conjugate gradient each) and equilibration, in which the restraint weights were lifted sequentially from 5 kcal/(mol $Å^2$) to 1 kcal/(mol $Å^2$). A final equilibration was performed for 500 ps with a restraint weight of 0.5 kcal/(mol $Å^2$) prior to production MD. Constant temperature (300 K) and pressure (1 bar) were controlled throughout the minimization protocol using a Berendsen thermostat with a 0.2 coupling time.[16]
All production MD simulations were performed using the GPU implementation of the Amber14 modelling suite[17,18] with Blue Waters K20X GPUs for at least 500 ns (each) in explicit solvent using a 4 fs time step, a Langeven thermostat[19] with a collision frequency of 5 ps^{-1} to control constant temperature and pressure,[20] a 10 Å non-bonded cutoff, default particle mesh Ewald treatment of electrostatics,[21] and SHAKE applied to bonds to hydrogen,[22] using a different random seed in each simulation to prevent synchronization artifacts, generated every 24 hours of simulation time.

Analyses of the MD trajectories were performed using the CPPTRAJ analysis toolset ,[23] which is distributed with AmberTools15. RMSD analyses were performed to monitor the structural variability of each system, while clustering analyses were performed to identify the most sampled structures throughout production MD. [24] A DSSP secondary structure analysis was performed to assess the helical content of each system.[25]

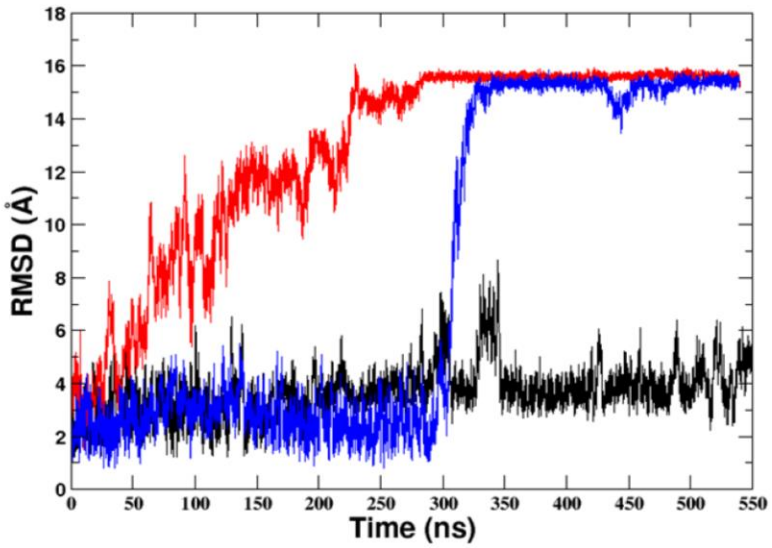

Figure S12. Time course of root-mean-square deviation (RMSD) of MD simulation structures as compared to the experimental reference structure.

RMSD analyses were performed to monitor the structural variance of (unstapled) protein 6 (black), (single stapled) 8(blue), and (double stapled) 10 (red) to that of the experimental reference structure (PDB: 1K1F) along the simulation trajectories. RMSD values between 0-6 are consistent with the extended peptide conformation in main body **Figure S12A**, while RMSD values between 14-16 are consistent with the collapsed peptide conformations observed in main body **Figure S12B** and **Figure S12C**. Results suggest that unstapled protein 6 exists in a single conformational state, while both protein 8 and 10 exist in least two or more conformational states.

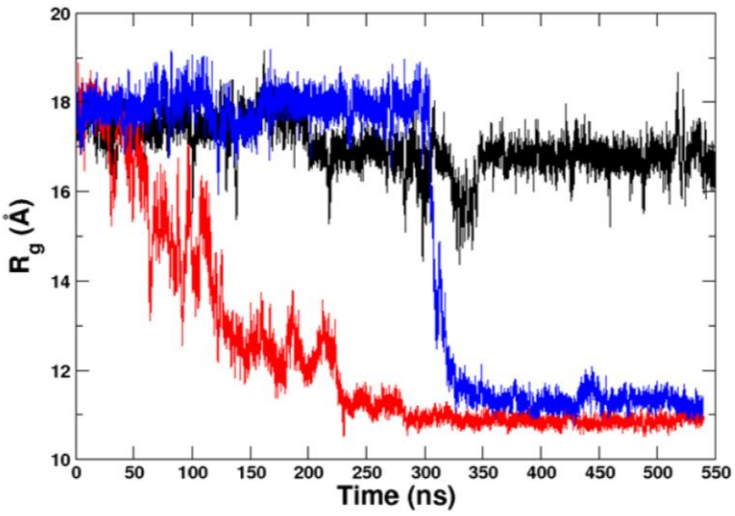

Figure S13. Time-course radius of gyration (R_g) of MD simulation structures.
The radius of gyration was calculated for each of (unstapled) protein 6 (black), and (stapled) proteins 8 (blue), and 10 (red) as a measure of relative structural compactness. Results outlined in **Figure S13** suggest a discrete re-ordering of stapled proteins 8 and 10 structure (but not of unstapled protein 6) – supporting the SEC results outlined in main body **Figure 2**.

System		Helicity (%)
Protein 6		**80.6**
Protein 8		**71.2**
Protein 10		**79.2**

Table S2. Helicity of Stapled protein 8 and 10 as relative to unstapled protein 6.
A DSSP analysis of secondary structure was conducted upon (unstapled) protein 6 and stapled protein 8 and 10 in order to assess the impact of molecular stapling on the overall helicity of the modified and unmodified proteins. While no significant change in helicity was observed in 10 relative to that of the 6, this variant (8) suffered from a marked loss of helicity, which may be attributed to its adoption of the collapsed conformation observed in **Figure 3**.

Table S3. Mass spectrometry for the compounds described in this manuscript.

Peptide	Calculated Mass in Da	Found Mass in Da	Method
1	2021.9	1012.1 [M/2 + H] 1023.1 [(M+ Na)/2]	ESI
5	2161.9	1082.5 [M/2 + H] 1093.6 [(M+ Na)/2]	ESI
7	8848.309	1770.4 [M/5 + H] 1475.2 [M/6 + H] 1264.7 [M/7 + H] 1106.7 [M/8 + H] 983.8 [M/9 + H] 885.8 [M/10 + H] 805.2 [M/11 + H]	ESI
8	8988.309	1798.4 [M/5 + H] 1498.8 [M/6 + H] 1284.7 [M/7 + H] 1124.3 [M/8 + H] 999.5 [M/9 + H] 899.6 [M/10 + H] 818.0 [M/11 + H]	ESI
9	8869.139	1774.8 [M/5 + H] 1479.0 [M/6 + H] 1267.7 [M/7 + H] 1109.4 [M/8 + H] 986.3 [M/9 + H] 887.8 [M/10 + H] 807.4 [M/11 + H]	ESI
10	9149.139	1525.8 [M/6 + H] 1307.9 [M/7 + H] 1144.3 [M/8 + H] 1017.5 [M/9 + H] 915.8 [M/10 + H] 832.7 [M/11 + H]	ESI
13a	2146.0	1074.1 [M/2 + H]	ESI
13b	2142.2	1072.5 [M/2 + H] 1083.6 [(M+ Na)/2]	ESI
15a	2612.8	1307.6 [M/2 + H] 1318.6 [(M+ Na)/2]	ESI
15b	2758.3	1380.2 [M/2 + H] 920.0 [M/3 + H]	ESI
16	889.4	890.4	ESI
17	332.2	1517.4 [M/2 + H]	ESI

		1011.8 [M/3 + H] 759.5 [M/4 + H]	
18	2441.7	1221.5 [M/2 + H]	ESI
19a	2565.8	1283.2 [M/2 + H]	ESI
19b	2561.8	1281.6 [M/2 + H]	ESI
20	3451.2	1726.3 [M/2 + H] 1150.9 [M/3 + H] 863.4 [M/4 + H]	ESI

LC-chromatogram and MS-spectrum

MS-spectrum for **5**

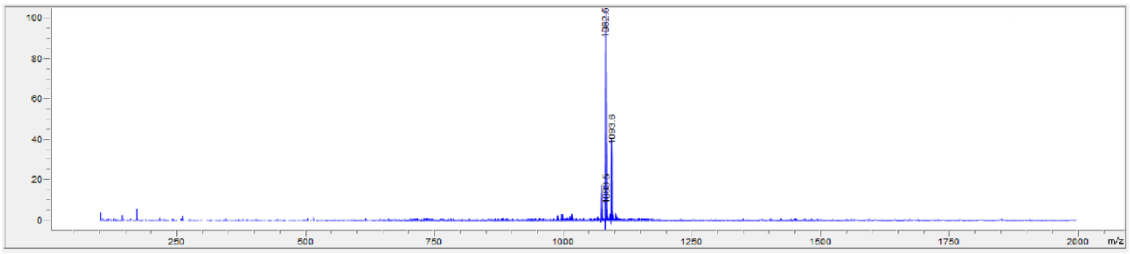

LC-chromatogram for **5**

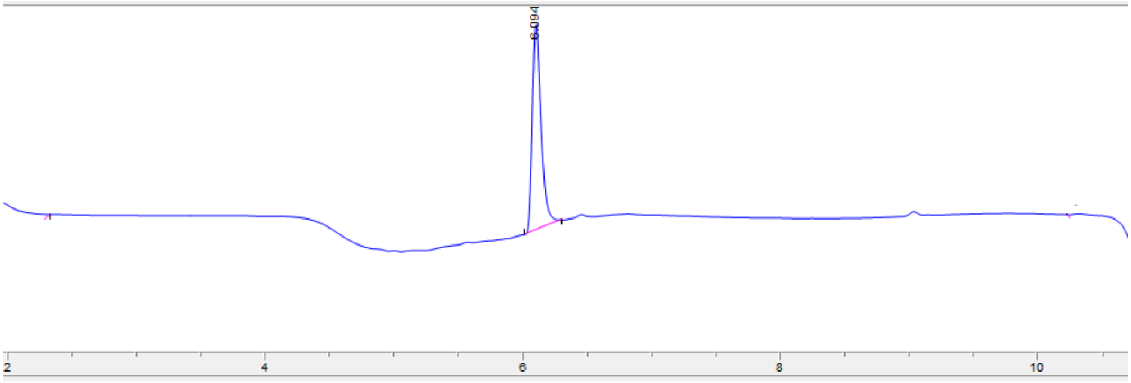

MS-spectrum for **7**

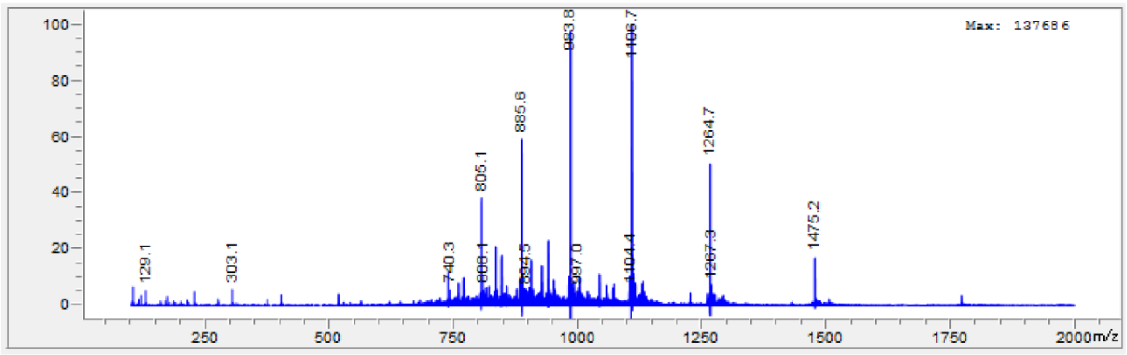

LC-chromatogram for **7**

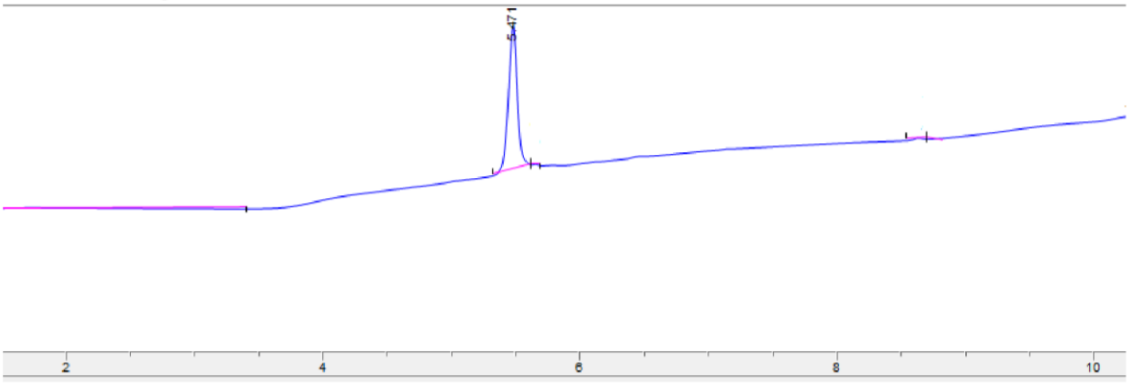

MS-spectrum for **8**

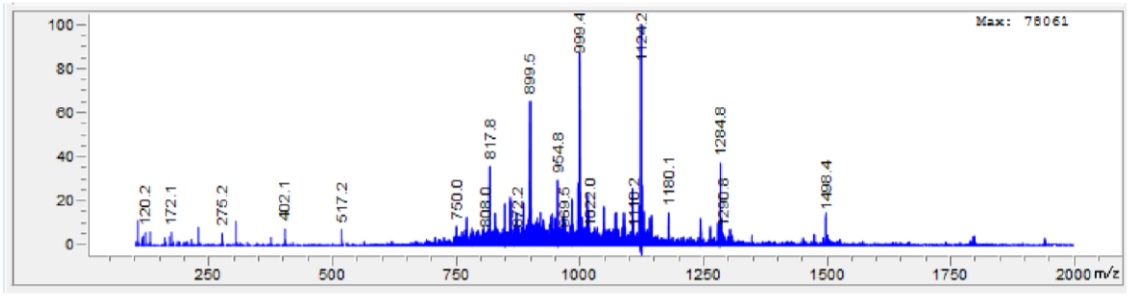

LC-chromatogram for **8**

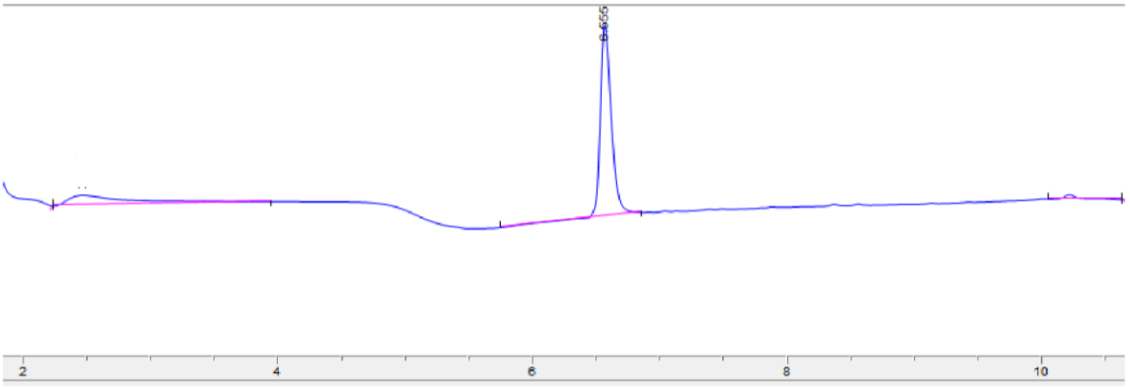

MS-spectrum for **9**

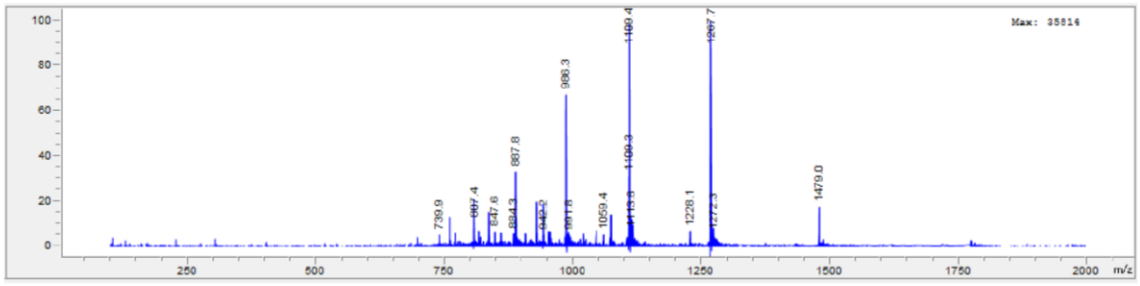

LC-chromatogram for **9**

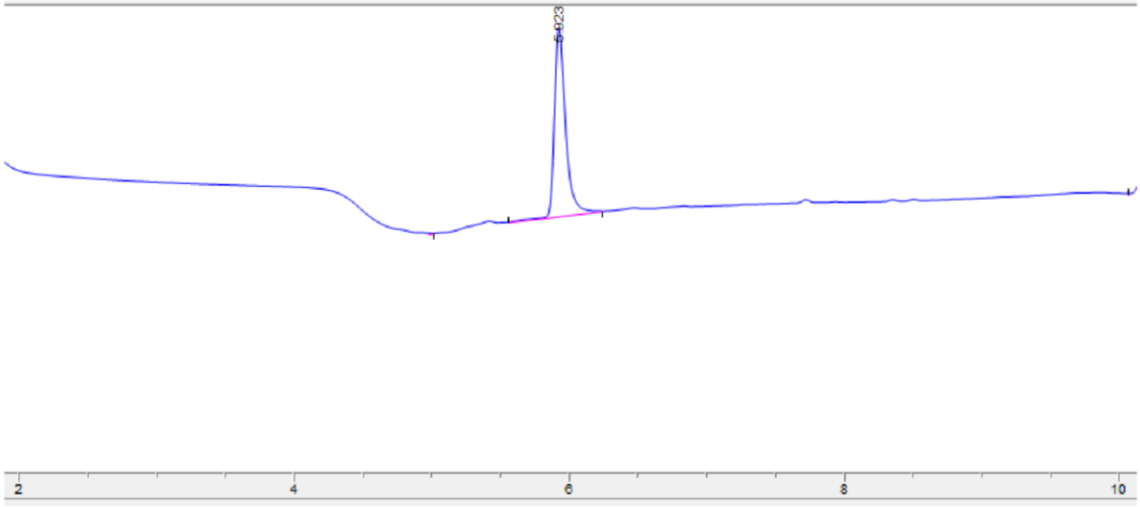

MS-spectrum for **10**

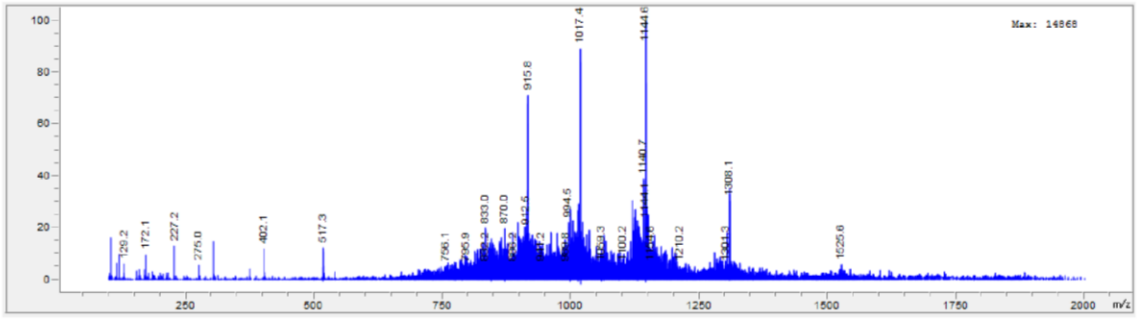

LC-chromatogram for **10**

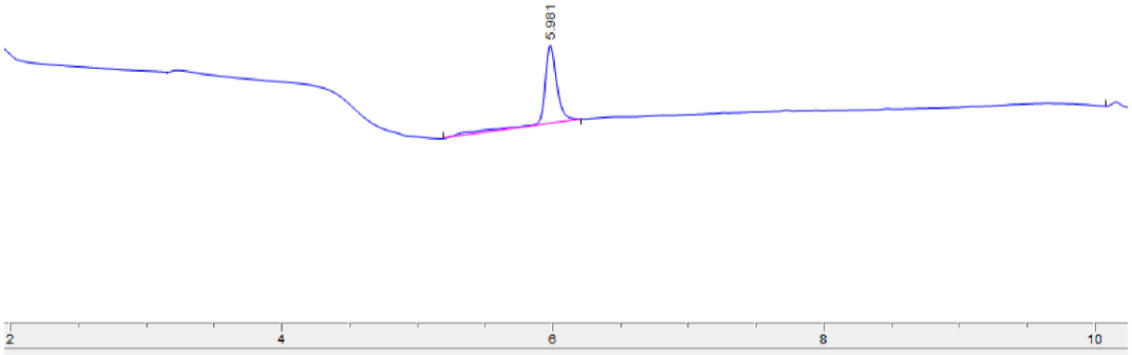

MS-spectrum for **13b**

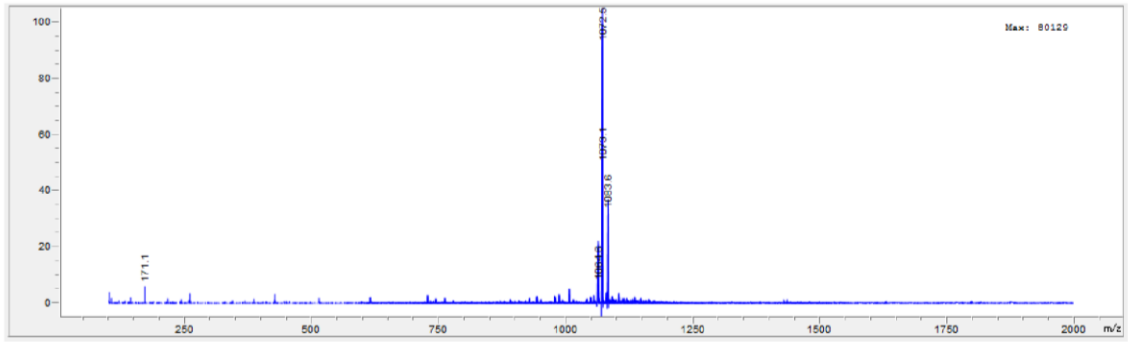

LC-chromatogram for **13b** (ZZ isomer)

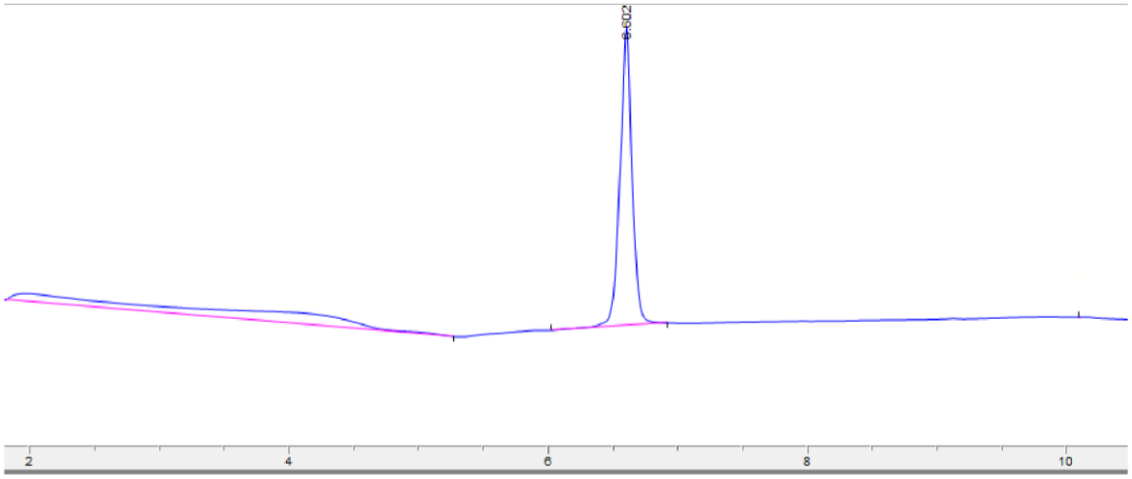

LC-chromatogram for **13b** (ZE+EZ+EE isomer)

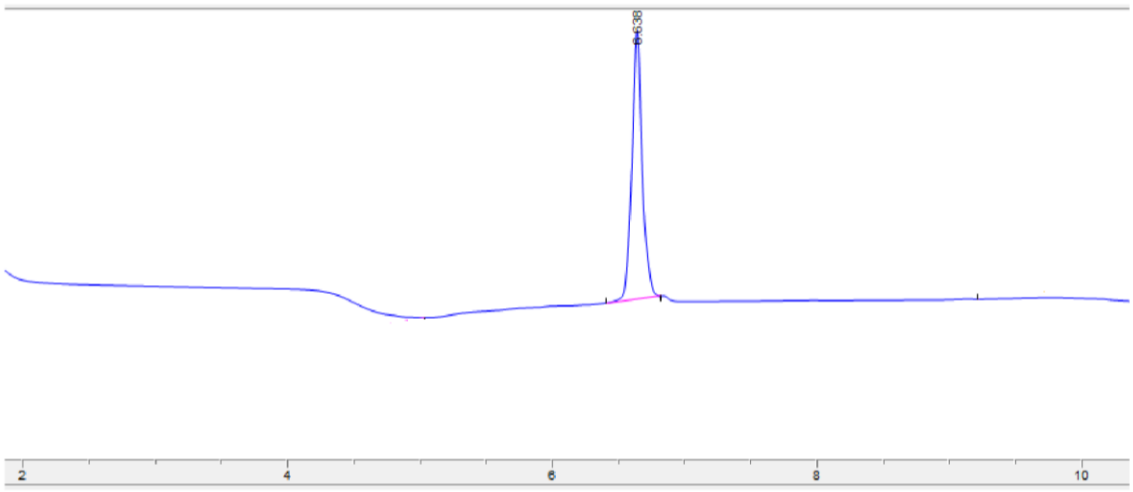

MS-spectrum for **15a**

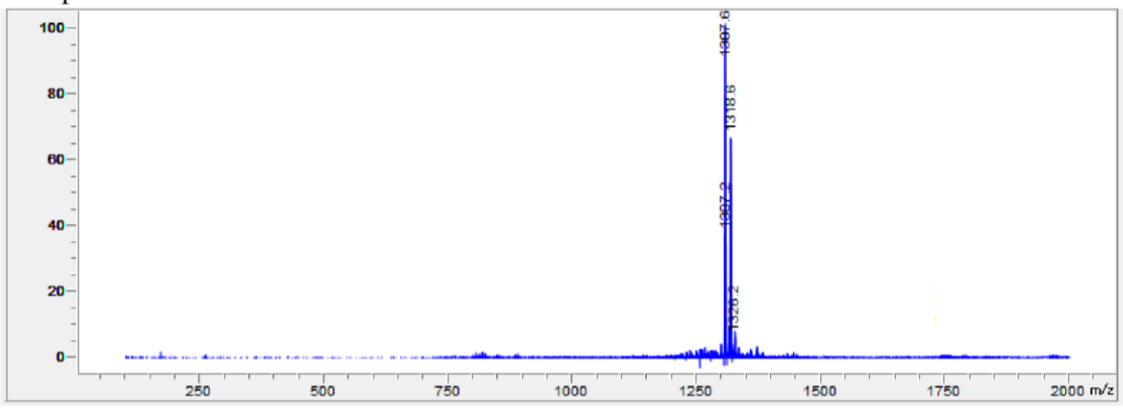

LC-chromatogram for **15a**

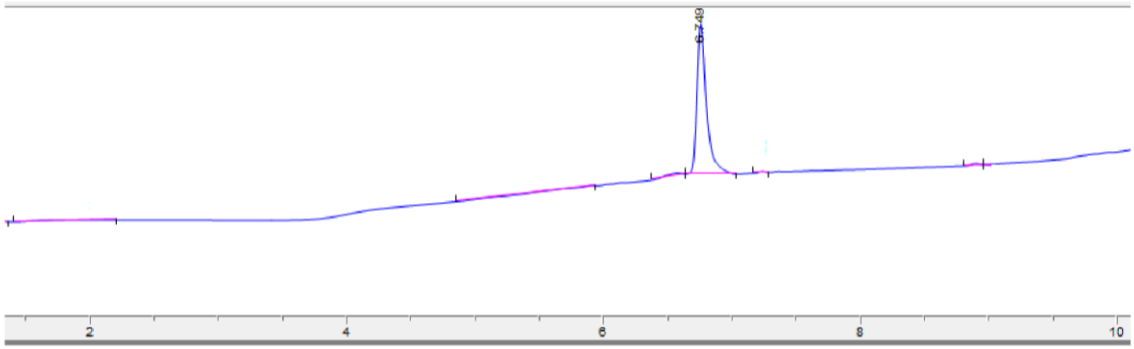

MS-spectrum for **15b**

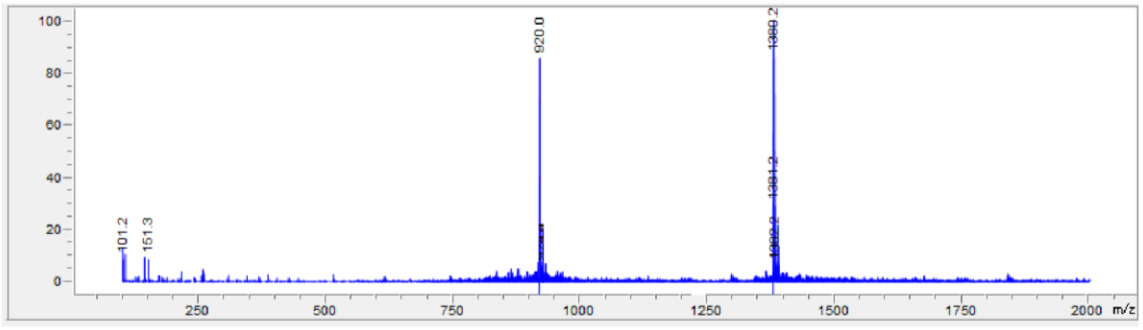

LC-chromatogram for **15b**

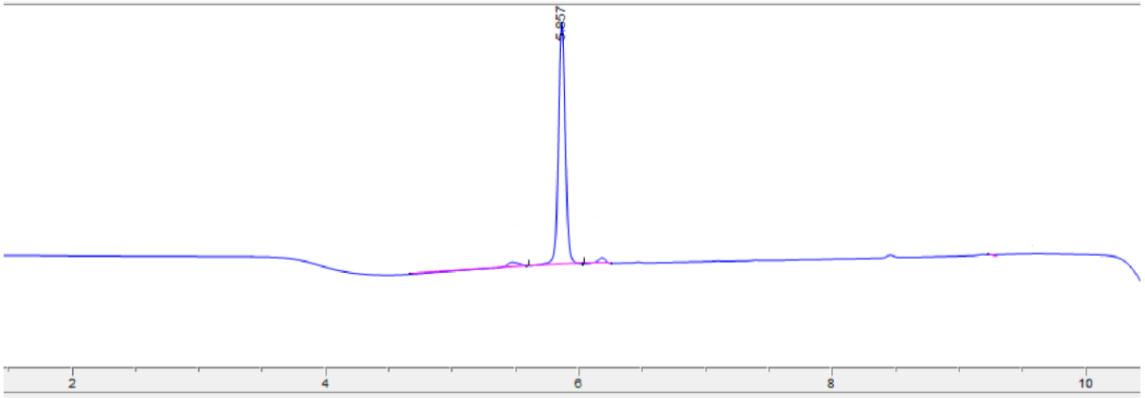

MS-spectrum for **16**

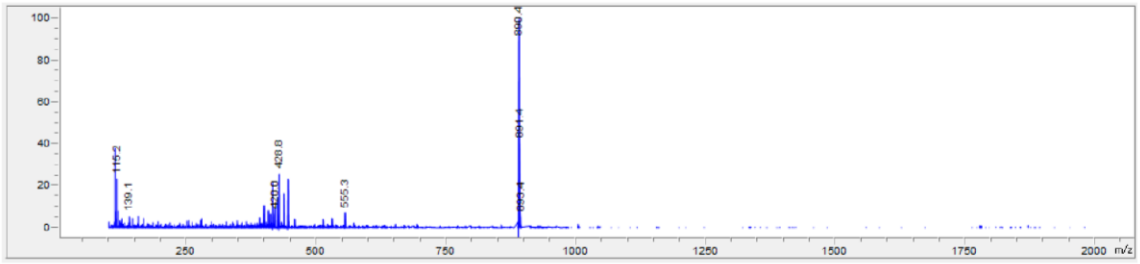

LC-chromatogram for **16**

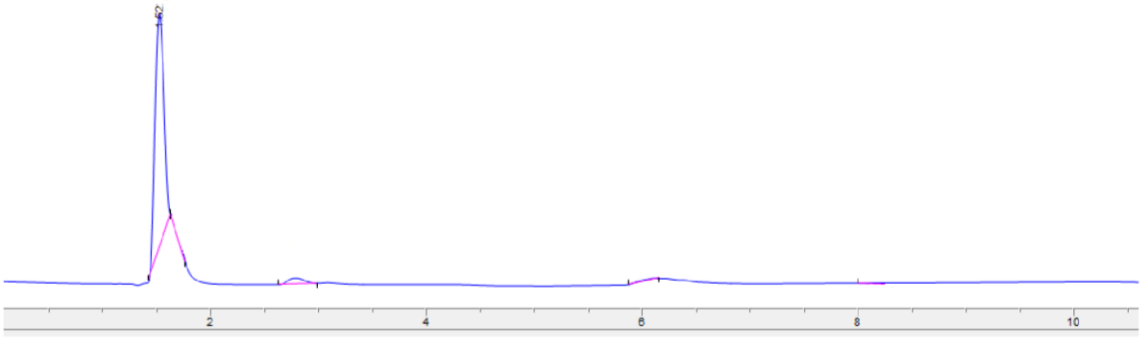

MS-spectrum for **17**

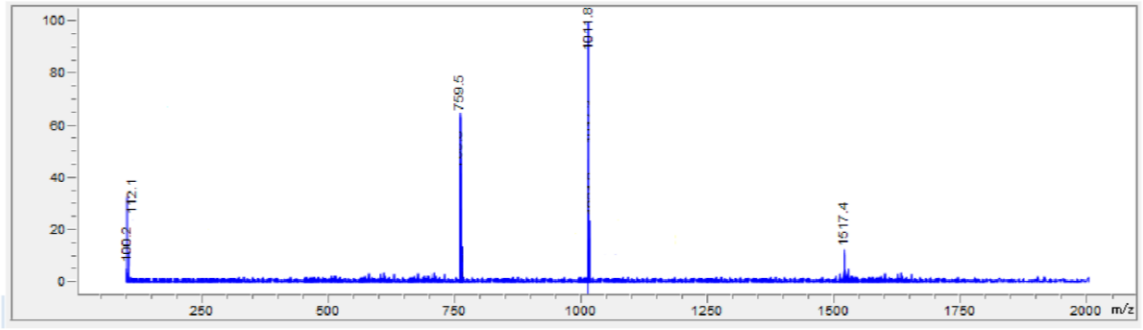

LC-chromatogram for **17**

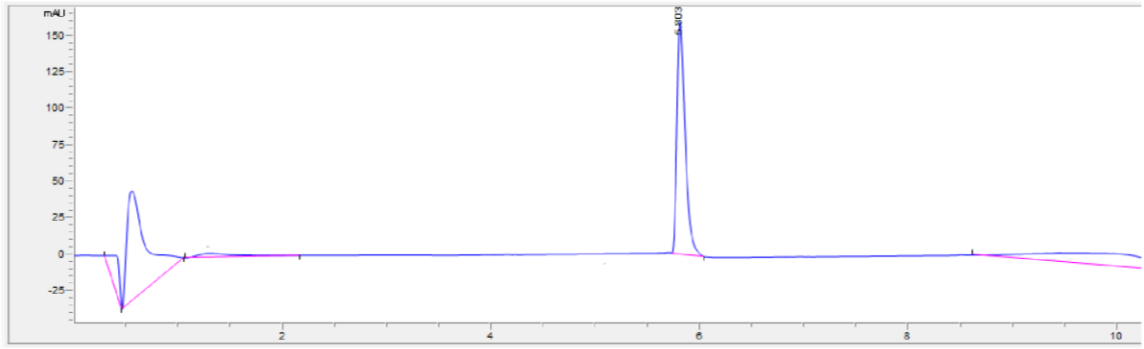

MS-spectrum for **18**

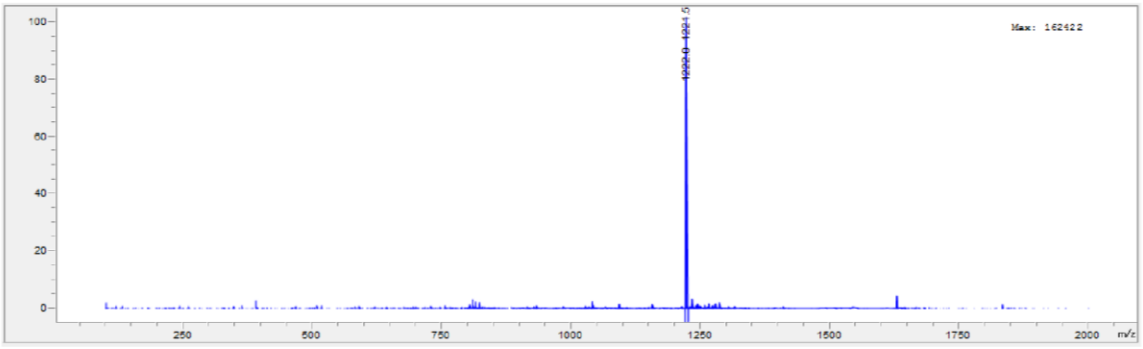

LC-chromatogram for **18**

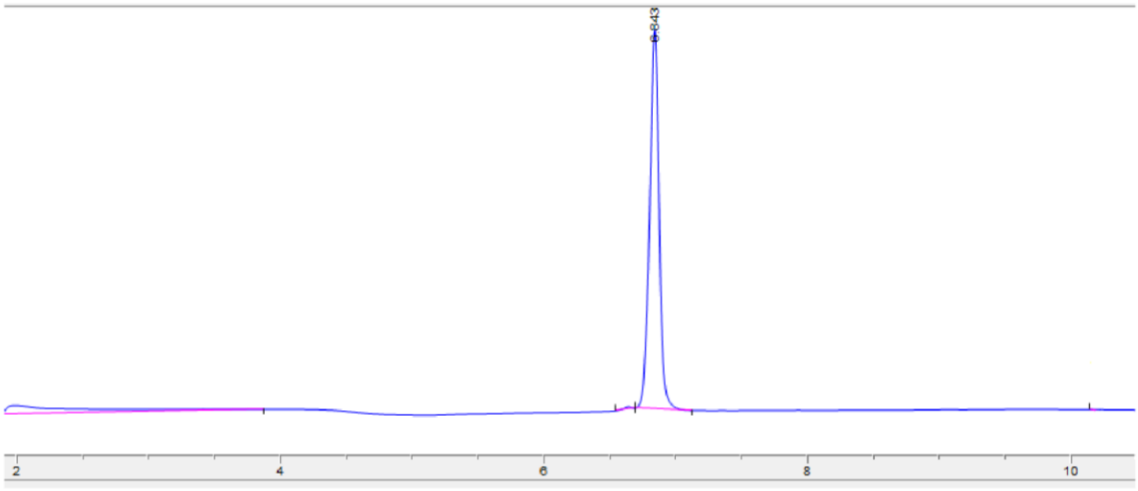

MS-spectrum for **19a**

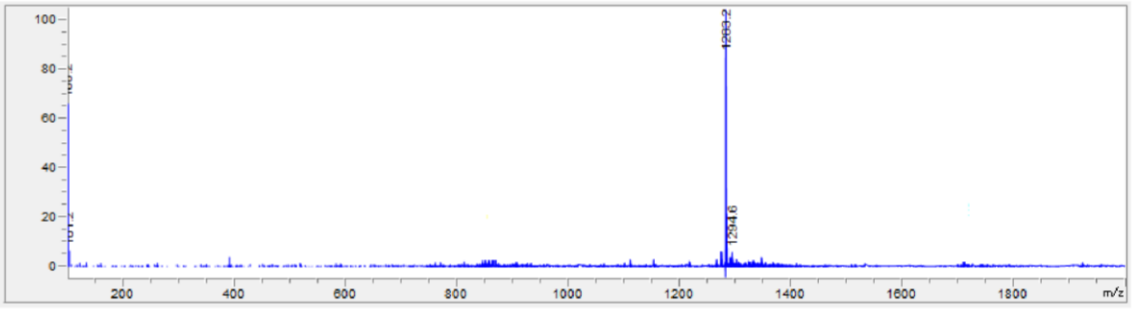

LC-chromatogram for **19a**

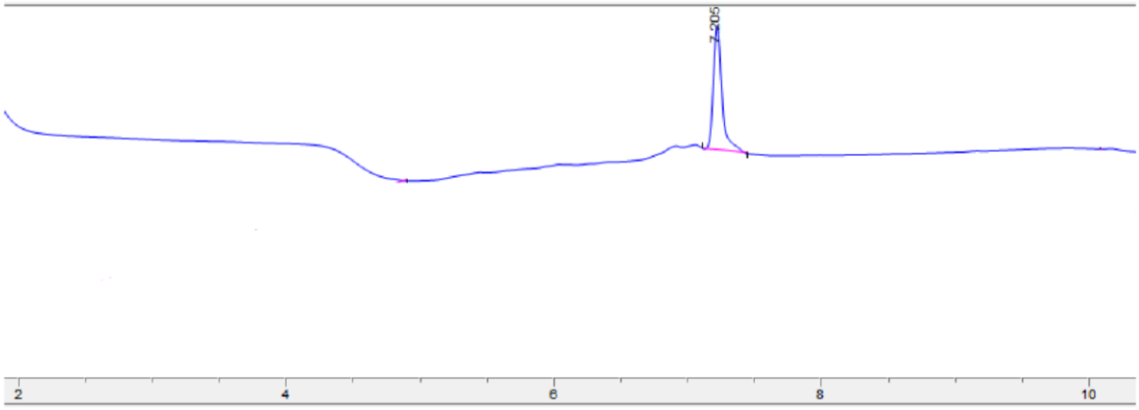

MS-spectrum for **19b**

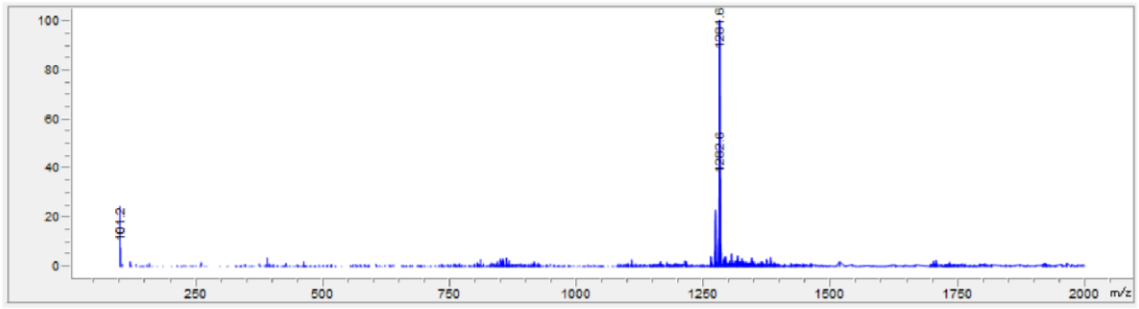

LC-chromatogram for **19b**

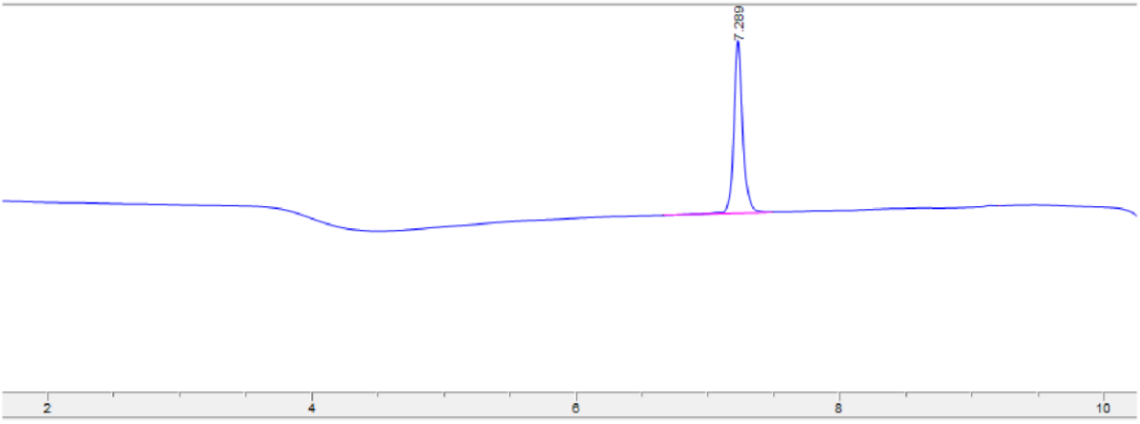

MS-spectrum for **20**

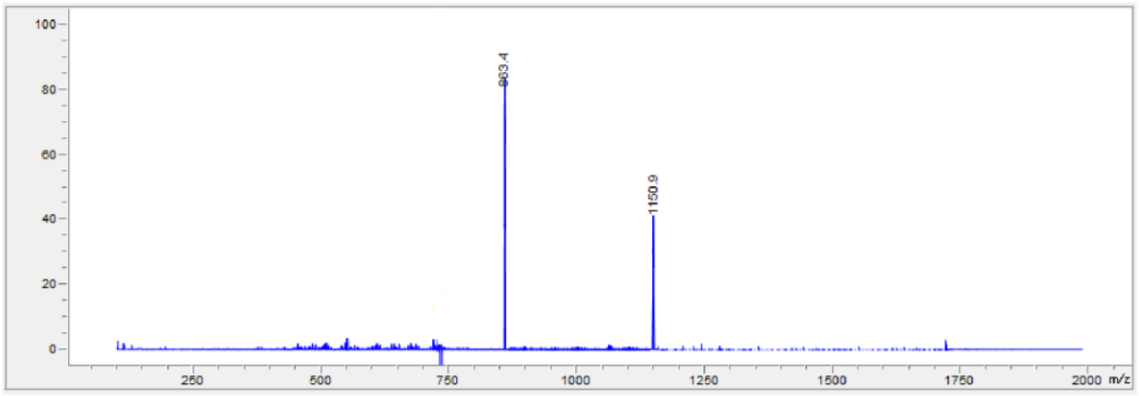

LC-chromatogram for **20**

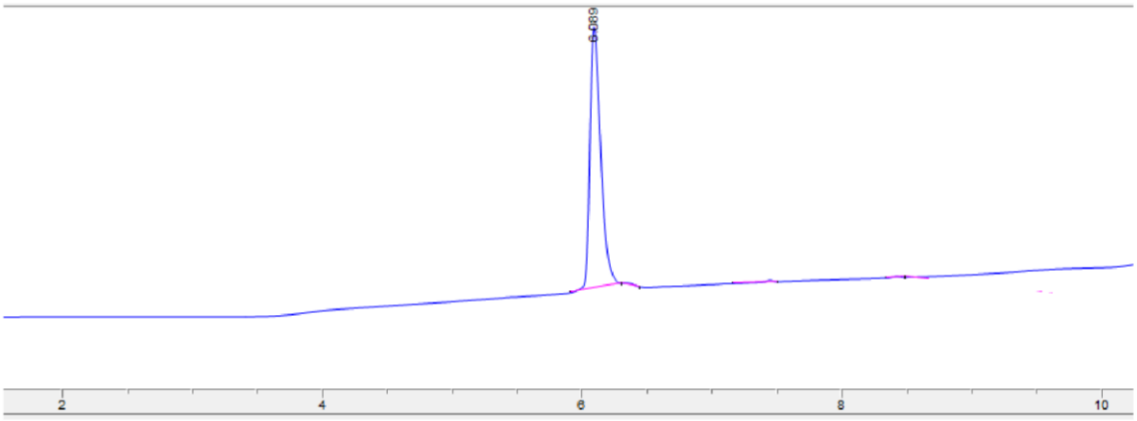

References

(1) Bruno, B. J.; Lim, C. S. *Mol Pharm* **2015**, *12*, 1412.

(2) Li, F.; Allahverdi, A.; Yang, R.; Lua, G. B.; Zhang, X.; Cao, Y.; Korolev, N.; Nordenskiold, L.; Liu, C. F. *Angew Chem Int Ed Engl* **2011**, *50*, 9611.

(3) Wright, T. H.; Brooks, A. E.; Didsbury, A. J.; MacIntosh, J. D.; Williams, G. M.; Harris, P. W.; Dunbar, P. R.; Brimble, M. A. *Angew Chem Int Ed Engl* **2013**, *52*, 10616.

(4) Chen, Y. H.; Yang, J. T.; Chau, K. H. *Biochemistry* **1974**, *13*, 3350.

(5) Pettersen, E. F.; Goddard, T. D.; Huang, C. C.; Couch, G. S.; Greenblatt, D. M.; Meng, E. C.; Ferrin, T. E. *Journal of Computational Chemistry* **2004**, *25*, 1605.

(6) Shapovalov, Maxim V.; Dunbrack, Roland L. *Structure* **2011**, *19*, 844.

(7) In *GaussView, Version 5, Dennington, Roy; Keith, Todd; Millam, John.*; Semichem Inc.: Shawnee Mission, KS; Vol. Version 5.

(8) Bayly, C. I.; Cieplak, P.; Cornell, W.; Kollman, P. A. *The Journal of Physical Chemistry* **1993**, *97*, 10269.

(9) Cornell, W. D.; Cieplak, P.; Bayly, C. I.; Kollmann, P. A. *J. Am. Chem. Soc.* **1993**, *115*, 9620.

(10) Vanquelef, E.; Simon, S.; Marquant, G.; Garcia, E.; Klimerak, G.; Delepine, J. C.; Cieplak, P.; Dupradeau, F. Y. *Nucleic Acids Research* **2011**, *39*, W511.

(11) Cornell, W. D.; Cieplak, P.; Bayly, C. I.; Gould, I. R.; Merz, K. M.; Ferguson, D. M.; Spellmeyer, D. C.; Fox, T.; Caldwell, J. W.; Kollman, P. A. *J. Am. Chem. Soc.* **1996**, *118*, 2309.

(12) Maier, J. A.; Martinez, C.; Kasavajhala, K.; Wickstrom, L.; Hauser, K. E.; Simmerling, C. *J. Chem. Theory Comput.* **2015**, *11*, 3696.

(13) Jorgensen, W. L.; Chandrasekhar, J.; Madura, J. D.; Impey, R. W.; Klein, M. L. *The Journal of Chemical Physics* **1983**, *79*, 926.

(14) Joung, I. S.; Cheatham, T. E. *The Journal of Physical Chemistry B* **2008**, *112*, 9020.

(15) Hopkins, C. W.; Le Grand, S.; Walker, R. C.; Roitberg, A. E. *J. Chem. Theory Comput.* **2015**, *11*, 1864.

(16) Berendsen, H. J. C.; Postma, J. P. M.; van Gunsteren, W. F.; DiNola, A.; Haak, J. R. *The Journal of Chemical Physics* **1984**, *81*, 3684.
(17) Salomon-Ferrer, R.; Götz, A. W.; Poole, D.; Le Grand, S.; Walker, R. C. *J. Chem. Theory Comput.* **2013**, *9*, 3878.
(18) Le Grand, S.; Götz, A. W.; Walker, R. C. *Computer Physics Communications* **2013**, *184*, 374.
(19) Zwanzig, R. *Journal of Statistical Physics* **1973**, *9*, 215.
(20) Loncharich, R. J.; Brooks, B. R.; Pastor, R. W. *Biopolymers* **1992**, *32*, 523.
(21) Essmann, U.; Perera, L.; Berkowitz, M. L.; Darden, T.; Lee, H.; Pedersen, L. G. *The Journal of Chemical Physics* **1995**, *103*, 8577.
(22) Ryckaert, J.-P.; Ciccotti, G.; Berendsen, H. J. C. *Journal of Computational Physics* **1977**, *23*, 327.
(23) Roe, D. R.; Cheatham, T. E. *J. Chem. Theory Comput.* **2013**, *9*, 3084.
(24) Shao, J.; Tanner, S. W.; Thompson, N.; Cheatham, T. E. *J. Chem. Theory Comput.* **2007**, *3*, 2312.
(25) Rost, B.; Sander, C. *Journal of Molecular Biology* **1993**, *232*, 584.

CHAPTER 5

CONCLUSIONS, FUTURE DIRECTIONS, AND ALTERNATIVE STRATEGIES

Conclusions

This dissertation has focused on advancing our rationally designed, Bcr-Abl dimerization inhibitor from gene therapy to a deliverable protein therapeutic. Unlike conventional CML therapies that target the Bcr-Abl tyrosine kinase domain, we aim to inhibit Bcr-Abl dimerization, a prerequisite to activation of the tyrosine kinase in Bcr-Abl. Past studies by Lim lab alumni Drs. Andrew Dixon and Geoffrey Miller created an optimized dimerization inhibitor, CC^{mut3}, which favors binding to Bcr-Abl and disfavors binding to itself. The next step towards creating a CC^{mut3} therapeutic was to create a CC^{mut3} protein capable of crossing cell membranes while maintaining activity (CPP-CC^{mut3}, Chapter 3). After this success, we focused on further modifying CC^{mut3} to improve its proteolytic stability. To this end, in collaboration with the Chou group, we utilized a novel method of stapling, which for the first time allowed the stapling of recombinant proteins. While we were able to staple full-length CC^{mut3}, the resulting proteins were more sensitive to proteolysis than their unstapled counterparts. Possible alternate strategies to overcome this are described in the following section.

Basics and Recent Advances in Peptide and Protein Drug Delivery

Today, there are more than 100 approved peptide/protein-based therapies on the market in the U.S.[1]. These large molecules can be highly selective for their target, much more so than the small molecules that have dominated medicine since time immemorial [1]. However, these peptide therapeutics face a number of unique problems, including low bioavailability, proteolysis (both in the GI and circulation), and limited cell penetration [2]. Cyclization, PEGylation, protease inhibitors, D-amino acids, and absorption enhancers have all been utilized to improve the oral bioavailability of peptide and protein therapeutics, with some successes [1, 3-8]. Beyond direct structural modifications, liposomal and nanoparticle delivery systems have been developed to increase the oral bioavailability [9, 10] and systemic resistance to proteolysis and opsonization [11, 12] [13].

Creating a protein therapeutic that is stable in circulation is, unfortunately, only half of the battle. The targets for many of these drugs are intracellular, meaning the protein therapeutic must cross the cell membrane. To that end, fusogenic liposomes [14] as well as compounds meant to help the protein therapeutic escape the endosome and subsequent degradation have been developed [14-19].

Of particular interest to this dissertation are cell penetrating peptides (CPPs) and peptide stapling. CPPs are short, water-soluble, polybasic peptides with a net positive charge that are able to penetrate cell membranes at low micromolar concentrations without causing membrane damage. Importantly, the CPP can be ionically or covalently linked to cargo – whether it be a peptide, protein, or small molecule [20-22]. Hydrocarbon stapling is a technique used to stabilize α-helical proteins, improve target affinity, cell penetration,

and serum stability [23-25]. Recent advances now allow for the stapling of recombinant proteins, whereas until recently only those peptides made by SPSS could be stapled [26].

Peptide and protein therapeutics, with their high target specificity and broad applicability, are already revolutionizing medical therapy. Clearly, there are still challenges to overcome in each of the areas discussed. As delivery and systemic stability are two overarching issues with protein and peptide therapeutics, overcoming these would likely lead to even further development of peptide and protein therapeutics with great therapeutic potential.

Inhibition of Bcr-Abl with a Coiled-Coil Protein Delivered via LS-CPP

Since the first cell-penetrating peptide (CPP) was discovered in 1988, many researchers have utilized CPPs to improve the intracellular delivery of protein therapeutics [27]. Of interest to this dissertation is the work by Nishimura and Kuniyasu which utilized phage display to isolate peptides that selectively internalize in leukemia and lymphoma cells [28]. We utilized this leukemia-specific cell-penetrating peptide (LS-CPP) for the selective delivery of CC^{mut3} to leukemic cells. CPP-CC^{mut3} was expressed, purified, and tested for its antioncogenic activity. Three purification schemes were unsuccessfully attempted (data not shown) before the successful purification scheme (Chapter 3) was optimized. After purity was demonstrated by SDS-PAGE analysis, the identities of the purified proteins were verified by mass spectroscopy.

Next, both leukemic (K562, Ba/F3) and nonleukemic (HEK-293, MCF7) cells were treated with CPP-CC^{mut3} and controls. As expected, this cell penetrating peptide delivered the constructs preferentially to leukemic cells, and those protein constructs lacking the CPP

did not enter any of the cell lines tested. CPP-CC^{mut3} had antioncogenic activity in Bcr-Abl+ leukemia cell lines K562 and Ba/F3 p210, but not in the Bcr-Abl-, pro-B cell line Ba/F3 (as evidenced by 7-AAD/Annexin V, colony forming assay, cell proliferation, and Bcr-Abl phosphorylation). This lead construct has two built-in safeguards against nonspecific toxicity. First, CC^{mut3} was shown to be nontoxic in Bcr-Abl- cell lines (Figure 5.1, unpublished data, collected by Dr. Andrew Dixon). These assays were carried out with CC^{mut2}, an earlier iteration of our dimerization inhibitor which differs from CC^{mut3} by one amino acid (K39E). Second, the LS-CPP will deliver the therapeutic preferentially to leukemic cells. Toxicity aside, unmodified CC^{mut3} would likely be sensitive to proteolysis in vivo, and attempts to ameliorate this problem are discussed in Chapter 4.

Stapling of Full-Length CC^{mut3}

Since all-hydrocarbon stapling of peptides was first pioneered by Schafmeister and Verdine in 2000 [29], α-helical peptide stabilization has become an exciting arena, and some stapled peptide therapeutics are even being tested in clinical trials [25, 30, 31]. However, most stapling chemistries require the incorporation of UAAs at the stapling sites (Table 2.7). Currently, incorporating UAAs into peptides requires that the peptide must be chemically synthesized, which limits the size of the peptide to 30-40 aa. As CC^{mut3} is 72 aa, stapling of full-length CC^{mut3} was unfeasible. Serendipitously, the Chou group (Biochemistry, University of Utah) developed a stapling scheme which required only cysteines at the staple site, thus removing the UAA requirement and associated peptide length limitations. Through mutagenesis, CC^{mut3} was modified to include two (single staple) or four (double staple) cysteines at i, i+7 spacing. Originally, an all-hydrocarbon

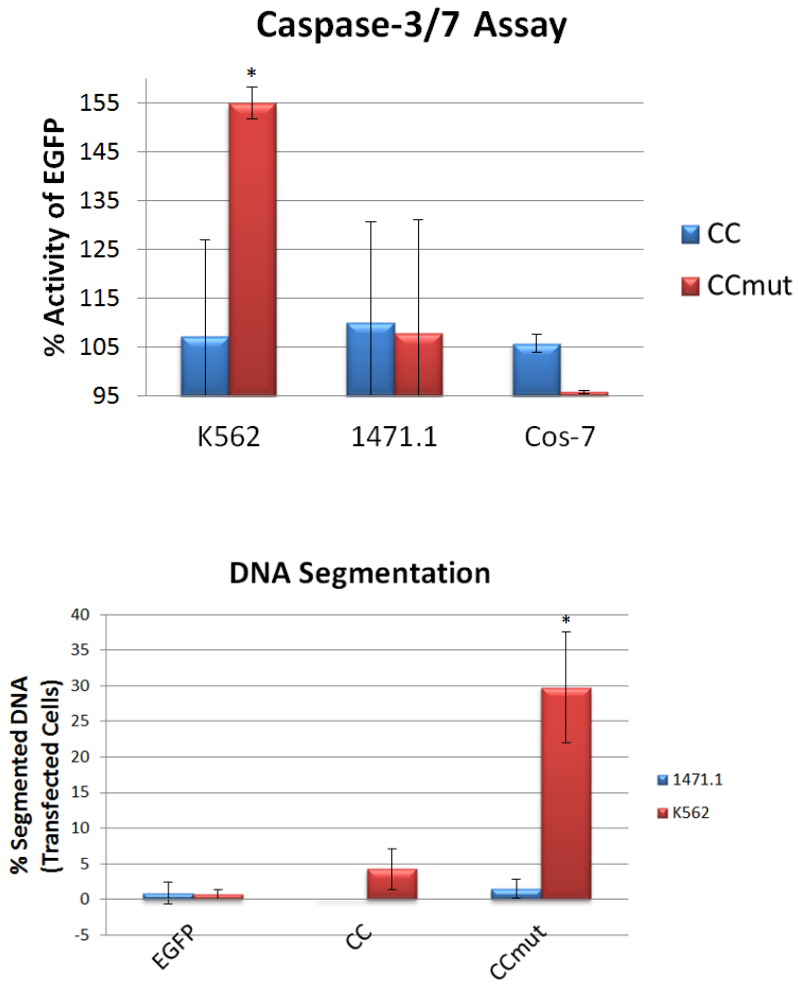

Figure 5.1 CC^{mut} construct is nontoxic to Bcr-Abl- cell lines 1471.1 and Cos7. Data collected by Dr. Andrew Dixon.

was to be used in this reaction. Unfortunately, miscibility issues (CC^{mut3}- hydrophilic, staple- hydrophobic) made this impossible. Therefore, the more hydrophilic (and untested) diallylurea staple was used. The stapling reactions were optimized, and single stapled (SS) and double stapled (DS) versions of CC^{mut3} were characterized by LC/MS, circular dichroism, and SDS-PAGE.

Following confirmation of the identity and alpha-helicity, stapled and unstapled (SS-U, DS-U) proteins were treated with three proteases: trypsin, chymotrypsin, and endoproteinase GluC. Surprisingly, the stapled proteins were more susceptible to proteolysis than both CC^{mut3} and cysteine-substituted, unstapled proteins SS-U and DS-U. Despite altering reaction conditions and attempting to control for all confounders, this result held. Further, mass spectroscopy analysis of digested SS and DS denoted rapid proteolysis of the proteins in all regions *except* those covered by the staple. Both native PAGE and size-exclusion chromatography suggest the stapled proteins exist in two conformations – one has approximately the same hydrodynamic radius as unmodified CC^{mut3}, while the other is about half the size as CC^{mut3}.

With this information, we hypothesize that the hydrophilic CC^{mut3} may refold to bury the relatively hydrophobic DAU staple when in aqueous solutions. Historically, hydrocarbon stapling has been performed on shorter, hydrophobic peptides [32]. The size and hydrophobicity of these peptides means there is little entropic penalty for solvating the additional hydrophobic staple. However, there is an entropic penalty for solvating the relatively hydrophobic DAU on the hydrophilic CC^{mut3}, and the increased length of CC^{mut3} means it may be able to refold and bury this hydrophobic patch, resulting in altered protein conformations. Computational modeling (performed by Sean Cornillie, Cheatham lab)

supports this conclusion, although exactly how the altered protein conformation results in increased sensitivity to proteolysis remains unclear.

Future computational modeling which analyzes the change in helicity of the proteins as a function of time could help to answer this question. Specifically, if our hypothesis is correct, we expect to see the stapled proteins demonstrate periods of decreased helicity (compared to unstapled control), during the time course of the simulation. The protein would be more susceptible to proteolysis when it loses its structure. A more detailed analysis of the phi-psi angles of the protein over the timecourse of the simulation could also add to our understanding of the increased proteolysis of the stapled proteins. More specifically, the simulations would focus on the torsion angles of the amino acids at and near the predicted protease cleavage sites. Previous computational and biological work has identified the required torsion angles/conformations required for protease-protein docking [33-35]. If our hypothesis is correct, we would expect the modeling to show the stapled proteins adopted these torsion angles more frequently compared to the unstapled proteins. Unfortunately, due to the constraints of collaborators and availability/cost supercomputer time to run these complex simulations, these simulations were not run.

Future Directions

Before discussing the future directions of this project, a brief overview of our initial attempt at making a stapled peptide is in order. As stated previously, classical hydrocarbon stapling requires the incorporation of UAAs, and therefore necessitates SPSS. To meet the requirements of SPSS, the Lim and Cheatham labs designed a stapled peptide version of

helix 2 of CC^{mut3} (aa 28-67). Computational modeling by Sean Cornillie and Dr. Thomas Cheatham revealed that, while truncating CC^{mut3} down to helix 2 reduced binding affinity with CC^{wt}, double hydrocarbon stapling these peptides restored the binding affinity to above that of full-length CC^{mut3}:CC^{wt} (Figure 5.2). Truncating CC^{mut3} to just helix 2 decreases the enthalpy of binding, but this loss is overcome by the reduced entropic cost of binding, as the peptide is already locked into its alpha helical conformation [36].

Based on these results and theoretical protection from proteolysis, we initiated a collaboration with the Walensky group (Harvard), and purchased three double-stapled helix 2 peptides at cost. These peptides each have two staples: 29/36-50/57 (St. #1), 30/37-50/57 (St. #2), and 29/36-43/50 (St. #3). The peptides were delivered with LC/MS data and a declaration that the proteins were >90% pure. Based on this information, I first tested to see if these stapled peptides could cross cell membranes. The peptides were fluorescently labeled, and therefore fluorescence intensity correlates with cell permeability. While all stapled peptides were able to enter K562 leukemic cells, stapled peptide #1 appears to demonstrate superior cell permeability (Figure 5.3, n=2).

Confocal microscopy was then performed to determine the location of the stapled peptides. A red membrane dye (Cell Mask far-red membrane dye, ThermoFisher) was used to stain the cell membrane. After a 4-hour incubation and washing with trypsin, heparin, and PBS, the stapled peptides appear to be associated with the membrane (Figure 5.4A). However, after the cells were allowed to grow for an additional 24 hours, the stapled peptides appeared to be truly intracellular (Figure 5.4B).

System	Copy (#)	$\Delta G_{binding}$ (kcal/mol)	Std. Err.
Control (Full)	cp1	-46.26	0.8
	cp2	-49.6	0.7
	cp3	-42.96	1.0
Control (Trunc)	cp1	-19.74	0.9
	cp2	-15.84	1.3
	cp3	-30.04	0.7

Staple 1	Staple 2	Copy (#)	$\Delta G_{binding}$ (kcal/mol)	Std. Err.
29/36	50/57	cp1	-54.8	0.8
		cp2	-49.4	0.8
		cp3	-56.4	0.7
30/37	50/57	cp1	-53.2	0.7
		cp2	-46.1	0.7
		cp3	-42.7	0.7
29/36	43/50	cp1	-43	0.7
		cp2	-44.1	0.9
		cp3	-49.8	0.9

Figure 5.2. Results of computational simulation between CC^{wt} and truncated, stapled CC^{mut3}.

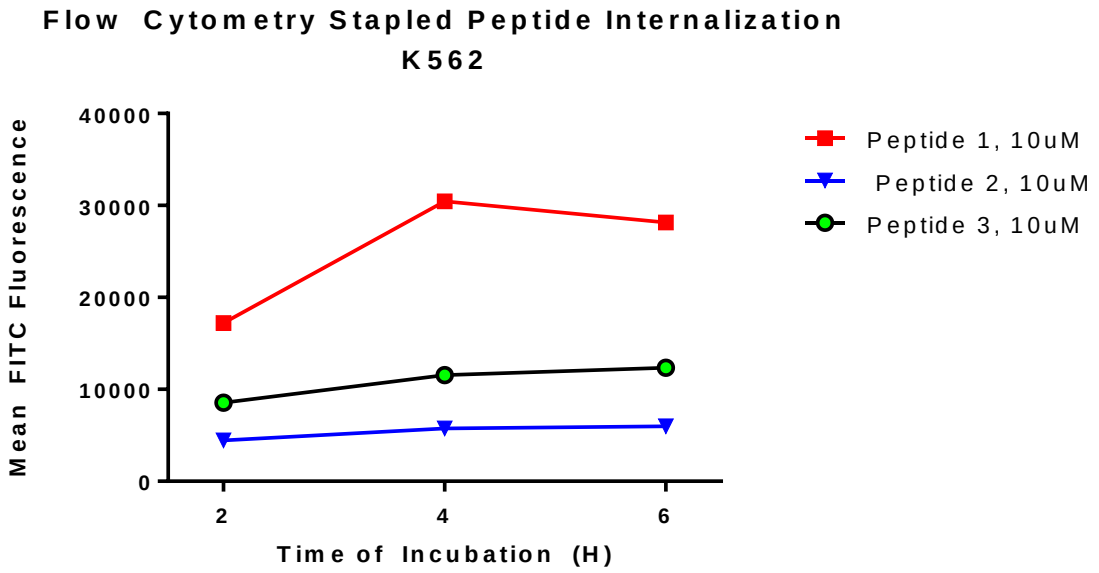

Figure 5.3. Stapled peptide internalization in K562 cells. Cells were treated in serum-free media, and at the indicated time, cells were washed to remove any membrane-bound, noninternalized peptide. Cells were then analyzed by flow cytometry, and FITC intensity connotates peptide internalization.

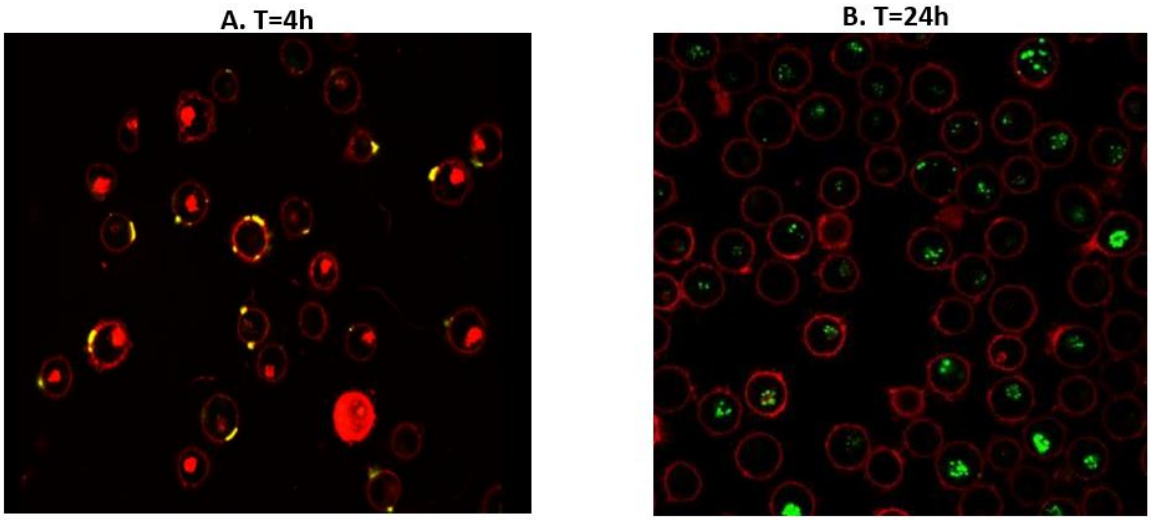

Figure 5.4. K562 cells treated with stapled peptide. #1 were imaged (A) immediately after a 4-hour incubation in serum-free media and washes and (B) 24 hours after the start of incubation, or 20 hours after washing the cells. The stapled peptide is membrane-associated at T=4, while at T=24 the stapled peptide appears to be truly intracellular. Red = cell membrane dye; green = stapled peptide.

With these data in hand, we proceeded to test the antioncogenic activity of the stapled peptides. For this purpose, 7-AAD, Annexin-V, MTT, colony forming and cell proliferation assays were performed. In all of these assays, surprisingly, none of the stapled peptides had any effect as compared to untreated cells (Figure 5.5). The positive control, small-molecule imatinib, demonstrated antioncogenic properties, as expected.

Following these results, we ran native PAGE with fluorescent imaging (Figure5.6A) and dynamic light scattering (DLS, Figure 5.6B) to determine if these peptides were forming aggregates. The native PAGE showed much of the proteins were stacking at the top of the gel, a sign of aggregation. Further, rather than one, clean band, the gel revealed a 'smear' of fluorescence, indicating the samples were not pure. Following this result, the peptides were analyzed by DLS. While controls (silver nanoparticles and albumin) appeared to be the appropriate size, all three stapled peptides appeared to be aggregating, with stapled peptide #1 forming the largest aggregates.

At this point, the purity/identity of the provided samples was in doubt. Therefore, the stapled peptides were analyzed via LC/MS. Figure 5.7 shows the LC data provided by the Walensky lab (A) and the report from our core facility (B). Whereas the LC plots from the Walensky group only denote one major peak and high sample purity, the LC data from the University core facility indicate there are numerous species in the samples. When discussing these results with Dr. Krishna Parasawar, co-director of the mass spectroscopy core, he stated these samples were well below 50% pure. It should be noted that, prior to LC/MS analysis, the peptides had been stored as lyophilized powder, and desiccated at -20 ^{o}C, meaning the samples were impure when received from the Walensky group. With this result, work on the truncated stapled peptide project was terminated.

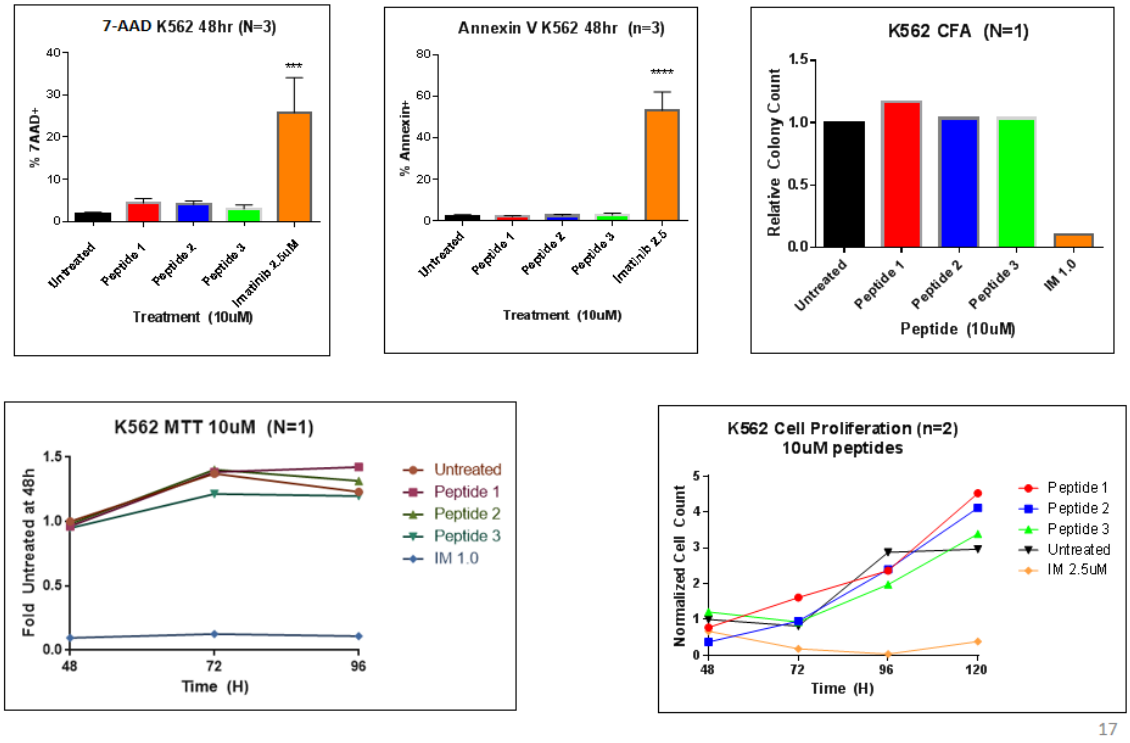

Figure 5.5. **Stapled peptide antioncogenic activity.** None of the stapled peptides demonstrated any antioncogenic activity in the K562 human leukemia cell line. Assays included 7-AAD and Annexin V for apoptosis induction, colony forming assay for transformative potential, and finally MTT and cell proliferation assays.

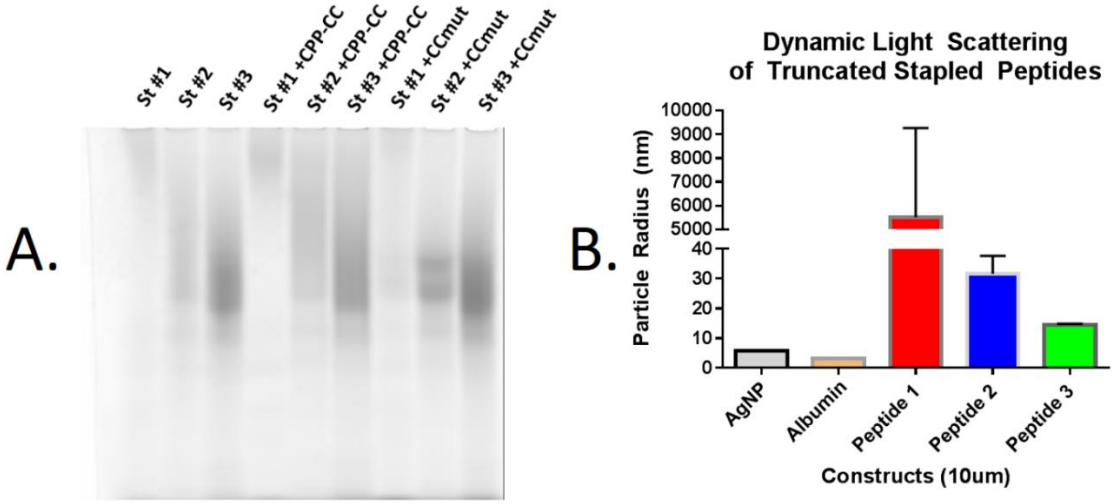

Figure 5.6. Analysis of stapled peptides by native PAGE and DLS. The native PAGE (A) indicates impure and aggregating samples, while DLS (B) confirms the stapled peptides are forming aggregates.

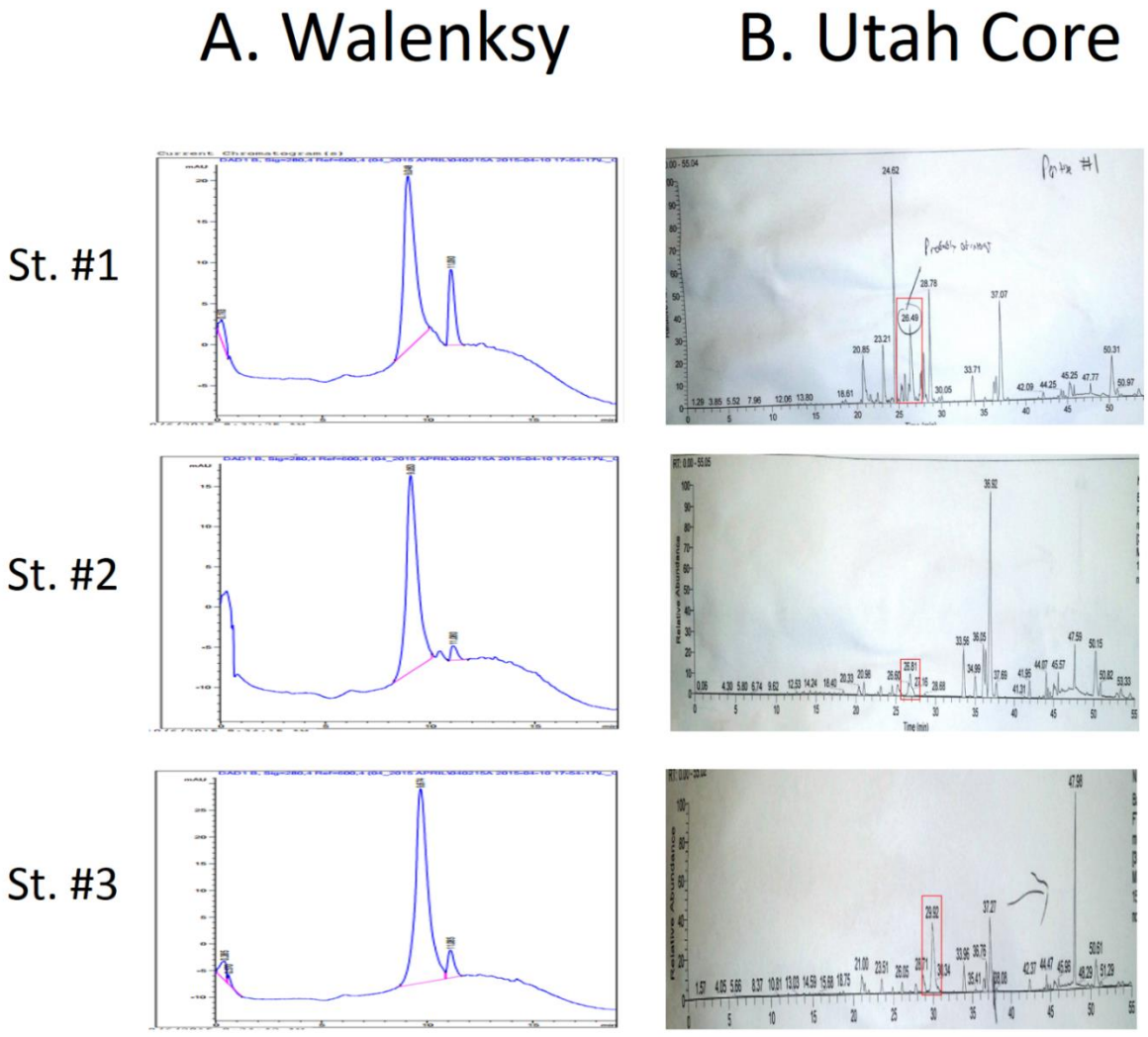

Figure 5.7. LC/MS analysis of stapled peptides. A. Data provided by the Walensky group. B. Data from Utah Mass Spectroscopy core facility. The red boxes in (B) indicate the LC peak corresponding to the protein of interest.

As mentioned in Chapter 4, immiscibility meant CC^{mut3} could not be stapled with an all-hydrocarbon staple. Peptide stapling is generally carried out in organic solvents, and the Chou lab was unable to dissolve CC^{mut3} in any hydrophobic solvents. The grand average of hydropathicity (GRAVY) is a measure of the overall hydrophobicity of a peptide. Most proteins found in nature range from -2 (hydrophilic) to +2 (hydrophobic) [37]. The GRAVY of full-length DS-U (CC^{mut3} with 4 cysteines) is -0.897, whereas the truncated helix 2 is more hydrophilic, -1.087 (as reported by the ProtParam tool on Expasy.org). Therefore, in retrospect, we handed the Walensky group the difficult (if not impossible) task of stapling a hydrophilic peptide with an all-hydrocarbon staple.

One important take-home message here is that *the truncated, stapled helix 2 (the stapled peptides from the Walensky group) has not been properly tested, since we received an impure sample that was impure and prone to aggregation*. As previously mentioned, the failure of stapled, full-length CC^{mut3} (Chapter 4) may be partially due to its size and ability to re-fold and bury the staple. Therefore, it may be possible to staple helix 2 with DAU or another, relatively hydrophilic staple. The log(p) of 1,8 nonadiene, a staple used by Walensky is 4.6, while DAU has a log(p) of 0.6.

The original modeling for the all-hydrocarbon stapled peptides (performed by Sean Cornillie) only looked at the constructs when bound to their target, CC^{wt}. Cornillie recently modeled the truncated, hydrocarbon-stapled peptides unbound in aqueous solution. Perhaps not surprisingly, the peptide folded in such a way to bury the hydrophobic staples (Figure 5.8A). This analysis was repeated with DAU-stapled helix 2, and the results were similar (Figure 5.8B). Therefore, even if the protein is truncated down just to helix 2, stapling with DAU is unlikely to succeed. Computational modeling can be used to screen

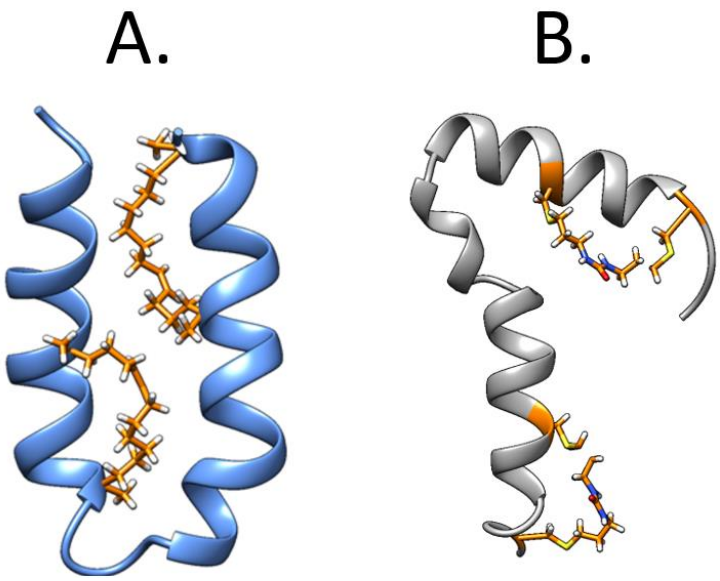

Figure 5.8. **Computational modeling of stapled helix 2.** (A) all-hydrocarbon stapled helix 2 and (B) DAU stapling of helix 2.

staple molecules with varying hydrophobicity, and those staples that do not show the sort of protein folding seen below can be created and tested.

Alternatively, full-length CC^{mut3} could be stapled with a more hydrophilic staple than DAU. For instance, the Wang and Chou attempted to use the compound 1,2-bis(4,5-dihydro-1H-imidazol-2-yl)propan-2-yl)diazene dihydrochloride as the staple in their original thiol-ene stapling work [26]. According to Molinspiration's log(p) calculator, this compound is more hydrophilic than DAU, and therefore may be better suited as a staple for CC^{mut3}. Alternatively, a charged linker could be used, although care must be taken, as this added charge may affect the cell penetration of the stapled protein. However, as the vast majority of stapled peptides use all-hydrocarbon or (at least) very lipophilic staples, this study would be quite an undertaking.

Alternative Strategies

Sortase Ligation of a Cell-Penetrating Peptide and St-CC^{mut3}

While using a hydrophilic staple may help maintain the secondary structure of CC^{mut3}, it may also reduce cell penetration. The internalization capacity of stapled peptides is thought to be due in part to the hydrophobicity of the hydrocarbon staple [32]; as Dr. Greg Verdine stated, "if you were an amphipathic α-helix bearing an all-hydrocarbon staple, would you prefer to live in aqueous culture medium or head to a lipid membrane[25]?" A possible solution is to include the LS-CPP (utilized in Chapter 3) to improve the delivery of the stapled, stabilized CC^{mut3}. The sequence of the LS-CPP is: CAYHRLRRC.

The cysteines in this CPP would likely cause problems during the stapling process,

as the Chou lab's technique adds a staple between two cysteine residues. Therefore, this CPP could be added to the peptide after the stapling reaction is completed. Specifically, CC^{mut3} was designed with an N-terminal triglycine sequence which can be used for sortase ligation [38]. Indeed, the Chou lab has successfully ligated the LS-CPP and CC^{mut3}; however, this work was performed on unstapled CC^{mut3} (data not shown). Another option is to use a different CPP, one without any cysteines present, to avoid the need for sortase ligation. As the Chou lab's current optimum conversion of CC^{mut3} to CPP-CC^{mut3} is quite low, near 20% (personal communication, Maria Disotuar, Chou lab), eliminating the need for this step would increase our final yield 5-fold. However, the leukemia-specific CPP is preferred, as it may decrease protein delivery to nonleukemic cells, thus reducing the required dose. Secondly, the LS-CPP cyclizes via formation of a disulfide bridge between two cysteines. As noted in Chapter 2, cyclic peptides tend to be more stable than their linear counterparts [39]. For these reasons, the cyclic, leukemiaspecific CPP is preferred to other nonspecific CPPs such as TAT or penetratin.

While CPPs are often successful in vitro, less success has been seen with systemic in vivo studies as well as in clinical trials. As of late 2016, 15 clinical trials using CPPs have been performed. However, only 2 of these are phase III clinical trials [40]. Further, nearly all clinical trials using CPPs are concerned with local (rather than systemic) delivery of a therapeutic peptide or protein. For instance, a c-Jun N-terminal kinase inhibiting peptide, known to reduce inflammation [41], was delivered via TAT using intraocular injection in an attempt to reduce postoperative intraocular inflammation in a phase III trial (results not yet published). The same process was used for intratympanic delivery for the treatment of acute hearing loss, with clinical benefits seen in a phase II trial (phase III trial

is currently recruiting) [42].

The systemic delivery of a therapeutic peptide via CPP was carried out in two phase I clinical trials. p28 is a 28 amino acid peptide known to penetrate cells and decrease the ubitquination of p53, and thus may be beneficial to treat those with p53+ tumors (by increasing the half-life of the antiapoptotic protein p53) [43]. While the trials showed it was well tolerated even at maximal doses, there was minimal evidence of antitumor activity, even at cumulative doses up to 140mg/kg over a 48-week period. For a 70kg adult, this equates to 10 grams of protein over the treatment course. For comparison, the recommended dose of adalimumab is 40mg every 2 weeks, or just over 1 gram per year. When one considers the molar differences in the drugs (2.9 kDa vs. 150kDa), the molar dose of p28 needed for the year of therapy is about 150x that of adalimumab. As CPPs require relatively high concentrations to trigger internalization, systemic treatment via CPP may require unrealistically high doses, considering the cost of biologicals today. Regardless of the cause, most CPP-based therapies falter in phase I/II trials, even those only aiming for topical or local delivery [40].

Protein Carrier Systems

While Chapter 2 covers many possible protein delivery modifications/systems, nearly all are impractical for the delivery of our therapeutic CC protein. First, we anticipate I.V. delivery of our protein, so none of the systems/modifications meant to increase oral stability/absorption need be considered. Further, most of the systems discussed in the 'systemic peptide stability' section aim for longer circulation time of the nanoparticle, resulting in controlled release of the protein therapeutic (e.g., liposomes, micelles, and

carbon nanotubes). As CPPs require high concentrations for internalization, the aforementioned systems are an irrational choice. Therefore, alternative systems aimed at directly increasing the stability/circulation time of our therapeutic CC will be discussed below.

PEGylation

As discussed in Chapter 2, PEGylation of proteins has the potential to improve the pharmacokinetic properties of the protein drug, such as increased half-life, reduced immunogenicity, and improved resistance to proteolysis [13, 44-46]. It is thought that PEG, which has a large hydrodynamic radius, shields the protein from proteases and antibodies [47, 48]. However, care must be taken when choosing a site to PEGylate; not all PEGylated proteins have the improved characteristics described above. Further, the specific conjugation strategy and linker characteristics alone can greatly alter the stability of PEGylated peptides and proteins [49]. In particular, cysteine-based PEGylation strategies confer less PK benefit than others (amide and triazole-based approaches), which is thought to be related to the relative flexibility of cysteine linkers [49]. Therefore, simply substituting cysteines at preferred PEGylation sites may not be the optimal strategy for stabilizing CC^{mut3}. While proteins can be PEGylated at the primary amine of lysine [50], that CC^{mut3} contains 5 lysines makes this approach impractical for our purposes. Other conjugation strategies are generally site-restricted (N- or C-terminus), nonspecific (glutamine-based) or require UAAs (Asn-PEGylation, azide- or alkyne- containing UAAs), and therefore are not be applicable or optimal for CC^{mut3} modification [49].

However, PEGylation may increase circulation time at the cost of reduced target

affinity [46, 51, 52]. For example, when Stigsnaes and colleagues PEGylated the α-helical peptide glucagon they noted it demonstrated improved biochemical stability, but PEGylation simultaneously disrupted the α-helical structure of the peptide [53]. Beyond the site chosen, the length and branching of the PEG chain used also affects conformational stability [49, 54], and this is an area of ongoing research. As an example, PEGylating the alpha-helical HIV-1 fusion inhibitor gp41 at the c and f sites of the heptad repeat (away from the binding interface, Figure 5.9) minimized loss of binding affinity, although the lead construct still saw a 2.7-fold reduction in binding affinity when compared to wild-type gp41 [51]. While PEGylation can reduce the binding affinity of the protein, increased serum half-life and plasma residence time can counteract this loss of affinity, resulting in greater in vivo activity [51]. Dual-PEGylation of two sites which independently provide improved PK profiles on one peptide can lead to synergistic, additive, or antagonistic effects [44]. Overall, PEGylation of CC^{mut3} has the potential to result in a bioactive, stable protein, although obtaining this construct would require extensive optimization and testing.

Nanoparticles

Nanoparticles have been used for the systemic protection and delivery of protein therapeutics [55]. However, they still face many problems including opsonization, cellular internalization, endosomal escape, and drug efflux pumps [56]. Despite these problems, 10 liposome-drug systems have been approved by the FDA [56]. Liposomal delivery of our CC^{mut3} construct is possible, and would require extensive liposome optimization in order to create stable, biocompatible liposomes with appropriate release kinetics. PLGA microspheres could also be used to protect our protein in vitro, although systemic

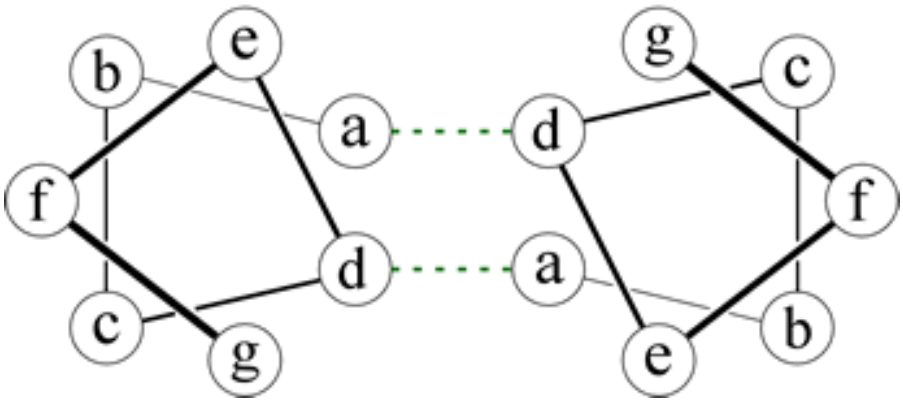

Figure 5.9. Coiled-coil helical wheel diagram. Residues in the heptad repeat are assigned a position: a and d are typically the hydrophobic amino acids leucine, isoleucine, valine and e and g are typically charged amino acids. Dimerization is driven by hydrophobic interactions of a and d residues as well as ionic interactions between g and e residues [57].

protection of the protein therapeutic requires harsh reaction conditions to synthesize the nanoparticle, which may in itself inactivate the protein therapeutic [46]. Gold nanoparticles are another attractive delivery option. These nontoxic and inert particles are relatively easy to synthesize, and can be readily functionalized through thiol linkages which can be tuned for intracellular drug release [58]. Indeed, gold nanoparticles have successfully been used for proteolytic protection of therapeutic proteins as well as the intracellular delivery of peptides, proteins, and nucleic acids [58, 59]. However, again it is difficult to engineer the particle surface for optimal therapeutic protein binding and release, bioavailability, and nonimmunogenicity [58]. Each of the systems discussed (and the multitude not mentioned) requires extensive optimization. While potentially viable as alternative options for the delivery of CC^{mut3}, it is beyond the scope of this dissertation.

Dual Target Therapy

As was shown by Dr. Geoffrey Miller, CC^{mut3} has additive (if not synergistic) effects when used in combination with the TKI ponatinib [60]. This study should be repeated with stapled CC^{mut3}, once a functioning construct is created. The work by Miller showed that, not only does simultaneously targeting two domains of Bcr-Abl have a greater therapeutic effect, but the required dose of ponatinib is reduced nearly 10-fold. Second and third generation TKIs have many off-target effects, and these effects are believed to be dose-dependent [61, 62]. In particular, ponatinib use is associated with an increased risk of cardiovascular events in a dose-dependent manner [63], which has been linked to ponatinib's potent inhibition of VEGFR signaling pathway [62]. Therefore, reducing the dose 10-fold (as seen in Miller's combinatorial therapy work), could reduce the

cardiotoxicity associated with ponatinib use. Another possibility is dual Bcr-Abl targeting with stapled CC^{mut3} and the allosteric inhibitor ABL001. As dual therapy with ABL001 and nilotinib reduced tumor regressions in mice [64], a dual (or possibly triple) therapy with ABL001 and stapled CC^{mut3} could have a similar effect.

Use of CC^{mut3} in Bcr-Abl-Independent Resistance

Bcr-Abl independent resistance has been associated with genetic variabilities in drug import and efflux [65-67], epigenetic modifications/upregulation of HDACs [68, 69], and the activation of alternative signaling pathways [68]. STAT3 has recently been implemented as a key mediator of Bcr-Abl independent resistance, and the Deininger group has successfully screened and tested a STAT3 inhibitor + imatinib, a combination that is synthetically lethal to CML progenitor cells that display Bcr-Abl independent resistance [70, 71]. Beyond synthetic lethality, the STAT3 inhibitor restored TKI sensitivity to cell lines that previously demonstrated Bcr-Abl independent resistance [70]. However, if the patient is unlucky enough to have both Bcr-Abl independent resistance AND a TKI-untreatable compound mutant (e.g., E255V/T315I) this combination therapy will likely not work. Studies performed by Drs. David Woessner and Geoffrey Miller showed CC^{mut3} is effective against mutant Bcr-Abl, including the compound mutant E255V/T315I [60, 72]. Therefore, a combination of CC^{mut3} + STAT3 inhibitor may have a place in therapy. Further, as many stem cells are insensitive to TKIs [73, 74], a therapy aimed at Bcr-Abl independent resistance may also eliminate CML stem cells.

Materials and Methods

Cell Culture and Transfections

K562 cells were cultured as in [75]. Cos-7 and 1471.1 cells were cultured and transfected as in [76]. Cos-7 and 1471.1 cells grow as monolayers in DMEM and RPMI (GIBCO, Invitrogen, Carlsbad, CA, USA), respectively, both supplemented with 10% FBS (Hyclone Laboratories, Logan, UT, USA), 1% penicillin-streptomycin (GIBCO), 0.1% gentamicin (Hyclone), and 1% L-glutamine (Hyclone). The cells were maintained in a 5% CO2 incubator at 37 °C. 1471.1 cells were grown to approximately 50% confluency, and 5 x 106 cells in 100 μL cold plain DMEM were transiently cotransfected via electroporation as previously described (22, 23). Transfections were performed using the Electrosquare Porator ECM 830 (BTX, Harvard Apparatus, Holliston, MA, USA) with 2 μg of EGFP-protein switch plasmid and 2 μg of DsRed plasmid along with 6 μg pGL3basic (Promega, Madison, WI, USA) carrier DNA for a total of 10 μg DNA. Three pulses of 140 V were applied for 10 msec. Following the electroporation, the cells were plated in complete DMEM in a 2-well live cell chamber (Lab-tek II chamber slide system, Nalge NUNC, Rochester, NY, USA), and incubated in a 5% CO2 incubator at 37 °C overnight. Cos-7 cells were seeded into a 2- or 4-well live cell chamber 24 hrs prior to transfection with Lipofectamine LTX (Invitrogen, Carlsbad, CA, USA) so the confluency was around 90% on the day of the transfection. Transfections were carried out as recommended by the supplier. Caspase 3/7 and DNA segmentation assays were carried out as in [77].

Stapled Peptide Internalization

Cells were treated with peptides washed as in [75]. Flow cytometric analysis was performed on a FACSCanto II analyzer (Becton Dickinson, Franklin Lakes, NJ, USA) using BD FACSDiva v6.13 software. Excitation and emission filters were as follows: FITC, 488nm excitation, emission filter 500-560. Laser intensity was held constant between samples and replicates.

Stapled Peptide Activity Experiments

K562 cells were treated with peptides as in [75]. 7-AAD, Annexin V, colony forming assays, and cell proliferation assays were performed as in [75]. MTT assay was carried out as in [72].

Native PAGE

Protein constructs (either alone, or in combination as noted in the image) were diluted to a concentration of 10μM in PBS. Samples were then run on Novex tris-glycine 4-20% gels with Novex tris-glycine native sample and running buffers. Gels were imaged using the Typhoon fluorescent gel imager (GE Healthcare), as in [78].

Confocal Microscopy

Following incubation of cells with peptides, cells were washed to remove bound, noninternalized peptide as in [75]. All images of K562 live cells were acquired on an Olympus IX81 FV1000-XY spectral confocal microscope (Imaging Core Facility, University of Utah) equipped with 405 nm diode, 488 nm argon, and 543 nm HeNe lasers

using a 60X PlanApo oil immersion objective (NA 1.45) using Olympus FluoView software. Excitation and emission filters were as follows: EGFP, 488 nm excitation, emission filter 500-530 nm; Cell Mask far-red membrane dye (ThermoFisher), 633 nm excitation, emission filter 555-655 nm. Images were collected in sequential line mode with exposure , and no channel crosstalk was observed. Pixel resolution was kept at 1024 x 1024 (0-2.5-fold digital zoom) with a pixel dwell time of 12.5 µs.

LC/MS

LC/MS was performed by the University of Utah Mass Spectroscopy core, as in [75].

References

[1] D.J. Craik, D.P. Fairlie, S. Liras, D. Price, The future of peptide-based drugs, Chem Biol Drug Des 81(1) (2013) 136-47.

[2] B. Aungst, Saitoh, H., Burcham, D., Huand, S., Mousa, S., Hussain, M., Enhancement of the intestinal absorption of peptides and non-peptides, J Control Release 41(1) (1996) 19-31.

[3] P. Calceti, S. Salmaso, G. Walker, A. Bernkop-Schnurch, Development and in vivo evaluation of an oral insulin-PEG delivery system, Eur J Pharm Sci 22(4) (2004) 315-23.

[4] C. McMartin, L.E. Hutchinson, R. Hyde, G.E. Peters, Analysis of structural requirements for the absorption of drugs and macromolecules from the nasal cavity, J Pharm Sci 76(7) (1987) 535-40.

[5] P. Vlieghe, V. Lisowski, J. Martinez, M. Khrestchatisky, Synthetic therapeutic peptides: science and market, Drug Discov Today 15(1-2) (2010) 40-56.

[6] R. Tugyi, K. Uray, D. Ivan, E. Fellinger, A. Perkins, F. Hudecz, Partial D-amino acid substitution: improved enzymatic stability and preserved Ab recognition of a MUC2 epitope peptide, Proc Natl Acad Sci U S A 102(2) (2005) 413-8.

[7] S. Fujii, T. Yokoyama, K. Ikegaya, F. Sato, N. Yokoo, Promoting effect of the new chymotrypsin inhibitor FK-448 on the intestinal absorption of insulin in rats and dogs, J Pharm Pharmacol 37(8) (1985) 545-9.

[8] M. Thanou, J.C. Verhoef, H.E. Junginger, Chitosan and its derivatives as intestinal absorption enhancers, Adv Drug Deliv Rev 50 Suppl 1 (2001) S91-101.

[9] G.S. Asane, S.A. Nirmal, K.B. Rasal, A.A. Naik, M.S. Mahadik, Y.M. Rao, Polymers for mucoadhesive drug delivery system: a current status, Drug Dev Ind Pharm 34(11) (2008) 1246-66.

[10] A. Bernkop-Schnurch, M.E. Krajicek, Mucoadhesive polymers as platforms for peroral peptide delivery and absorption: synthesis and evaluation of different chitosan-EDTA conjugates, J Control Release 50(1-3) (1998) 215-23.

[11] T. Jung, W. Kamm, A. Breitenbach, E. Kaiserling, J.X. Xiao, T. Kissel, Biodegradable nanoparticles for oral delivery of peptides: is there a role for polymers to affect mucosal uptake?, Eur J Pharm Biopharm 50(1) (2000) 147-60.

[12] A. Kumari, S.K. Yadav, S.C. Yadav, Biodegradable polymeric nanoparticles based drug delivery systems, Colloids Surf B Biointerfaces 75(1) (2010) 1-18.

[13] B.W. Bailon P, Polyethylene glycol-conjugated pharmaceutical proteins, Pharm Sci Technol Today 1 (1998) 352-356.

[14] A.K. Varkouhi, M. Scholte, G. Storm, H.J. Haisma, Endosomal escape pathways for delivery of biologicals, J Control Release 151(3) (2011) 220-8.

[15] G. Fuertes, D. Gimenez, S. Esteban-Martin, O.L. Sanchez-Munoz, J. Salgado, A lipocentric view of peptide-induced pores, Eur Biophys J 40(4) (2011) 399-415.

[16] E. Prchla, C. Plank, E. Wagner, D. Blaas, R. Fuchs, Virus-mediated release of endosomal content: different behavior of adenovirus and rhinovirus serotype 2, J Cell Biol 131(1) (1995) 111-23.

[17] J. Sun, E.E. Pohl, O.O. Krylova, E. Krause, Agapov, II, A.G. Tonevitsky, P. Pohl, Membrane destabilization by ricin, Eur Biophys J 33(7) (2004) 572-9.

[18] M. Ogris, R.C. Carlisle, T. Bettinger, L.W. Seymour, Melittin enables efficient vesicular escape and enhanced nuclear access of nonviral gene delivery vectors, J Biol Chem 276(50) (2001) 47550-5.

[19] K. Sandvig, B. Spilsberg, S.U. Lauvrak, M.L. Torgersen, T.G. Iversen, B. van Deurs, Pathways followed by protein toxins into cells, Int J Med Microbiol 293(7-8) (2004) 483-90.

[20] P. Jarver, U. Langel, Cell-penetrating peptides--a brief introduction, Biochim Biophys Acta 1758(3) (2006) 260-3.

[21] F. Madani, S. Lindberg, U. Langel, S. Futaki, A. Graslund, Mechanisms of cellular uptake of cell-penetrating peptides, J Biophys 2011 (2011) 414729.

[22] S. El-Andaloussi, T. Holm, U. Langel, Cell-penetrating peptides: mechanisms and applications, Curr Pharm Des 11(28) (2005) 3597-611.

[23] L.D. Walensky, A.L. Kung, I. Escher, T.J. Malia, S. Barbuto, R.D. Wright, G. Wagner, G.L. Verdine, S.J. Korsmeyer, Activation of apoptosis in vivo by a hydrocarbon-stapled BH3 helix, Science 305(5689) (2004) 1466-70.

[24] G.L. Verdine, G.J. Hilinski, Stapled peptides for intracellular drug targets, Methods Enzymol 503 (2012) 3-33.

[25] L.D. Walensky, G.H. Bird, Hydrocarbon-stapled peptides: principles, practice, and progress, J Med Chem 57(15) (2014) 6275-88.

[26] Y. Wang, D.H. Chou, A thiol-ene coupling approach to native peptide stapling and macrocyclization, Angew Chem Int Ed 54(37) (2015) 10931-4.

[27] K.M. Wagstaff, D.A. Jans, Protein transduction: cell penetrating peptides and their therapeutic applications, Curr Med Chem 13(12) (2006) 1371-87.

[28] S. Nishimura, S. Takahashi, H. Kamikatahira, Y. Kuroki, D.E. Jaalouk, S. O'Brien, E. Koivunen, W. Arap, R. Pasqualini, H. Nakayama, A. Kuniyasu, Combinatorial targeting of the macropinocytotic pathway in leukemia and lymphoma cells, J Biol Chem 283(17) (2008) 11752-62.

[29] C. Schafmeister, Po, J, and Verdine, GL, An all-hydrocarbon cross-linking system for enhancing the helicity and metabolic stability of peptides, J Am Chem Soc 122 (2000) 5891-5892.

[30] A.P. Higueruelo, H. Jubb, T.L. Blundell, Protein-protein interactions as druggable targets: recent technological advances, Curr Opin Pharmacol 13(5) (2013) 791-6.

[31] C.S. Higman, J.A. Lummiss, D.E. Fogg, Olefin Metathesis at the dawn of implementation in pharmaceutical and specialty-chemicals manufacturing, Angew Chem Int Ed 55(11) (2016) 3552-65.

[32] M.R. Chu Q, Hilinski GJ, Kim YW, Grossmann TN, Yeh JTH, Verdine GL, Towards understanding cell penetration by stapled peptides, Med Chem Commun 6 (2015) 9.

[33] S.J. Hubbard, F. Eisenmenger, J.M. Thornton, Modeling studies of the change in conformation required for cleavage of limited proteolytic sites, Protein Science : A Publication of the Protein Society 3(5) (1994) 757-68.

[34] A.A. Belushkin, D.V. Vinogradov, M.S. Gelfand, A.L. Osterman, P. Cieplak, M.D. Kazanov, Sequence-derived structural features driving proteolytic processing, Proteomics 14(1) (2014) 42-50.

[35] M.D. Kazanov, Y. Igarashi, A.M. Eroshkin, P. Cieplak, B. Ratnikov, Y. Zhang, Z. Li, A. Godzik, A.L. Osterman, J.W. Smith, Structural determinants of limited proteolysis, J Proteame Res 10(8) (2011) 3642-51.

[36] T. Rao, G. Ruiz-Gomez, T.A. Hill, H.N. Hoang, D.P. Fairlie, J.M. Mason, Truncated and helix-constrained peptides with high affinity and specificity for the cFos coiled-coil of AP-1, PloS One 8(3) (2013) e59415.

[37] M.R. Wilkins, E. Gasteiger, J.C. Sanchez, A. Bairoch, D.F. Hochstrasser, Two-dimensional gel electrophoresis for proteome projects: the effects of protein hydrophobicity and copy number, Electrophoresis 19(8-9) (1998) 1501-5.

[38] C.S. Theile, M.D. Witte, A.E. Blom, L. Kundrat, H.L. Ploegh, C.P. Guimaraes, Site-specific N-terminal labeling of proteins using sortase-mediated reactions, Nature Protocols 8(9) (2013) 1800-7.

[39] H. Kaminski, Cyclosporine is derived from a fungus and is a cyclic undecapeptide with actions directed exclusively on T cells, in: H. Kaminski, Myasthenia Gravis and Related Disorders, Blackwell Publishing, 2008, p. 393-405.

[40] G. Guidotti, L. Brambilla, D. Rossi, Cell-penetrating peptides: from basic research to clinics, Trends Pharmacol Sci 38(4) (2017) 406-424.

[41] K. Reinecke, S. Eminel, F. Dierck, W. Roessner, S. Kersting, A.M. Chromik, O. Gavrilova, A. Laukevicience, I. Leuschner, V. Waetzig, P. Rosenstiel, T. Herdegen, C. Sina, The JNK inhibitor XG-102 protects against TNBS-induced colitis, PloS One 7(3) (2012) e30985.

[42] M. Suckfuell, G. Lisowska, W. Domka, A. Kabacinska, K. Morawski, R. Bodlaj, P. Klimak, R. Kostrica, T. Meyer, Efficacy and safety of AM-111 in the treatment of acute sensorineural hearing loss: a double-blind, randomized, placebo-controlled phase II study, Otology & Neurotology : Official Publication of the American Otological Society, American Neurotology Society [and] European Academy of Otology and Neurotology 35(8) (2014) 1317-26.

[43] M.A. Warso, J.M. Richards, D. Mehta, K. Christov, C. Schaeffer, L. Rae Bressler, T. Yamada, D. Majumdar, S.A. Kennedy, C.W. Beattie, T.K. Das Gupta, A first-in-class, first-in-human, phase I trial of p28, a non-HDM2-mediated peptide inhibitor of p53 ubiquitination in patients with advanced solid tumours, British Journal of Cancer 108(5) (2013) 1061-70.

[44] P.B. Lawrence, Y. Gavrilov, S.S. Matthews, M.I. Langlois, D. Shental-Bechor, H.M. Greenblatt, B.K. Pandey, M.S. Smith, R. Paxman, C.D. Torgerson, J.P. Merrell, C.C. Ritz, M.B. Prigozhin, Y. Levy, J.L. Price, Criteria for selecting PEGylation sites on proteins for higher thermodynamic and proteolytic stability, J Am Chem Soc 136(50) (2014) 17547-60.

[45] Y.S. Youn, J.Y. Jung, S.H. Oh, S.D. Yoo, K.C. Lee, Improved intestinal delivery of salmon calcitonin by Lys18-amine specific PEGylation: stability, permeability, pharmacokinetic behavior and in vivo hypocalcemic efficacy, J Control Release 114(3) (2006) 334-42.

[46] D.S. Pisal, M.P. Kosloski, S.V. Balu-Iyer, Delivery of therapeutic proteins, J Pharm Sci 99(6) (2010) 2557-75.

[47] C.S. Fishburn, The pharmacology of PEGylation: balancing PD with PK to generate novel therapeutics, J Pharm Sci 97(10) (2008) 4167-83.

[48] F.M. Veronese, A. Mero, The impact of PEGylation on biological therapies, BioDrugs 22(5) (2008) 315-29.

[49] P.B. Lawrence, W.M. Billings, M.B. Miller, B.K. Pandey, A.R. Stephens, M.I.

Langlois, J.L. Price, Conjugation strategy strongly impacts the conformational stability of a PEG-protein conjugate, ACS Chem Biol 11(7) (2016) 1805-9.

[50] N. Stefan, M. Zimmermann, M. Simon, U. Zangemeister-Wittke, A. Pluckthun, Novel prodrug-like fusion toxin with protease-sensitive bioorthogonal PEGylation for tumor targeting, Bioconjug Chem 25(12) (2014) 2144-56.

[51] M. Danial, T.H. van Dulmen, J. Aleksandrowicz, A.J. Potgens, H.A. Klok, Site-specific PEGylation of HR2 peptides: effects of PEG conjugation position and chain length on HIV-1 membrane fusion inhibition and proteolytic degradation, Bioconjug Chem 23(8) (2012) 1648-60.

[52] P. Bailon, A. Palleroni, C.A. Schaffer, C.L. Spence, W.J. Fung, J.E. Porter, G.K. Ehrlich, W. Pan, Z.X. Xu, M.W. Modi, A. Farid, W. Berthold, M. Graves, Rational design of a potent, long-lasting form of interferon: a 40 kDa branched polyethylene glycol-conjugated interferon alpha-2a for the treatment of hepatitis C, Bioconjug Chem 12(2) (2001) 195-202.

[53] P. Stigsnaes, S. Frokjaer, S. Bjerregaard, M. van de Weert, P. Kingshott, E.H. Moeller, Characterisation and physical stability of PEGylated glucagon, Int J Pharm 330(1-2) (2007) 89-98.

[54] B.K. Pandey, M.S. Smith, C. Torgerson, P.B. Lawrence, S.S. Matthews, E. Watkins, M.L. Groves, M.B. Prigozhin, J.L. Price, Impact of site-specific PEGylation on the conformational stability and folding rate of the Pin WW domain depends strongly on PEG oligomer length, Bioconjug Chem 24(5) (2013) 796-802.

[55] K.S. Wong N, and Dai H, Carbon nanotubes as intracellular protein transporters: generality and biological functionality, J Am Chem Soc 127 (2005) 6021-6026.

[56] E. Blanco, H. Shen, M. Ferrari, Principles of nanoparticle design for overcoming biological barriers to drug delivery, Nat Biotechnol 33(9) (2015) 941-51.

[57] Y.B. Yu, Coiled-coils: stability, specificity, and drug delivery potential, Adv Drug Deliv Rev 54(8) (2002) 1113-29.

[58] P. Ghosh, G. Han, M. De, C.K. Kim, V.M. Rotello, Gold nanoparticles in delivery applications, Adv Drug Deliv Rev 60(11) (2008) 1307-15.

[59] M. Chanana, P. Rivera Gil, M.A. Correa-Duarte, L.M. Liz-Marzan, W.J. Parak, Physicochemical properties of protein-coated gold nanoparticles in biological fluids and cells before and after proteolytic digestion, Angew Chem Int Ed Engl 52(15) (2013) 4179-83.

[60] G.D. Miller, D.W. Woessner, M.J. Sirch, C.S. Lim, Multidomain targeting of Bcr-Abl by disruption of oligomerization and tyrosine kinase inhibition: toward

eradication of CML, Mol Pharm 10(9) (2013) 3475-83.

[61] G.D. Miller, B.J. Bruno, C.S. Lim, Resistant mutations in CML and Ph(+)ALL - role of ponatinib, Biologics : Targets & Therapy 8 (2014) 243-54.

[62] J.J. Moslehi, M. Deininger, Tyrosine kinase inhibitor-associated cardiovascular toxicity in chronic myeloid leukemia, Journal of Clinical Oncology : Official Journal of the American Society of Clinical Oncology 33(35) (2015) 4210-8.

[63] D.J. Dorer, R.K. Knickerbocker, M. Baccarani, J.E. Cortes, A. Hochhaus, M. Talpaz, F.G. Haluska, Impact of dose intensity of ponatinib on selected adverse events: Multivariate analyses from a pooled population of clinical trial patients, Leuk Res 48 (2016) 84-91.

[64] A. Wylie, J. Schoepfer, G. Berellini, H. Cai, G. Caravatti, S. Cotesta, S. Dodd, J. Donovan, B. Erb, P. Furet, G. Gangal, R. Grotzfeld, Q. Hassan, T. Hood, V. Iyer, S. Jacob, W. Jahnke, F. Lombardo, A. Loo, P.W. Manley, A. Marzinzik, M. Palmer, X. Pelle, B. Salem, S. Sharma, S. Thohan, S. Zhu, N. Keen, L. Petruzzelli, K.G. Vanasse, W.R. Sellers, ABL001, a potent allosteric inhibitor of BCR-ABL, prevents emergence of resistant disease when administered in combination with nilotinib in an in vivo murine model of chronic myeloid leukemia, Blood 124(21) (2014).

[65] S. Dulucq, S. Bouchet, B. Turcq, E. Lippert, G. Etienne, J. Reiffers, M. Molimard, M. Krajinovic, F.X. Mahon, Multidrug resistance gene (MDR1) polymorphisms are associated with major molecular responses to standard-dose imatinib in chronic myeloid leukemia, Blood 112(5) (2008) 2024-7.

[66] L.C. Crossman, B.J. Druker, M.W. Deininger, M. Pirmohamed, L. Wang, R.E. Clark, hOCT 1 and resistance to imatinib, Blood 106(3) (2005) 1133-4; author reply 1134.

[67] L. Wang, A. Giannoudis, S. Lane, P. Williamson, M. Pirmohamed, R.E. Clark, Expression of the uptake drug transporter hOCT1 is an important clinical determinant of the response to imatinib in chronic myeloid leukemia, Clin Pharmacol Ther 83(2) (2008) 258-64.

[68] D. Bixby, M. Talpaz, Mechanisms of resistance to tyrosine kinase inhibitors in chronic myeloid leukemia and recent therapeutic strategies to overcome resistance, Hematology Am Soc Hematol Educ Program (2009) 461-76.

[69] W. Fiskus, M. Pranpat, P. Bali, M. Balasis, S. Kumaraswamy, S. Boyapalle, K. Rocha, J. Wu, F. Giles, P.W. Manley, P. Atadja, K. Bhalla, Combined effects of novel tyrosine kinase inhibitor AMN107 and histone deacetylase inhibitor LBH589 against Bcr-Abl-expressing human leukemia cells, Blood 108(2) (2006) 645-52.

[70] A.M. Eiring, B.D. Page, I.L. Kraft, C.C. Mason, N.A. Vellore, D. Resetca, M.S. Zabriskie, T.Y. Zhang, J.S. Khorashad, A.J. Engar, K.R. Reynolds, D.J. Anderson, A. Senina, A.D. Pomicter, C.C. Arpin, S. Ahmad, W.L. Heaton, S.K. Tantravahi, A. Todic, R. Colaguori, R. Moriggl, D.J. Wilson, R. Baron, T. O'Hare, P.T. Gunning, M.W. Deininger, Combined STAT3 and BCR-ABL1 inhibition induces synthetic lethality in therapy-resistant chronic myeloid leukemia, Leukemia 29(3) (2015) 586-97.

[71] A.M. Eiring, I.L. Kraft, B.D. Page, T. O'Hare, P.T. Gunning, M.W. Deininger, STAT3 as a mediator of BCR-ABL1-independent resistance in chronic myeloid leukemia, Leukemia Supplements 3(Suppl 1) (2014) S5-6.

[72] D.W. Woessner, A.M. Eiring, B.J. Bruno, M.S. Zabriskie, K.R. Reynolds, G.D. Miller, T. O'Hare, M.W. Deininger, C.S. Lim, A coiled-coil mimetic intercepts BCR-ABL1 dimerization in native and kinase-mutant chronic myeloid leukemia, Leukemia 29(8) (2015) 1668-75.

[73] C. Bellodi, M.R. Lidonnici, A. Hamilton, G.V. Helgason, A.R. Soliera, M. Ronchetti, S. Galavotti, K.W. Young, T. Selmi, R. Yacobi, R.A. Van Etten, N. Donato, A. Hunter, D. Dinsdale, E. Tirro, P. Vigneri, P. Nicotera, M.J. Dyer, T. Holyoake, P. Salomoni, B. Calabretta, Targeting autophagy potentiates tyrosine kinase inhibitor-induced cell death in Philadelphia chromosome-positive cells, including primary CML stem cells, J Clin Invest 119(5) (2009) 1109-23.

[74] S.M. Graham, H.G. Jorgensen, E. Allan, C. Pearson, M.J. Alcorn, L. Richmond, T.L. Holyoake, Primitive, quiescent, Philadelphia-positive stem cells from patients with chronic myeloid leukemia are insensitive to STI571 in vitro, Blood 99(1) (2002) 319-25.

[75] B.J. Bruno, C.S. Lim, Inhibition of bcr-abl in human leukemic cells with a coiled-coil protein delivered by a leukemia-specific cell-penetrating Peptide, Mol Pharm 12(5) (2015) 1412-21.

[76] A.S. Dixon, C.S. Lim, The nuclear translocation assay for intracellular protein-protein interactions and its application to the Bcr coiled-coil domain, BioTechniques 49(1) (2010) 519-24.

[77] A.S. Dixon, S.S. Pendley, B.J. Bruno, D.W. Woessner, A.A. Shimpi, T.E. Cheatham, 3rd, C.S. Lim, Disruption of Bcr-Abl coiled coil oligomerization by design, J Biol Chem 286(31) (2011) 27751-60.

[78] H.X. Hao, O. Khalimonchuk, M. Schraders, N. Dephoure, J.P. Bayley, H. Kunst, P. Devilee, C.W. Cremers, J.D. Schiffman, B.G. Bentz, S.P. Gygi, D.R. Winge, H. Kremer, J. Rutter, SDH5, a gene required for flavination of succinate dehydrogenase, is mutated in paraganglioma, Science 325(5944) (2009) 1139-42.